THE UNIVERSITY OF QUEENSLAND

AUSTRALIA

Behaviour of stiff, fine-grained soil during the installation of screw auger displacement piles

Martin Larisch

Dipl.-Ing

A thesis submitted for the degree of Doctor of Philosophy at

The University of Queensland in 2014

School of Civil Engineering

Geotechnical Engineering Centre

Abstract

Screw auger displacement piling tools have been successfully used throughout the global piling and ground engineering industry for decades. The technique can be used to install circular concrete elements referred to either as piles, to transfer structural loads into stiffer layers; or as rigid inclusions (known as drilled displacement columns, CSC, CMC, etc.), to reinforce and strengthen unsuitable ground as a soil improvement technique. The effect of installation parameters on screw auger displacement pile performance and load capacity in hard clay formations has not been investigated in detail and is the main scope of this research work.

For both applications, it is desirable that the pile or column toes are embedded into a displaceable dense, stiff or hard bearing layer. Loads from the structure are then transferred directly (via piles) or indirectly (by settlement of the soft layer and the resulting negative skin friction along the column shaft) into this bearing layer. As the design methodologies for these applications are different, this research work introduces the latest applications and design philosophies for both screw auger displacement piles and rigid inclusions.

As the typical diameters for screw auger displacement piling tools range from 270 mm to 610 mm, the working loads to be transferred are typically limited to 500 kN to 2,500 kN, depending on tool diameter and ground conditions. Both displacement piles and rigid inclusions are economical for use in projects with low to medium structural load-transfer requirements, like warehouses, embankment approaches or tanks.

For soil improvement projects, rigid inclusions are usually designed by calculating the settlements of the entire soil block (as reinforced with rigid inclusions), typically using finite element methods. Analytical design methods cannot practically reflect the complex interaction between the stiff concrete columns and the softer surrounding soil; therefore, this interaction needs to be modelled by numerical means.

For screw auger displacement piles, the additional load capacity caused by the soil displacement effect around the shaft and the base can be taken into account for the design work if there is sufficient evidence about the degree of the potential improvement. By considering increased skin friction because of soil displacement created during the pile installation process, piles could be designed to be shorter and more economical than would be possible using the traditional approaches used for conventional bored piers without any known improvement effects. The traditional 'α-c_u' method and the approach for screw auger displacement piles developed by Bustamante and Gianeselli (1998) are introduced and used in this work.

To compare the results of the design calculations with real load-settlement data, two different screw auger full-displacement piles (progressive displacement versus rapid displacement tools) and one small diameter Continuous Flight Auger (CFA) pile were installed with 4.0 m penetration into hard clay at a fully monitored field test site at Lawnton, QLD (Australia). The three piles were installed with different tool penetration rates and the pile load capacities (using axial static pile load tests) were compared in relation to installation parameters in similar ground conditions.

CPTs were carried out before, during and after the installation process of the three piles to measure and analyse *in situ* stresses in the ground. The measurements show that the declining penetration rates of the drill tool (which was the result of the underpowered piling rig installing the three initial test piles) reduces the cone pressure q_c around the pile after installation, particularly below pile toe.

To verify the finding that tool penetration rates are critical for stress development in the soil formation and to pile load capacity, an additional screw auger full-displacement pile was installed with a more powerful piling rig (140% additional rotational torque and 100% more vertical thrust). This setup was able to maintain a constant penetration rate during the entire installation process. It could be observed that the *in situ* stresses after the installation process for this pile were considerably higher (more than 60% on average) compared to for the test piles installed with insufficient installation energy. Moreover, the measured soil-heave volume was reduced by about 50% when penetration rates were held constant during the penetration of the hard clay. Back calculations from the static load tests using Fleming's method (1992) incorporating the *in situ* stress measurements before and after tool installation indicated an up to 25% higher load capacity for the pile installed under the constant penetration rate compared to under declining penetration, using similar auger shapes and diameters in the same soil formation.

This research work highlights the importance of utilising sufficiently equipped piling rigs with suggested minimum torque capacities of 250 kNm and vertical pull-down forces of 250 kN for the most effective installation of screw auger full-displacement tools into stiff/ hard clay bearing layers.

Additionally, site trials should be carried out prior to the installation of the working piles/columns to proof that penetration rates can be kept constant with smaller piling equipment to achieve the proposed embedment lengths into the base stratum. As insufficiently powerful piling equipment caused load reductions for screw auger displacement piles and columns, the author recommends the introduction of installation factors to reflect the influence of installation parameters on pile/column load capacities.

Declaration by author

This thesis is composed of my original work, and contains no material previously published or written by another person except where due reference has been made in the text. I have clearly stated the contribution by others to jointly-authored works that I have included in my thesis.

I have clearly stated the contribution of others to my thesis as a whole, including statistical assistance, survey design, data analysis, significant technical procedures, professional editorial advice, and any other original research work used or reported in my thesis. The content of my thesis is the result of work I have carried out since the commencement of my research higher degree candidature and does not include a substantial part of work that has been submitted to qualify for the award of any other degree or diploma in any university or other tertiary institution. I have clearly stated which parts of my thesis, if any, have been submitted to qualify for another award.

I acknowledge that an electronic copy of my thesis must be lodged with the University Library and, subject to the policy and procedures of The University of Queensland, the thesis be made available for research and study in accordance with the Copyright Act 1968 unless a period of embargo has been approved by the Dean of the Graduate School.

I acknowledge that copyright of all material contained in my thesis resides with the copyright holder(s) of that material. Where appropriate I have obtained copyright permission from the copyright holder to reproduce material in this thesis.

Publications during candidature

It is expected that eight research papers will be published based on the findings of this research project.

Five peer-reviewed conference papers and one journal paper have been accepted or published to date (July 2014). These are detailed below.

Currently, the author is preparing two additional journal papers; the first of which will present the results of the field test with a particular focus on methodology and outcomes, while the second will present the overall findings of the research with a specific focus on installation parameters and failure modes for the installation of screw auger displacement piles. The submission of the journal papers is scheduled for late 2014.

To promote the results of the research internationally, the author will present another conference paper, showing the results of the research, at the XVI European Conference on Soil Mechanics and Geotechnical Engineering in Edinburgh in September 2015.

Below are the details of the six papers published or accepted for publication that have arisen from this research to date.

Journal paper (peer-reviewed)

Larisch, MD, Nacke, E, Arnold, M, Williams, DJ and Scheuermann, A 2013, 'Simulation of auger displacement pile installation', *International Journal of Geotechnical Engineering (IJGE)*, accepted

Conference papers (peer-reviewed)

Larisch, MD, Scheuermann, A and Williams, DJ 2012, 'Fundamentals of the behaviour of piles and columns installed using screw auger displacement techniques in stiff clays', *Proceedings of the 2nd Symposium of Soil Improvement*, Vienna, Austria, pp. 83–98 (in German)

Larisch, MD, Williams, DJ and Slatter, JW 2012, 'Load capacity of auger displacement piles', *Proceedings of the International Conference on Ground Improvement and Ground Control (ICGI 2012)*, Wollongong, Australia, pp. 739–745

Larisch, MD, Arnold, M, Uhlig, M, Schwiteilo, E, Williams, DJ and Scheuermann, A 2013, 'Stress and displacement monitoring of auger displacement piles', *Proceedings of Pile 2013—State of the Art of Pile Foundations and Case Histories*, Bandung Indonesia, B3, pp. 1–13

Larisch, MD, Williams, DJ, Scheuermann, A and McConnell, A 2014, 'Stress monitoring using a raked CPT during screw auger pile installation', *Proceedings of the 3rd International Symposium on Cone Penetration Testing (CPT2014)*, Las Vegas, pp. 1121-1128

Larisch, MD, Williams, DJ and Scheuermann, A 2015, 'Effects of installation parameters of drilled displacement piles on in situ stress conditions in stiff clays', *XVI European Conference on Soil Mechanics and Geotechnical Engineering*, September 2015, Edinburgh, accepted

Publications included in this thesis

No publications included.

Contributions by others to the thesis

The following contributions by others were made to the thesis.

Execution of the laboratory tests

Dr-Ing. Michael Arnold	Senior Lecturer, Institute of Soil Mechanics and Geotechnical Engineering, Technical University of Dresden, Germany (until 2012)
Dipl.-Ing. Erik Schwiteilo	Lecturer, Institute of Soil Mechanics and Geotechnical Engineering, Technical University of Dresden, Germany

Development of the finite element model

Dr-Ing. Michael Arnold	Senior Lecturer, Institute of Soil Mechanics and Geotechnical Engineering, Technical University of Dresden, Germany (until 2012)

Collection of research data and documentation of standard testing methods

Mr Andrew Acton	Undergraduate student, The University of Queensland (until 2/2014)
Mr Heath Utting	Undergraduate student, The University of Queensland
Mr Michael Connors	Undergraduate student, The University of Queensland

General advice about auger mechanics and auger design

Dr James W Slatter	Director, Foundation Specialist Group (previously Piling Contractors)

Editing

Elite Editing Services

Statement of parts of the thesis submitted to qualify for the award of another degree

None.

Acknowledgements

I would like to acknowledge the valuable contributions of all of the people who were involved in this research project. Without them, this project would not have been possible.

Firstly, I want to thank my supervisor and Principal Advisor Professor David J. Williams for the opportunity to do my PhD within the Geotechnical Engineering Centre at The University of Queensland in part-time. David's support, guidance and advice throughout the last five years were exceptional and the foundation for the success of this research. I also want to thank my Associate Advisor Dr-Ing Alexander Scheuermann for his support and involvement over the last four years.

This research project would not have been possible without the generous funding of Piling Contractors Pty Ltd. The support of the company directors during the last five years needs to be highlighted separately and the efforts of Mr Mark Kliner, Mr Mark Dagge, Dr James Slatter and Mr Tony Mitchell stand out separately.

The test program would not have been possible without the substantial efforts of Mr Paul Pickering, Mr Steve Dowse and the team of Piling Contractors' employees who were involved in the field test site preparation and pile installation.

I also want to thank Mr Andrew Acton, Mr Heath Utting and Mr Michael Connors for their valuable support in helping with the field test preparations and data collection during the UQ Summer School programs in 2012 and 2013.

The efforts and great support of industry partner IGS, and in particular Mr Allan McConnell, were essential for the success of the project. All CPT and DMT data were collected by IGS.

I want to thank Golder Associates for their support as the third industry sponsor and particularly highlight the efforts and practical guidance of Dr Chris Haberfield and Dr Gary Chapman.

I am very grateful for the support of the ARC Linkage Program and for their considerable and generous funding of the research project.

I also extend my gratitude to the Go8 and DAAD for the support of the exchange program with the Technical University of Dresden in 2011 and 2012. The collaboration was very beneficial for the development of the FE model and without the contributions of Dr-Ing. Michael Arnold and Dipl-Ing. Erik Schwiteilo, the development of the current model would not have been possible.

Finally, I thank my wife Karen for her loving support and patience over the last five years.

Keywords

Auger mechanics, displacement piles in clay, hypo-plasticity, penetration rate, pile installation factor, pile design, raked CPT, rigid inclusions, static load tests, stiff clay penetration

Australian and New Zealand Standard Research Classifications (ANZSRC)

ANZSRC code: 090501, Geotechnical Civil Engineering, 100%

Fields of Research (FoR) Classification

FoR code: 0905, Civil Engineering 100%

CONTENTS

LIST OF TABLES

LIST OF FIGURES

LIST OF ABBREVIATIONS

ADP	Auger Displacement Pile
API	American Petroleum Institute
BAP	Bored and Augered Piles
CD	Consolidated drained
CFA	Continuous Flight Auger
CPT	Cone penetration test
CU	Consolidated undrained
DMT	Marchetti Dilatometer Test
FDP	Full-Displacement Pile
FE	Finite element
IGS	In situ Geotech Services
MPT	Menard pressuremeter test
nd	no date of publication
NSW	New South Wales
OCR	Over-consolidation ratio
QLD	Queensland
SID	Socket Inspection Devices
SPT	Standard penetration test
TDR	Time domain reflectometer
UQ	University of Queensland
US	United States
UU	Unconsolidated undrained

CHAPTER 1: INTRODUCTION

1.1 Scope of research

The construction of buildings, infrastructure and resources projects is a crucial part of Australia's economy. Limited land availability in major cities, the remote locations of mines or resource projects and the alignment of road or rail tracks sometimes make it necessary to build on ground that is not suitable for construction without additional measures. These additional measures include soil improvement and piling. The first of these improves the unsuitable soil directly by the addition of binders, inclusions or consolidation. Alternatively, the unsuitable ground can be bridged by piles, which are stiff elements transferring loads from the structures directly into stiffer soil layers below the unsuitable ground. In Australia, the volume of the piling and soil improvement markets is estimated by the author to be around AUS$900 million per year.

Both the piling and the soil improvement market offer various techniques and methodologies for piling and soil improvement; a few of these will be introduced in this research work. However, the focus of this research work is set on a particular and unique technique that can be applied to both fields: Screw auger displacement piles and columns.

Screw auger displacement piles were developed about 40 years ago in Europe (Van Impe 1988) and the technique has since been further improved by researchers and the industry. Screw auger displacement tools have the capability to improve unsuitable ground conditions during the installation process due to soil displacement and compaction. The created circular concrete elements (henceforth referred to as piles or columns) have the ability to improve the unsuitable ground directly as 'rigid inclusions' to reduce the overall settlement of the soil to be treated. Alternatively, they can be used as piles to bridge the unsuitable soil layer, offering potentially enhanced load-bearing capacities in certain ground formations due to possible soil improvement effects during installation. The execution technique for both options is similar, only the design process is different. Screw auger displacement tools do not create any spoil, as the ground is displaced. This is an advantage because no spoil removal is required, which is particularly important for contaminated ground conditions.

Some research work has been carried out in the last years to investigate the behaviour of screw piling augers in granular soil conditions (Slatter 2000, Schmitt and Katzenbach 2003); however, only very limited experience is reported about the behaviour of the technique in cohesive or fine-grained ground conditions.

Over the past 10 years, the author has been personally involved in the design and execution of numerous screw auger displacement projects in Germany and Australia. In his personal experience,

the majority of the projects were carried out in cohesive ground conditions, where the piles or columns were embedded in stiff to hard cohesive or dense granular bearing layers. In various instances, the embedment length could not be achieved due to early tool refusal inside the stiff layer. This occurred when the resistance of the soil to be displaced was larger than the installation energy of the piling rig, applied by rotational torque and vertical pull-down force. Consequently, projects needed to be re-designed and additional columns were required. Soil heave was another issue in need of monitoring due to the development of soil displacements in the ground during the installation process, resulting in potential damages on adjacent structures and freshly installed piles.

Overall, these effects can cause significant damages in cost and time to projects. The problem seems to be that the technique is not understood well enough to avoid these damages. The lack of understanding of screw auger displacement techniques was supported by the extensive literature review conducted for this research, which indicated that the gaps in the theoretical understanding of screw displacement auger behaviour in cohesive soil conditions are significant. This has previously been highlighted by van Impe (2003), who concluded in his paper that practical developments and state of practice are usually ahead of the theoretical understanding of screw auger piling for full-displacement and partial-displacement tools and techniques (Figure 1). During the last decades, contractors have developed new screw auger displacement piling applications, tools and technologies with the aim to get an advantage in the competitive market and to improve production rates and installation efficiency. Most of these new technologies were tested and proven in field applications, providing acceptable results in respect to economical as well as technical and load-settlement criteria. After the successful implementation of new technologies, research activities (sometimes) commence to understand the theories behind the new applications and systems.

Contractors are usually not interested in sharing their knowledge and research with the public, to protect their investments in the research and development of new technologies for as long as possible. There is currently a substantial gap between the current screw auger piling systems being used for foundation engineering purposes and their real theoretical understanding.

Screw auger displacement pile behaviour in fine-grained soil has not been investigated in detail in the past. Likewise, detailed investigation has not been done on the influence of different types of screw auger displacement augers and tools in relation to soil improvement capabilities; the stress and displacement in the soil caused by screw augers of different shapes during installation and extraction; or the influence of pile capacity, auger shape and installation parameters such as torque and penetration rate. Therefore, the scope of this research work is to narrow the current gap in understanding this technology.

A better and deeper theoretical understanding of screw auger displacement piling processes by detailed research will help to optimise pile designs and construction methodologies. The aim of this thesis is to narrow the knowledge gap, as shown in Figure 1, and to improve the general understanding of screw auger displacement pile behaviour in hard, fine-grained soil conditions. It is important to focus on these conditions, as the majority of the projects involving this technique require embedment into a stiff to hard cohesive layer.

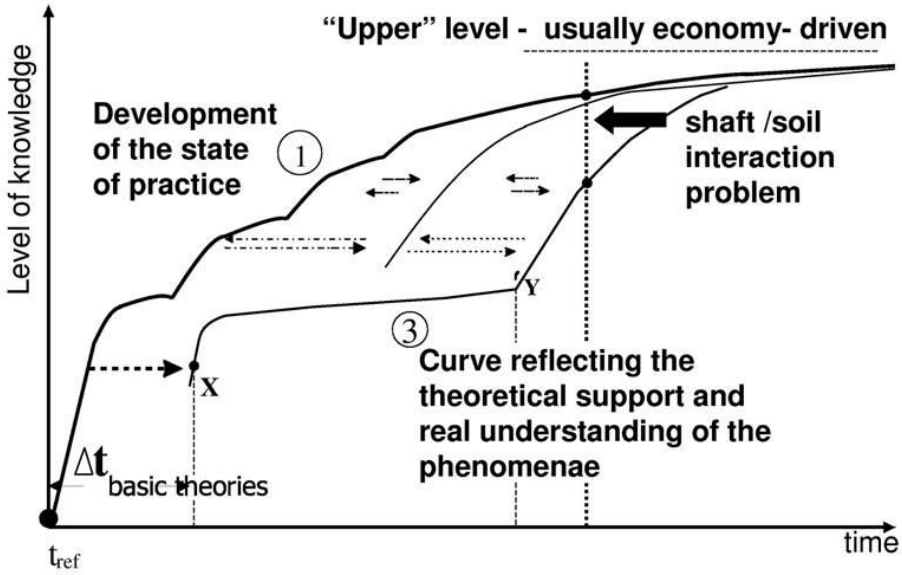

Figure 1 – Foundation engineering developments typically driven by the development of the state of practice, after Van Impe 2003

The estimated construction volume of screw auger displacement piles, carried out as piles or rigid inclusions for the Pacific Highway Upgrade and other infrastructure projects in New South Wales (NSW) is estimated to be about $20M for 2014. All of the projects are designed with penetration into stiff or hard clay formations.

It will be investigated whether embedment lengths can be reduced to a minimum to optimise the design and productivity on site. Further, it will be investigated whether installation parameters and the shape of different screw auger displacement tools affect pile or column load capacity.

1.2 Research supervision and collaborators

The Principal Advisor of the ARC Linkage Project that funded the thesis was Professor David Williams, Director of the Geotechnical Engineering Centre within the School of Engineering at The University of Queensland (UQ). The Associate Advisor of the project was Dr-Ing Alexander Scheuermann who is a Senior Lecturer in the Geotechnical Engineering Centre.

Professor Williams has an international reputation, developed over 30 years, in the application of soil mechanics principles to mining and mineral processing issues, as well as civil engineering applications.

Dr-Ing Alexander Scheuermann, has an international reputation, developed over almost 20 years, in the application of soil mechanics and hydraulic research topics.

Dr James Slatter was a Partner Investigator for Piling Contractors Pty Ltd. Besides providing the major industry funding to the project, he provided valuable technical advice, in particular regarding auger mechanics and field test set-up. Piling Contractors also provided their Lawnton yard for the pile tests and supported the project by supplying piling equipment and crews for the installation of the test piles and associated works.

Dr Chris Haberfield and Dr Gary Chapman of Golder Associates were Partner Investigators in the research project and provided valuable assistance and advice on theoretical matters and regarding the execution of the field tests at Lawnton.

Mr Allan McConnell of In situ Geotech Services (IGS) was a Partner Investigator in the research project and generously provided advice with respect to soil investigation activities as well as the execution of the CPT and DMT tests on site.

Dipl-Ing Martin Larisch, the author of this thesis, has 15 years of international experience in the piling and soil improvement industry. Martin carried out his PhD research on a part-time basis, while he was employed as a Project Manager and later as the National Technical and Quality Manager for Piling Contractors Pty Ltd.

1.3 Layout of research

This PhD research, 'Behaviour of stiff, fine-grained soil during the installation of screw auger displacement piles', covers the following:

- Introduction (Chapter 1)

  The research background, scope and layout are summarized and an overview of the research team and collaborators is provided in this introductive chapter of the thesis.

- Review of the available literature-

  - Screw piling technology (Chapter 2)

    The most common screw auger displacement piling systems are introduced in this chapter with a focus on full, partial and non-displacement methods and their distinct working principles.

- Auger mechanics (Chapter 3)

  In this chapter, the fundamental behaviour of screw piling augers is explained and the three basic auger actions (cutting, transport and displacement) are discussed in detail. The most common screw auger models identified in the literature are introduced by the author. Further, state of the art rig monitoring systems together with the most vital data influencing screw auger pile installation are presented in this chapter, too.

- Applications of screw auger displacement piles (Chapter 4)

  The basic principles of main applications and the major differences in design approaches and philosophies for screw auger displacement piles and columns are discussed in this chapter. Even though the construction of piles/columns on site is almost identical, the design for each application is fundamentally different.

- Critique of and gaps in the available literature (Chapter 5)

  The findings of the literature review are summarized and the most obvious gaps are highlighted in this chapter.

- Work program (Chapter 6)

  The work program of the research project is introduced in detail with explanations of the different steps starting from the literature review and chosen research methods to the execution of the tests and the final data analysis.

- Research methodologies applied for this project (Chapter 7)

  The research methodologies which were used for the research are introduced in detail in this chapter. The focus is placed on the general description of the chosen methodologies and the specific use or modification for each methodology for this research project to suit the particular scope.

- Results of the research carried out (Chapter 8)

  Chapter 8 shows the results of the methodologies and tests applied for the research.

- Analysis and interpretation of the results (Chapter 9)

  The detailed analysis and interpretation of the results is carried out in this section of the document. The focus is set on the influence of pile installation parameters on load test results for the different test piles as well as the interpretation of inclinometer, CPT and DMT tests carried out before and after pile installation, indicating the effect of the pile installation process on stress changes and displacements in the ground.

- Benefits and technology transfer (Chapter 10)

  Opportunities for future technology transfer with industry partners and Universities as well as benefits and results of existing transfer activities for the research are discussed and presented by the author.

- Conclusions and recommendations for further research (Chapter 11)

  In this chapter, the author presents the conclusions of the research project. Based on the findings and gaps identified during the literature review (Chapter 5), each gap identified is addressed individually. Additionally, several conclusions which are beyond the original gaps identified during the literature review are presented in this section of the thesis.

  In a separate step, the author discusses opportunities for further research based on the findings of this work.

- References

CHAPTER 2: SCREW PILING TECHNOLOGY

2.1 General overview

The development of screw auger piles started more than 40 years ago with the commercial application of Continuous Flight Auger (CFA) piles on hydraulic drilling rigs in the 1970s (Legrand 2001). In Figure 2, Van Impe (2003) summarises the developments of screw (auger) piling technology from the first generation of non-displacement auger systems in the early 1970s to the second and third generation of screw auger displacement auger systems.

Screw Piles 1 TECHNOLOGY EVOLUTION	
* Continuous flight auger - small ϕ stem, cast in situ - large ϕ stem, cast in situ	First generation (bored piles)
* Partial flight auger on steel casing - prefabricated - cast in situ * Prefabricated pile type (torque ≤ 70 kNm) * Lost auger head + regained casing type - screwing down usually combined with pulling up of the casing	Second generation (displacement auger systems)
* Screwing down (torque 150-500 kNm) screwing up and down with specific auger tip design features	Third generation (displacement auger systems)

Figure 2 – Technology evolution in the field of screw (auger) piling, after Van Impe 2003

Screw auger piles can be classified as displacement or non-displacement systems (Van Impe 1988, Van Impe 2003, Peiffer 2008), depending on the auger shape and the cutting, transport and displacement action of the screw piling auger or drill tool. The penetration and extraction process of the screw auger drill tool displaces soil vertically and horizontally.

Massarsch, Brieke and Tancre (1988) describe the use of partial screw auger displacement piles (VB piles). It is important to note that the auger shape and geometry of these piles for 500 mm diameter drill tools are identical to 'classic' CFA piles (which are typically defined as non-displacement piles), as the ratio between the outside of the inner stem and the pile diameter is identical (see Table 1 in Section 2.3. Henceforth, in the literature review of this thesis, all CFA will be referred to as non-displacement piles.

Consequently, screw auger piles can be differentiated into three groups, depending on their soil displacement behaviour and particular auger mechanics:

- Screw auger full-displacement piles;
- Screw auger partial-displacement piles; and
- Screw auger non-displacement piles (in the literature and commonly, these are referred to as CFA piles)

It is important to introduce the basics of auger mechanics at this early stage of the literature review, as the behaviour of different screw augers strongly depends on their mechanical behaviour. Figure 3 shows the basic working principle of a non-displacement (CFA) auger.

Numerous authors (Metcalf 1965, Van Weele 1988, Thornburn, Greenwood and Fleming 1993, Viggiani 1993, Fleming 1995, Slatter and Seidel 2000, Bustamante 2003) have tried to define suitable theoretical auger models to describe the complex process of cutting, transport and displacement. The pile–soil interaction and load capacity between full-displacement, partial-displacement and non-displacement piles can vary considerably, as the auger action in the soil is different for all three systems. Slatter (2000) describes screw auger action as a function between the cutting, transport and displacement of soil. A CFA drill tool (Figure 3) is designed and built mainly to cut and transport soil, whereas a full-displacement Atlas pile drill head (see Figure 16 in Section 2.4.1) is designed predominately to cut and displace the soil during installation.

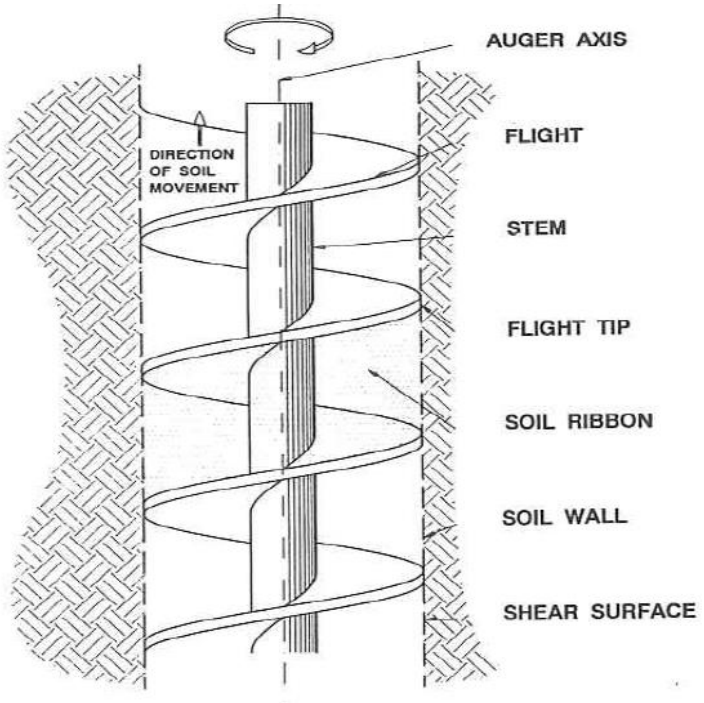

Figure 3 – Basic working principle of a non-displacement (CFA) auger, after Thornburn, Greenwood and Fleming 1993

Van Impe (1988) compared the different screw auger piling technologies with the behaviour of a metal screw (full-displacement) and a drill (non-displacement) penetrating in a piece of wood (Figure 4). The metal screw displaces the wood during the installation process and the structural interaction between wood and screw is improved; no spoil is created during the installation process of the screw. The removal of wood while boring a hole into the material using a drill bit creates spoil, and the drilling process does not improve the friction values of the wood. However, this model simplifies the installation process of screw augers in soil, as the behaviour and composition of granular soil (sand) and cohesive soil (clay) is different and cannot be compared with wood.

The general installation energy to install a screw is significantly higher than for drilling a hole into the same material, regardless of whether the task is being carried out in wood or any type of soil. Slatter (2000) demonstrated in his research that the smart design of displacement screw augers for applications in sand could save up to 30% of installation energy while providing similar pile load capacities. He did not extend his research to applications in cohesive soil. Therefore, this research aims to conduct an analysis of screw auger behaviour in fine-grained soils with respect to the correlation between installation capacities, installation parameters and the load-settlement behaviour of the piles.

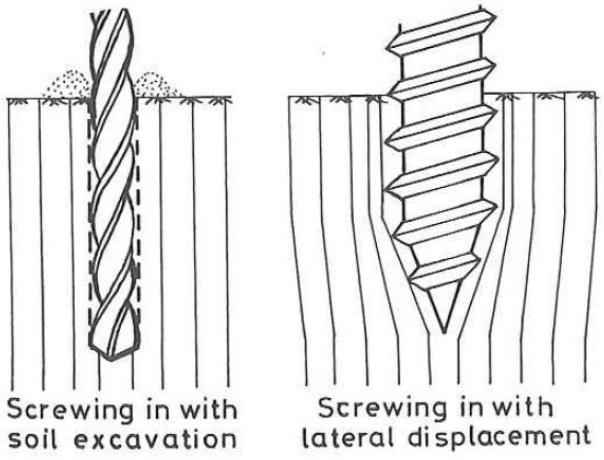

Figure 4 – Analogy between non-displacement and displacement piles, after Van Impe 1988

In contrast to conventional rotary bored piles, where an open excavation is created prior to pouring the pile, as shown in Figure 5, screw auger piling applications do not rely on Kelly bars for the transmission of installation forces. Rotary bored piles with Kelly bars can be installed with diameters of up to 3.5 m and to excavation depths exceeding 100 m. Screw piles are usually limited to diameters of 1.5 m for CFA piles and to between 270 mm and 610 mm for screw auger displacement piles. Drilling depths of up to 40 m are possible with the latest generation of screw piling rigs (e.g. Fundex F3500), with operational weights in excess of 120 ton and rotational torque capacities up to 500 kNm and vertical pull-down forces up to 1,000 kN.

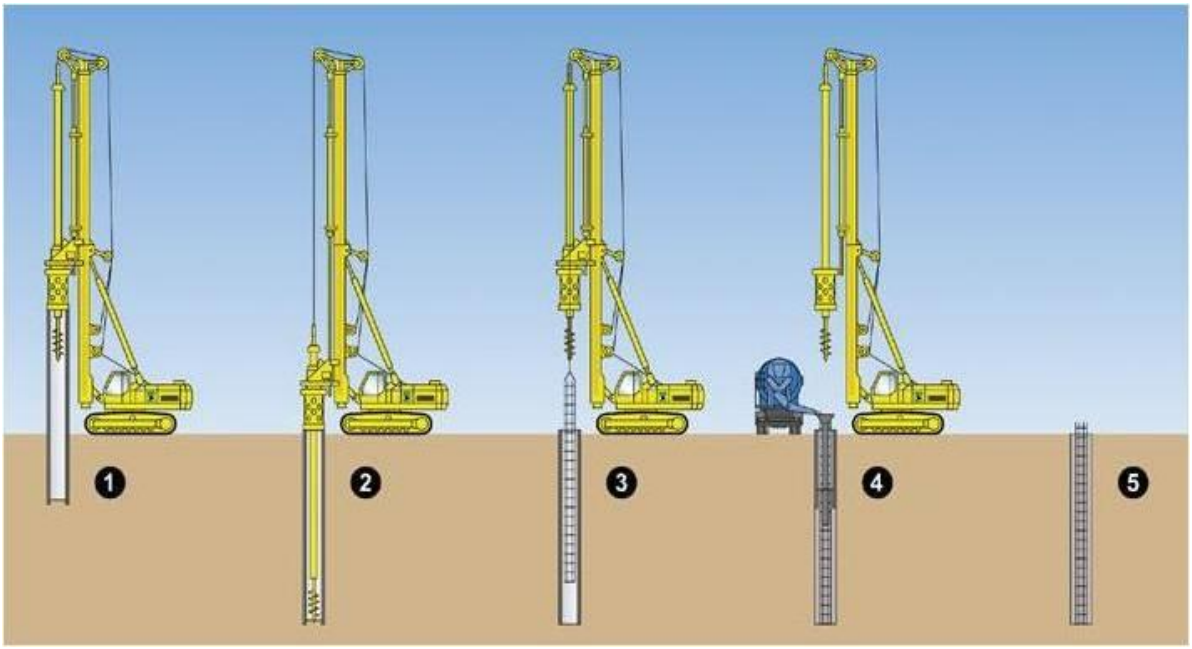

Figure 5 – Installation sequence for cased rotary bored piles, after Brueckner nd

The typical working sequence for the installation of conventional cased rotary bored piles installed with Kelly bars can be summarised as follows:

1. Installation of the temporary or permanent steel casing by rotating, vibrating or driving;
2. Excavate soil or rock inside the casing or the stable unsupported borehole wall with suitable conventional drill tools (e.g. auger, bucket). Clean the pile base using purpose-built cleaning buckets;
3. Control socket length and the cleanliness of the pile base before the reinforcement cage is lowered down into the excavated, open hole. Ensure cage spacers are in place and that the reinforcement cage is located at the correct level;
4. Insert tremie pipe and place concrete according to project requirements; and
5. Extract temporary casing and finish pile head according to project requirements.

Contrary to rotary piling with Kelly bars, screw augers are directly attached to the drill head of the piling rig and always have a hollow stem for concrete placement. The most significant distinction to conventional bored piles is that screw auger piles do not create an open excavation. The auger and the soil inside the auger flights act like an internal support to the borehole walls and keep the excavation open. Screw auger piles must be poured while the auger is extracted; concrete fills the potential cavity created by the extracted auger. The construction methodology for screw auger displacement and screw auger non- or partial-displacement piles is quite similar, with the only difference being the shape of the drill tool (Figure 6).

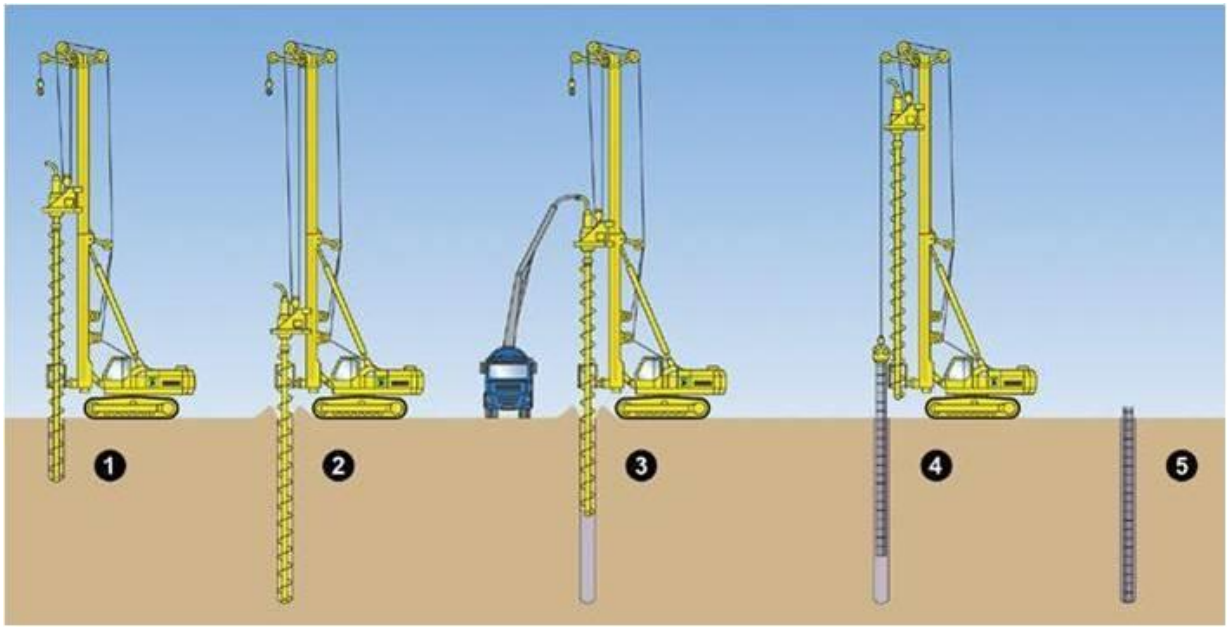

Figure 6 – Installation sequence of CFA screw auger piles, after Brueckner nd

The typical working sequence for the installation of continuous flight auger (CFA) piles can be summarised as follows:

1. Set up the rig at the pile location and close the tip of the hollow auger stem with a plastic cap or other suitable device to avoid water ingress during drilling. The screw auger is drilled into the soil strata. The penetration rate has to be specified before the drilling process based on ground conditions and auger shape;
2. The auger is drilled to design depth, maintaining a constant penetration rate to avoid over excavation and uncontrolled horizontal auger feeding. The auger filled with soil acts like an internal hole support and prevents the hole from collapsing;
3. After the final depth is reached, highly workable concrete is pumped through the hollow auger stem while the auger is extracted from the bore. The auger is extracted without rotation and concrete fills the volume in the ground created by the auger. It is important to maintain a positive pressure and keep the auger embedded into the fresh concrete to ensure pile integrity;
4. Clean the pile head and, if required, plunge pile reinforcement into fresh concrete; and
5. Finish pile head according to project specifications.

Screw auger piling techniques are commonly used in Australia and around the world, and sophisticated hydraulic piling rigs as well as a range of screw auger displacement tools to install different pile types can be bought ‘off the shelf’ from various suppliers in Europe, Asia and America (Fleming 1995, Pagliacci et al. 2003).

Figure 7 shows the difference between a piling rig installing CFA piles and a conventional rotary bored piling rig with a Kelly bar.

Figure 7 – Screw piling application using CFA augers (left and centre) and a conventional rotary bored piling application (right)

2.2 Non-displacement screw piling system: CFA

CFA piles are defined as a non-displacement system. This method was used first in the United States (US) in the early 1940s (Gupte 1989). Fleming (1995) reports of the implementation of CFA piles in Europe about 40 years later in the early 1980s, with the development of equipment that allowed the use of concrete rather than sand-cement grouts.

The CFA auger consists of a hollow stem with constant auger flight pitches and flights with a constant outer diameter (Figure 8). The tip of the auger is sealed with a temporary end cap to prevent soil or water ingress into the hollow stem of the auger during installation. Auger diameters reach between 400 mm and 1,500 mm, and drilling depths of up to 40 m can be achieved with modern piling equipment.

The working principles for the drilling process of CFA piles are described by Peiffer et al. (1993) and are displayed in Figure 6 above. The auger (with a sealed auger tip) is rotated through the soil, continuing in the same direction throughout the whole auger penetration. Soil is cut and transported upwards out of the borehole, while the auger (filled with soil) maintains the integrity of the borehole and prevents it from collapsing. The penetration rate must be carefully selected to ensure that the volume of soil being transported by the rotating auger flights corresponds to the volume being cut and loosened by the auger tip. This is important to avoid soil decompression in granular soils, which can occur when penetration is too slow (Thornburn, Greenwood and Fleming 1993, Viggiani 1993).

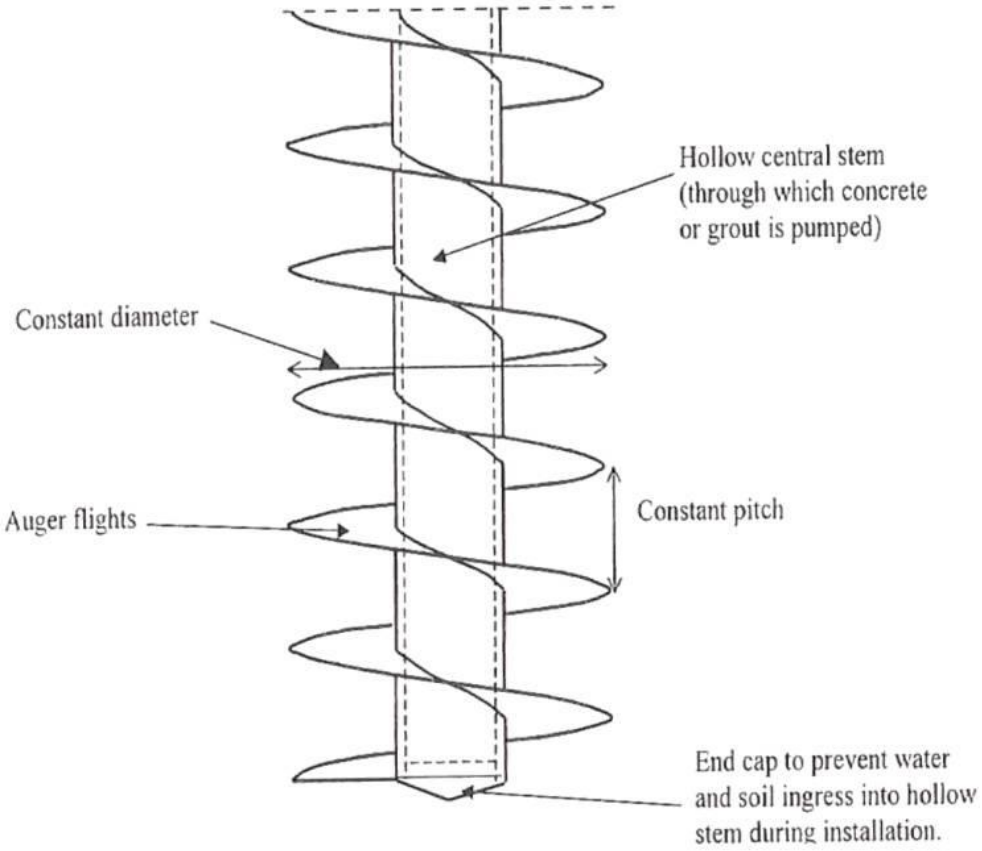

Figure 8 – Schematic of CFA string, after Slatter 2000

When penetration is too slow, more soil is transported inside the auger flights than is supplied by the cutting action at the base of the excavation. This potentially leads the soil at the borehole wall to collapse into the insufficiently filled auger flights. The borehole wall becomes unstable and surface settlements may occur due to lateral auger feeding. Reduced skin friction values of the loosened soil along the pile shaft lower pile capacities. It is important to establish a perfect balance between auger penetration and soil transport.

As a rule of thumb, Van Weele (1988) recommends that during the auger penetration, the downward speed should always be greater than the pitch of the flights multiplied by the number of auger rotations. If this criterion is achieved, no soil decompression should occur, as soil transport and soil cutting actions are similar. The author disagrees with this recommendation, as the volume of the inner stem and the auger flights have to be considered. A more realistic rule of thumb recommendation would be to aim for a penetration rate of about 2/3 of the height of the auger pitch per rotation (author's personal experience). If penetration rates are lower than the recommended values given above, more soil is transported upwards, which causes a decrease in soil pressure at the auger tip, potentially leading to over-excavation and significantly reduced skin friction and pile load capacity.

When the proposed toe level is reached, auger rotation is stopped and the first batch of pumped concrete is discharged through the hollow auger stem into the pile excavation. Lifting the auger prior to discharging the concrete must be avoided to prevent potential cavity collapses of the borehole wall. Due to the concrete pressure being 1–5 bars inside the stem, the end cap at the auger tip is blown off. The auger is lifted slightly, pushed back to toe level and rotated 1–2 turns inside the fresh concrete to fill the auger flights with concrete and eliminate any debris from the pile base.

The auger is then lifted with a constant rate without any rotations. Further spinning of the auger would transport the fresh concrete through the auger flights towards the surface, potentially leading to excessive concrete overconsumption and the risk of not maintaining the required positive concrete pressure, possibly causing borehole wall collapses. Concrete is continuously pumped through the hollow auger stem and a positive concrete pressure has to be maintained at all times. The extraction rate of the auger is dependent on the concrete pressure, and the auger tip must be embedded in the fresh concrete by at least half a metre to ensure shaft integrity. After the concrete reaches the surface of the working platform, a reinforcement cage can be installed in the fresh concrete. The use of cage vibrators should be avoided due to the risk of segregation of the high slump (self-compacting) concrete. The required reinforcement should be installed under gravity or by pushing the cage gently in a controlled manner with the bucket of an excavator (Larisch et al. 2013).

The main advantage of CFA piles is the high production rate that can be achieved with the system. This makes CFA piles very economical. The installation is vibration free and the lateral stress relief associated with bored piles (Viggiani 1993) can be reduced notably if the pile construction is carried out correctly. Provided the installation parameters are maintained and monitored correctly, it is also possible to construct CFA piles in water-saturated or instable soils without using any additional excavation-stabilising measures such as casings or drilling fluids. The drawbacks of this system include that the risk of soil decompression or over-excavation in granular soils when penetration rates are too slow might cause unwanted settlement of adjacent structures. Pile load capacities are also strongly dependent on installation parameters and operator skill (Van Weele 1988, Fleming 1995). Pile capacities can differ significantly due to uncontrolled soil transport or insufficient concrete pressure. Compared with conventional bored piles, verification of the pile excavation is not possible because the concrete is poured while the auger is being extracted. Pile diameters and pile lengths are limited compared with rotary piling applications.

2.3 Partial-displacement screw piling system: VB pile

The VB pile is a partial screw auger displacement pile, developed by Franki International in the late 1980s. This piling system can be carried out with an optional compacted base (Massarsch, Brieke and

Tancre 1988). The VB auger looks similar to a CFA auger, but has a large hollow stem that can be up to 80% of the full pile diameter (Figure 9). Despite its development in Sweden, the system has mainly been used in Germany and the Netherlands to date. However, because highly specialised piling equipment is required for drilling and base compaction, VB piles have been used solely without base compaction during the last decades by several different contractors besides Franki Grundbau, mainly in the German and Dutch market (author's personal experience).

The system combines the advantages of the vibration-free installation of the screw auger piles with increased shaft capacities and the opportunity to install full-length reinforcement cages without the need of plunging them into the fresh concrete and the associated risk of inadequate cage penetration.

Partial-displacement systems were developed to compact and improve the soil surrounding the pile shaft and to increase the pile shaft capacity. However, not all soil surrounding the auger is compacted by the large stem of the auger during penetration. A certain amount of soil is cut and transported to the surface, similar to in CFA applications. Dense soil layers can be penetrated by the auger (cutting and transport of material) and compressible layers can be sufficiently compacted (displacement action of large stem). Pile shaft friction can be increased in those layers. However, the system still relies on soil transportation and, to avoid soil decompression, it is crucial that the volume of the auger introduced in the ground is always greater than the volume of excavated soil. The system is very sensitive to soil decompression if penetration rates are too slow due to hard layers or cobbles in the ground, similar to in the CFA applications introduced earlier.

Figure 9 – VB auger with large hollow stem (left) and VB piling rig (right)

Soil decompression (Massarsch, Brieke and Tancre 1988) and over-excavation (Bustamante 2003) can be avoided by using a large hollow stem auger correctly. It has been demonstrated by Viggiani (1993) that augers with a large hollow stem are particular effective in soil displacement action during

auger installation. On the one hand, the large stem maximises the volume of the auger during penetration by acting like a displacement body; on the other, the soil volume transported to the surface contained in the auger flights is minimised.

Another advantage of the VB system is that the installation of the reinforcement cage inside the hollow stem can be carried out before the concrete placement process. The cage installation after casting a screw auger pile can be difficult because the cage has to be plunged into the fresh concrete, which might cause issues if concrete workability or stability is insufficient.

The installation process, illustrated in Figure 10, is similar to that for a standard CFA pile. The hollow stem auger is plugged with an end cap at the auger tip before it is screwed down to design level with a penetration rate at which the volume of cut material is equal to the volume of transported soil, to avoid soil decompression.

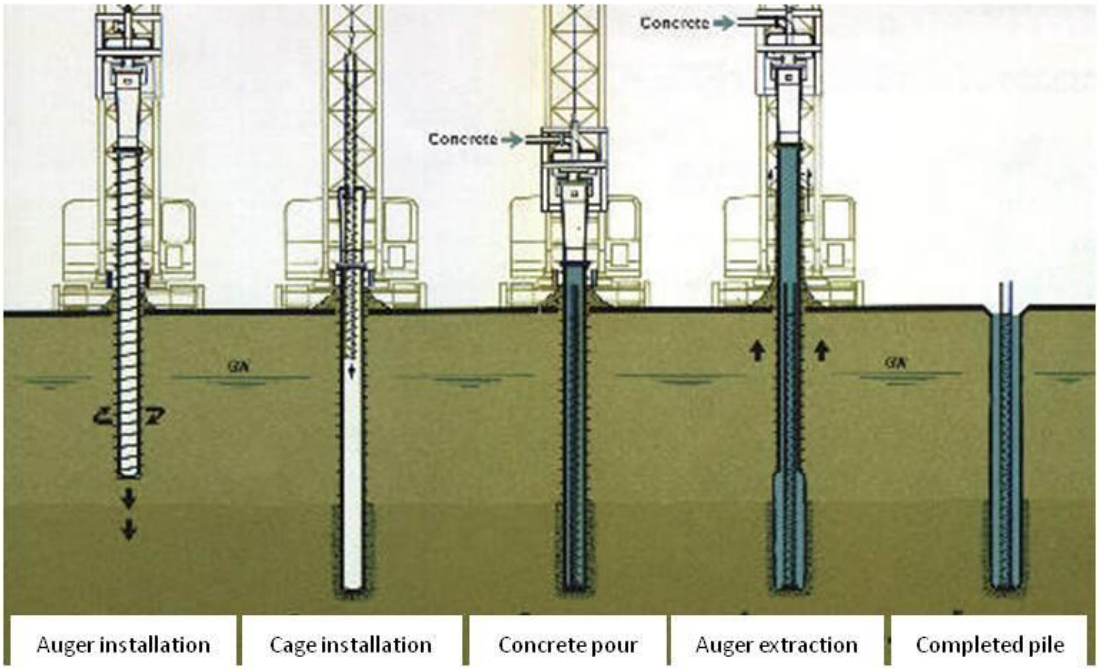

Figure 10 – Construction procedure of a VB pile, after Massarsch, Brieke and Tancre 1988

Unfortunately, no detailed information was given by Massarsch, Brieke and Tancre (1988) about the influence of soil conditions (e.g. water-saturated sand, stiff or soft clays) on the cutting and transport process of the VB auger. After reaching the designed pile toe level, the reinforcement cage is installed inside the hollow auger stem. A drop hammer can be lowered down the hollow auger stem and the compacted pile base can be formed. The use of the hammer is optional; however, this will increase pile capacities, as the loosened base caused by the auger cutting action will be improved and compacted.

The hollow stem is filled with concrete before the auger is extracted without rotating (similar to in CFA operations). It is important to note that during the extraction of the auger, the level of concrete inside the hollow stem must be at least a meter above the auger tip to maintain positive concrete pressure in the pile excavation.

While the VB system has not been implemented in Australia, this research will include the auger behaviour of VB piles in fine-grained soil because this system is a combination between a classic non-displacement CFA system and a full-displacement system. Small diameter CFA augers of 500 mm (the size used for this research project) have the same dimensions as 500 mm VB piling augers. As standard tool couplings need to be used, and the volume of concrete pumped through the stem should be minimised, the outer diameter of the inner (hollow) stem has similar dimensions to the CFA pile. The typical dimensions and ratios for CFA and VB piles are displayed in Table 1.

Table 1 – Comparison between auger cutting diameters, outer stem diameters and volumes for typical VB and CFA piles

VB Pile					
A	B	C	D	E	
Auger cutting diameter [mm]	Outer diameter inner stem [mm]	Ratio (A/B)	Auger cutting volume [mm^3]	Volume inner stem [mm^3]	Ratio (D/E)
420	267	0.63	82,587	56,012	1.47
500	318	0.63	116,974	79,454	1.47
560	406	0.73	116,886	129,514	0.90
640	508	0.79	116,064	202,765	0.59
CFA Pile					
Auger cutting diameter [mm]	Outer diameter inner stem [mm]	Ratio (A/B)	Auger cutting volume [mm^3]	Volume inner stem [mm^3]	Ratio (D/E)
420	267	0.63	82,587	56,012	1.47
500	318	0.63	116,974	79,454	1.47
600	318	0.53	203,402	79,454	3.56
750	406	0.54	312,450	129,514	3.41
900	406	0.54	506,914	129,514	4.90

Based on the data displayed in Table 1, all l 420 mm and 500 mm CFA piles can also be classified as VB piles, as the ratios between the outer cutting and inner stem diameters are the same. In current design applications, the potential of partial soil displacement by small CFA augers has not been considered. If installation parameters can be defined to suit ground conditions, soil improvement can be taken into account, resulting in improved pile capacities for small diameter CFA piles.

With increasing pile diameter, these systems' volume ratios between the outer cutting and inner stem diameters divert in opposite directions such that a 600 mm CFA pile has about five times the transport volume of a VB pile with a comparable diameter.

2.4 Full-displacement screw Auger piling systems

Full-displacement screw augers are designed to displace the soil completely during auger penetration and the auger configuration generates a specific influence radius in the soil (creating stresses and displacements around the auger) during installation and extraction. The aim of all screw auger full-displacement piles is to increase the shaft capacity of piles by lateral and vertical soil displacement. That these systems are noise- and vibration-free and avoid spoil, which is especially important in contaminated areas, is another significant advantage of these systems.

Screw auger displacement piles were developed in the 1980s in Europe (Bustamante and Gianeselli 1998). The Atlas pile was a pioneer bored, full-displacement pile, introduced in the 1980s by Franki International in Belgium. About a decade later, the Omega pile was developed as the flagship of the next generation of screw auger displacement piles (Figure 11 and Figure 12). With the development of standardised hydraulic piling rigs and the increasing rotational torque and vertical pull-down force capacities of these machines, screw auger displacement piles became more economical. Over the past few decades, several different auger shapes and geometries have been developed by different manufacturers. Prezzi and Basu (2005) collated a summary of the most popular full-displacement piling systems and this is displayed in Figure 11.

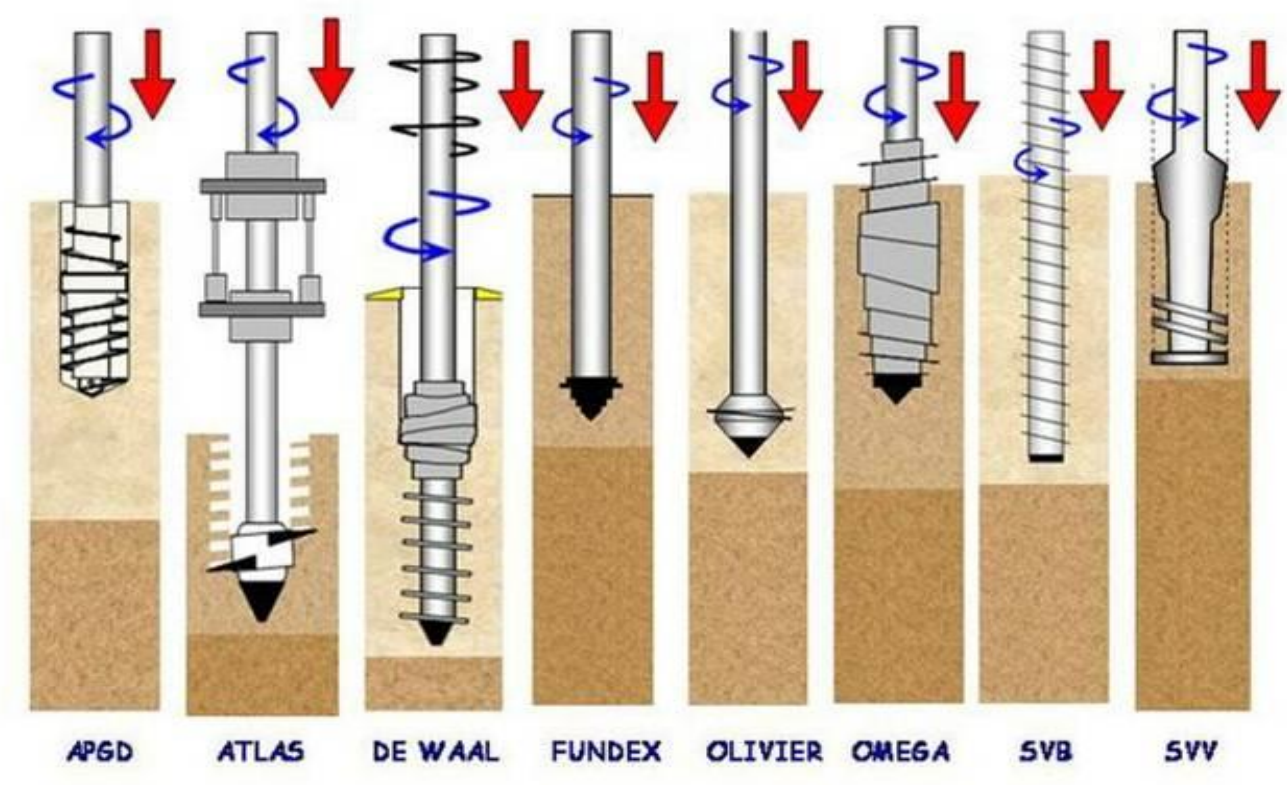

Figure 11 – Summary of the most popular screw auger full-displacement piling systems, after Prezzi and Basu 2005

The augers shown in Figure 11 and Figure 12 are all full-displacement pile augers, but can be distinguishes as either:

(i) Short displacement auger systems (Atlas, Fundex, Olivier); or

(ii) Long displacement auger systems (Omega, de Waal, APGD, SVV and others).

As shown in Figure 12, the Atlas and Fundex systems rely on a short, single, full-helical flange to cut the soil and act as a displacement body, with little or no soil transport.

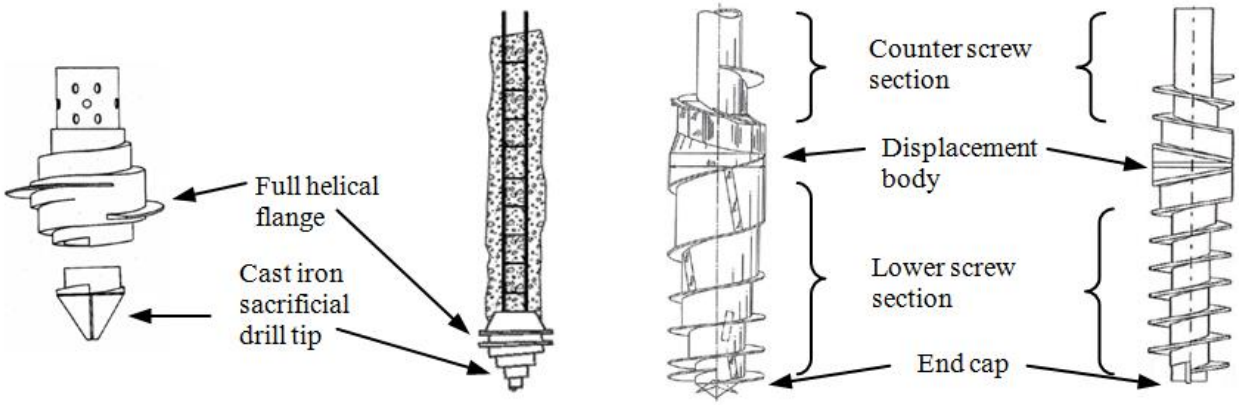

Figure 12 – Different full-displacement piling augers: Atlas and Fundex (left), representing short displacement auger systems; and Omega and de Waal (right), representing long displacement auger systems

Usually, high torque capacities are required for these pile types, as a large amount of soil displacement. In the Fundex system, the iron-cast, auger-shaped drill head is sacrificial. In contrast, when the Atlas drill head (see Figure 14 in Section 2.4.1) is extracted, only the drill tip is left in the ground. In this system, the helical-shaped single-screw auger head is used to give the pile shaft its unique appearance (see Figure 16 in Section 2.4.1). For both systems, reinforcement is installed prior to concrete placement via the hollow casing or auger stem, dissimilar to in the methodology described in Figure 6 for typical screw auger piling applications using long displacement augers like CFA and VB systems.

Short full-displacement tools are usually not as sensitive to over-excavation and soil decompression as CFA or VB piles because virtually no soil transport takes place, only soil displacement. Improved load-settlement curves are typically expected for short full-displacement piles. Soil is displaced and compacted by the auger head or displacement body when the installation force is greater than the soil resistance.

In general, long full-displacement augers are designed with longer flighted sections, and the lower auger sections are used for cutting and transporting the soil to the displacement body of the auger (Figure 12). The counter-screw sections, located above the displacement body, re-displace any soil that has collapsed into the cavity behind the auger during the extraction process. Omega and de Waal displacement augers are introduced here as typical examples of two types of long full-displacement augers: the progressive displacement auger and the rapid displacement auger. The auger geometry of Omega and de Waal augers seems similar, and visually the augers are comparable. However, the Omega auger is a typical progressive displacement auger, with the stem diameter of the lower auger section progressively increasing towards the displacement body. During penetration, soil is displaced progressively along the lower auger section, finding its peak at the location of the displacement body. Omega augers require high installation torque. The de Waal auger can be defined as a typical rapid displacement auger, since the displacement body has a larger diameter than the auger stem. Soil displacement occurs rapidly at the displacement body and no displacement is expected below and above this zone (Figure 13).

Installation torque and pile capacities in sand should be lower for rapid displacement augers compared to progressive displacement augers (Slatter 2000). For cohesive soil, no reliable research data were available at the time of the literature review. Therefore, one aim of this research is to investigate the behaviour and load capacity of rapid and progressive displacement augers in fine-grained soil conditions.

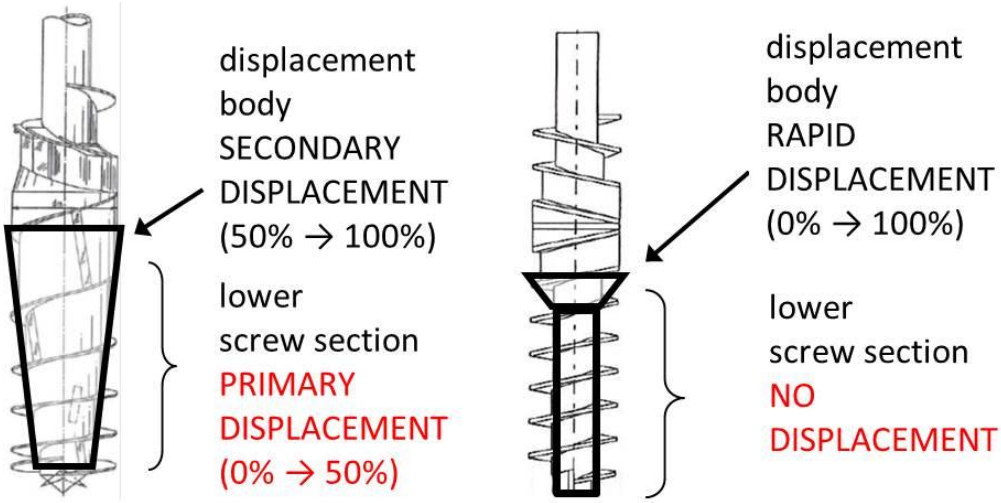

Figure 13 – The de Waal rapid displacement auger (right) and the Omega progressive displacement auger (left)

Several different long full-displacement auger shapes have been developed over the last decade (see Figure 11 above), with some augers introducing cutting and transport actions to different degrees in the soil. It has not been investigated in detail how the cutting action influences the pile capacities of

different pile types, and currently, similar auger shapes are used for piling in granular and cohesive soils. Full-displacement screw auger piling applications are limited to soil conditions that allow soil compaction or displacement. For that reason, these piling techniques are not particularly suitable for dense granular material and rock formations.

Slatter (2000) developed a theoretical auger model for screw auger full-displacement augers installed in granular soil formations. In his opinion, further research is required to correlate installation parameters to pile capacity, and further studies are necessary in relation to secondary soil displacement during the auger extraction and placement of concrete under pressure. However, he highlights the fact that his model has not been extended to cohesive soil conditions.

In addition to Slatter's suggestions regarding further research activities in the field of full-displacement screw piling applications, it is fundamental to understand the effects of different auger shapes in different soil conditions. Besides the Atlas pile as the pioneer screw auger full-displacement piling system, two other full-displacement screw auger systems are relevant to this research project and are introduced in the following sections of this chapter; namely, the Omega pile (progressive displacement) and Piling Contractor's in-house rapid displacement auger system. The latter system was developed with a long lower auger section to cut and transport soil to enable penetration of hard layers or obstructions. It is debatable whether this system is a real full-displacement technique or whether it belongs to the group of partial-displacement piles. While the shaft capacity might be increased by the displacement body, the area of the pile toe can be disturbed by CFA-like auger action (cut and transport of material) if the penetration rate is insufficient, as the displacement body creates additional penetration resistance during the installation process. This topic will be discussed in more detail in the following sections and will be thoroughly investigated throughout the thesis.

2.4.1 Atlas pile

The Atlas pile was one of the first full-displacement screw piling systems introduced to the market in the early 1980s (Bustamante and Gianeselli 1998). The system combines pile installation by jacking and screwing of a purpose-built screw auger. Atlas piles require purpose-built piling rigs, and current equipment can mobilise 450 kNm drilling torque used to rotate the casing at 8 rpm. The maximum thrust or pull-down capacity is 250 kN.

Atlas piles are usually installed to maximum depths of up to 21 m with standard equipment; however, piles up to 36 m have been installed successfully (Bustamante and Gianeselli 1998). Pile rakes of 1:3 can be constructed (author's personal experience).

The typical Atlas full-displacement screw auger piling rig and the typical auger are displayed in detail in Figure 14. Atlas piles are installed vibration free. The pile capacity of Atlas piles is high compared to CFA piles in similar soils, as the Atlas system has excellent soil compaction characteristics.

The system is very sensitive towards obstructions in the ground and hard layers, as the auger provides only minimum cutting action. The small diameter of reinforcement cages (usually 180–240 mm) does not allow the transfer of high bending moments.

Atlas piles are usually installed with diameters of 410/510 mm, 460/560 mm or 510/610 mm, where the first number describes the diameter of the inner core of the pile and the second describes the diameter of the outer flanges (Figure 14).

$Ø_c$ = diameter inside the helical flights

$Ø_b$ = diameter outside the helical flights

$Ø_f$ = diameter of the auger flight

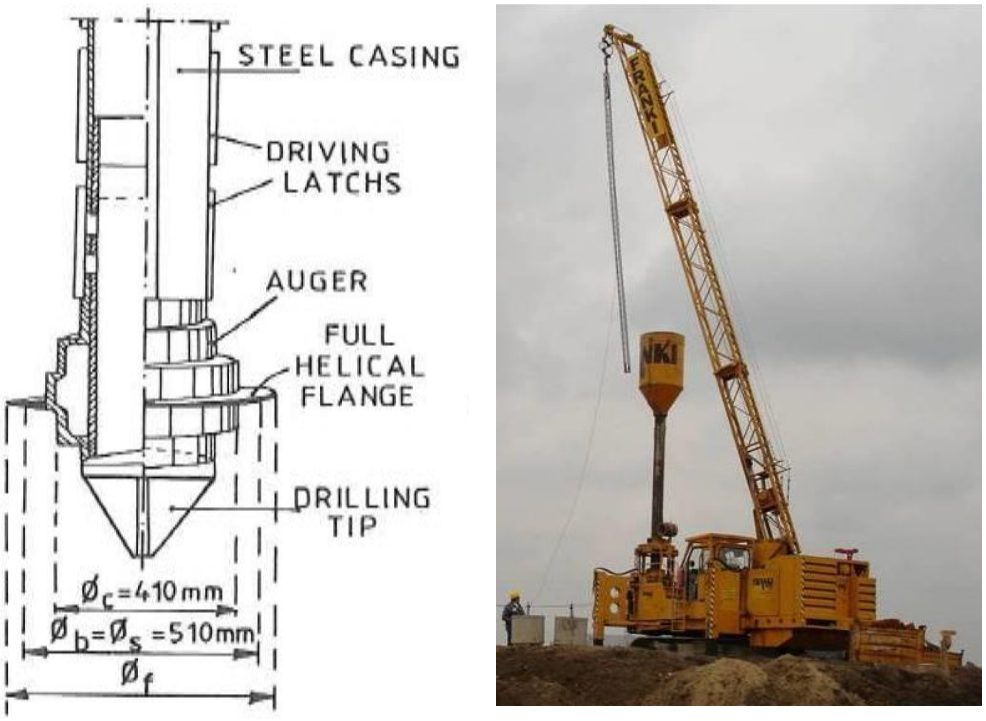

Figure 14 – Atlas screw piling auger, after Van Impe 1988 (left) and a typical Atlas piling rig (right)

The installation process of Atlas piles is described and illustrated in Figure 15. The auger is plugged with a sacrificial drilling tip before being rotated down to the required depths. Due to the high pull-down forces and torque capacity of purpose-built Atlas piling rigs, the auger is pushed in the ground under clockwise rotation with an almost constant penetration rate.

There are several penetration rates from which to choose. When the penetration rate is close to the pitch of the auger, the outer helical flight forms a constant ridge along the outer surface of the pile. When the penetration depth is reached, rotation stops, and a reinforcement cage is installed inside the hollow auger casing.

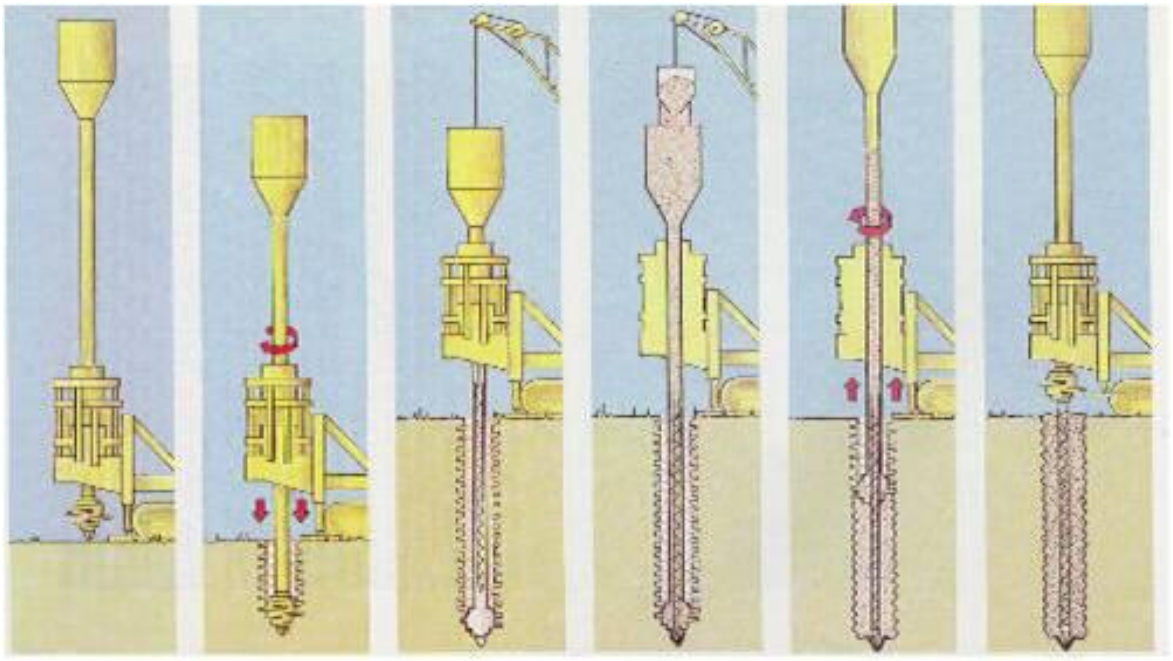

Figure 15 – Typical installation process of an Atlas pile, after Franki SA nd

The Atlas auger consists of a short and thick displacement body located immediately above the sacrificial auger tip that plugs the hollow stem (Figure 16), similar to in the screw piling auger system described earlier. A single helical flight is attached to the displacement body. The auger is connected to a hollow steel casing that is fitted with driving latches along its surface.

Figure 16 – Typical single helical flight of an Altas pile (left) and a characteristically screw-shaped Atlas pile shaft, resulting in increased skin friction (right)

A series of four driving latches, orientated at an angle of 90° to each other from a plane view, is used as key sections for the hydraulic rams of the drill head of the Atlas piling rig. Then, concrete is placed in the hopper installed on top of the auger casing. The sacrificial drilling tip is displaced by the concrete pressure that builds up inside the auger stem under the self-weight of the concrete.

It is important that the auger stem remain filled with concrete to maintain a positive pressure while extracting the auger. Auger extraction is carried out by counter-clockwise rotation (n_u) and a constant penetration rate (v_u). Extraction forces (N_t) are significant as the crowd of the drill head is applied directly to the auger stem via the driving latches (Figure 17).

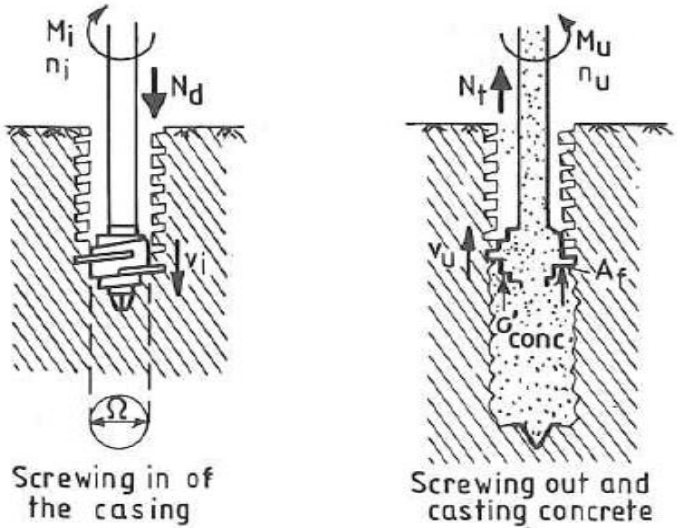

Figure 17 – Installation and extraction forces for Atlas piles, after Van Impe 1988

A constant extraction rate with a similar magnitude as the penetration rate is important to create the typical screw shape of the Atlas pile (Figure 18). The thickness of the flanges, created by the passage of the helical single auger flight, can be varied depending on penetration and extraction rates. Figure 18 shows that higher extraction rates (N_t) create bigger concrete flanges d_f and pitches R.

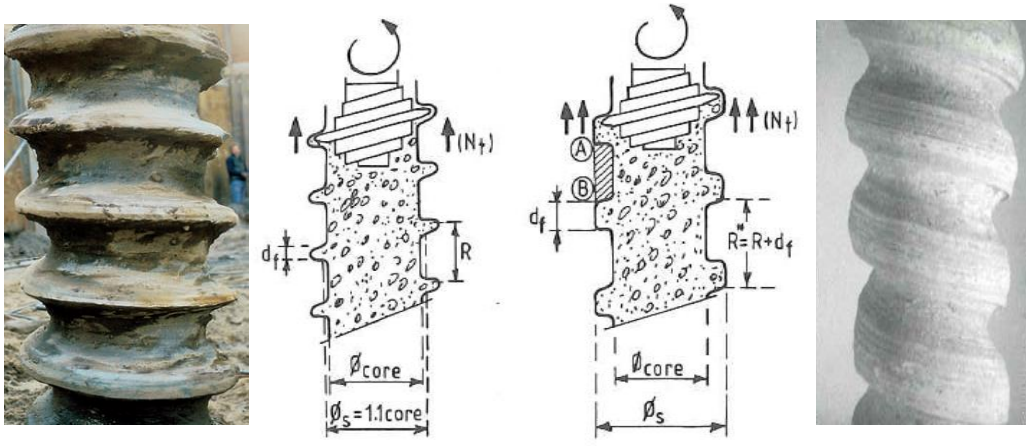

Figure 18 – Difference in flange thickness Atlas Piles after Van Impe 1988

Van Impe (1988) points out that in fine-grained ground conditions, the cohesive soil plugged between the flanges (in the zone AB of Figure 18) indicated an important re-moulding and compaction effect of the soil in the direct vicinity of the flanges and section AB between the flanges due to the displacement work of the auger. He conducted soil tests on samples plugged between the flanges in section AB and found that the soil consisted of successive very thin lenses of soil squeezed together. The shear strength of these cohesive soil samples indicated significantly higher values than the surrounding natural soil (unfortunately, no further details and data were provided in the paper). Van Impe concluded that, in this case, the outer diameter of the Atlas pile (diameter of the flanges) could be taken into account for the calculation of shaft capacity. The soil re-moulding and compaction phenomenon was not observed at low extraction speed with thin flanges (Figure 18). In this case, the diameter of the core section of the Atlas pile needs to be taken into account for pile shaft design.

Van Impe's research leads to the conclusion that higher (but constant) pile installation rates cause soil compaction along the shaft between the flanges, achieving better shaft friction results. As the Atlas auger is a pure displacement auger with no soil transport (there is almost no transport action due to the single helical flight), penetration rates remain constant but are higher in soft or loose soils and slower in dense or stiff formations.

Anderson (1988) shows through instrumented laboratory-scale pile element tests that different pile construction methods are likely to cause slightly different orientations of clay plates within the disturbed zone surrounding the pile which could influence pile load capacities.

2.4.2 Omega pile

The Omega pile is a cast-in-place long screw auger full-displacement piling system developed by Van Impe in 1994 (Slatter 2000) and introduced to the market in 1995 (Bustamante and Gianeselli 1998). The system was developed as a result of research carried out on Atlas piles by Van Impe at the University of Ghent in Belgium.

The Omega pile system aims to improve the soil based on the Atlas piling system by optimising energy input, control of soil displacement and penetration rate. The auger shape is shown in Figure 19 and can be divided into three different sections: the lower screw section, the displacement body and the upper screw section. The lower screw section has a conical shape, with variable auger flight pitches and flights with a constant outer diameter. This section loosens the soil during penetration, displaces some soil laterally and transports the loosened soil towards the displacement body. The displacement body is a cylindrical sector with the same outer diameter as the outer auger flights of the lower section.

Transported soil from the lower auger section cannot pass the displacement body and it is pushed into the surrounding borehole wall by the displacement body. The upper auger section is also called the counter screw section. This section is conical and consists of four overlapping flights. The flights are positioned in the opposite direction to the flights of the lower auger section. Soil that falls into the cavity created by the Omega auger is transported towards the displacement body by the counteraction of these flights during normal drilling operations. During auger extraction, the upper auger section ensures that no soil is transported to the surface.

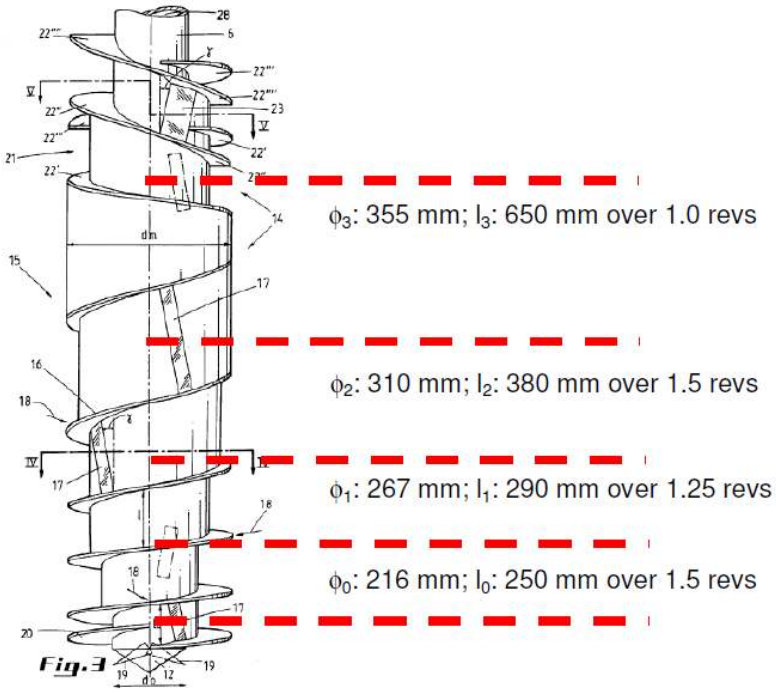

Figure 19 – Omega pile screw head, indicating the different stem diameters and section lengths, after Bustamante and Gianeselli 1998

Van Impe at al. (1998) point out that the auger was designed and developed in such a way that the increasing volume of the transported soil between the auger flights of the screw can be stored at each level at a given rotational speed and vertical penetration speed (which were not specified in the research paper). This results in an efficient screwing process of the auger head, with low energy consumption, higher penetration rates and improved soil displacement.

The ratio between the discontinuously increasing diameter of the lower auger stem and the continuous screw flights with a variable height of pitches has been geometrically optimised to ensure an effective transport and displacement action during pile penetration. This is the reason that the Omega auger is categorised as a progressive displacement auger; that is, the soil is transported and displaced progressively. The auger can be screwed in with lateral soil displacement, and additional pull-down forces can be activated if required. Figure 19 above shows the different stem diameters and influence lengths for the Omega auger.

In comparison to the Atlas pile, Omega displacement augers can be fitted on standard CFA piling rigs. Over the past decades, several manufacturers and contractors have tried to modify the Omega auger, sometimes without understanding the initial sophisticated auger design and the progressive soil transport and compaction mechanism (in Figure 11, a few of these systems are introduced). The introduction of rapid displacement screw auger tools has been mainly owing to a lack of understanding of the progressive auger work. These tools consist of a CFA-like lower screw section and a displacement body that causes a rapid increase of the diameter of the inner auger stem. The mechanics of this type of tool are described earlier in this chapter and the influence on stresses during installation and load capacity in cohesive soil will be investigated in this research work.

The installation process for the Omega pile (Figure 20) is similar to the installation process for CFA piles described earlier (Figure 6 in Section2.1).

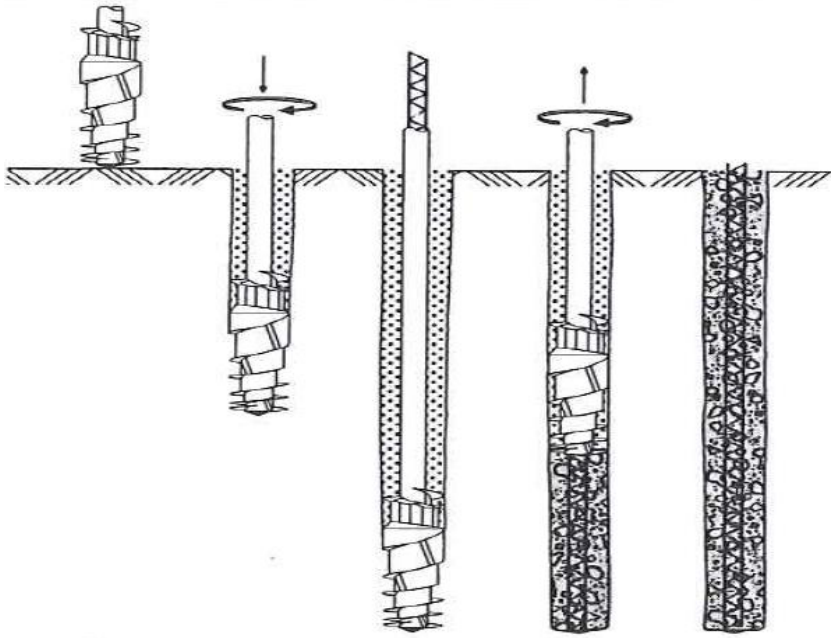

Figure 20 – Installation procedure for Omega piles, after Bottiau et al. 1998

The biggest advantage of Omega piles is the high production rate of 200–600 lm per day (average pile production) compared with CFA, VB or Atlas piles. The system causes no vibrations during the piling process and no spoil is generated during pile installation.

Soil that falls into the cavity above the displacement body created by the stem is transported towards the displacement body by the counter screw section and pushed into the borehole wall. However, because the lower section of the Omega auger is also designed for the cutting and transport of soil and not solely for the displacement of soil, the risk of soil decompression at the pile base and of a ‘soft toe’ must be taken into consideration when using Omega screw auger displacement piles with insufficiently low tool penetration rates.

2.4.3 Omega B* pile

The Omega B* pile is an Omega pile with an enlarged pile base made of dry concrete, which enables high base capacities if ground conditions are suitable.

Soil profiles without distinctive bearing strata (‘floating foundation’) or with intermediate soft layers are particular suitable for this piling technique. Depending on the geotechnical conditions, the Omega B* pile offers the opportunity to install Omega piles of different design loads with a similar auger of the same diameter, which makes the system economically attractive.

Similar piling equipment and tools as for the installation of the standard Omega pile can be utilised; however, the installation sequence of Omega B* is different from the standard Omega application, as described in Figure 21 (Bottiau et al. 1998).

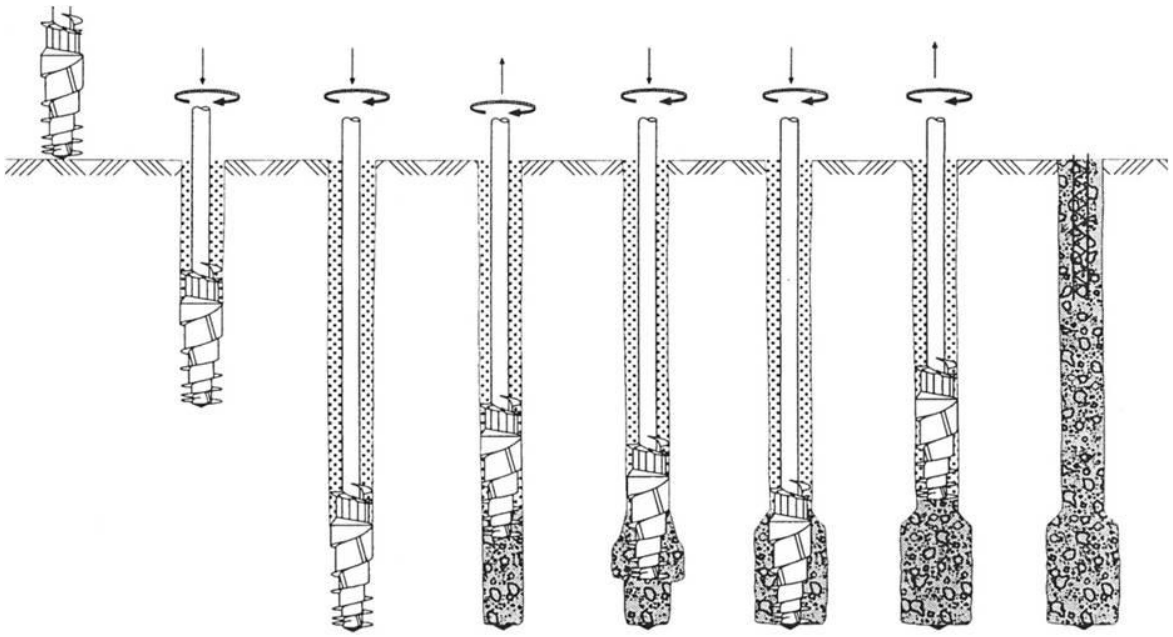

Figure 21 – Installation procedure for Omega B* piles, after Bottiau et al. 1998

The target design depth of the pile toe is determined by geotechnical investigation before drilling on site. The auger is drilled down clockwise with a constant penetration rate to allow balanced soil cutting, transport and displacement action.

Once the design depth is reached, dry concrete is pumped from the concrete pump to the top of the auger stem at the masthead. The auger rotates constantly (clockwise) and is withdrawn slowly over a distance of about a meter above the target toe level. The concrete pressure inside the hollow auger stem, measured at the swan neck close to the drill head, should be in the range of 5–10 bars. The formation of the enlarged base starts by re-inserting the Omega auger a number of times into the freshly cast dry concrete.

On the way down, constant auger rotation, the high penetration rate and the distinctive displacement shape of the Omega auger forces the concrete to be pushed aside, enlarging the diameter of the pile section over a pre-defined height. The lower auger section is not able to transport the entire volume of concrete towards the displacement body and a certain amount of concrete is displaced laterally in the soft ground. Throughout the pile base construction process, the stem rotates continuously and concrete is pumped through the hollow stem.

A concrete pressure of about 10 bars, measured at the top of the hollow stem, indicates that the lateral resistance of the soil will not allow any further lateral soil displacement and that the auger must be extracted immediately using a constant extraction rate. The concrete pressure while forming the pile shaft should be in the range of 6–8 bars as suggested by Bottiau et. al (1998).

The theoretical volume of concrete required for the installation of the pile base should be determined before construction by the number of times and the distance the auger needs to be pushed into the fresh concrete. During pile execution, concrete consumption should be monitored carefully to compare design volumes with as-built volumes.

Attempts to form an enlarged pile base in dense or stiff ground conditions might lead to problems, as lateral soil displacement might be difficult and efforts to reinsert the auger into the freshly poured concrete might fail, resulting in potential auger blockages.

Despite the numerous advantages of the Omega B* pile, a major concern is the capability to pump dry concrete through the system. Usually, concrete needs high slump criteria to be suitable for concrete pumping. The use of dry concrete might block concrete supply lines.

2.4.4 Bauer Full-displacement Pile

The Bauer Full-displacement Pile (FDP), which looks very similar to the de Waal piling auger (Figure 11 and Figure 12), is manufactured by the German piling equipment manufacturer Bauer Maschinen AG. Piling Contractors Pty Ltd, one of the industrial partners of this research project, introduced the system in 2005 in Australia.

The FDP system has been used for several displacement piling projects in Australia and it is introduced here to represent rapid screw auger full-displacement tools in general. For rapid displacement augers, the displacement body has a larger diameter than most sections of the inner auger stem and the flights have approximately the same diameter as the outside of the displacement body. The auger pitch at the lower auger section is constant and is not reduced towards the displacement body as for Omega piles. This indicates that no constant soil volume is transported

towards the displacement body and that soil displacement occurs rapidly at the displacement body, below which no or potentially only minor displacements are expected.

Soil decompression might occur along the lower section of the auger if penetration rates are too slow or are not optimised for the ground conditions encountered. In Figure 22, a typical FDP auger head is illustrated. The auger sections are similar to the sections defined in Figure 12 and Figure 13; the installation process for the system is identical to that for Omega piles.

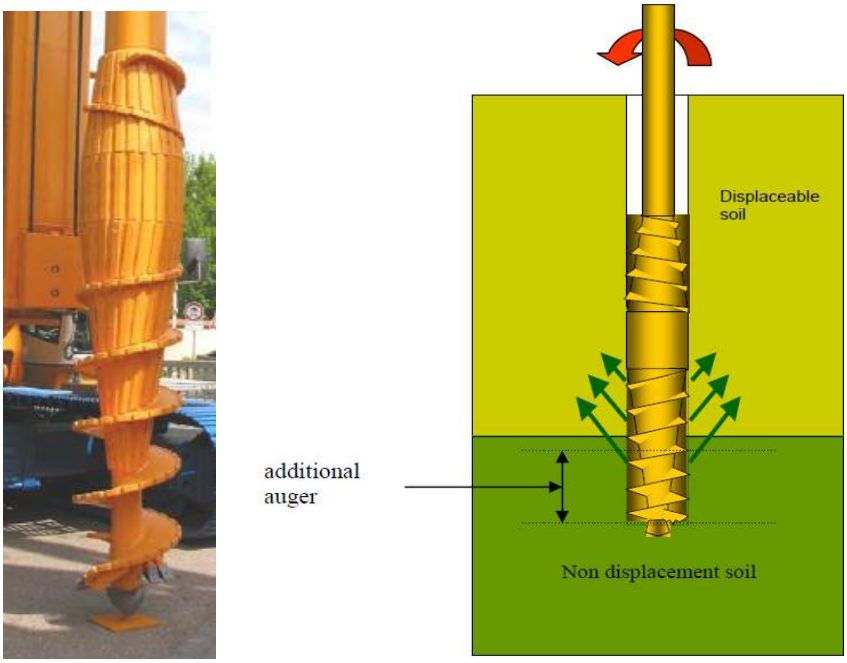

Figure 22 – The Bauer FDP auger

Figure 22 shows that an additional auger can be attached to the lower section of the FDP auger. This indicates that, in comparison to the progressively shaped Omega auger, the FDP system relies more on cutting and transport below the displacement body and on rapid soil compaction at and above the displacement body. The bottom part of the FDP auger looks very similar to a CFA auger and it will be investigated whether soil compaction occurs along the lower auger section. The auger design allows for the penetration of hard layers and the removal of small obstructions. It is able to break up or loosen cemented soils or granular soils containing cobbles or gravel, with the loosened particles then transported towards the displacement body. The shaft friction capacity at and above the displacement body may be improved by displacement action.

No research work could be found by the author on the behaviour of this particular auger type in cohesive soil conditions. The author assumes that the lower auger section of the FDP auger behaves more like a non- or partial-displacement system than a full-displacement system. This hypothesis will be further investigated during the course of the research. The observation and analysis of pile

installation parameters is of great importance for this system, to avoid soil decompression along the lower auger section, which results in lower shaft friction and potentially causes reductions in pile capacities.

2.5 Summary of screw auger technologies

Screw piling augers can be separated into non-displacement, partial-displacement and full-displacement types. Screw auger action is described by several authors in detail and auger action in the ground can be divided into three different processes:

(i) Cutting of soil;
(ii) Transporting of soil; and
(iii) Displacement of soil.

During the installation of screw piling augers, regardless of their shape or function, all three distinct actions described above are taking place to a different extent. The literature explains that CFA augers are mainly designed to cut and transport soil; soil displacement during CFA drilling is minimal. By contrast, the large stem of partial-displacement auger systems (VB pile) allows for some displacement. However, considering that the auger shape and geometry for typical 420 mm and 500 mm CFA and VB (partial-displacement) augers are similar, small diameter CFA augers should be able to displace some soil during the installation process, thereby enhancing the load capacity of the piles in suitable ground conditions.

Soil displacement is the main action of an Atlas auger, which is classified as a short full-displacement auger. For this system, cutting and transporting are not desired, and their influence during the pile execution is minimal.

Long displacement augers like the Omega auger are carefully designed to ensure a very effective transport and displacement action during pile penetration. This is shown by the conical shape of the lower auger section, the discontinuously increasing diameter of the lower auger stem and the continuous screw flights with variable height of pitch. The Omega system is defined as a progressive displacement auger due to the constant and progressive soil displacement effort.

The FDP system, and other systems that were not introduced in this work, are mainly based on rapid displacement action. Despite these augers seeming near identical to progressive displacement augers, the lower stem section of the FDP auger has a CFA-like design. Hard layers and obstructions can be penetrated, but no or only marginal soil displacement is expected to occur in this zone. As for CFA, soil decompression is a risk that can occur with this system.

Installation parameters for all auger types must also be considered, as different penetration rates can cause significant changes in cutting, transport and displacement actions for similar screw augers. Screw auger piling in general is a 'blind process' that strongly relies on monitoring during construction and the analysis of installation data after the piling process to produce accurate piles on site (Larisch et al. 2013).

The control of conventional bored piles is much easier, as dry holes can be inspected visually after pile excavation. Before the installation of reinforcement cages and concrete, the pile socket and shaft can be inspected and assessed in detail. Even if the pile is installed under a supporting drilling fluid, the excavation can be inspected using Socket Inspection Devices (SID), as described by Holden (1988). However, screw auger pile sockets and shafts cannot be inspected visually or by SIDs, as the auger is located inside the pile excavation when the toe is reached and it keeps the bore wall stable. Concrete is poured while the auger is extracted and visual inspections of the pile excavations are impossible. Construction monitoring of screw auger piles is very important to manage and control the quality of the executed piles (England and Harding 1993, Larisch et al. 2013).

Scott et al. (2006) describe state-of-the-art rig monitoring for screw auger piling applications, and several authors have highlighted the importance and urgent need of sound construction monitoring as a quality control tool during the execution process of screw auger piles (Van Impe 1988, Van Weele 1988, England and Harding 1993). Some of these recommendations have been successfully implemented. The rapid development of computer technology could not have been predicted in the early days of screw piling. The state-of-the art in pile monitoring techniques, as described in the literature, is now presented.

2.5.1 Construction monitoring

During the early days of screw piling installation in the 1960s and 1970s, construction monitoring and analysis was very poor and it was almost impossible for site crews and rig operators to monitor penetration rates, torque, extraction rates and concrete pressure reliably during pile execution. The lack of understanding, especially of non-displacement screw piling techniques, caused numerous failures and led to a negative perception of these techniques by many major clients (Fleming 1995).

Besides construction monitoring of screw piles, instrumentation of pile installation is an important management tool for the quality control of piling works (England and Harding 1993). With all types of screw auger piles, construction problems must be identified as soon as possible to allow for immediate rectification. Scott et al. (2006) point out that rig instrumentation assists the rig operator to construct an appropriate pile on site. However, the installation parameters must be defined prior to pile installation and construction records must be checked as soon as possible after the execution of

the pile. Both tasks should be conducted by an experienced engineer, as in-depth knowledge of pile design, pile loads and ground conditions are required to analyse and interpret the installation parameters correctly. Rig operators or site crews are generally not able to carry out these tasks without assistance from engineers.

Potential problems with respect to the pile construction have to be identified quickly to avoid identical issues for the remaining piles to be constructed on site. Provided the piling rig is still on site, defective piles can be replaced relatively easily.

Typically, the following parameters are monitored during operations as shown in Figure 23 as used by Scott et al. (2006):

- Date, pile number, rig specification, etc.;
- Installation depth;
- Penetration rate and time;
- Rotational torque;
- Pull-down force;
- Rotations of the auger stem;
- Concrete pressure;
- Concrete volume; and
- Extraction rate and time.

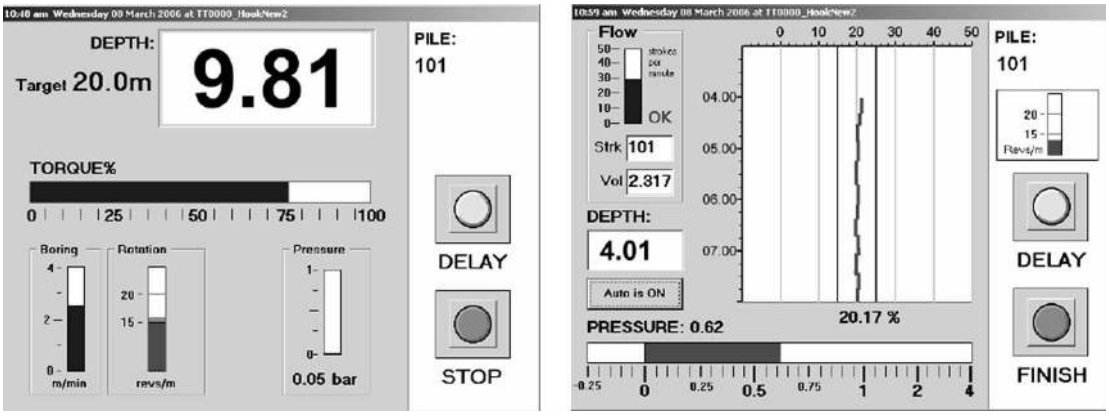

Figure 23 – Display during penetration (left) and concreting process (right), after Scott et al. 2006

However, engineers should not rely solely on the construction monitoring data; they should also control and challenge those data to detect errors. Slatter (2000) summarised the typical errors in rig monitoring systems as:

(i) Under high pressure and in soft ground conditions, concrete can be forced past short augers (full-displacement augers), leading to an apparently oversized pile shape.

(ii) If the auger flights are not completely filled with soil (i.e. if the transport volume is less than the cutting volume, which also indicates potential soil decompression), concrete might be forced up the auger flights. Some monitoring programs will indicate bulging of the pile in this section

(iii) The printout of the pile shape on the construction record sometimes shows necking or bulging of a particular pile section. This plot is based on concrete delivery related to auger extraction rate. However, the concrete delivery rate is not measured at the auger tip but rather at the top of the mast; therefore, these plots can provide misleading information.

(iv) Concrete pumps do not always deliver full strokes of concrete in the supply line. Since the computer system counts each stroke as a full stroke, the concrete supply will be overestimated. The use of electromagnetic flow meters can avoid this source of error.

It can be summarised from the literature review that construction instrumentation should be used as a quality control and management tool for the installation of screw auger piles. It can also be used for design verification. Rig operators are able to monitor real-time drilling and concreting parameters during the pile execution while also controlling the installation parameters.

Today, highly developed computer monitoring systems are readily available, and pile installation should not be carried out without a pile installation monitoring system. The records produced by rig computers are valuable quality assurance and management tools, and much information is provided to engineers to assess and analyse these records. However, it is important to understand how the monitoring system works, how the data relate to each other, which data are important for the pile installation and the common errors that may arise during the recording of construction data. Engineering judgment is still required to assess whether piles are of good or poor quality, and it should be considered that errors could be included in the printouts.

Van Weele (1988) states that the influence of the installation parameters on the finished piles introduced by the piling rig operator are more important than the actual soil parameters for CFA piles in granular, saturated soils. However, Bustamante (2003) points out that, despite the development of sophisticated installation monitoring computer software and hardware in recent years, it remains difficult to establish any unquestionable and quantitative relationship between drilling parameters, soil characteristics and completed pile capacity for all types of screw auger piles.

Further details of the rig monitoring system that was used for this research project are discussed in Section 7.3.1. The next chapter continues the literature review, turning to a discussion of auger mechanics.

CHAPTER 3: AUGER MECHANICS

3.1 General

It is important to understand the principle behaviour of screw piling augers working in soil formations to be able to verify and optimise installation parameters. Existing auger models and the most accepted theories about them are briefly presented in this chapter to provide a general overview of the topic. These models are used to analyse the behaviour of helical screws to predict and model the behaviour of screw augers in granular material, as no models for cohesive material exist to date.

In soft cohesive ground conditions, soil tends to behave more like a fluid than a granular material, and theories valid for granular materials have to be adapted to reflect this. The effect screw auger mechanics might have in stiff, cohesive soil if the borehole stays open is debatable. However, as stated by Van Impe (1988), stiff clay characteristics and parameters can be significantly influenced and changed during the pile installation process.

Potentially, the principles of the existing theories can be used or simplified models can be adopted. Nevertheless, it is important to understand the existing auger models for granular material first in order to use, modify, extend or decline these approaches for application to stiff, cohesive soils.

Screw piling augers consist of a helical flight that coils across a central stem, which is generally hollow. Cutting teeth or blades are installed at the leading edge of the flights to allow penetration of the auger into the ground. Screw piling augers are installed in the ground by a combination of external rotational torque and pull-down forces (Figure 24) applied by the piling rig.

Q = Pull-down force applied by piling rig
M = Torque applied by piling rig
P = Soil resistance at auger tip
N = Auger weight
z = Auger length/drill depth
τ = Friction between surrounding soil and soil in auger
l = Auger pitch
d = Outer auger diameter
d_0 = Auger stem diameter

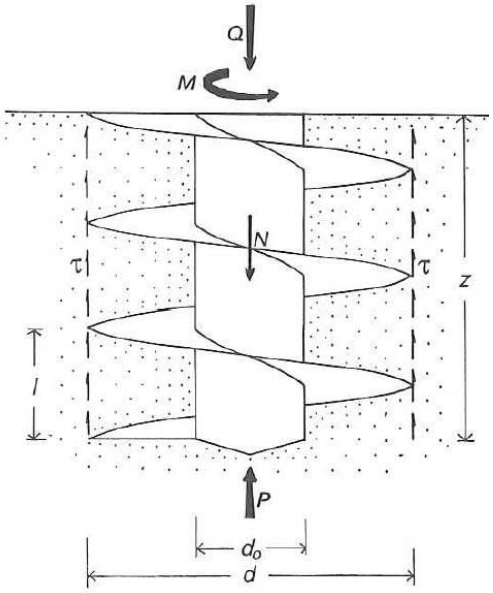

Figure 24 – Forces acting on the auger during the drilling process, after Viggiani 1993

During the installation process, screw augers are designed to cut material at the auger tip and to transport the loosened material through the auger flights towards a displacement body (long displacement augers) or the surface (CFA or VB augers).

Over the last decades, a few theoretical auger models have been presented by different authors (Metcalf 1965, Massarsch, Brieke and Tancre 1988, Van Weele 1988, Thornburn, Greenwood and Fleming 1993, Viggiani 1993, Fleming 1995, Slatter 2000, Bustamante 2003); however, no particular soil model for fine-grained soils has been developed to date. Some of the most accepted models for granular soils are based on the Archimedean screw principles. The basics of this theory, as well as the most relevant auger models developed for sandy soils, will be briefly explained and outlined in this chapter. This research work utilises existing models for application in stiff, fine-grained soil. The development of a new screw auger model for fine-grained soils is not within the scope of this thesis.

3.1.1 Cutting action at the auger tip

The cutting action of the bottom edge of the auger flights in sand has been presented by Thornburn, Greenwood and Fleming (1993). The authors assume that material at the auger tip is loosened and cut by overcoming a combination of bearing and passive resistance. Sand cut by the teeth passes onto the auger flights at a relative density close to that at which it shears at constant volume. Sheared dense sand will have a tendency to dilate, whereas loose sand may be compacted during the process. Thornburn, Greenwood and Fleming (1993) recommend typical figures of 10–15% for the reduction of volume of loose sands. It is important to note that the volume of the material before it moves onto the auger blades is different from the volume of the material that will be transported through the auger flights to the surface.

For sands below the water table, the authors point out that immediately beneath or behind the auger tip, temporary suction is created by the cutting process and the excavation of the soil. This suction might destabilise the wall of the borehole behind the sweep of the auger. As a result, the hydraulic gradient in the soil surrounding the borehole tends towards instability due to the removal of material and loss of internal soil pressure caused by the excavation. In dry sands, the cutting action might cause instability caused by stress changes behind the cutting blade of the auger. However, in a usual moist sand case, the moisture would tend to stabilise the walls of the excavation temporarily.

Vertical pull-down forces, rotational torque and rotation speed are crucial parameters for soil cutting action.

3.1.2 Soil transport

After sandy soil is loosened and cut by the auger tip, the material is transported to the auger flights, which become filled with the disturbed sand. The transport mechanism and the borehole stability are driven by the fact that the auger flights are completely filled with sand.

Resistance to rotation of the soil contained in the auger flights occurs due to contact between the moving soil inside the auger flights and the immobile soil of the borehole wall. The material transport process is driven by the force generated by this contact.

When the rotational speed of the soil inside the auger flights is slowed to a point at which it is lower than the speed of the auger itself, an upward force is applied to the soil as the flight slides past the bore wall. If this vertical force exceeds the shear resistance at the borehole wall, upward movement of the soil inside the auger flights occurs.

The final direction of soil movement inside the auger flights is a complex function of auger geometry, rotational speed, characteristics of the transported material and the friction coefficients between the soil and the auger. The determination of the material transport is outside the scope of this research project.

Figure 25 shows the pitch angle (α) and the angle of soil movement (β), both of which are measured against the horizontal. The transport angle (β) indicates the efficiency of the soil transport on the auger. Pure soil rotation would not be efficient at all (β = 0°) and soil transport along the axis of the auger would be 100% efficient (β = 90°).

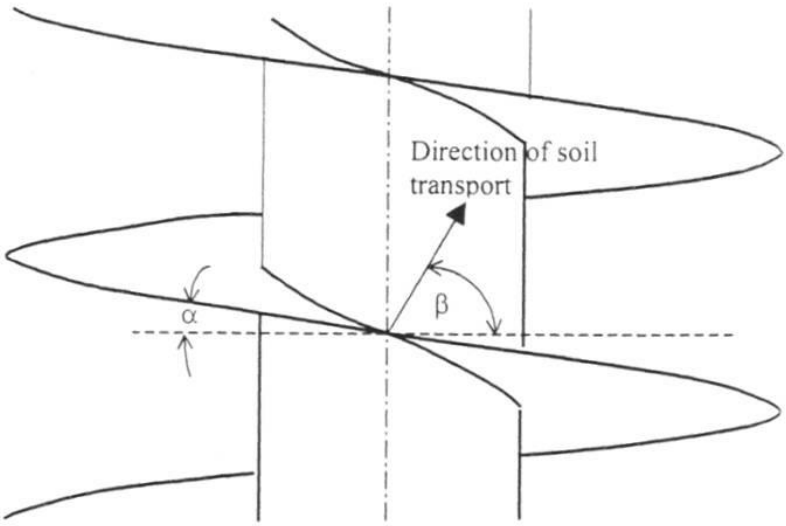

Figure 25 – Movement of soil on auger, after Slatter 2000

Slatter (2000) states that low-contact stresses, which occur when the auger flights are only partially filled with soil, such as at the auger/borehole wall interface, usually result in low transport efficiencies. Under these circumstances, material remains on the flights (not moving upwards) until a continuous ribbon of soil is re-established from the auger tip and is driven upwards by the soil entering the tip of the auger. This theory seems debatable to the author, as during practical CFA operations in sand, clay or heterogeneous soil, soil transport can be observed to take place even if the auger flights are only partially filled.

Slatter correctly concludes that the efficiency of soil transport can be increased by maximising frictional forces promoting transport (acting along face 4, Figure 26) or by minimising frictional forces resisting soil transport (acting along faces 2 and 3). The force acting along face 1 in Figure 26 is negligible (Slatter 2000).

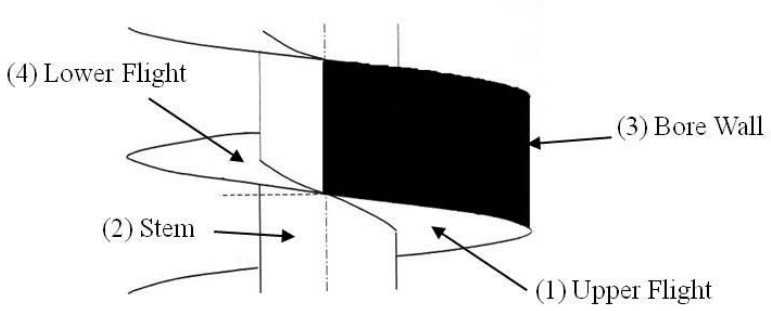

Figure 26 – Faces on which forces promote or oppose soil transport action, after Slatter 2000

High transport efficiency has significant benefits, despite its potential to cause soil decompression and over-excavation due to increased levels of soil transport. An auger enters the soil by cutting material from the tip and transports the soil inside the auger flights towards the displacement body or to the surface. Maximum transport efficiency is achieved when the quantity of materials cut and transported are equal. When auger rotation continues but the cutting process decreases (e.g. when a hard layer is encountered or in the case of a lack of rotational torque and vertical pull-down force), the risk arises of over-excavation from the borehole wall. This situation is characterised by decreased skin friction values of the surrounding soil and potential settlements around the borehole.

Penetration rates should be maintained in such a way that the forces supporting soil transport are maximised and the forces preventing soil transport are minimised (Slatter 2000). When the pitch of the auger flight is increased, the contact area between the bore wall and the soil inside the flight is also increased, which results in increased supporting forces for soil transport. The reduction of the auger pitch would increase the preventing forces of soil transport, as the contact area between the borehole wall and the soil inside the auger is reduced relative to the flight surface.

Figure 27 shows two augers with different pitch angles. The auger displayed on the left would be expected to have superior soil transport characteristics compared to the auger displayed on the right.

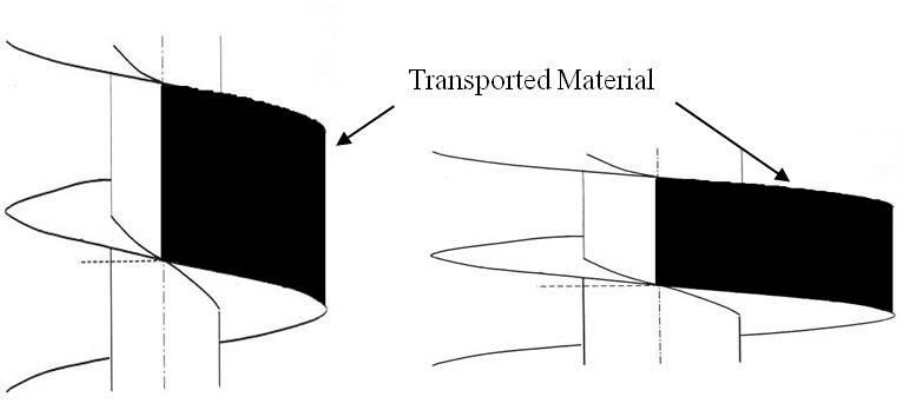

Figure 27 – Effect of auger configuration on soil transport, after Slatter 2000

Soil transport criteria are only one element influencing the soil transport characteristics of an auger. The pitch angle α influences the preventing forces as well as the coefficient of friction between auger flight and soil. Soil transport for stiff cohesive soil is not very different to that for granular material, as the borehole wall will always be stable.

3.1.3 Soil displacement

Simultaneous to soil transport, the penetration of the auger in the ground as a volume metric body creates the potential for soil displacement (Slatter 2000). For displacement augers, between 20% (at the auger tip or lower screw section) and 100% (at the displacement body) of the excavation can be filled by the body of the auger itself; CFA augers fill about 15–40% of the borehole, depending on the relevant diameters (Table 1). Whether material is displaced by the auger into the surrounding soil or drawn onto the auger from the surrounding ground is determined by a volume balance.

Slatter (2000) summarised the definition of a volume balance as follows:

> If, for any given flight, the volume of the auger introduced is greater than the volume transported, soil must be displaced from the auger into the wall of the bore (or displaced at surface). By contrast, if the volume of the auger introduced is less than the volume transported, then the walls of the bore will collapse (unless the soil is stable), allowing additional material to enter the flight, thus loosening the surrounding soil. If the volume of the auger introduced and volume of material transported are equal over any given section, then the flights of the auger remain full and no material is displaced. Furthermore the fully packed flight supports the borehole wall and prevents additional material from entering the auger.

The statement is also valid for stiff cohesive soil conditions; however, it can be assumed that the borehole walls in stiff clay will be stable and no short-term collapses will occur. Moreover, the soil

transport will be different due to the cohesiveness of the clay and the increased frictional forces between the auger flights and the soil. The influence of water will change these forces. Clearly, the auger mechanics for cohesive soil conditions add complexity to the process.

3.2 Archimedean screw principle

The installation of screw piling augers has the potential to transport and/or displace material, thus resulting in a corresponding loosening or densification action of the surrounding soil. The estimation of the level of densification and/or loosening potential of a specific auger in specific ground conditions is critical for the design of the pile load capacity of a screw auger pile and its construction.

A number of established and well-accepted screw auger theories (for granular soil conditions) rely on the Archimedean screw piling principle (Figure 28). The Greek mathematician Archimedes discovered that rotating screws could be used to transport free flowing materials. The original Archimedean screw comprised a helical pipe on an axis inclined from the vertical with its lower end in water. When the auger was rotated, water could be transported to a higher level.

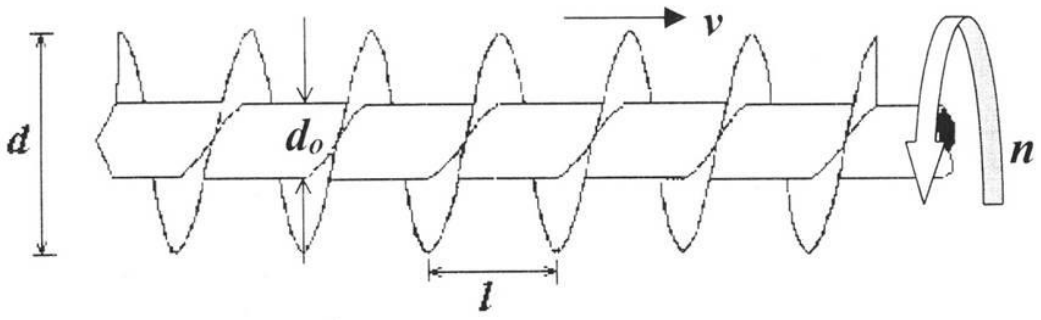

Figure 28 – Schematics of an Archimedean screw, after Slatter 2000

Archimedes subsequently developed screws consisting of a cylindrical stem wound around by a helical flange to form the flight. These screws typically operated inside a casing and they were used to transport loose, cohesion-less materials, such as grain. These screws are still in use today and are commonly known as screw conveyors or feeders. On an Archimedean screw, the flights have a constant pitch 'l', a constant stem diameter 'd_0' and a constant outer diameter 'd', as illustrated in Figure 28. Archimedean screws typically do not operate vertically; they usually work at 20–60º from the horizontal plane.

From first principles, and ignoring the volume of the auger flights and the friction between the transported material and the auger, the velocity v of material transported along the stationary auger with a pitch of l rotating to a rate of n is expressed in Equation 1:

$$v = n \cdot l \qquad (1)$$

From Figure 28, the cross-sectional area of the flight can be expressed as Equation 2:

$$\text{X-Sect area} = ¼ \cdot \pi(d^2 - d_0^2) \quad (2)$$

The volume of material transported by a stationary Archimedean screw over time Δt is equal to the cross-sectional area multiplied by the velocity. Using (1) and (2), this can be written as Equation 3:

$$V_t = ¼ \cdot \pi(d^2 - d_0^2) \cdot (n \cdot l \cdot \Delta t) \quad (3)$$

There are a number of similarities between the configurations of an Archimedean screw and a CFA piling auger, including the continuous stem diameter, constant pitch flights and constant flight diameter. There are also similarities in the material transport. However, as identified below, there are some major differences in the behaviour between an Archimedean screw and a screw piling auger.

The purpose of an Archimedean screw is solely to transport material. The effects of inserting a screw piling auger into the particular material to be transported and the cutting and displacement actions inside this material are not considered. However, the cutting of stiff cohesive soils could only be achieved by pushing the rotating auger into the material to be transported. The displacement effect is a function of the volume of material cut at the base and the volume that can be transported. The displacement effect depends on the vertical penetration rate in piling applications.

Archimedean screws and conveyors operate inside casings and the effect on the surrounding material is not considered. The screw inside the casing is completely isolated from the surrounding material and operates in an environment with very low horizontal stresses. By contrast, screw piling augers lack a protective casing and completely penetrate the material in which they operate. Screw piling augers also operate under considerably higher radial stresses, particularly in the case of displacement augers and/or in cohesive soil formations.

Archimedean screws are only fed from the bottom at a constant rate, as they are embedded in a fluid or in loose material. For stiff cohesive soil conditions, the borehole wall is stable such that it can be compared with an operation inside a casing after shearing the cohesive soil from the borehole wall. Further, the Archimedean screw does not work when it is positioned vertically, whereas screw pilings are positioned vertically in most cases.

The Archimedean screw theory assumes constant auger geometry, which might be valid to analyse CFA augers but is limited when more complex displacement auger configurations are used (e.g. Atlas, Omega). The last assumption that all material is free flowing and cohesion-less is adopted by all auger models. However, this assumption does not reflect the behaviour of stiff, fine-grained cohesive soils by definition.

3.3 Screw auger model, after Massarsch, Brieke and Tancre (1988)

Massarsch, Brieke and Tancre (1988) presented a method of predicting the soil transport and displacement characteristics of CFA type screw piling augers. The approach adopted by the authors is almost entirely based on the Archimedean screw principle.

However, Massarsch, Brieke and Tancre addressed one of the major limitations of the Archimedean screw theory by accounting for the displacement of material caused by the introduction of the auger stem into the soil. For an auger advanced into the soil at a rate v_a over a time Δt, Massarsch proposed that the volume of soil displaced by the auger stem V_d is as expressed in Equation 4:

$$V_d = ¼ \cdot \pi \cdot d_0^2 \cdot v_a \cdot \Delta t \quad (4)$$

Where, 'd_o' is the diameter of the auger stem.

The volume of soil cut by the auger V_c is shown in Equation 5:

$$V_c + V_d = ¼ \cdot \pi \cdot d^2 \cdot v_a \cdot \Delta t \quad (5)$$

Where, d is the diameter of the auger flights, which is equal to the diameter of the borehole.

From this, Massarsch, Brieke and Tancre stated that 'in time Δt the auger will pump a volume of re-moulded soil V_p where':

$$V_p = ¼ \cdot \pi \cdot n \cdot l \cdot \Delta t \cdot (d^2 - d_0^2) \quad (6)$$

Massarsch, Brieke and Tancre then proposed that, for loosening of the surrounding soil to occur, 'the volume pumped is greater than the volume moved ($V_p + V_c$)'. From this, they concluded that to avoid loosening of the surrounding soil when installing a VB (or CFA) pile, the pile should be installed at a rate of $v_a = n \cdot l$ (Equation 1).

Assuming the Archimedean screw principle, Equation 1 stated that the velocity of material relative to the auger is equal to $n \cdot l$. Therefore, if the velocity as the auger penetrates the soil is also equal to $n \cdot l$, the velocity of the material on the auger, relative to the surrounding soil must be zero (corkscrew effect). Massarsch, Brieke and Tancre's conclusion suggests that to install CFA and VB piles without loosening the surrounding soil, no material can be excavated from the borehole.

While Massarsch, Brieke and Tancre took into account the soil displacement of the auger stem, they did not consider the effect of the penetration rate of the auger on the amount of material excavated from the borehole.

3.4 Screw auger model, after Viggiani 1993

In a paper discussing the use of CFA piles in Italy, Viggiani (1993) carried out a detailed analysis of the soil transport and displacement characteristics of CFA augers. Like Massarsch, Brieke and Tancre's (1988) research activities described above, Viggiani's approach also relied on the basic principles of the Archimedean screw theory.

Viggiani also assumed no friction between the soil inside the auger flights, the auger itself and the wall of the bore, which oversimplifies the model in the author's opinion. However, he did implement the introduction of the auger stem into the ground, similar to in the approach presented by Massarsch, Brieke and Tancre (1988) (Equation 4).

A new equation for the volume of material removed from the borehole V_r was introduced:

$$V_r = ¼ \cdot \pi \cdot (d^2 - d_0^2)\ (nl - v_a) \cdot \Delta t \qquad (7)$$

By using the term $(n_l - v_a)$, Viggiani correctly accounted for the reduction in the volume of material removed from the borehole as the penetration rate of the auger increased. For example, if the velocity of the auger $v_a = 0$, then Equation 7 is reduced to the volume transported by a stationary Archimedean screw (Equation 3). If the auger is inserted at the pitch of the flights ($v_a = nl$), then no material is removed from the bore.

By equating the volume of the auger stem introduced with the volume of material removed during installation (Equations 4 and 7), Viggiani derived the following equation for the minimum velocity at which a CFA auger could be installed without loosening the surrounding soil:

$$V_{a(min)} \geq nl\ (1 - (d_o^2/d^2)) \qquad (8)$$

Equation 8 indicated that augers could be installed at a rate less than v = nl, as proposed by Massarsch, Brieke and Tancre (1988), without loosening the surrounding soil.

From the above, it is evident that the ratio of stem diameter to flight diameter (d_o/d) also influences the permissible penetration rate.

The greater the value (d_o/d), the lower is the penetration rate required to avoid loosening of the surrounding soil because of the increased displacement imposed by the stem.

While the work of Viggiani modified the Archimedean screw principle to account for soil displacement and the effect of auger movement on the amount of material excavated from the bore, it still has many of the fundamental deficiencies associated with the Archimedean screw principle.

The two most significant limitations of Viggiani's model are, firstly, that consideration is not given to the friction between the soil inside the auger flights and the auger itself during transport and the walls of the borehole. Secondly, since the model is based on the Archimedean screw principle, it is assumed that the piling auger does not work in the vertical plane, which does not accurately reflect the reality.

However, both limitations seem negligible for stiff cohesive soil, as the borehole wall is stable such that it acts like a casing. The friction between the clay and the auger flights themselves is significant and soil is transported even if the flights are partially filled. Auger cleaners are used at the surface to clean sticky cohesive soil off the flights. For displacement augers, the soil is pushed into the ground using the displacement body as a kind of auger cleaner.

Two additional, albeit minor, limitations also need to be addressed:

(i) The volume of the flights is not considered in the volume of the auger introduced. However, since the volume of the flights is only 5–10% of the total auger volume, it can be ignored for the simplified approach used in this research work.

(ii) The model has been specifically designed for CFA piling augers and therefore assumes that the geometry of the auger is constant. Modifications of the model to make it applicable to augers with variable geometry would potentially increase its application.

3.5 Conclusion

All auger models described in this chapter define the augering process as a process on its own, unrelated to the surrounding material. Stresses and displacement caused by auger action inside the surrounding material (soil formation) are not integrated in the models. However, the auger–soil interaction is an important part in predicting screw auger behaviour and in understanding the entire process. The principles of the Archimedean screw do not seem ideal for modelling a screw piling auger in granular soil, as Archimedean screws are designed to transport material only and not to carry out excavation, transport and displacement actions in different kinds of material.

In stiff cohesive soil conditions, the stable borehole wall acts like a casing, so the soil transport process can be separated from the surrounding material. The Archimedean screw theory might be more applicable in these soil conditions, even though the material being transported inside the auger flights is not granular and the cohesive nature of the clay creates a stronger friction between the auger flights and the soil.

Viggiani's auger model seems suitable for the simplified description of screw auger behaviour in stiff cohesive soil as a starting point to evaluate minimal penetration rates. The amount of soil displacement depends on the installation parameters. The fact that the piling auger is vertical is not a serious issue in the author's opinion, as the only difference to the Archimedean screw is the implication of a vertical pull-down force to cut material (soil) at the bottom site of the screw. Only that material that has been cut at the base will be transported; no material can enter laterally if the borehole is stable.

In the author's opinion, it is more important to investigate how the surrounding soil can be improved by the displaced soil inside the auger flights. There must be a point at which the borehole wall becomes over-stressed and a kind of failure mode occurs, weakening the surrounding soil.

Despite the need to develop an advanced auger model for screw piling augers in cohesive soils, the aim of this research is to find a suitable existing model that reflects the fundamental geotechnical interaction between screw piling augers and the surrounding cohesive soil. Viggiani's auger model seems suitable to describe the minimum penetration rates for stiff cohesive soil conditions, as it incorporates soil displacement and calculates a minimum penetration rate of the drill tool.

The next chapter continues the literature review, with the focus shifting to applications for screw auger displacement piles.

CHAPTER 4: APPLICATIONS FOR SCREW AUGER DISPLACEMENT PILES AND COLUMNS

4.1 General

In this section, the general applications for screw auger displacement piles are highlighted. Typically, screw auger displacement piles can be utilised for piled foundations (classic deep foundation) or as rigid inclusions for soil improvement applications, (Figure 29). The design concepts for piles and rigid inclusions are profoundly different, although the construction methods are similar.

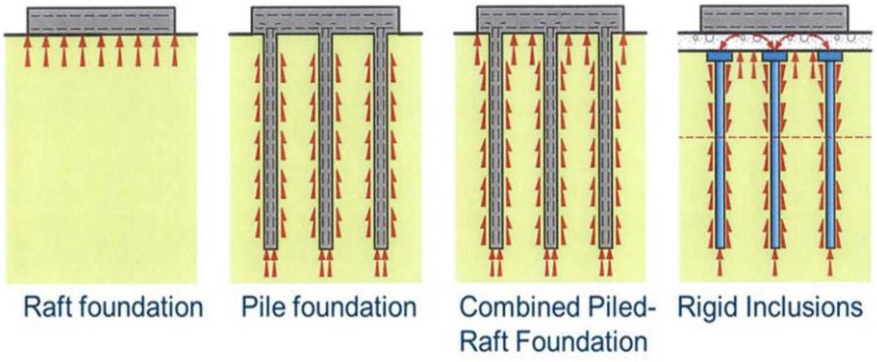

Figure 29 – A sample of foundation concepts

4.2 Piled foundations

4.2.1 General load transfer of single piles

In general, piled foundations are used to transfer structural loads into deeper and stiffer soil formations. The piles are directly connected to the structure via pile caps or slabs and the loads are directly transferred into the piles. Load transfer occurs via shaft friction and base resistance. Figure 30 (Van Weele 1957) shows the typical load distribution for a single pile, demonstrating that the shaft resistance will be activated to a certain level when it has reached its full capacity.

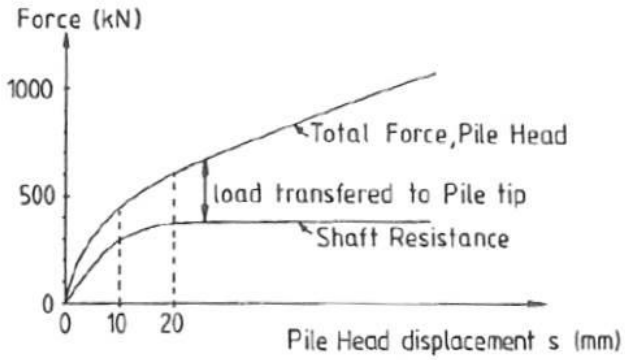

Figure 30 – Pile head displacement versus force, after Van Weele 1957

The load transferred to the pile tip (base resistance) develops with further pile loading. It can be concluded from Figure 30 that piles installed in soils with shaft resistance activate their full shaft capacity first, before the base resistance is fully utilised.

Other authors have developed models for the load-transfer mechanism in compression piles and tension piles (e.g. Smoltczyk 2006). Figure 31 shows the load-transfer mechanism for compression piles under a single load applied at the pile head. The development of a compression zone under the pile base is highlighted. The settlement of the soil adjacent to the pile causes arching inside the soil, which affects the skin friction distribution. In the area of the arching, the author concludes that the skin friction is reduced, as shown in Figure 31.

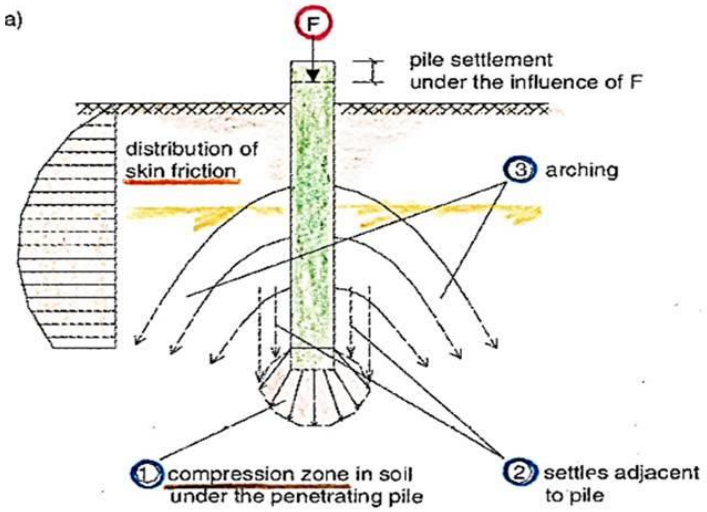

Figure 31 – Load-transfer mechanism for piles in compression

For tension piles, the authors assume a different load-transfer mechanism, as shown in Figure 32. Under pile heave, no base resistance develops and the load transfer relies solely on skin friction, which gradually decreases towards the surface, as shown in Figure 32.

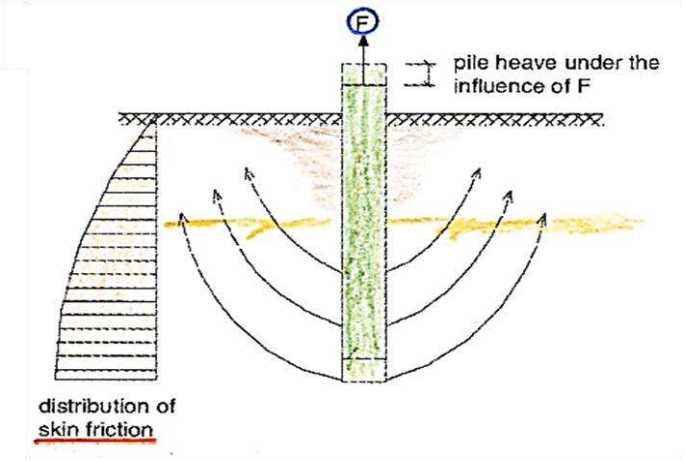

Figure 32 – Load-transfer mechanism for piles in tension

4.2.2 Load capacity of screw auger piles

The principles of the load-transfer methods introduced in the previous section of this work are also applicable for screw auger piles. However, the load distribution in the ground strongly depends on the shape of the drill tool and the relevant ground conditions. According to the author's personal experience and based on numerous static load test results on screw auger displacement piles installed in medium dense sands in North West Germany, the adhesion factor α when using the α-cu method for pile design (refer to section 7.5.1) can be increased to the following values depending on the associated pile types:

- Atlas pile 1.5
- Fundex pile 1.25
- SVB/VB pile 1.1

Unfortunately, none of the test results that were used to verify the factors mentioned above can be made available for this research. Typically, designers allowed a reduction factor for CFA piles in medium-dense sands of 0.5 to 0.9 due to the risk of uncontrolled soil excavation or decompression.

Screw auger pile capacities in sand and clay are usually determined by empirical methods, previous experience and load test results for particular projects (Tchepak 1998, Ayfan et al. 2003, Huybrechts and Maertens 2008) rather than by numerical modelling. What is really happening during the screw auger piling installation process is not yet known and properly understood.

De Cock, Van Impe and Peiffer (2001) collected and analysed 27 static pile tests carried out on screw auger displacement piles in sand and clay between 1970 and 2000 and demonstrated different load-settlement behaviour for different pile types in different soil conditions. In their research, they focused on the behaviour of the completed pile only (once the concrete developed its full strength after at least 28 days). They did not investigate the stresses in the soil caused by drilling, pouring and extracting using different auger types and shapes, installation parameters or concrete properties; nor did they attempt to develop a theoretical model to explain the results or allow for reliable predictions for future applications.

Well-accepted piling codes and standards (e.g. AS2159-2009, BS EN 12699:2001) do not allow for shaft friction adjustments for different screw auger displacement auger types like Atlas, Fundex, Omega, de Waal or others. Some authors (Van Impe 1988, Bustamante and Gianeselli 1998) have developed general design methods for screw auger displacement piles, mainly relying on *in situ* soil test results (i.e. CPT, SPT, PMT), but none of the authors incorporates adjustment factors for

different auger depth profiling geometries or *in situ* installation parameters into the design. Bustamante and Gianeselli's (1998) approach will be introduced later in Section 7.5.2.

Skin friction values for different pile types with different auger shapes, installation parameters and toe resistance factors for clay and sand are mainly based on experience and back analysis, rather than on geotechnical modelling. Bustamante (2003) concluded more than a decade ago that further research is required to establish a trustworthy and reliable link between drilling parameters, soil characteristics and pile capacities for screw piling applications. During the last years, efforts have been made by some researchers to correlate installation energy with actual pile capacities (NeSmith 2003, Schmitt and Katzenbach 2003, Scott et al. 2006, NeSmith and NeSmith 2008), mainly for granular soil formations.

Van Impe et al. (1998) and Bottiau et al. (1998) describe a research project carried out on four screw displacement piles in Feluy, Belgium. Four different screw piles of the same diameter (360mm) were installed and tested using static load tests in similar ground conditions with comparable installation parameters (torque, pull-down force, penetration rate, extraction rate).

For each pile, a different concrete casting technique was applied. The load test results clearly showed that the pile capacities and load-settlement curves were different for each pile. This particular research program will be discussed in more detail in the following sections of this thesis.

It is not only the concrete pouring method and installation parameters that influence the pile capacities of screw auger piles; auger shape can also affect pile load-settlement curves. Identical screw piling auger heads and tools are considered for application in both granular and cohesive soils. However, auger action (cutting, transport and displacement), soil behaviour and soil composition differ greatly between granular and cohesive soils, which thus require separate research (Slatter 2000). For example, in loose sands, a displacement auger thoroughly compacts the soil during penetration causing skin friction values to increase; however, in stiff clay, the same auger causes different soil behaviour, re-moulding rather than compacting and resulting in reduced pile capacities.

In the next section, the load-settlement behaviour of different screw auger displacement piles installed in granular and cohesive formations will be investigated, including by discussing load test results from completed research projects.

4.2.3 Load-settlement behaviour of different screw auger pile types

Between 1998 and 2002, a research project on screw auger displacement piles was conducted in Belgium (Holeyman 2001, Maertens and Huybrechts 2003) to investigate the load-settlement behaviour of this pile type in granular (at Limelette) and cohesive soils (at Sint-Katelijne-Waver).

Load-settlement behaviour of ADP in granular soil

For the test campaign in Limelette, several different screw auger displacement pile types were installed in the heterogeneous soil, which consisted of three distinctive soil layers:

(i) Silty clay;
(ii) Clay; and
(iii) Clayey sand.

Figure 34 shows the static load test results for Omega, de Waal and Fundex piles (refer to Figure 11 in Section 2.4 for details on these different pile types) with similar diameters (Omega and de Waal: 410 mm; Fundex: base diameter 450mm, shaft diameter 380mm) and pile lengths (9.50 m). The load settlement curves as displayed in Figure 33 were documented by Maertens and Huybrechts (2003) and no information on the installation parameters was made available in the literature. It is assumed that the parameters reflecting installation energy were different for the Omega, de Waal and Fundex piles, as the resistance caused by the different drill tools is fundamentally different such that it would not be possible to achieve a constant penetration rate for the different piles.

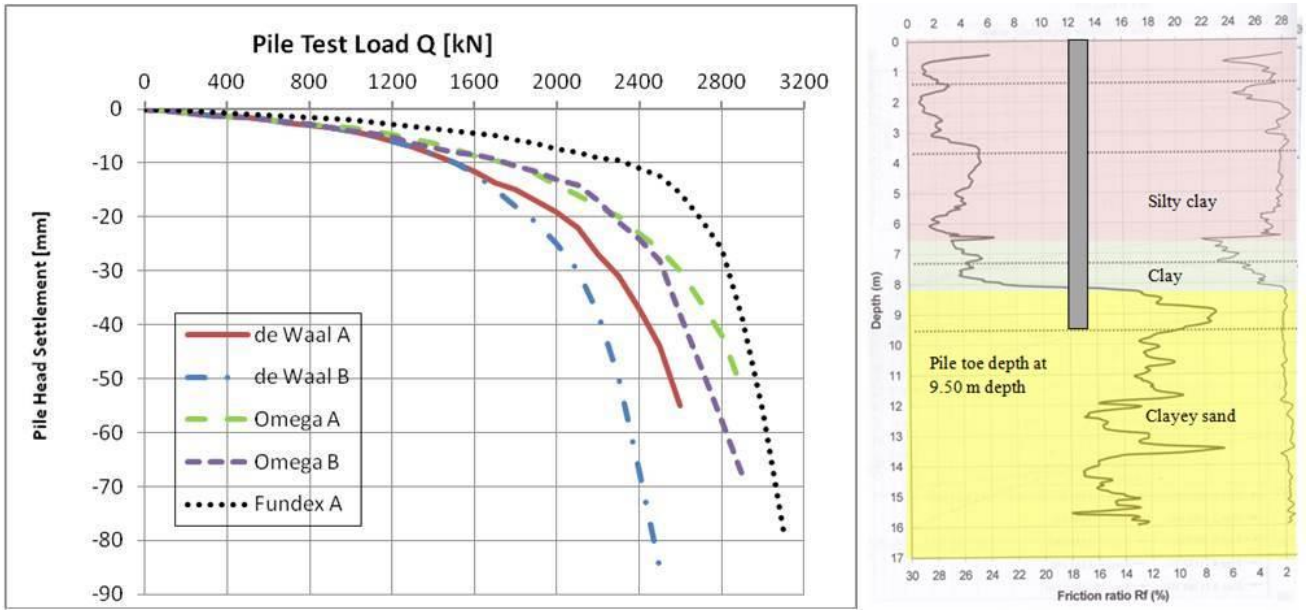

Figure 33 – Static load test results from the Limelette campaign for Omega, Fundex and de Waal piles in granular soil

Figure 33 illustrates the load-settlement behaviour, the soil profile, a typical CPT and the pile toe level for the Limelette test campaign for Omega piles, de Waal piles and Fundex piles. The load-settlement curves show a stiff response for the Fundex pile, resulting in the highest shaft capacity of all piles tested on site. The predominant auger action of this pile type is soil displacement at the auger

tip, and during the installation process, the clayey sand around the lower pile shaft located in sandy soil was compacted well, increasing the skin friction in this location. The skin friction capacity of the Fundex pile is superior, as indicated by the shallow load-settlement curve.

The load-settlement responses of the other pile types show a generally lower stiffness, indicating an increased shaft capacity for the Omega pile compared to the de Waal pile, in the range of 10–25%. The base responses of the de Waal and Omega piles, indicated by the steeply angled end part of the load-settlement curve, are comparable and the gradients are in the same range. The short Fundex pile shows a similar response for base capacity.

Load-settlement behaviour of ADP in cohesive soil

For the test campaign in Sint-Katelijne-Waver (Belgium), a setup similar to that described for the tests in granular soil was used. Omega, de Waal and Fundex piles of identical lengths and similar diameters (see above) were installed into stiff clay, as documented and published by Holeyman (2001) and as shown in Figure 34. Two different pile toe levels (7.60 m and 11.70 m) were used. No information was provided on the pile installation parameters. Figure 34 shows almost identical behaviour for the long Fundex and Omega piles. The short Fundex pile shows a weaker toe response, but its shaft resistance shows comparable stiffness. In general, the de Waal piles have a less stiff response compared to the other pile types, as well as a reduced shaft capacity by 5–10%. The base resistance of all long piles is in the same range. The de Waal and Omega piles show slightly stiffer toe responses compared to the Fundex reference pile.

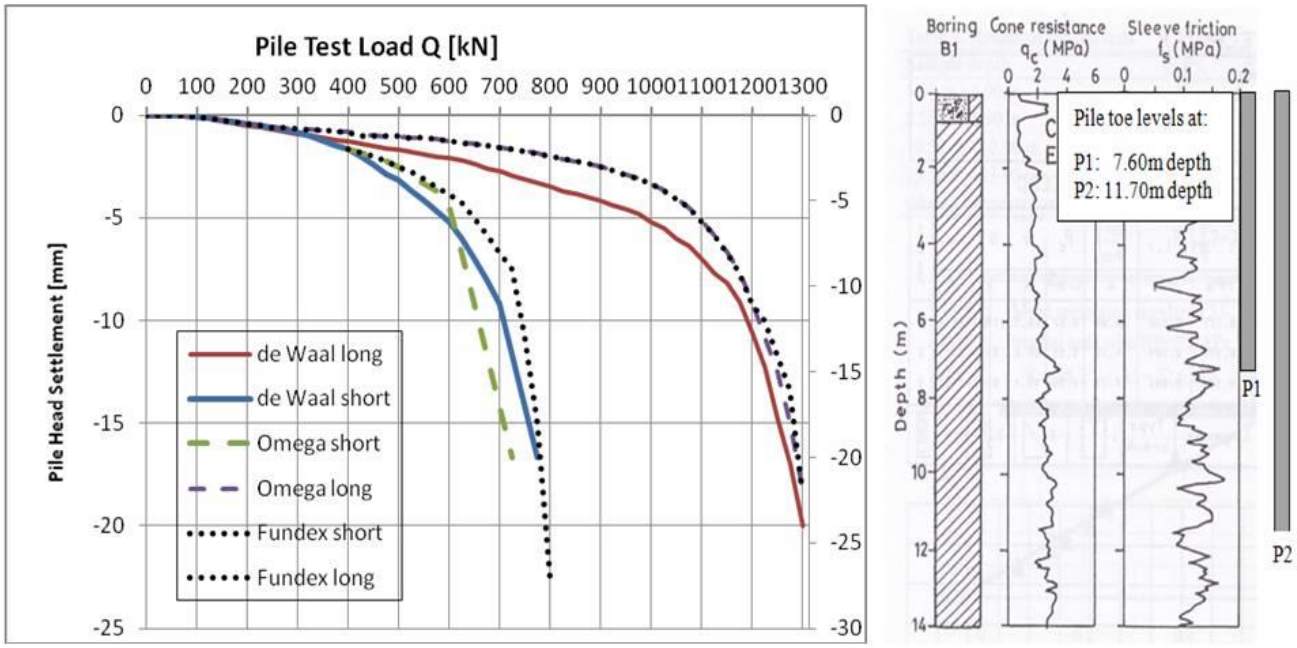

Figure 34 – Static load test results from the Sint-Katelijne-Waver campaign for Omega, Fundex and de Waal piles in cohesive soil conditions

Load-settlement behaviour of Omega piles in cohesive soil

At a test site in Feluy in Belgium, four almost identical Omega piles (refer to Figure 19 in Section 2.4.2) were installed in similar cohesive soil conditions to assess pile load capacity, estimate the installation coefficients, and control and analyse load-settlement behaviour in clayey soil using different concrete installation parameters.

Several authors (Bottiau et al. 1998, Peiffer et al. 1998, Van Impe et al. 1998) were involved in this research program and their findings are summarised below.

Two Omega piles and two Omega B* piles with identical diameters (360 mm) and pile lengths were installed in Ypsian clay. The two Omega B* piles were installed 11 m deep into the cohesive formation, while the two Omega piles were installed at a depth of 14.5 m. All piles were installed using different concrete pressures and the results are displayed in Figure 35. The authors provided no information about the particular installation parameters for each pile.

The four test piles were load tested (Figure 36) and it was proven that using a higher concrete pressure during the pouring process resulted in improved load capacities for all piles.

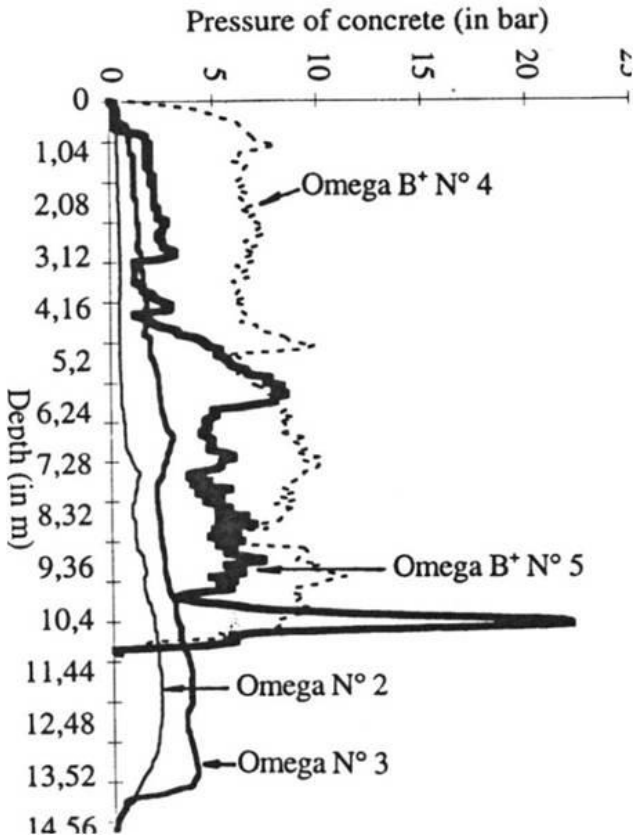

Figure 35 – Concrete pressure recorded during pile installation at Feluy, after Bottiau et al. 1998

All test loads were recorded for a settlement of 0.15 pile diameters to define a common baseline and to compare the load test results.

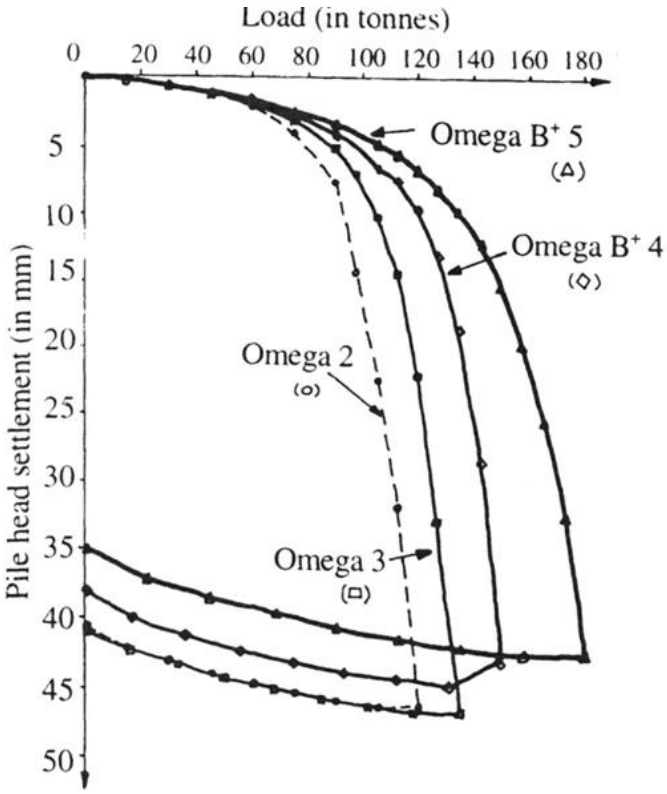

Figure 36 – Load v. pile head displacement for Omega piles at Feluy, after Bottiau et al. 1998

The authors involved in the Feluy research program successfully demonstrated by field tests that soil decompression at the auger base can be reverted by installing concrete under high pressure for Omega B* piles and that high concrete installation pressure can increase pile capacities in general for Omega piles. However, it should be noted that the reinforcement cage installation becomes more difficult if concrete is placed under high pressure.

Omega B*5 was poured with a lower pressure than that used for Omega B*4 during the auger penetration and at an extremely high pressure (25MPa) when forming the extended pile base. As a result, the overall bearing capacity of this pile was increased in comparison to the Omega B*4 test pile.

Unfortunately, no attempt has been made to verify the test results using numerical analysis or modelling to obtain a numerical, theoretical model of Omega piles in clay. Further, no installation records were made available showing the different penetration rates, torque, pull-down forces and extraction rates for each individual pile.

4.3 Rigid inclusions

4.3.1 Introduction

Rigid inclusions are a soil improvement method developed in France in the 1990s. Over the past two decades, many projects using this method have been carried out, not only in France but also in other parts of Europe, Asia, America (Plomteux and Lacazedieu 2007) and Australia (Wong and Muttuvel 2011). Rigid inclusions are usually installed by piling equipment, but this soil improvement technique has a completely different load-transfer behaviour to piled foundations. It is important to understand that rigid inclusions are not piles (even though they could be installed by piling equipment). This concept has caused some confusion within the global geotechnical community about the general idea of this technique.

Typically, soil improvement with rigid inclusions aims to reduce the settlement of a soil block that is subject to loads applied by a structure. This technique does not necessarily improve the soil itself; in most cases, the actual soil mechanical characteristics remain unchanged after the installation of the rigid inclusions. Instead, the soil is reinforced by creating a composite in which the structural loads are distributed between soil and inclusions. This foundation concept requires the presence of a load-transfer platform between the inclusion heads and the structure they are supporting. The general concept of a soil block reinforced by rigid inclusions was shown in Figure 29 in Section 4.1, above.

Shallow or raft foundation design methods (Figure 29) for soil improvement by rigid inclusions are typically chosen if:

(i) The soil formation provides sufficient stability; and
(ii) The predicted settlements are acceptable for the structure.

If at least one of these two criteria is not met, the usual alternative solution is to design deep foundations to carry the structural load. These loads are transferred to piles via rigid elements (pile caps or slabs), which distribute the structural loads into the piles.

In some cases, the shallow or raft foundation concept is not suitable (e.g. due to high settlements) and the deep foundation solution is over-designed (and therefore too expensive) in comparison with what is structurally required. This situation can be solved by simultaneously taking into account the respective load-bearing capacities of the rigid elements (pile cap or slab) and the piles themselves. It is assumed that a part of the structural load is transferred to the piles while another fraction is transferred to the soil between the inclusion heads, underneath the cap or slab (similar to in the shallow foundation concept).

This is known as a piled raft foundation and it is particularly attractive for soils featuring 'average' strength and homogeneous characteristics. The advantage of this system is to decrease the individual pile loads, resulting in reductions in the required pile lengths or diameters.

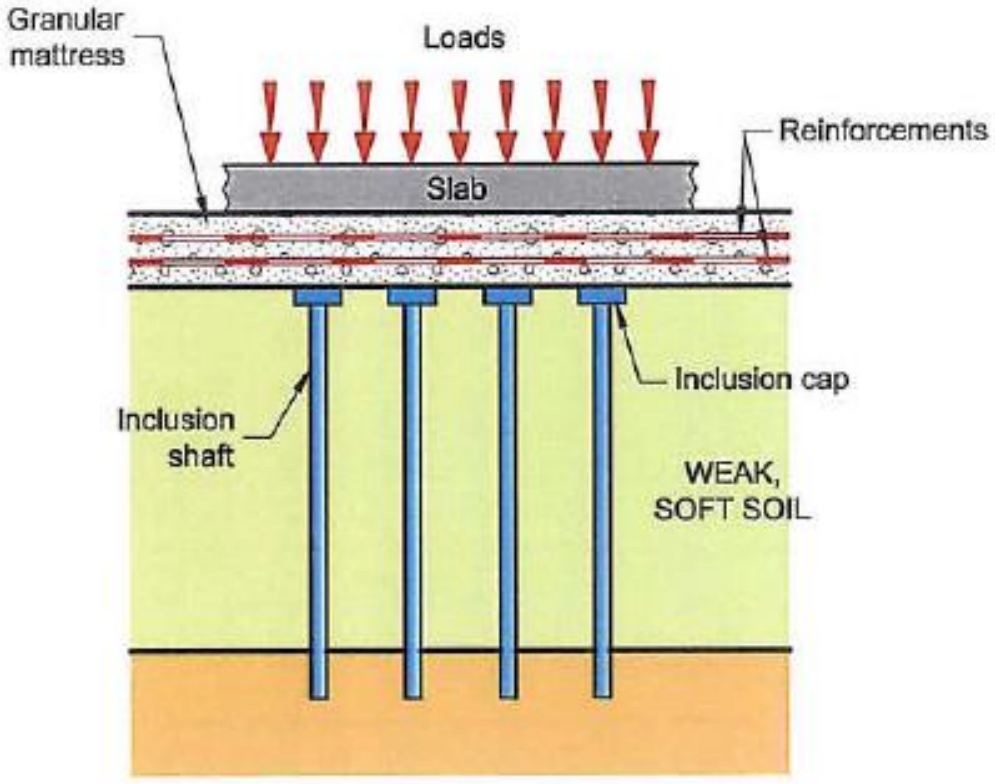

Figure 37 – The components of a rigid inclusion foundation system, after ASIRI 2011

The typical components of a soil reinforced by rigid inclusions are shown in Figure 37 and can be summarised as:

- A slab or other structural component to transfer the structural loads into the load-transfer layer, similar to in the shallow or raft foundation concept;
- A load-transfer layer (referred to as the granular mattress), which is typically reinforced with geosynthetics. The load-transfer layer further transfers the structural loads into the rigid inclusion heads or the soil between the rigid inclusion heads;
- Rigid inclusions (with or without caps for improved load transfer), which will transfer part of the structural load into the soil;
- A 'weak, soft soil' layer, which will settle due to the load transfer by the granular mattress. As this settlement will be larger than that for the rigid inclusions, a negative skin friction will occur at the inclusion shafts, up to the point at which the soil settlement and the rigid inclusion settlement are equal; and

- A competent soil layer as an embedment layer for the rigid inclusion. This ensures the load transfer into the stiffer ground via the inclusion base and shaft friction below the point of equal settlement. (The concept of equal settlement will be discussed in the following sections and is referred to in Figure 40 in Section 4.3.2).

Figure 38 shows the range of interactions, with a differential settlement at the base of the load-transfer layer. This generates a direct load transfer onto the inclusion head via load arching occurring inside the load-transfer layer. Further, the load is transferred onto the soil between the inclusions, causing the soil to settle and to apply negative friction along the rigid inclusion shaft.

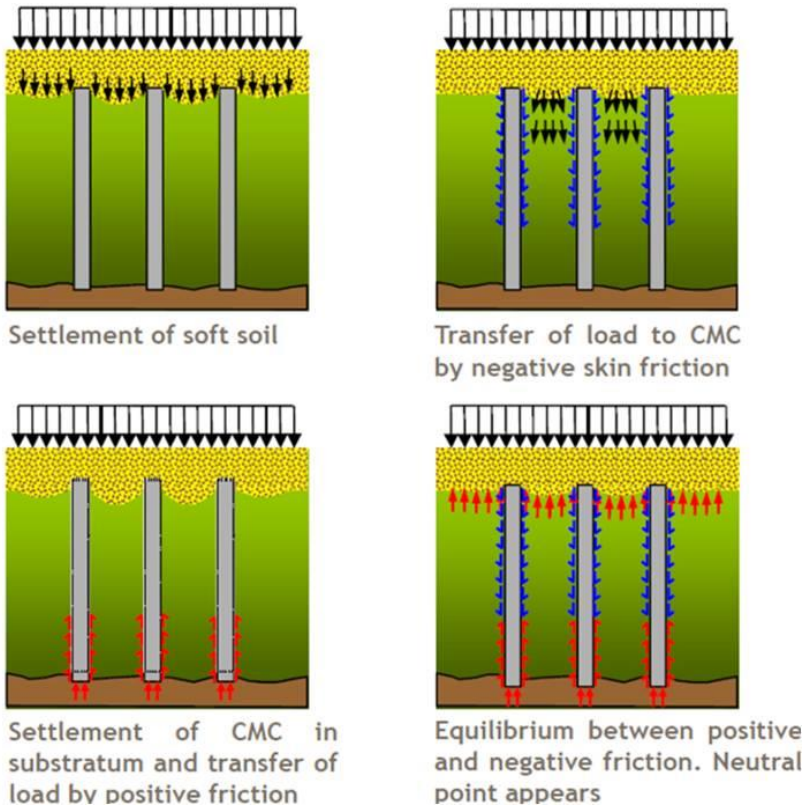

Figure 38 – Rigid inclusion (CMC) working principles, after Menard

The working principle of rigid inclusions is shown in Figure 29, Figure 38, Figure 39 and Figure 40. It is related to the piled raft foundation approach in which the structural load is partly transferred into the pile/column and the soil between the piles/columns. The load transferred through the soil between the column heads is partly carried out by the concrete column via negative skin friction, as shown in Figure 38.

A load distribution layer is placed on top of the rigid inclusions to transfer the loads from the structure above into the columns and into the soil between the column heads. It is important to note that there is no rigid or mechanical connection between the inclusions and the load-transfer layer.

Typically, the load distribution layer consists of granular material and can vary in thickness, depending on the ground conditions and design approach.

Combarieu (1974, 1985, 1988) and others developed a theoretical model of the system, as shown in Figure 39. However, a great variety of implementation techniques, component materials and design methods can be observed.

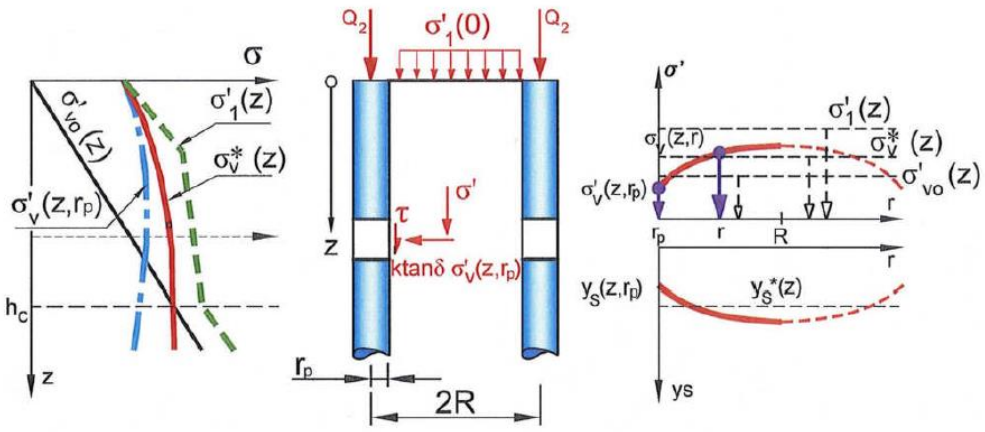

Figure 39 – Negative skin friction model, after Combarieu 1985

Even the brand names of rigid inclusions differ, resulting in confusion in the industry. The French construction company Menard claims to be the inventor of the system. They named their columns Controlled Modulus Columns or CMC (Figure 39). The Keller Group (one of the leading global ground-engineering contractors) branded their rigid inclusion system as Controlled Stiffness Columns (CSC), and for various projects in Australia, the rigid elements have been referred to as Concrete Injected Columns (CIC) or Drilled Displacement Columns (DDC). The design and working principles of the rigid inclusion products named above are similar to one another and differ from the concept of screw auger displacement piles described in Section 4.2 of this chapter.

4.3.2 Working principle of rigid inclusions

The concept of rigid inclusions includes various modes of interaction between:

(i) The inclusions themselves;
(ii) The load-transfer platform directly supporting the foundation; and
(iii) The soil and load transfer between the inclusions.

Combarieu (1985) highlighted these principles as shown in Figure 39, and Simon and Schlosser's (2006) illustration of the shear mechanism of an embankment founded on rigid inclusions is given in Figure 40. The load applied by the embankment in Figure 40 causes the settlement of the load-

transfer layer above the column heads u_p and of the soil surrounding the columns u_s. The settlement of the soil and column at the 'equal-settlement upper plane' is similar. However, below this level, the settlement u_s of the soil is greater than the column settlement u_p, which causes the stiffer rigid inclusion to punch into the load-distribution layer.

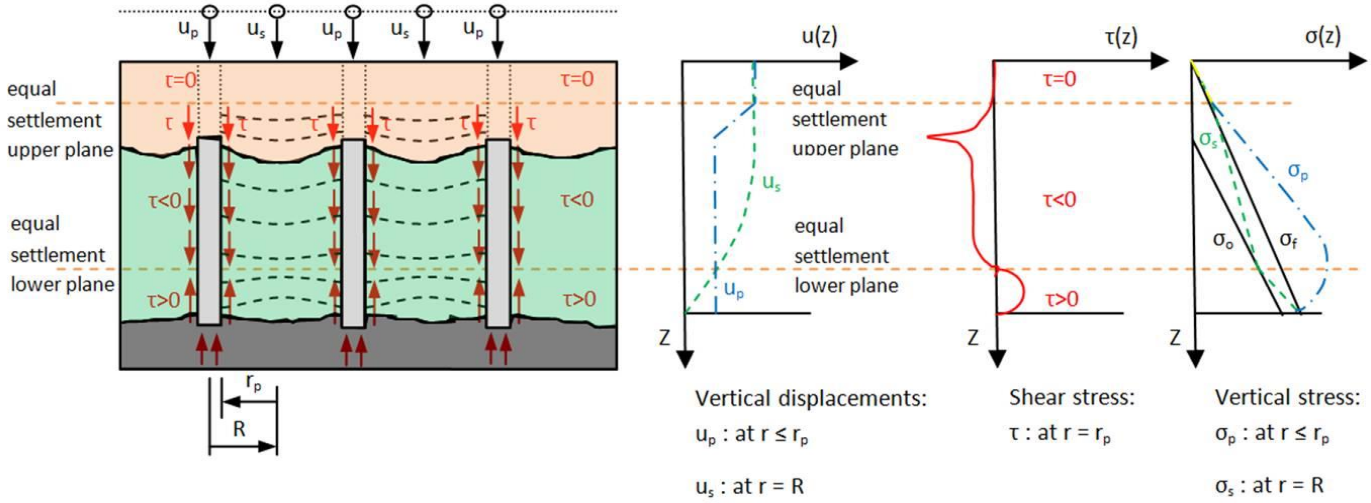

Figure 40 – Shear mechanism of an embankment founded on rigid inclusions, after Simon and Schlosser 2006

The soil surrounding the upper part of the column applies negative skin friction to the shaft of the column until the settlements of the soil u_s and column u_p reach equilibrium at the neutral point, corresponding to the 'equal-settlement lower plane'. Below the neutral point, the column settlement u_p is larger than the soil settlement u_s, which causes the rigid inclusion to develop positive shaft resistance and base resistance below the toe of the column. Eventually, stress equilibrium occurs over the full length of the inclusion.

In general, the design of rigid inclusions is based on the equilibrium of external loads, applied by the structure and the column resistance in the ground. Plomteux and Lacazedieu (2007) define the condition of equilibrium by Equation 9:

$$Q + R_{s+} = R_{s-} + R_B \qquad (9)$$

where:

Q = vertical load at the head of the rigid inclusion;

R_{s-} = negative skin friction, applied above the equal-settlement lower plane;

R_{s+} = positive skin friction, mobilised below the equal-settlement lower plane; and

R_B = tip resistance in the anchorage layer.

Wong and Muttuvel (2011) define equilibrium as load sharing between the soil and the rigid inclusion, combining:

(i) Compressibility of the columns;
(ii) Yielding of the column toe; and
(iii) Load sharing via a load-transfer platform.

Rigid inclusions, in the strict sense of the term, contain elements that are slender, often cylindrical in shape, mechanically continuous and typically vertical with constant cross sections. They are typically spaced in a regular grid pattern, designed to suit the structural loads and the project-specific soil conditions.

The adjective ‘rigid’ is required whenever any material displays a strong permanent cohesion, resulting in a level of stiffness that is significantly greater than the stiffness of the surrounding soil. However, this stiffness may vary depending on the selected inclusion material, which can range from lime columns to steel sections, gravel columns injected with a cement slurry, mortar or concrete (reinforced or plain). Concrete columns are the most common form of rigid inclusions. They are typically installed using screw auger displacement tools and equipment.

The rigid inclusion concept assumes that column stability is provided without any lateral confinement of the surrounding soil, which contradicts with the concept of stone column design. The load able to be applied at the top of the inclusion depends on the strength of the inclusion material, which can vary considerably even for concrete columns (e.g. 5–40 Mpa compressive strength). Consequently, the design of rigid inclusions requires a minimum internal strength of the rigid elements and must incorporate interactions with the surrounding soil by shaft friction and forces at the top and base of the inclusions. Therefore, the inclusion dimensions can be highly variable. In most cases, the inclusion length extends the thickness of the relevant soft soil layer socketing in stiff or dense formations. Shorter rigid inclusions would be less efficient due to a lack of load-bearing capacity at the base. This is an important design principle, as the penetration into stiff soil layers is a crucial part of the rigid inclusion concept. For rigid inclusions installed with screw piling auger equipment, this concept results in the requirement of the installation of ‘sockets’ into stiff/hard clay or dense sand; neither of these soil conditions is ideally suited for screw auger displacement techniques.

Numerical analysis is typically employed, both quantitatively and qualitatively, to examine characteristics of behaviour of rigid inclusions.

4.3.3 Load-transfer platform

The design and working principle of load-transfer layers are not part of this research project and this topic is only introduced briefly in this section. The focus of this work is on the behaviour of the rigid inclusions themselves with respect to load distribution, load transfer and the consequences for design and installation with screw auger displacement tools.

The rigid inclusion concept implies that the rigid inclusions are not structurally connected to the structure, which is fundamentally different to the classic piled raft foundation concept. Load transfer is provided by a load-transfer layer between the rigid inclusions and the structure and it is assumed that the column heads punch into the load distribution layer. Different failure modes are possible, as shown in Figure 41.

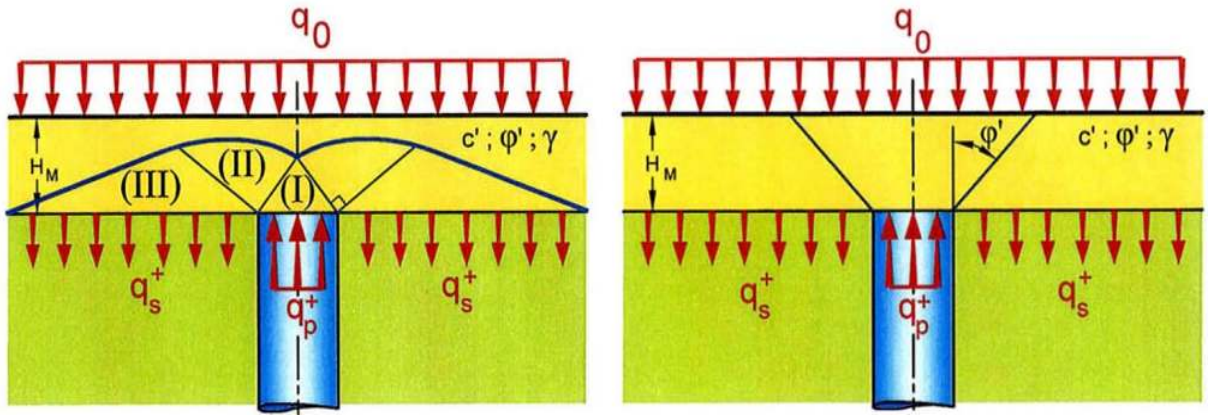

Figure 41 – Punching effects at rigid inclusion heads, after ASIRI 2011. Prandtl failure mechanism (left), shear cone type failure mode (right)

The load-transfer layer typically comprises:

(i) Single layers of well-compacted granular material;
(ii) Layers of soil treated with hydraulic binders; or
(iii) Layers of soil reinforced by horizontal geosynthetics or geotextile.

The load-transfer platform is responsible for distributing the structural loads partially into the column heads and partially into the soil between the rigid inclusions.

The system consisting of rigid inclusions, load-transfer layer and geotextile creates a composite or reinforced soil body, which tends to be stronger and less deformable than the initial soil, allowing the structure to be founded as a shallow foundation.

For the load-transfer platform, a minimum thickness of typically 400–1200 mm is required to allow for appropriate load transfer between inclusions and soil. This is essential for an optimal design of the supported structure, particularly with the aim of reducing bending moments in the slab or base plate.

For granular material layers, it is important to obtain a high level of compactness, which results in a high modulus of deformation. For load-transfer layers treated with hydraulic binders (lime or cement-lime mortar), sufficient flexibility needs to be retained to avoid cracking. Typically, load-transfer layers are made of granular soil reinforced with geosynthetics or geotextiles. This is a very efficient measure to control lateral loads.

4.3.4 The rigid inclusion (columns)

This section focuses on the general load-transfer mechanism of the rigid inclusion (column) itself in the soil formation, highlighting the critical areas close to the column toe of this particular system component and the applicable requirements.

The design of rigid inclusions relies mainly on shaft friction values for the determination of the load-settlement behaviour of the rigid inclusion. It is critical for the design of the system to understand the two main contributing aspects governing the skin friction capacity of the rigid inclusion:

(i) The *in situ* shear strengths of the soil; and

(ii) The capability of the installation method to increase or decrease this shear strength.

Single rigid inclusions experience negative skin friction above the neutral plane of equal settlements, as shown in Figure 42.

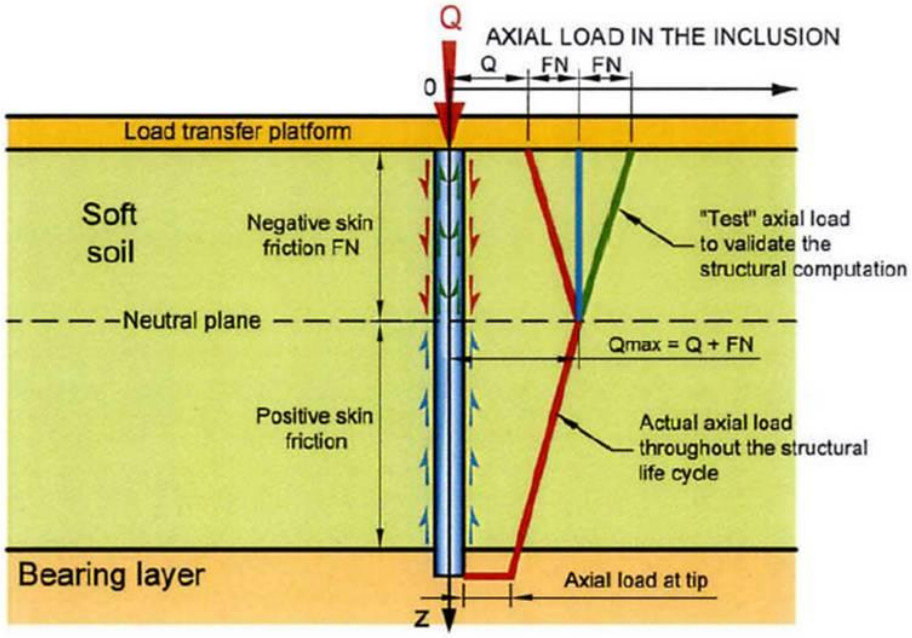

Figure 42 – Axial load distribution inside a rigid inclusion, after ASIRI 2011

To validate the structural capacity of each inclusion, the negative skin friction needs to be taken into account in the design. The actual axial load might be smaller than the assumed load, as the structural load is partly transferred into the soil between the column heads.

The maximum 'active' load ($Q + F_n$) is applied at the neutral plane. It is critical to mobilise sufficient reaction forces below the neutral plane to reach equilibrium. Typically, the neutral plane is located in soft soil conditions (above the bearing layer) and the positive skin friction able to be mobilised in the soft layer is negligible. Consequently, the rigid inclusion needs to be embedded into a stiff layer to mobilise sufficient reaction forces. Typical embedment lengths into stiff soil reach 2–4 m and it is important that sufficient base resistance and shaft friction can be mobilised to keep the system in balance. If the required reaction forces cannot be mobilised, the neutral plane moves downwards, resulting in increased settlement of the soil block.

Even though rigid inclusions are a soil improvement system, it is critically important to ensure that the inclusion resistance is given by sufficient base and shaft capacities in the bearing layer (below the neutral plane), as shown in Figure 42.

In general, rigid inclusions are un-reinforced; however, sometimes the addition of a single rebar is required to resist potential damage caused by installation effects (lateral forces act on the columns as a result of soil displacement during the installation of adjacent inclusions). Reinforcement cages might be required at embankment edges or other critical locations at which sliding might occur in order to provide sufficient bending and/or shear resistance.

4.3.5 Applicable soil conditions

Rigid inclusions are generally applicable to loose granular or soft cohesive soil conditions above medium-dense or stiff bearing layers. It should be noted that peat and all materials containing organic substances require special attention because they are subject to secondary compression settlements.

Rigid inclusions are not suitable for penetration of obstructions, hard soils or rock. Their use in very soft soils ($c_u < 15$ kPa) should also be considered carefully, as the lateral concrete pressure inside the column might be greater than the lateral soil resistance, resulting in excessive concrete overconsumption and a potential failure to pour the columns to platform level.

It is important to understand that a foundation on rigid inclusions is a soil improvement system and will therefore experience settlements higher than for pile foundations.

4.3.6 Fields of application

Generally, soil improvement systems are applicable for designs allowing moderate to high settlement. Rigid inclusions improve the original soil formation, and structures can be designed for shallow foundations.

Typical applications for rigid inclusions are displayed in Figure 43. They include, but are not limited to:

(i) Slabs and foundations for industrial and commercial buildings;
(ii) Storage reservoirs and tanks (water, oil products or liquid chemicals);
(iii) Retention systems, such as reinforced earth walls;
(iv) Highway embankments; and
(v) Railway embankments.

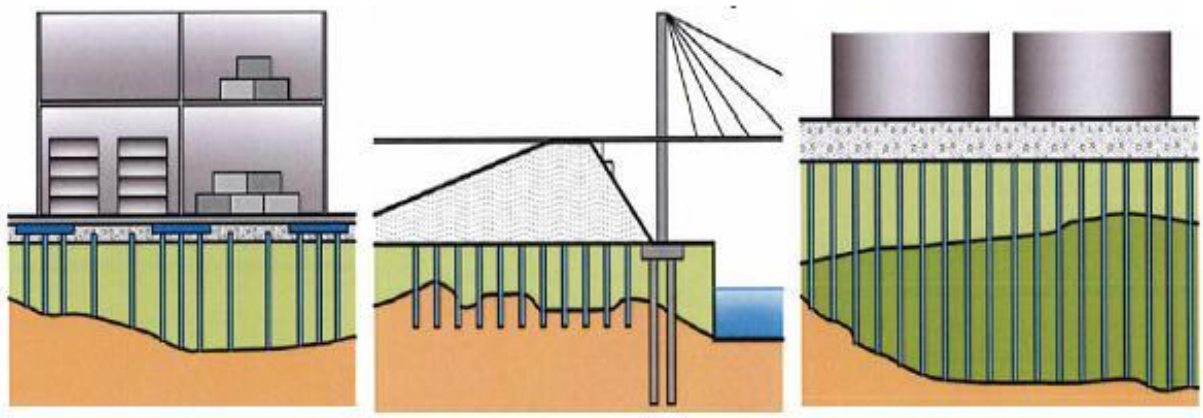

Figure 43 – Examples of rigid inclusion applications, after Menard nd

In contrast to piled foundations, in which high structural (point) loads are applied and the settlements are small, rigid inclusions are not suitable for high-rise buildings, large bridges or structures with high lateral load, point loads or bending resistance.

4.3.7 ASIRI National Project

The ASIRI National Project ('L'amelioritionn des sol de foundation par inclusions rigides', which translates as 'Soil Improvement by Vertical Rigid Inclusions') was carried out in France between 2005 and 2011, with a total budget allocation of €2.7 million.

The scope of the research involved the investigation of soil improvement by the installation of vertical rigid inclusions using screw auger displacement piling tools and equipment. The project was supported by 39 partner firms and organisations and it received the financial support of the French Government.

Rigid inclusions were used for the first time in France during the 1990s, despite their having been developed some two decades earlier. Similar foundation systems had been used before this (Combarieu 1974, 1985, 1988) in other European countries, where embankments were founded on a grid of concrete piles, timber piles or other rigid elements, separated by a load-transfer layer from the structure to be supported. However, no specifications or standards arose from this and the general design principles remained poorly understood, with different interpretations in different countries. The aim of the ASIRI project was to develop a set of dedicated and adapted guidelines for the design and execution of rigid inclusions for France and the international geotechnical community.

The ASIRI project focused on the design, execution and analysis of a series of tests, experiments and numerical models as a fundamental step towards understanding the working principles of this innovative foundation system. The project provided detailed results about the load-transfer mechanism, including the load transfer from the structure into the load-transfer layer and the column heads, as well as the load distribution along the column shaft. It was highlighted that rigid inclusions needed to be both structurally and geotechnically designed and that the equilibrium of forces and stresses inside the column depended on the base resistance and positive shaft capacity of the column.

Unfortunately, no research data about the influence of the installation techniques of the rigid inclusions could be found by the author. Further, no attempts appear to have been made to investigate the influence of the drill tool, installation parameters or installation techniques on the base capacity and positive shaft resistance of rigid inclusions.

4.4 Summary

Screw auger displacement piles can be used for the installation of piles or soil improvement projects with rigid inclusions. The difference between the two applications is solely in the design approach. For piling applications, the structural load is completely transferred into the piles, with the loads then transmitted into the soil formation via shaft friction and base resistance.

The use of different screw auger displacement tools results in different load capacities in similar soil conditions. Pile load tests in Belgium proved that the load capacities for short displacement augers (Fundex piles) as compared to long screw displacement augers (Omega and de Waal piles) were superior in both granular and cohesive ground conditions. For the long screw auger displacement pile tools, the progressive Omega pile outperformed the rapidly displacing de Waal pile.

The load test results indicate that the end-bearing capacity of all pile types is similar, with the key difference being in the shaft capacity of the different pile types. National and international standards do not differentiate with respect to pile load capacities for the use of different screw piling auger

tools or types. No distinctions between short, long, progressive and rapid displacement auger types are made, even though the load test results in Belgium showed different load capacities between these auger types.

Unfortunately, no information about the installation parameters were provided by the authors of the research carried out in Belgium. It is critical to compare the installation parameters to evaluate whether the specified penetration rates were achieved as per the recommendations of Maasarsch et al. (1988), Viggiani (1993) and others. Slatter (2000) highlights the importance of installation parameters for using screw auger displacement augers in granular formations, to avoid uncontrolled lateral soil excavation or soil decompression.

The research in Belgium also highlighted that using an increased concrete pressure for the installation of progressive displacement piles in clay improved the load capacity considerably. The shape of the static load test curves indicated an increased skin friction capacity for the piles installed with high concrete pressure. Unfortunately, high concrete pressures can cause concrete segregation or line blockages. From personal experience, the author of this report does not recommend this technique to increase pile shaft capacities.

Screw auger displacement piling tools and equipment have been successfully used for the installation of rigid inclusions as a soil improvement system. Rigid inclusions are typically installed as concrete columns, which act to transfer the majority of the structural load from the structure into the soil. These inclusions rely on load transfer via base resistance and shaft capacity in stiff bearing layers (e.g. dense granular material or stiff cohesive formations).

No recommendations for the installation of rigid inclusions were found in the literature to specify column capacities based on the type of drill tool installation parameter or installation method when using screw auger displacement piling tools.

For both screw auger displacement auger and tool applications—piling and soil improvement using rigid inclusions—the tool is often required to penetrate into stiff or dense bearing layers and load transfer in the soil occurs via shaft friction and end bearing, even though rigid inclusions are designed as a settlement reduction method.

Having presented the literature on screw piling technology, auger mechanics and screw auger displacement pile applications, the following chapter provides a critique of the literature and defines the gap in the current research that this thesis aims to fill.

Figure 44 – Identical screw auger full-displacement equipment can be used for both piling and soil improvement applications

CHAPTER 5: CRITIQUE AND GAPS IN CURRENT RESEARCH

Screw auger displacement piling is an under-investigated area. The majority of the sources used for this literature review come from the conference proceedings of the five Deep Foundations on Bored and Augered Piles (BAP) conferences, held quinquennially in Ghent, Belgium between 1988 and 2008. Over that period, most research activities were carried out in Belgium, the Netherlands and Germany, with a particular focus on granular ground conditions and a basic understanding of screw auger displacement piling in general.

Most references for the design and construction of rigid inclusions were found in the French guideline ASIRI (and related literature), which was published in 2011. The PhD thesis of Dr James Slatter (2000) also provided valuable background information and further references in the area of screw auger mechanics. The remaining sources were drawn from papers, reports and publications from international conferences, journals or private correspondence with fellow researchers.

The literature review identified some considerable gaps in the field of screw auger piling applications in stiff fine-grained soils. Whereas the behaviour of screw auger piles in granular soil conditions has been the topic of two PhD theses (Slatter 2000, Schmitt 2006), the performance of this pile type in stiff cohesive formations has not been researched in detail to date.

Due to the numerous gaps in the research area of this thesis, it was important to focus on the defined scope of this research work (i.e. How do installation parameters and auger shape influence the load capacity of screw auger piles in fine-grained soil) and to avoid digressions. Consequently, the author identified numerous research topics that were beyond the scope of this research work or that might arise from this research (refer to Section 11.2).

The following gaps identified in the literature review are addressed in this research work:

(i) Screw auger pile behaviour in stiff, cohesive soils has not been investigated in detail. Stiff or hard clays are often used as bearing layers for piles and rigid inclusions, and it is important to understand the interaction of screw piling augers and the surrounding soil formation, particularly as regards the influence of auger shape and installation parameters in relation to possible load capacities, stress changes and soil behaviour in the soil formation around the pile shaft;

(ii) There are no qualifications in design standards and specifications with respect to the performance of different drill tools and auger geometries, despite the auger mechanics being different for each individual tool;

(iii) Over the last two decades, numerous screw auger displacement tools have been developed and manufactured by various suppliers around the world; yet no classification of the different auger types has been carried out. The author of this research has proposed a classification scheme comprising long, short, progressive and rapid displacement tools;

(iv) Several researchers have conducted pile load tests to compare the load capacities of different screw auger types in similar ground conditions. However, no efforts have been made to compare and account for the particular installation parameters (penetration rates, pull-down forces and rotational torque readings) or to investigate whether those parameters affect pile capacity and stress development in the soil formation;

(v) There is no evidence for whether the current theoretical auger models introduced in this thesis sufficiently describe screw auger behaviour in cohesive soil conditions. All current auger models are based on the Archimedean screw principle, which might not perfectly reflect the real behaviour of screw piling augers. Despite this, this principle is considered a sufficient starting point to investigate the fundamental screw auger behaviour in stiff and hard clays;

(vi) The effects of lateral soil displacement and heave for screw auger displacement piles are well known from practical experience on numerous piling projects but are not understood in detail. Heave has not been related to installation parameters and has not been applied to designs or specifications for screw auger displacement piles or rigid inclusions;

(vii) Load tests have indicated an improvement of the skin friction of screw auger piles due to soil displacement or re-moulding processes in stiff clay formations, but no detailed research has been carried out in regards to the potential weakening of the surrounding pile by insufficient installation parameters; and

(viii) The influence of installation parameters (penetration rate, pull-down force, torque, rotations) for different screw piling auger types has not been studied in detail and no theoretical models are available to predict pile capacities in relation to different installation parameters.

Screw auger displacement piles have been used for decades, both as load-bearing piles and as rigid inclusions for soil improvement projects. Despite this, little research has been conducted on the fundamentals of the auger mechanics, the influence of installation parameters on shaft and base capacities and the overall behaviour (particularly as regards the stresses and displacements around the shaft and toe area during and after the installation process) in stiff or hard cohesive clay formations.

CHAPTER 6: WORK PROGRAM

The work program for this research work is illustrated in Figure 45. The five-year research period is shown, indicating the main working steps. These steps, which are briefly outlined in the remainder of this chapter, are:

i) The literature review and study of the relevant publications directly and indirectly related to the field of research;

ii) The development of a simple basic finite element (FE) model to simulate the penetration of a rigid body into stiff cohesive clay;

iii) The execution of the field and laboratory tests to determine the geotechnical parameters of the proposed field test site at Lawnton;

iv) The preparation of the field test site and execution of the test piles at Lawnton;

v) The analysis of the field test data and the formulation of the results and conclusions; and

vi) Thesis finalisation and submission.

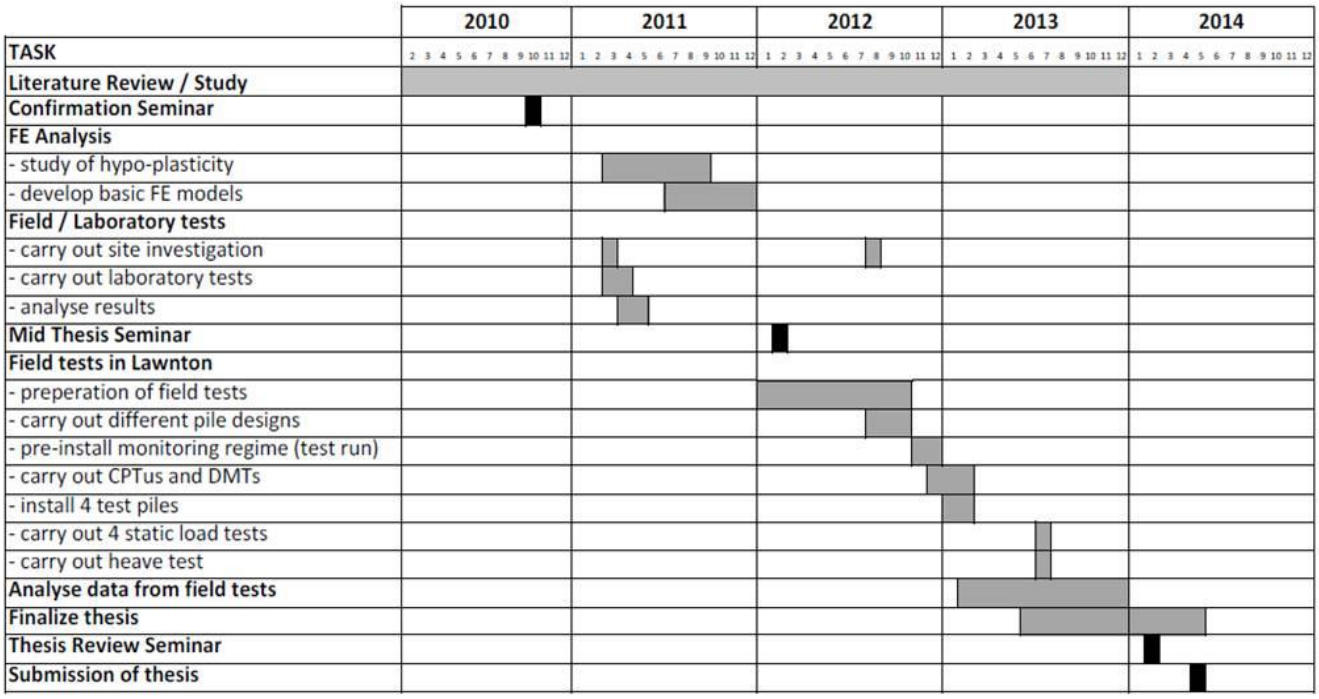

Figure 45 – Work Program

6.1 Literature review

The review of relevant literature was an ongoing process, beginning with the commencement of the research work. The main challenge was to find literature relevant to screw auger displacement piles and rigid inclusion, which is a sub-topic of piling and soil improvement.

Some research was found to have been carried out in the countries in which most of the auger types and techniques were originally developed: the Netherlands, Germany, France and Belgium.

The author found the proceedings of the five international BAP conferences, held quinquenially between 1988 and 2008, very helpful in gaining an in-depth understanding of the history and state-of-the-art of the research in this field. These conferences were a global forum for researchers involved in the study of screw auger displacement piles.

Additional research papers were collected from other international conferences and from personal contact with researchers in related areas. Despite screw auger piles being an effective and economical foundation system, only a few researchers have published data that might allow the academic community to further their understanding of and develop this topic. It seems that much information remains hidden in the folders of numerous piling companies around the world.

The literature review included not only information about screw auger piles in general, but also about auger mechanics, rig instrumentation and different design methods for piles in general and screw auger piles in particular. In relation to the design and numerical modelling of screw auger piles, the investigation of different constitutive soil models was carried out, which greatly broadened the knowledge of the author.

The review and critical discussion of relevant literature is an important part of this work and it is crucial to continue to study relevant literature and to challenge the new ideas and findings of this research with existing models and opinions.

As the literature review remained an ongoing process, and due to the great personal interest of the author in the field of screw auger piles, some new components about rigid inclusions were added to the thesis during 2013. In France, a research project about soil improvement with rigid inclusions (ASIRI project) was finalised in 2011. As the majority of rigid inclusions are installed using screw auger displacement tools of different shapes and geometries, some of the findings and background knowledge of the ASIRI project were relevant for, and thus included in, this work.

This thesis and the publications arising from it are an important step to stimulating future research in this area. It will also help to guide future researchers in their literature reviews and help to inform their research efforts.

6.2 Finite element modelling

After the completion of the general literature review, the field tests were prepared. It was intended to install different monitoring equipment to measure stresses and displacements in the soil during the installation process of different screw auger (displacement) piles in stiff clay. To evaluate the stress and displacement fields around the piles during installation, a basic numerical model was developed to simulate the installation of a rigid body into a stiff cohesive clay formation.

This numerical model was not intended to model the installation process in detail, but rather to provide an understanding of the stress field and the displacement during the installation process, to help to locate the monitoring equipment correctly around the individual test piles.

For the numerical simulation of the 4.0 m penetration and extraction of a screw auger displacement pile into stiff Lawnton Clay, the FE code Abaqus Standard was used. Hypo-plastic soil behaviour for fine-grained soil (clays) after Mašín was implemented using an UMAT (user material) routine. An axisymmetric, two-dimensional FE model was developed to simulate the process, and this model was found to simplify greatly the real geometry and process. It was evident that, when modelling the complex penetration of a screw piling auger into any soil formation, current FE codes and hardware applications are not capable of considering the cutting, transport and displacement processes and allowing for the rotation and vertical movement of the auger. The simplified penetration of a cone-shaped rigid body only 4.0 m into clay took the program around 10 hours to calculate. Therefore, the author decided instead to choose a greatly simplified installation simulation with an advanced constitutive soil model. It was decided that hypo-plastic soil behaviour should be used to analyse the penetration of the rigid body (to simulate the auger). Hypo-plasticity is a nonlinear constitutive theory that is able to describe dissipative behaviour, plastic flow and nonlinear effects with a single tensorial equation (Niemunis 2002).

The FE model was developed in cooperation with the Technical University of Dresden (Germany), generously funded by a DAAD/Go8 scheme in 2011 and 2012.

6.3 Field and laboratory tests

Prior to the development of the numerical model, initial soil investigation was carried out at the proposed field test site in Lawnton. In February 2011, two initial CPTs were conducted at Lawnton. These were accompanied by two boreholes (BH1 and BH2) providing undisturbed soil samples next to the CPT locations, reaching about 3.0 m below the proposed design toe level of the test piles. The undisturbed soil samples were used in laboratory tests to determine the index values and soil parameters for the hypo-plastic soil model and pile design at a later stage.

6.4 Field tests at Lawnton

The field test site at Lawnton is located in the yard facility of Piling Contractors Pty Ltd, one of the industry partners of this research. Piling Contractors made an area available and provided sufficient access and a granular working platform for the safe operation of piling equipment and heavy machinery during the tests.

Prior to the commencement of the tests, pile design analysis was carried out using the α-cu method as well as the method after Bustamante and Gianeselli (1998) using the parameters determined by triaxail tests (refer to 7.2.1 and 8.2.1). The anticipated pile loads varied from 427 kN to 1,006 kN (refer to Table 13 and Table 14) geotechnical capacity for the 4.0 m deep piles (diameter of 450 mm).

Also before testing, the required monitoring equipment was purchased and assembled, and safe work method statements and risk assessments for the different activities on the field test site were developed and communicated with all personnel involved in the tests.

Overall, four test piles were installed to a depth of 4.0 m into stiff Lawnton Clay. Three different piling augers were used:

(i) Screw auger piling partial-displacement auger (CFA);
(ii) Screw auger piling progressive displacement auger; and
(iii) Screw auger piling rapid displacement auger.

This third auger type was used to install the fourth test pile (pile A) to calibrate the results if necessary and to prove repeatable results. Unfortunately, the pile was damaged during the tests and no valid results were retrieved.

After completion of the numerical model, the locations for the monitoring equipment were finalised. It was decided that inclinometers would be used to measure the soil displacement, and three inclinometers were installed per test pile location in varying distances from the pile axis.

The same distances were used to carry out the CPT and DMT tests after the pile installation, to measure the stress changes in the soil before and after pile penetration and extraction. The initial CPT and DMT measurements were carried out at the pile location prior to pile installation.

The stress changes during pile installation were monitored by raked CPT cones, which were left in the ground 225 mm from the pile edge, about 1.5 m below surface level. During the pile installation, the soil was pushed against the stationary cone and the stress changes and pore water pressure

changes in the soil formation were measured. The displacement of the surface (heave) around each pile was also measured and recorded.

In July 2013, a few months after the pile installation, the initial four piles were load tested using static load tests with reaction piles. The tests were conducted in line with AS2159-2009 (Standards Australia 2009), although a few minor modifications were made for primarily practical reasons.

In addition, another heave test was carried out to collect further detailed results. The heave measurements during the tests conducted in February 2013 were taken using minimal survey points, as no significant heave was expected in stiff clay. However, this was a wrong assumption. The new heave tests consisted of drilling an un-instrumented fifth test pile (pile E) with a rapid displacement auger to the same design depth of 4.0 m for the sole purpose of measuring the heave. Another, more powerful piling rig was used, as the original rig was not available.

Unfortunately, this test pile was damaged after construction and could not be load tested. However, theoretical comparisons of the CPT readings of the pile were made with the readings at the other test pile locations and back calculations of the static load tests were used to estimate the load capacity of test pile E.

6.5 Data analysis and formulation of results

After completion of the initial test piles in February 2012 (just a day before the annual wet season started), the analysis of the field test site data commenced. The CPT graphs of the initial test piles and the additional test pile E (installed in July 2013) were analysed and plotted against each other to show the difference in stresses before and after installation for each pile. The installation parameters of each pile were analysed and plotted and the stress changes during penetration were studied in detail. The displacement (vertical and horizontal) was examined and plotted to allow for meaningful comparisons.

Further, the static load test results (carried out in July 2013) were studied and back calculated to determine the base and shaft capacities for each pile. The CPT results after pile installation were compared with the initial results and the conclusions and recommendation for further research were formulated. The results and recommendations resulting from this research are summarised in Chapter 11 of this thesis.

The next chapter details the research methodology employed in this research project.

CHAPTER 7: RESEARCH METHODOLOGY

7.1 Finite element analysis

7.1.1 Hypo-plasticity

Constitutive models are used in numerical and FE analysis to describe the mechanical behaviour of a soil, relating stress and strain or their respective rates. Besides stresses and strains (which are both tensorial quantities), additional parameters such as material constants and state variables are used in constitutive equations. Reliable constitutive models are required to describe material behaviour as accurately as possible. Hypo-plasticity is a nonlinear constitutive theory that is able to describe dissipative behaviour, plastic flow and nonlinear effects with a single tensorial equation (Niemunis 2002).

Several hypo-plastic constitutive models express the stress rate as a function of a given strain rate and the state variables of stress and void ratio. Provided T denotes the tensorial quantity stress, D denotes the tensorial quantity stretching tensor and e denotes void ratio, this can be expressed by the general form of the hypo-plastic equation (Kolymbas 2001), as stated in Equation 10 below:

$$\dot{T} = \quad h(\dot{T}, D, e) \tag{10}$$

The basic stress–strain rate relationship is expressed in Equation 11 (Gudehus 1996):

$$\dot{T} = \ f_s \ (L : D + \ f_d \ N \ \|D\|) \tag{11}$$

with L and N being fourth- and second-order constitutive tensors and f_s and f_d representing two scalar factors, known as the barotropy (influence of stress level) factor and the pyknotropy (influence of density) factor, respectively. The hypo-plastic relationship expressed in Equation 11 seems simple, as there is only one equation for loading and unloading. It assumes non-elastic deformations occurring from the beginning of the loading process. Hypo-plasticity does not distinguish between elastic and plastic deformations.

Hypo-plasticity after Mašín

Research on hypo-plastic models started more than 20 years ago. Many of the early models were developed by researchers of the University of Karlsruhe in Germany and focused on granular materials (von Wolffersdorff 1996, Niemunis and Herle 1997). However, hypo-plastic models for clays have since also been developed (Niemunis 2002, Herle and Kolymbas 2004, Mašín 2005).

Mašín's (2005) hypo-plastic constitutive model for clays, which has been used for modelling the clay for this research project, is based on the general approach to hypo-plasticity developed at Karlsruhe. Mašín's basic model requires only five constitutive constants, which can be determined from standard laboratory tests. Despite this simple and practical approach, several effects of nonlinear soil behaviour are described by the model: (i) the variation of stiffness during loading and unloading; (ii) the influence of relative density (over-consolidation ratio [OCR]) on the stiffness, contractancy and dilatancy in the volumetric behaviour; and (iii) the dependence of peak friction angles on the state.

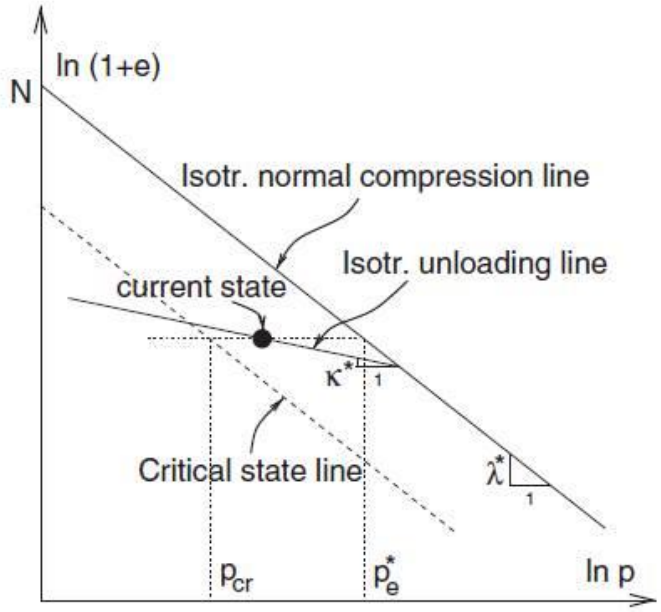

Figure 46 – Definition of parameters N, λ* and κ* (Mašín 2005)

The basic model comprises several principles of critical state soil mechanics. It also uses a similar set of five constitutive constants determined by standard laboratory tests. The interpretation of the parameters is similar to in the modified Cam Clay Model (Roscoe and Burland 1968).

Parameters N and λ* define, respectively, the position and slope of the isotropic normal compression line (Figure 46), following the formulation of Butterfield (1979), stated in Equation 12:

$$\ln(1+e) = N - \lambda^* \ln(p/p^r) \quad (12)$$

The parameter, κ*, controls the slope of the isotropic unloading line (Figure 46).

Further information about Mašín's hypo-plastic constitutive model for clays and further refinements of this model can be obtained from Mašín (2005) and Mašín and Khalili (2008).

7.1.2 Numerical model

For the definition of the location of the proposed field monitoring equipment and the numerical simulation of the penetration and extraction of a screw auger displacement pile, the FE code Abaqus Standard was used. Hypo-plastic soil behaviour for fine-grained soil (clays) after Mašín was implemented using an UMAT (user material) routine. The soil parameters for the hypo-plastic analysis were obtained by laboratory tests and further details are provided in sections 7.1.1 and 8.1.1. An axisymmetric, two-dimensional FE model was developed to simulate the process, with this model greatly simplifying the real geometry and process.

The drill head of the screw auger displacement pile was modelled as a cone-shaped rigid body, with a 60-degree cone angle and a total auger height of 1.5 m, representing the lower, tapered auger section of a full-displacement screw auger drill head up to the displacement body. As the soil cutting and transport process of the auger has not been modelled, it was assumed that the auger flights would stay completely filled with soil throughout the process. To avoid excessive mesh distortion at the beginning of the penetration process, the cone was partly pre-installed into the soil and the soil and the cone were modelled to be in full contact before penetration commenced.

In the past, the 'zipper technique' method has been used successfully (Cudmani 2001, Henke 2010) to model pile penetration into a soil continuum. Using this method, a smooth rigid tube with a diameter d = 1 mm was discretised at the axis of penetration. The cone-shaped, rigid screw auger displacement body slid over the rigid tube and separated the soil from the tube. The cone established contact with the soil and was able to deform the meshed continuum, thus simulating penetration and the resulting soil displacement. The surface-to-surface contact between the penetrating object (screw auger displacement auger) and the surrounding soil was based on the master–slave principle. The friction coefficient between the deformable soil and the piling auger was assumed to be tan (φ_c / 3), based on Coulomb's friction law.

The diameter of the displacement auger head was taken to be 450 mm and the penetration depth into the soil continuum was taken to be 4.0 m. Pile installation was modelled progressively with constant penetration and extraction rates of 0.03 m/sec (equivalent to 1.8 m/min, refer to section 8.3.1 and Figure 94). However, since the constitutive model is rate-independent, the rates were of no impact. Soil behaviour has been assumed to be undrained during penetration (constant volume), as penetration occurs too rapidly to allow substantial drainage.

Four-node bilinear axisymmetric mesh elements (CAX4) were used to represent the soil continuum, and unacceptable mesh distortions were avoided due to the use of an adaptive meshing technique (re-meshing rule). Small strain was assumed by the FE code to allow for sufficient mesh deformations.

The model could not be used with elastic-plastic constitutive laws, as the mesh distortion proved excessive and the simulation was aborted by the program after a penetration of less than 10 mm.

The stress field, soil displacements and pore water pressures needed to be obtained during screw auger full-displacement pile installation for the entire installation process up to the point of reaching the design depth as well as during the extraction process up to surface level.

The reliability and verification of the suitability of the proposed FE model and the methods adopted was difficult as Abaqus was the only FE software available to the candidate, which was able to simulate the penetration process of a cone shaped body into a soil continuum.

7.2 Laboratory tests

Soil samples were taken at the field test site at Lawnton (QLD) to determine the soil profile of the test location and to find the relevant soil parameters of the Lawnton Clay as shown in Figure 47.

Figure 47 – The field test site at Lawnton during early soil investigation works

The soil samples were taken at two locations at the field test site, which were spaced about 4.50 m apart. BH1 was investigated up to 8.50 m below the surface, while the second location at BH2 was explored up to 7.25 m depth (refusal). Soil samples were obtained by pushing 50 mm diameter steel tubes of 450 mm length into the ground to acquire undisturbed soil samples for further laboratory testing, as shown in Figure 48.

Figure 48 – Steel tubes were pushed into the ground to obtain undisturbed soil samples

The individual steel tubes were sealed to avoid moisture loss. They were then labelled for future reference on the outside of the tube with the borehole identification and the depth of the soil probe (Figure 49).

Figure 49 – Labelling of the undisturbed soil samples on site

After completion of the soil investigation on site, the sealed tubes were delivered to the soil laboratory in Brisbane and tests were conducted to profile the soil formation and determine the most important soil parameters like undrained shear strength and Young's modulus.

Further, CPTs were carried out in the direct vicinity (a distance of about 500 mm) of the two boreholes. The CPT data were correlated to the undisturbed borehole data and were mainly used to confirm the soil profile of the test site. This is discussed in more detail in Section 8.4.2.

Details of the borehole locations with respect to the initial CPTs and the relevant test piles are displayed in Figure 52 in Section 7.4.1.

7.2.1 Triaxial tests

Triaxial tests are used to test cylindrical soil specimen, typically of 50 mm in diameter and with a height to diameter ratio of about two. The soil sample is subjected to a constant all-around pressure, defined as the cell pressure or confined pressure.

There are three test types for the triaxial test, each of which can be used to determine the strength parameters of the relevant soil specimen.

For the unconsolidated undrained (UU) test, the saturated soil sample is unable to drain itself for the entire duration of the test. The confining stress σ_3 is applied to the specimen, allowing no initial consolidation and axially loading until failure. With no drainage or consolidation required, this test is quicker than the other two types, and is applicable for most practical situations (i.e. foundations). In the UU test, the internal friction angle is typically $\varphi = 0$, with the undrained cohesion calculated from the test results. The peak strength is measured from the deviator stress versus axial strain diagram.

In the consolidated drained (CD) triaxial test, the application of the confining lateral stress σ_3 causes a reduction in volume of the soil sample. By leaving the drainage lines open until full consolidation is achieved (pore water pressures are zero), the specimen is axially loaded under full drainage and consolidation until failure occurs. The test is run numerous times with varying confining lateral stresses and is applicable for conditions in which the soil is expected to fail under a long-term constant load with drainage allowed (Dettman 2010).

The consolidated undrained (CU) test is similar to the CD test, in that the applied confining stress compresses the sample, causing volumetric decrease. However, the drainage pipes are only left open until initial consolidation is achieved. After initial consolidation, they are closed so that no drainage can occur within the test specimen. The soil sample is then loaded axially under deviatoric stress until failure. This test is also repeated under differing confining stress conditions (100kpa, 200 kPa and

400 kPa for this research project) and is used to determine soil parameters in cases in which sudden failures may occur. The results are typically displayed in a τ v. σ_n space using stress–strain diagrams.

To determine the strength parameters for this research project, CU tests were used to simulate the conditions inside the soil formation. The penetration of the screw auger occurred quickly, with the soil having no time to drain, and initial consolidation occurred under the load applied by the auger.

Although the earth pressures induced in the soil by the displacement tools during penetration could be larger than 400 kPa, the maximum confining stresses applied during the laboratory tests was selected at 400 kPa as no data were available at the time of the geotechnical investigation and soil sampling undertaken at the site.

Tests were conducted for soil samples collected in two different boreholes and the soil modulus was determined for every meter of depth. The CU results were also used to determine the parameters for the hypo-plastic soil model (section 7.1.1).

7.2.2 Oedometer test

The hypo-plastic soil parameters of the fine-grained soil samples collected at the field test site at Lawnton were determined by one-dimensional compression tests carried out in oedometers.

7.3 Pile installation

For the installation of the test piles, three different augers were used (Figure 50). The dimensions and other important details of these augers are displayed in Table 2.

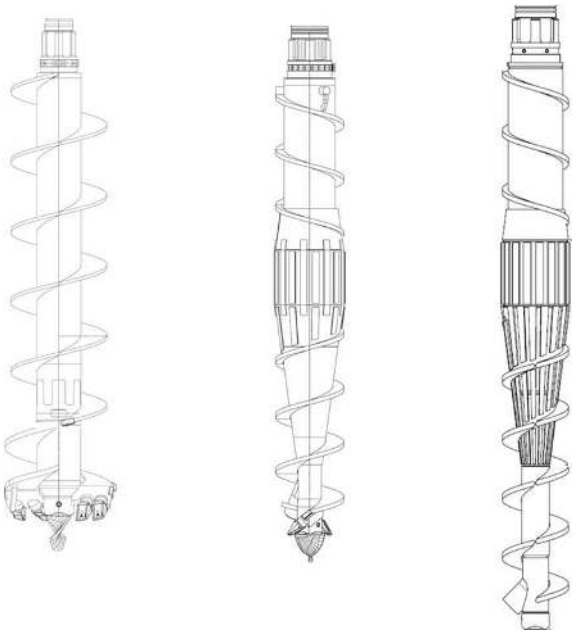

Figure 50 – The three different auger types used for this research project: CFA auger (left), progressive displacement auger (centre) and rapid displacement auger (right)

Table 2 – Auger details

Auger Details	***Continuous* Flight Auger (PILE B)**	***Progressive* Displacement Auger (PILE C)**	***Rapid* Displacement Auger (PILE D & E)**
Outer diameter (flights and displacement body)	500 mm	450 mm	450 mm
Inner stem diameter (inner tube at the bottom)	318 mm	250 mm	250 mm
Height			
Lower Section	N/A	1,000 mm	1,500 mm
Displacement Body	N/A	500 mm	500 mm
Counter Screw Section	N/A	1,000 mm	1,000 mm
Total	**9,000 mm**	**2,500 mm**	**3,000 mm**
Height Flight Pitch	300 mm	250 mm	250 mm
Bottom Flight Pitch	300 mm	100 mm	100 mm

Pile B was installed using a 500 mm diameter CFA. The inner stem was 318 mm in diameter and the ratio between inner stem to cutting diameter was 0.63 (refer to Table 1 in Section 2.3). This auger can also be referred to as a partial-displacement auger due to the relatively thick inner stem diameter compared to the outer flights. The shape of this auger is fundamentally different from that of the full-displacement augers used to install piles C, D and E. The CFA auger has improved soil transport characteristics during the installation process and soil resistance is expected to be smaller than for screw auger full-displacement piles.

Pile C was installed with a progressive full-displacement auger. Soil cutting occurred at the pile base and the soil was transported inside the flights of the tapered short lower auger section towards the displacement body. At the displacement body, the soil was pushed at the borehole wall resulting in a re-moulding of the clay (Van Impe 1988).

Depending on the degree of the re-moulding process, the soil can be strengthened, as mentioned by Van Impe (1988), provided the stresses applied to the borehole wall are smaller than the applied stresses that push the displaced soil against the borehole wall. When progressive screw auger full-displacement piles are used, the soil is transported and progressively displaced immediately after cutting at the auger tip. Typically, the resistance during the installation process is very high with this auger type.

Piles D and E were installed using a rapid full-displacement auger. This auger had a longer lower auger section, comparable to a CFA auger section. The soil was cut at the auger tip and transported inside the lower auger section towards the displacement body. Soil displacement towards the borehole wall did not occur immediately after cutting; first, the soil was transported for 500–700 mm upwards inside the auger flights. When the displacement body was reached, the soil was pushed

towards the borehole wall rapidly. This process can cause high drilling resistance, which, for rapid full-displacement augers is typically lower than for progressive full-displacement augers but considerable higher than for CFAs. For rapid full-displacement augers, the displacement body has a larger diameter than most sections of the inner auger stem of the lower auger section (the flights have the same diameter as the displacement body). Soil displacement occurs rapidly at the displacement body and only minor displacements are expected below it. Potential soil loosening might occur (in granular soil) along the lower section of the auger if penetration rates are too slow or are not optimised for the ground conditions encountered.

The overall height of the rapid displacement auger used for this research was about 500 mm more than the height of the progressive full-displacement auger, mainly due to the longer lower screw section of the rapid displacement auger.

Both augers have identical outer diameters (450 mm), but the taper from the displacement body to the smaller inner diameter at the auger base is different. The progressive displacement auger is tapered over three pitches (about 750 mm) while the rapid displacement auger is only tapered only two pitch heights (about 500 mm), which explains its more rapid displacement process.

7.3.1 Pile monitoring records

Modern piling rigs are fitted with electronic and mechanical sensors and measurement devices to monitor construction parameters during the execution of screw auger piles. In Figure 51, the typical positions of standard sensors measuring the required construction parameters (depth, rotational torque, rotations of the auger stem, vertical pull-down force, penetration rate and time, drilling depth, concrete pressure and concrete volume) are illustrated after Scott et al. (2006).

However, the positions and working principles of the sensors might vary, as different rig manufacturer use different construction monitoring technology. It is necessary that construction records be taken for every pile on site and that pile execution is electronically documented. During pile execution, the data are displayed on a computer screen in the cabin of the piling rig observed by the operator, as illustrated in Figure 23 in Section2.5.1. These data can be accessed at any time and downloaded in the office using remote transmission technology. Modern state-of-the-art monitoring systems are equipped with this technology and the monitoring data can be displayed ‘live’ during execution on the monitor in the office if a suitable internet connection is available. All these installation parameters are interrelated and must be analysed in combination. It is important for all parameters to be well balanced during the pile execution. The most important parameters are introduced below.

Depth, penetration rate and extraction rate

The progression and depth of the auger tip in the ground is measured by depth meters, which measure the length of a cable fed out as the drill head travels down the mast. This is the most widespread type of depth measurement device. The cable length is measured by counting the number of turns of a guide wheel attached to the top of the mast. Depth, penetration and extraction rates of the auger can be calculated, as the diameter of the wheel is known. Depth measurement is important for the identification of the design toe level and the sensors should be calibrated before the start of every shift to ensure that measurements are correct. In some cases, extreme temperature changes or fatigue can cause elongation of the cable, resulting in incorrect depth and auger progressing data.

The knowledge and measurement of penetration and extraction rates is of great importance, as penetration should be kept constant to achieve a continuous auger cutting and transport action. Decreasing penetration rates with constant rotations indicate a risk of potential soil decompression along the pile shaft, particularly in granular soil conditions, as described by Viaggiani (1993). In his opinion, this risk is negligible for the installation of screw auger displacement in cohesive soils. This research work will investigate the accuracy of this statement.

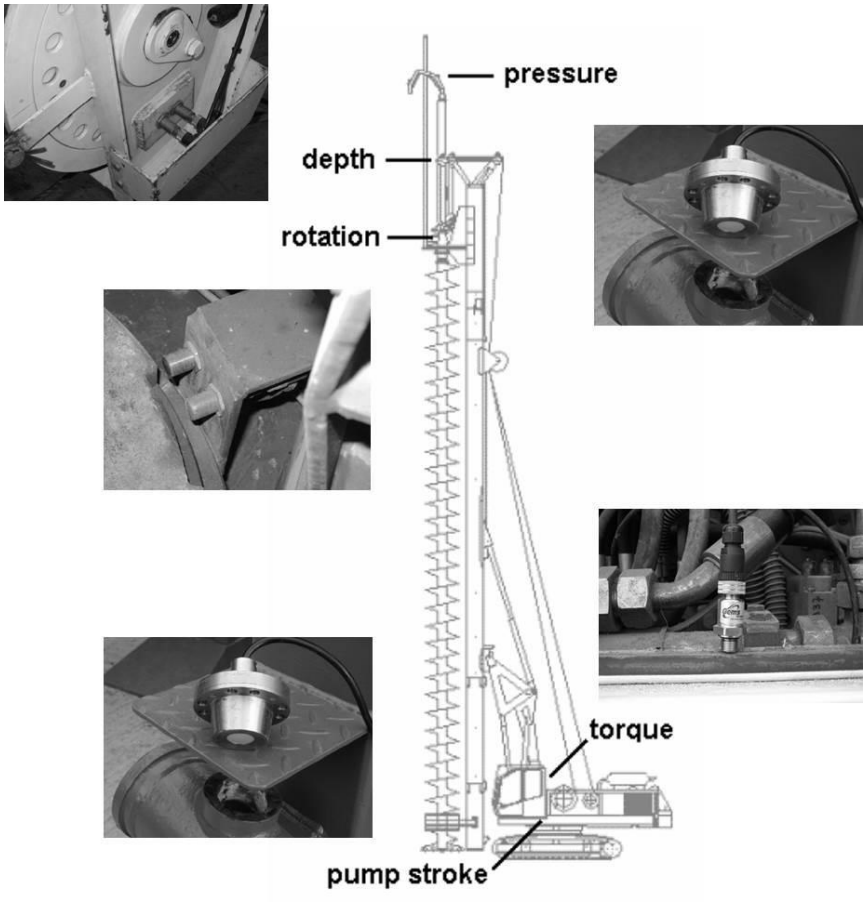

Figure 51 – Typical position of standard sensors for screw auger pile monitoring (Scott et al. 2006)

Penetration rates are sometimes used to identify hard or dense soil layers. Despite some authors' (Derbyshire et al. 1989, Slatter 2000) experience that penetration rate is a more reliable indicator of drilling conditions than torque measurement, progressing rates of augers should always be considered in combination with rotational torque readings.

The combination of constant penetration rates and increasing rotational torque readings might be an indication of dense/stiff soil layers, but should not be used as definitive evidence, as augers work differently than do static cones. Boreholes or other soil investigation data should be considered for final statements. In the author's opinion, all screw auger piles should be installed with pre-defined and project-specific penetration rates, regardless of auger configuration or soil conditions to balance the soil cutting, transport and displacement actions during the penetration process of the drill tool.

Extraction rates should also be kept constant, with these data requiring analysis in conjunction with concrete pressure and volume. Increasing extraction rates and falling concrete pressure might indicate potential integrity problems (necking), whereas decreasing extraction rates might cause increased concrete pressure, which might force the concrete inside the cavity to escape upwards, passing the auger.

Rotational torque

Rotational torque is usually monitored by direct measurement with a load cell located between the drive head and the auger stem, or by comparing the hydraulic pressure applied to the rotary head expressed as a percentage of the total torque capacity.

Bustamante and Gianeselli (1998) point out that torque capacities are of greatest importance to maintain constant penetration rates for screw auger piles, as rotational torque can be used as an indicator for auger resistance in the soil. They generally point out (but do not provide further details) that the shape of the auger head and the ground conditions are the most important factors in how much penetration energy must be activated to install a screw auger with constant penetration rates.

It is critical for all types of screw auger piles (non-, partial- or full-displacement piles) that rigs with sufficient rotational torque capacities are used for pile installation. This is particularly true in granular soil conditions, to avoid soil decompression and uncontrolled lateral soil transport.

If rotational torque increases, the penetration rate should be held constant to ensure the constant cutting and transport action of the screw auger. Unfortunately, piling rig operators, aiming not to want to overload or damage their machines, often reduce penetration rates when rotational torque readings increase, despite the machines having sufficient torque capacities. An increasing rotational torque reading usually indicates the penetration of a dense or stiff soil layer.

A potential problem with the latest generation of piling rigs that provide torque capacities of up to 500 kNm is the ability to snap off the auger connection to the hollow stem when the auger resistance becomes greater than the structural strength of the connection. Modern rigs can be so powerful that the drilling equipment can become the weakest part. Operators are trained to avoid material damages under all circumstances, as they result in additional costs and delays. It is important for operators to control torque readings carefully and to find the balance between maintaining a constant installation rate and the avoidance of equipment damage.

Vertical pull-down force or thrust

If rotational torque capacities together with auger self-weight are insufficient to establish or maintain constant penetration, additional pull-down forces need to be activated by the rig operator. These extra forces should only be used to establish constant penetration or extraction rates. Pull-down forces are usually measured by comparing the hydraulic pressure required for pull-down actions expressed as a percentage of the total pull-down capacity.

Rotation of the auger

Auger rotations are usually measured by a device that is mechanically activated by a pin attached to the auger stem. At each full rotation of the auger, the device is activated to count the rotation. Alternatively, a laser device can be activated at each full rotation by a reflector attached to the auger stem. Auger rotations should be constant during the piling process to ensure a constant transport rate of the soil inside the auger flights. During the pile extraction, no rotation of the auger (for CFA piles) should occur, as auger rotation during auger extraction can cause significant concrete overconsumption (the concrete pumped through the hollow stem is transported to the surface by the rotating auger) and insufficient concrete pressure, potentially leading to a deficiency in the integrity of the pile shaft.

Concrete pressure

Typically, two concrete pressure requirements must be met for screw auger piling applications:

- Concrete must be pumped from the concrete pump to the drill head of the rig at the top of the mast. Usually, pressures of 10–25 bars are required for this task; and
- Additional concrete pressure is necessary for the construction of the pile shaft and is measured as an installation parameter. This pressure is usually in the range of 1–5 bars.

The device to measure the concrete pressure usually consists of a disk-shaped membrane mounted to the concrete line, which is linked to the computer system of the rig. The calibrated membrane is

shifted by the concrete pressure in the supply line and it transmits the current pressure in the system. Concrete pressure cells are usually located close to the drill head or on top of the hollow auger on the 180-degree bend of the steel supply line, also referred to as the 'swan neck'. Such pressure cells can only be used when the supply lines and auger stem are filled with concrete. The cell will register positive concrete pressure while concrete is pumped through the stem.

If the hollow auger stem is not completely filled and concrete is free falling through the measuring device, negative or zero concrete pressures will be registered at the drive head of the rig. However, this does not indicate that the concrete pressure at the auger tip is also zero or negative; the hollow stem could be partially filled with concrete, causing positive concrete pressure at the auger tip. In this case, the monitoring program would indicate zero concrete pressure and a possible pile-necking issue in the area of the auger tip. This issue can be avoided by pumping concrete with excellent workability criteria continuously through the supply lines, without any air pockets.

Concrete pressure is an important indicator during the auger extraction and concrete placement process. Ideally, this pressure should be kept constant throughout the pouring process. The concrete pressure inside the stem must be positive at all times to maintain the integrity of the pile shaft.

A positive concrete pressure usually indicates that the auger tip is embedded in the fresh concrete and that the concrete pressure inside the bore is equal to the horizontal stresses at the bore wall. A negative concrete pressure might indicate that the auger tip is not embedded in the fresh concrete, indicating the risk that wall collapse might occur inside the gap between the auger tip and the surface of the concrete column inside the pile excavation. This condition must be avoided, as it will generate defective piles.

Concrete volume

Concrete volume is usually measured by flow meters attached to the concrete supply line of the rig. Typically, these meters are fitted to the rig externally and the velocity of the concrete flowing through the line is measured using electromagnetic techniques. Slatter (2000) points out that concrete travels as a plug inside a supply line. This plug is assumed to be in motion as one piece, separated from the supply line by a thin boundary layer of grout.

It is important to calibrate the flow meter occasionally to ensure that concrete volume is being correctly recorded. This is usually achieved by counting the strokes of the concrete pump, knowing the volume of concrete that is pumped per blow and comparing this value with the volume measured by the flow meter.

All test piles installed for this research project were constructed using automatic installation records. The rig monitoring system 'Jean Lutz' was utilised in the piling rigs that installed the piles on the field test site and the required data as introduced in this chapter were collected and are presented in Chapter 8 of the thesis.

7.4 Field test observation methods

7.4.1 Layout details

The three initial test piles were installed in February 2013 following a triangular pattern, as shown in Figure 52. Test pile A was not used; the location was intended as a backup if required. Test pile E was installed in July 2013, about four months after the installation of the other piles, and the location is indicated in Figure 52.

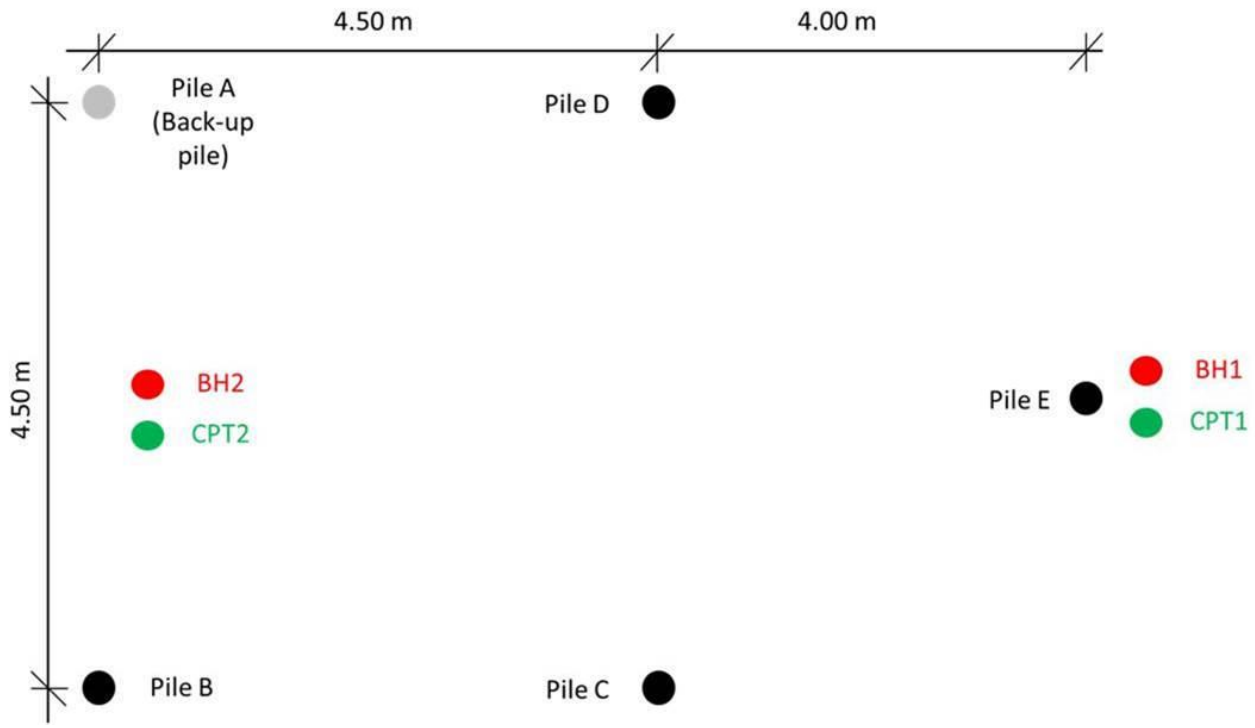

Figure 52 – General layout of pile locations for test piles B, C, D and E

The test piles were spaced at a distance of 4.50 m from pile centre to pile centre (equivalent to 10 pile diameters), based on the assumption that the influence ratio would be below this value, particularly in stiff or hard clay formations. In the author's personal experience, the influence ration of displacement piles is assumed as three to five pile diameters per pile.

Pile E was installed about four months after the installation of the other test piles (at the CPT1 location) using a rapid displacement auger. The initial purpose of installing pile E was to investigate the heave or vertical displacement of rapid displacement augers. Heave measurements were taken for

piles C and D before and after installation; however, survey points were only taken in two axes across the piles. Therefore, pile E was to be used to obtain additional data using four axes.

Pile E was installed without inclinometers, TDR, DMT or raked CPT instrumentation, and no static load test was executed after installation. A single vertical CPT was carried out before installation at the pile axis (CPT1) and two CPTs were taken after installation 225 mm off the edge of the pile shaft at opposite sites. Heave measurements were also taken.

For operational reasons (i.e. the original rig was not available), test pile E was installed with a different piling rig: a much stronger and more powerful Bauer BG28 rig with automated drill assistant. The results are discussed in Chapter 8.

The initial boreholes, BH1 and BH2, as well as the corresponding CPT locations, CPT1 and CPT2 (Figure 52), were carried out in February 2011. The CPT positions were located about 500 mm from the boreholes and the boreholes were located about 4.50 m from each other, with equal distances to the relevant pile locations.

CPT and DMT tests were carried out close to the pile axes of each individual test pile before pile installation to determine the *in situ* stresses in the soil formation.

Spatial time domain reflectometer (TDR) pressure sensors (Scheuermann and Huebner 2009) were used for the first time to measure stresses in the ground during pile installation. The working principle, assembly, installation and measurement results of the TDR for this research project will be presented in a separate publication and are not part of this thesis. Nonetheless, the TDR sensors need to be mentioned here, as they influenced the location of the CPT, DMT and inclinometer tests around the test piles. The basic setup was similar for each pile location to give similar reference points for each pile and each test.

For the monitoring of horizontal soil displacements, a series of inclinometer tubes was installed around each test pile, as shown in Figure 53. The tubes were installed and grouted into 100 mm diameter holes, drilled by a subcontractor. Three sensors were lowered down each tube before and after the test pile installation to measure lateral soil displacements before and after the installation of the test piles. Measurements were taken every 100 mm over a depth of 6.00 m. It was important to measure potential changes below pile toe level, as the FE model indicates stresses up to 1.0 m below the proposed pile toe.

Figure 53 shows the general location of the monitoring equipment used for this research. Table 3 summarises the target locations and compares them to the actual locations as installed on site.

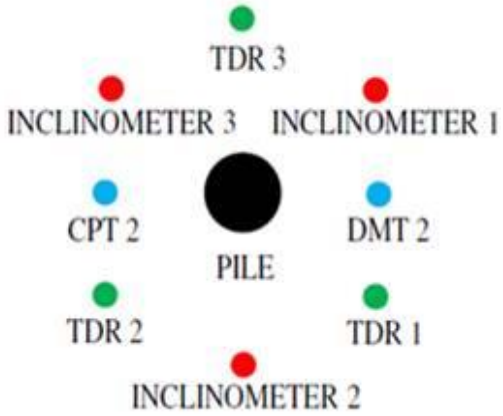

Figure 53 – Typical universal field test site layout for piles B, C and D to measure stresses and displacement during pile installation (not to scale)

The actual locations vary from the target locations owing to construction tolerances during the installation process, caused by obstructions in the working platform or inaccuracies during equipment set up. However, all tolerances are acceptable and it is not expected that these slight deviations from the target locations will significantly influence the monitoring results.

Table 3 – Target distance of the field test monitoring devices from each test pile

TEST	***TARGET DISTANCE***	
	Distance to pile axis	Target (mm)
CPT 1	0.00 d	0
CPT 2	1.00 d	450
DMT 1	0.00 d	0
DMT 2	1.00 d	450
Inc. 1	1.00 d	450
Inc. 2	1.25 d	563
Inc. 3	1.50 d	675
TDR 1	0.72 d	325
TDR 2	1.00 d	450
TDR 3	1.50 d	675

Note: TDR measurements are not discussed as part of this thesis.

CPT1 and DMT1 were installed at the proposed pile locations, somewhere within the 450 mm circular pile diameter. Both tests were carried out at opposite edges of the proposed pile location to achieve the greatest possible clearance and to avoid any interaction effects between the CPT and DMT tests. CPT2 and DMT2 for each pile were installed within 10 mm of tolerance from the target location, which is an acceptable value.

The inclinometer tubes were installed using small augers and the actual locations were within 15 mm from the target location, which is an acceptable tolerance. The TDR assemblies were installed up to 70 mm out of tolerance and the data are listed in Table 3, even though the test results are not part of this research.

The typical layout on site is shown in Figure 54. Each pile centre was marked by a nail (the red cross) and was connected by a string line to the other test pile centre locations. The TDR sensors were placed in holes, which were then back-filled with sand, and the inclinometer tubes were covered with red protective plastic caps.

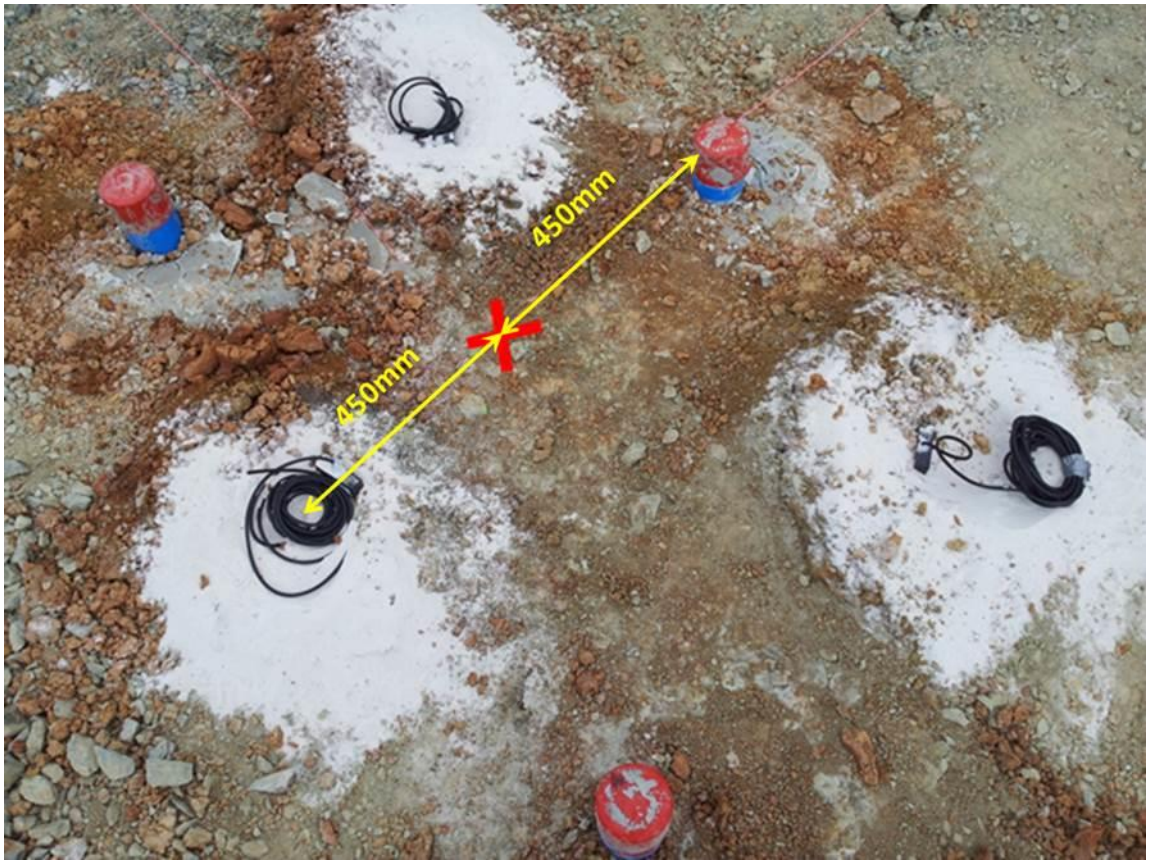

Figure 54 – Typical pile layout on site (Pile B) with inclinometer tubes and TDR

7.4.2 CPT

Cone penetration testing (CPT) is a fast and reliable method of conducting *in situ* soil exploration for support of embankments, retaining walls and pavement subgrades, or for bridge foundations and the determination of pile load capacities. The results produced by CPT should only be used in combination with borehole-sampling methods.

For the screw auger displacement research project at Lawnton, CPTs were carried out to determine the stresses in the soil formation before and after pile installation. Figure 55 shows the typical setup for the initial tests.

Figure 55 – CPT units at the field test site at Lawnton(vertical tests): truck-mounted CPT (left), cone (centre) and hydraulic jacking system (right)

These initial tests prior to pile installation were carried out at the pile axis, whereas the tests after the installation were conducted at 0.5 pile diameters (225 mm) from the edge of the piles. The CPTs were installed vertically at least 2.0 m below the pile toe design level, to measure the stresses below the pile base.

Raked CPT

Several authors have compared the stresses in the ground before and after screw auger displacement pile installation in granular (Slatter 2000) and cohesive ground conditions (Huybrechts 2001, Larisch et al. 2013) using CPT or DMT. Some authors have measured the stress changes during pile installation using DMTs (Slatter 2000, Peiffer 2008), but there is no evidence in the literature of stress changes during the installation of screw auger piles being measured with cone penetration (raked or vertical CPT) devices. The advantage of the latter technique is the inclusion of pore water pressure measurement during the installation process.

Stress changes in the soil formation during the installation of screw auger piles are an important indicator of soil behaviour and can provide vital information for the pile design.

For granular soil, several researchers (Slatter 2000, Schmitt and Katzenbach 2003) have proven that there is compaction around the pile shaft due to the installation process of screw auger full-displacement piles. Van Impe (1988) discovered the improvement of cohesive soils as a result of the installation process of screw auger full-displacement piles. As mentioned earlier, in Section 2.4.1 on Atlas piles, van Impe found that, during the installation of Atlas full-displacement piles in clay, the soil was displaced and re-moulded along the pile shaft, which resulted in improved shear strength of the displaced clay near the shaft. Laboratory tests on samples of the displaced clay indicated that the shear strength of these cohesive soil samples had significantly higher values than the surrounding natural soil. However, no installation records or other data were published by van Impe.

For the measurement of the stress changes in the soil formation during the installation of the screw piles at the Lawnton field test site, a raked CPT was installed, as shown in Figure 56.

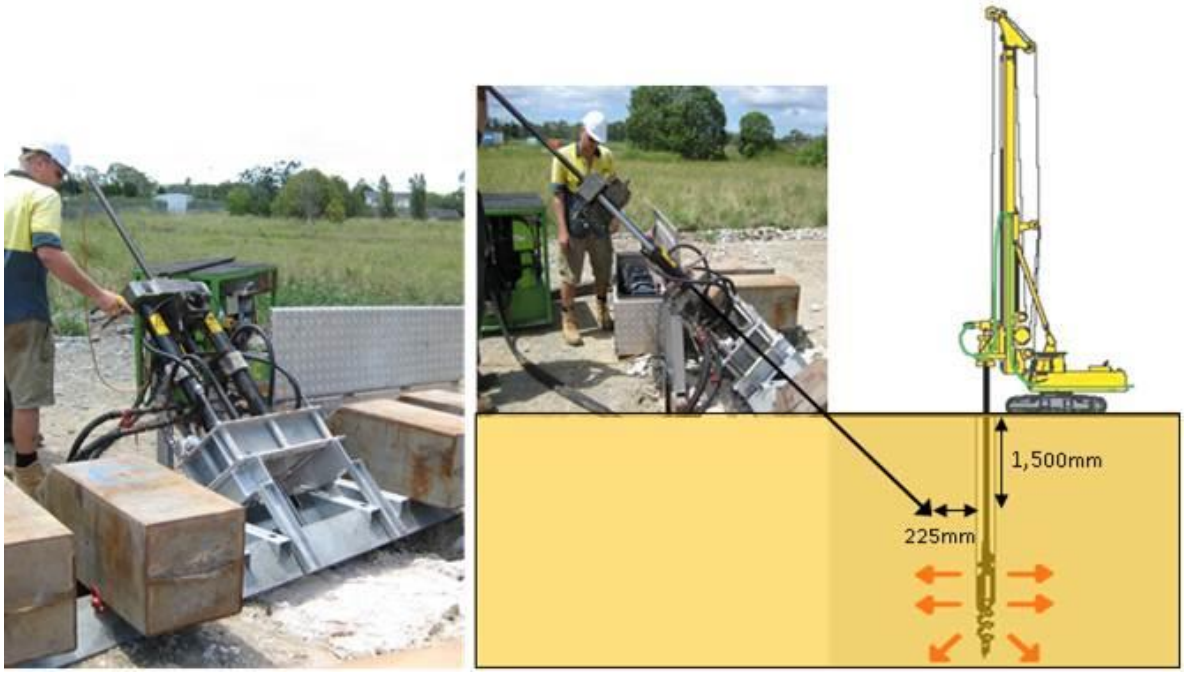

Figure 56 – Setup and schematics of the raked CPTs carried out at Lawnton

The 25 MPa CPT cone was installed at an angle of 45° and was left in the ground during the pile installation process. A purpose-built frame was designed and built by a sponsor of the research project, IGS. The idea behind this approach was to measure the lateral stress changes in the soil (total stresses and pore water pressures) caused by displacement of the soil during the pile installation process. Measurements were taken every five seconds and recorded manually. The distance between the tip of the cone and the edge of the proposed pile was selected to be 225 mm, which is equivalent to 0.5 pile diameters.

The raked CPT approach provides better results compared to stress measurements taken using a static DMT (Peiffer 2008), as it allows the pore water pressure in the soil to be measured. This is a major advantage over the use of the DMT or standard earth pressure cells. In particular, the latter require more effort to install, resulting in a potential disturbance of the soil around the test piles.

During the set-up process, as displayed in Figure 56 and Figure 57, the frame was lifted into place by an excavator or small crane. Then, four dead weights (concrete blocks) were placed on the frame to provide sufficient reaction forces during the operation of the 6 ton hydraulic jack. The cone was then pushed through the pre-excavated holes (the pre-excavation was necessary due to obstructions close to the surface) penetrating the working platform and the rods were extended as required.

Figure 57 – Raked CPT setup on site during the installation of a test pile (Pile C)

To allow for pore water pressure dissipation, the stationary CPT cone was installed 100 mm short of its final position, extracted and the cavity was filled with water. Then, the cone was reinstalled, pushed a further 50 mm into the stiff clay and left in that position overnight. The following morning, before the start of auger installation, the cone was pushed the remaining 50 mm to its proposed final position, 1.5 m below the surface and 225 mm from the edge of the planned pile location. This procedure ensured that enough time was allowed for the pore water pressure to dissipate so that the stress changes due to pile installation could be measured unaffected by pore water pressure caused during cone installation.

7.4.3 DMT

The DMT is a static penetration test used for *in situ* sampling of soils. The setup on site makes DMTs executable with a variety of field equipment. It can be used to determine design parameters such as undrained shear strength, friction angle, elastic modulus and permeability.

The test is initiated by inserting the dilatometer into the soil using steel rods to transfer the installation force. This can be done either by driving it with a hammer or static pushing. The method of constant penetration is preferred (Figure 58), as it has been shown that driving the dilatometer can significantly affect results, particularly in clay formations (TC16 2001).

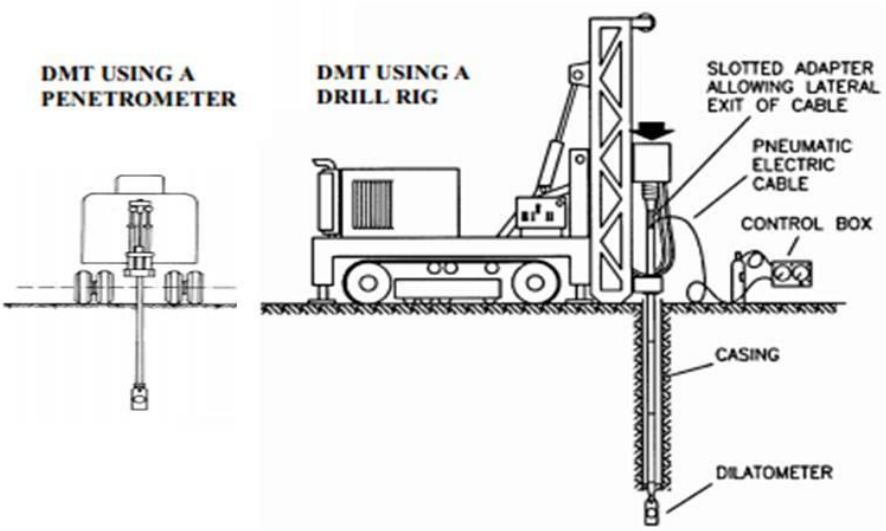

Figure 58 – Methods of constant penetration, after TC16 2001

A Flat Dilatometer test (DMT) was used to measure the *in situ* stresses in the soil before and after the installation of the screw auger piles. For test piles B, C and D, one DMT was carried out at the pile centre position prior to installation of the test piles. After the three test piles (pile B, C and D) were installed, additional DMTs were conducted at a distance of one pile diameter (450 mm) from the centre of the pile, to compare the stresses in the soil formation before and after pile installation.

7.4.4 Inclinometers

Inclinometers are geotechnical investigations instruments capable of measuring relative displacements. Inclinometer probes use accelerometers to measure tilt in two perpendicular planes, allowing for the determination of displacement magnitude and direction. The sensors are typically used in landslide investigations and to monitor slope stability, retaining structures, excavation walls, the settlement of embankments, the deformation of pavement bases and performance during tunnelling. Inclinometer casings are either installed within vertical boreholes with the base grouted in place to be used as a stable reference or installed horizontally and embedded into the surface.

Inclinometer casings for the field test site at Lawnton were installed to a depth of 6.0 m below the working platform, which is equivalent to 2.0 m below the toe levels of the test piles. It was desirable to detect any potential deflection below the pile toe to understand fully the displacement behaviour of the different screw auger piles.

Data acquisition units (or readout boxes) recorded the measurement data at each depth interval. The boxes feature an internal rechargeable power supply for prolonged use and can store large amounts of field data. Data management software was used to provide a communication channel between the

data acquisition unit and the computer, allowing for data to be edited, and for the production of simple graphs and tabular results.

Figure 59 shows a data readout unit consisting of a data logger used in combination with a multiplexer, allowing for the recording of data from more than one inclinometer probe at once. The data logger is programmed via software to collect data at designated time intervals using a wired or wireless system (Machan and Bennett 2008).

Figure 59 – Data readout unit used for the tests at Lawnton

The appropriate method of installing and testing strongly depends on the scope of the inclinometer readings. The drilling of the boreholes for the inclinometers is shown in Figure 60.

Figure 60 – Boreholes were drilled to install the inclinometer casings

Figure 61 – Installation of the inclinometer probes at Lawnton

For the field test site at Lawnton, traversing inclinometers were used to measure the horizontal displacements in the ground before and after pile installation. The probes were lowered down inside the casings before the pile installation to measure the 'zero' reading of the tubes (Figure 61). Then, the probes were pulled back out and the piles were installed. After the pile installation process, another reading was carried out to provide data on the soil movement during the pile installation.

7.4.5 Heave

Taking pile heave measurements was not a major research aim of this project, and the test piles were located so as not to interfere with each other (Ten diameters spacing between the piles). It was expected that the installation of the screw auger full-displacement piles into stiff and hard clay formations would cause failure mechanisms inside the soil formation, which causes vertical and horizontal soil movement during pile installation, as quantitatively shown in Figure 62.

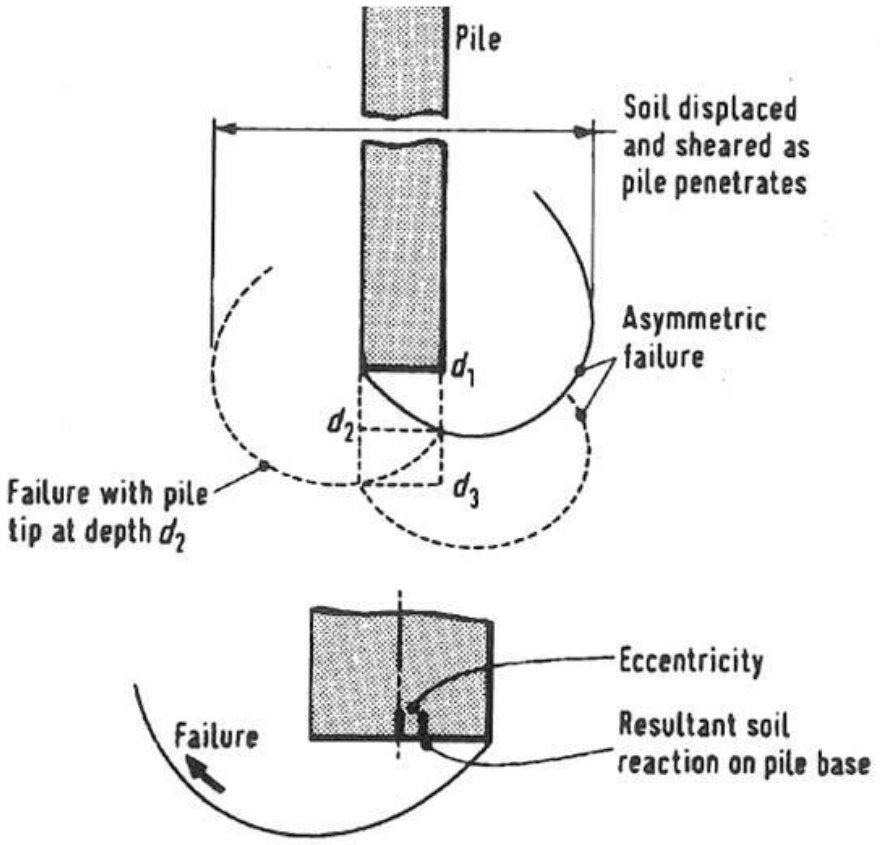

Figure 62 – Idealised mode of soil displacement and failure modes for displacement piles, after Hanna 1968

No detailed research has been carried out to date on the heave behaviour of stiff clay during installation of screw auger full-displacement piles. A few authors have investigated heave in cohesive soil conditions for driven piles, but this topic was not included in this research project. Therefore, heave measurements were carried out for the full-displacement tests piles C, D and E, both to monitor vertical soil movements and to provide test data for future research projects at UQ in this area.

For the measurement of heave or vertical soil movement, survey data were obtained and a series of surface points were measured before and after pile installation to obtain a magnitude of potential heave at each pile location, as shown in Figure 63.

Figure 63 – Heave measurements after pile installation were carried using standard survey equipment

For test piles C and D, only 10 points along one axis through the centre of each test pile were measured, spanning a radius of 1.0 m from the edge of each pile. The data were used to draw a heave profile for each pile after pile installation, meaning the heave profiles were based on 20 data points located on a single axis. Having only two representative axes of data points bears the potential risk of over- or underestimating vertical soil movements. Therefore, another test pile (pile E), using two additional axes, was installed, to increase the number of heave profiles to four and confirm the data acquired by the tests for piles C and D.

The layout for the heave measurements for test pile E is shown in Figure 64. The survey points were located in 100 mm intervals up to 1.0 m from the pile edge. Each point was surveyed prior to installation using dumpy levels, and this procedure was repeated after pile installation.

Care needed to be taken after pile installation, as some data points were covered by spoil. These data points were left out so that only freely accessible data points were used for the data collection. Finally, all acquired data were summarised and an average heave profile was prepared for each individual test piles installed for this research project (section 8.4.5), except for test pile B.

Figure 64 – Survey points for the determination of vertical soil movements during pile installation at four different axes for test pile E

Test B was installed using a CFA auger. Due to the spoil creation during the pile installation process, no noteworthy vertical pile movements were measured as the survey points were covered by drill spoil. As the majority of the soil volume is transported to the surface by the auger flights of the CFA, only minimal (assumed to be negligible) vertical soil movement was expected.

7.5 Pile design

The three different test piles for this research project were designed using methods, which have been successfully used by practitioners around the world for pile designs in clay. These methods are:

(i) Alpha-c_u method;
(ii) Method after Bustamante and Gianeselli for screw auger piles; and
(iii) Fleming method to predict load-settlement curves.

The first two methods are used to calculate pile strength and are based principally on the undrained shear strength c_u parameters of the clay, which can be determined by *in situ* tests such as CPT and DMT or by laboratory tests. Laboratory tests require undisturbed soil samples and can be more

expensive and time consuming than direct *in situ* tests. A key aim of this research is to use practical, quick and dependable methods based on *in situ* soil investigation results to determine reliably and accurately the capacity of screw auger displacement piles.

The Fleming method (Fleming 1992) is based on the input of calculated base and shaft capacities, which are provided by the first two methods mentioned above and introduced in this chapter. Fleming's method also requires the soil modulus (E) at the pile base and a dimensionless shaft flexibility factor. Fleming's method can be used to predict the load-settlement curve of piles and has been commonly used by practitioners to back-calculate design parameters from static pile load tests.

Back-calculations were used to compare the shape of the three different load-settlement curves, to compare the design predictions made using the two different pile design methods with the actual load-settlement data obtained by static load tests. Further, correlations between the *in situ* soil investigation results carried out after the pile installation and the actual pile performance were formulated, with a particular focus on pile installation factors.

7.5.1 α-c_u method

One of the most commonly used methods for the design of piles is the 'α-c_u' method. It is based on the assumption that the pile load will be distributed into shaft friction $Q_{u,S}$ and base resistance $Q_{u,P}$, as expressed in Equation 17 below:

$$Q_u = Q_{u,P} + Q_{u,S} \tag{17}$$

Where: $Q_{u,P}$ = ultimate capacity at the pile tip

$Q_{u,S}$ = ultimate friction capacity mobilised along the full shaft length

The equation can be further refined as follows (Equation 18):

$$Q_u = \alpha c_u A_s + N_K c_u A_b \tag{18}$$

Where: α = Adhesion factor derived from empirical relationships with shear strength

c_u = Mean undrained cohesion over the length of the pile shaft (kPa)

A_s = Pile shaft area (m^2)

N = Bearing capacity factor (~ 9.0)

c_u = Undrained cohesion at pile base (kPa)

A_b = Pile base area (m^2)

Several authors have defined the adhesion factor α differently, depending on the installation techniques for different pile types.

In 1984, the American Petroleum Institute (API) proposed the following values for α for the installation of driven piles, considering the displacement effect during pile installation:

$\alpha = 1.0$ for clays with $c_u < 25$ kPa
$\alpha = 0.5$ for clays with $c_u > 75$ kPa

Values of 25–75 kPa need to be interpolated and the skin friction is solely dependent on the cohesion of the soil. Effective stress changes with depth are disregarded with this method.

Fleming et al. (1985) proposed slightly lower values for bored piles in clay, at about 70% of the API values:

$\alpha = 0.7$ for clays with $c_u < 25$ kPa
$\alpha = 0.3$ for clays with $c_u > 75$ kPa

Values of 25–75 kPa need to be interpolated and the skin friction is solely dependent on the cohesion of the soil. Effective stress changes with depth are disregarded with this method.

It is obvious that this simple method for pile design strongly depends on the adhesion factor α and the correlation factor N_K when converting the cone resistance of a CPT to the undrained shear strength. The author has assumed a value of N_K=15, which is used in many practical applications.

The pile design for the screw auger piles of this research project will be carried out according to the API method, as screw auger piles displace the soil and thus show behaviour comparable to that of driven piles.

Data to obtain undrained shear strength were taken from *in situ* DMT and CPT soil tests and from undisturbed samples in the laboratory using triaxial CU tests; the results are discussed in Section 8.2.1 of the following chapter.

7.5.2 Method after Bustamante and Gianeselli (1998)

This method was originally based on the prediction of the bearing capacity and settlement of displacement piles installed by simultaneous screwing and jacking, with special emphasis on the Atlas pile (see Section 2.4.1). The method has since been used successfully by many practitioners (including the author) for screw auger displacement piles installed with long screw displacement augers such as the Omega, de Waal, CMC or Bauer FDP augers, to name only a few. Bustamante and Gianeselli's original design method was based on the analysis of 24 Atlas piles, tested on 17 different projects in France and Belgium between 1984 and 1988; however, it clearly distinguishes between two different pile types:

(i) Cast-in-place screw pile; and (Atlas pile)

(ii) Cased screw pile (Fundex pile)

With reference to Figure 11 in Section 2.4 above, and based on the practical design experience of the author with this method, it is assumed that all full- and partial-displacement screw auger piling systems can be treated and categorised as cast-in-place screw piles, regardless of the auger geometry and anticipated auger actions. The method does not distinguish between long, short, progressive or rapid displacement augers. Even CFA piles for some projects in Australia have been designed using Bustamante and Gianeselli's method and the first category, and the results were successfully verified by load tests on site. It appears that auger shape does not have a significant influence if one design method covers a wide range of different screw auger tools.

This design method can be used in displaceable soil only (e.g. sand, gravel, silt, clay, marl and chalk) and is based on *in situ* soil investigation data, such as measured by a CPT, Menard pressuremeter test (MPT) or standard penetration test (SPT). However, the design method is largely based on CPT and MPT test data and the SPT has only an indicative character. SPT tests have limitations when penetrating hard layers, organic soil formations or strata with complex structures. The correlation from CPT and MRT data to SPT values should be carried out with caution.

Calculation of the ultimate pile capacity Q_u

The ultimate pile capacity Q_u is calculated using Equation 17 as given in Section 7.5.1 above:

$$Q_u = Q_{u,P} + Q_{u,S}$$

Where: $Q_{u,P}$ = Ultimate capacity at the pile tip

$Q_{u,S}$ = Ultimate friction capacity mobilised

Independent of the type of chosen *in situ* test method, the author has formalised each term of the bearing capacity, as shown in Equation 19 and 20:

$$Q_{u,P} = K * S_p * \alpha \quad (19)$$

$$Q_{u,S} = q_{s,i} * S_{lat,i} \quad (20)$$

Where: K = Non-dimensional empirical base bearing capacity factor—depends on the type of *in situ* test and is determined by k_p (pressuremeter), k_c (CPT) or k_N (SPT), according to the selected tests

S_p = Cross-sectional area of the pile base (m^2)—depends on the design diameter D_s

α = Defines the density of the soil in the direct area of the pile base—a function of the point resistance q_c (CPT), the ultimate pressure p_l (pressuremeter) and the number of blows N (SPT)

$q_{s,i}$ = Ultimate unit skin friction (MPa) as mobilised in different soil layers—depends on the type and density of the soil and the type of screw auger pile

$S_{lat,i}$ = Shaft area of the pile at different levels—depends on the design diameter D_s

For the selection of the different input parameters necessary for the pile design, the values of Table 4 and Table 5 are to be utilised. For the calculation of the ultimate pile capacity, it was assumed by the author that the pile head settlement at this particular load was 10% of the pile diameter. Shortening of the shaft has not been taken into account for this design method as the test piles were only 4 m deep.

Selection of the design diameter D_s (m)

The design diameter D_s needs to be reduced by a factor of 0.9 for Atlas piles due to the unique shape of this pile type. It is assumed that the flanges will have an influence on the shaft area $S_{lat,i}$ and the cross-sectional section of the pile base S_p. For all other screw auger piles, the design diameter D_s is equal to the actual pile diameter.

The selection of the base bearing capacity coefficient K

For different soil types and *in situ* tests, different K factors need to be applied, as shown in Table 4. For gravels, chalks and marl, conservative values were adopted by the authors, as only a small amount of test data were available for these soil types. Conversely, since most screw auger displacement piling projects have been carried out in clays and sands, it was possible to select more justifiable values for these soil formations.

Table 4 – Selection of the base capacity coefficient K

Type of soil	K_p	K_c	K_N
Clay	1.60–1.80	0.50–0.65	0.90–1.20
Sands	3.60–4.20	0.50–0.75	1.80–2.10
Gravels	≥ 3.60	≥ 0.50	Undetermined
Chalks	≥ 2.40	≥ 0.60	≥ 2.60
Marl	≥ 2.40	≥ 0.70	≥ 1.20

The choice of α

The alpha factor characterises the soil density at the pile base and is determined by pressure meter, CPT or SPT tests. Soil conditions at the pile base must be representative for the entire soil formation.

The characterisation of the soil strength using this parameter is based on the use of equivalent ultimate pressure p_{le}, equivalent cone tip resistance q_{ce} or equivalent number of SPT blows N_e.

Each of these equivalent parameters is calculated from the corresponding geotechnical profile over a height of 'a', counted above and below the pile base. The equivalent pressure p_{le} for the pressure meter approach is calculated using Equation 21:

$$p_{le} = \sqrt[3]{p_{l1} * p_{l2} * p_{l3}} \quad (21)$$

The equivalent pressure q_{ce} for the CPT approach corresponds to an arithmetic mean of the cone resistance q_c measured along a height of 'a' above and below the pile base, as shown in Figure 65. Typically, 'a' is equal to 1.5 pile diameters (D). The equivalent cone resistance is calculated in several steps. Firstly, the q_c profile of the CPT is smoothed to eliminate local irregularities before, in a second step, the mean of the strengths between '-a' and '+a' q'_{ca} is calculated from the smoothed curve, as shown in Figure 65.

***In situ* Tests**	**Description of α (MPa)**	***a***	
SPT	$^{a}1000 \times \sqrt[3]{N_1 \times N_2 \times N_3}$	0.5m	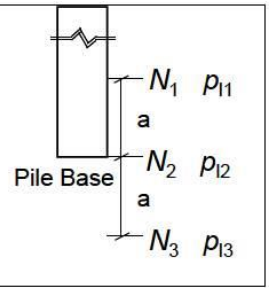
CPT	Arithmetic Mean of q_{ce}	1.5 D_b	
PMT	$\sqrt[3]{p_{l1} \times p_{l2} \times p_{l3}}$	0.5m	

Figure 65 – Calculation of the equivalent CPT pressure q_{ce}

Finally, the equivalent cone resistance q_{ca} is calculated after clipping the smoothed curve. The clipping is carried out to eliminate values greater than 1.3 q'_{ca} below the pile tip (to avoid over-estimating the capacity) and values larger than 1.3 q'_{ca} and smaller than 0.7 q'_{ca} above the pile toe.

For the SPT approach, the equivalent blows N_e are calculated from Equation 22:

$$N_e = \sqrt[3]{N_1 * N_2 * N_3} \quad (22)$$

Here, the value for 'a' is assumed to be 0.5m and the final value of N_e needs to be multiplied by a factor of 1,000 to obtain $Q_{u,P}$ expressed in MN.

The choice of the unit friction q_s (MPa)

The unit friction to be obtained for the relevant screw auger pile design depends on the category of the pile and the type density of the soil. The unit skin friction for the pile design is obtained from Table 5 and Figure 66 (next page).

Table 5 – Selection criteria for Bustamante and Gianeselli design method

Soils	*Curves qs (MPa)*		p_l (MPa)	q_c (MPa)
	Screw auger full-displacement piles	**Other screw piles with casings (Fundex pile)**		
Clay	Q1	Q1	< 0.30	< 1.00
Clayey silt	Q3	Q2	> 0.50	> 1.50
Sandy silt	Q4	Q2	≥ 1.00	≥ 3.00
Sand or gravels	Q1	Q1	< 0.30	< 1.00
	Q4	Q2	> 0.50	> 3.50
	Q5	Q2	> 1.20	> 8.00
Chalk	Q4	Q2	> 0.50	> 1.50
	Q5	Q2	> 1.20	> 4.50
Marl	Q4	Q2	< 1.20	< 4.00
	Q5	Q2	≥ 1.50	≥ 5.00

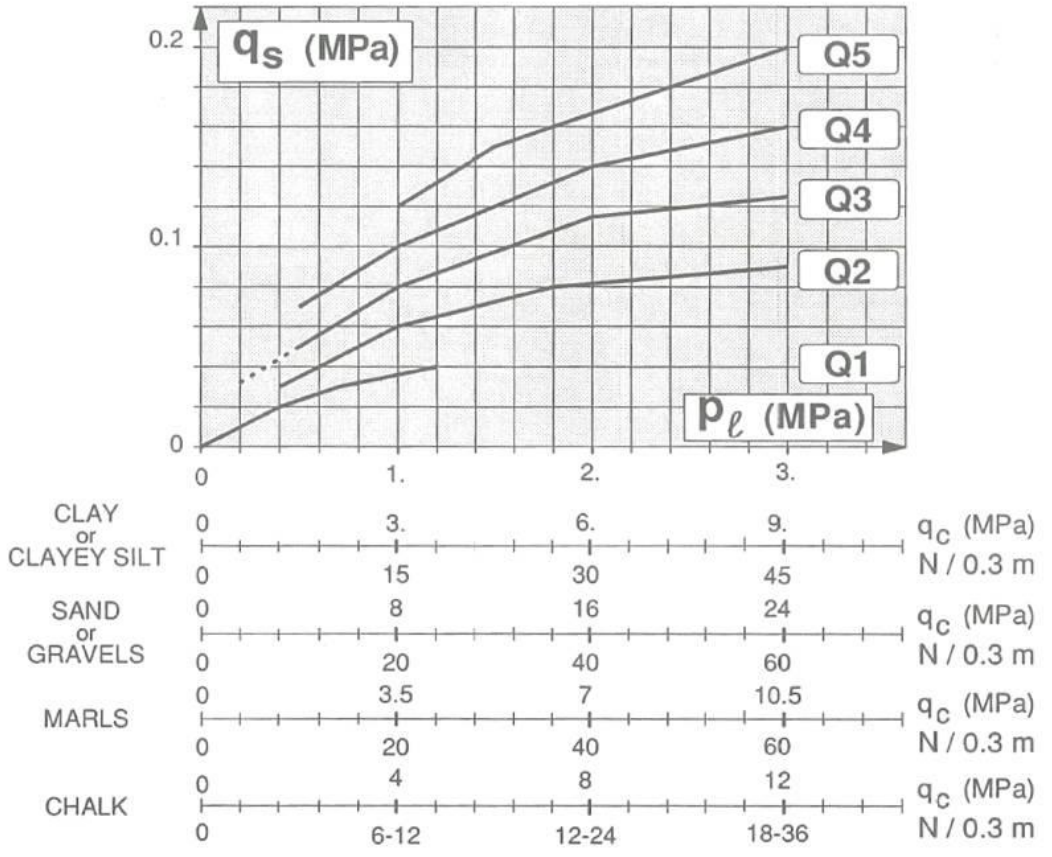

Figure 66 – Design curves, after Bustamante and Gianeselli 1998

The values of the design parameters of this method were obtained based on *in situ* tests performed by specific test equipment, like the pressuremeter after Menard and defined as per French Standard AFNOR Pr P-94-110 (1991). The CPT cone was a mechanical cone type 'Gouda M1', as defined by the ISSMFE standards TC-16 (1989).

It is advisable to amend the q_c values (as per Equation 23) if a mechanical cone is used:

$$q_c\text{mechanical} = \beta * q_c\,\text{electrical} \quad (23)$$

Where: β = 1.40 to 1.70 for cohesive soils

β = 1.30 for saturated sands

The Bustamante and Gianeselli approach has been used successfully over the last decade by the author of this thesis to design screw auger displacement piles and CFA piles in Australia and Europe for several projects and proposals.

7.5.3 Fleming's method (1992)

Pile settlement and differential settlements are important features in pile design. At least the performance of a single pile needs to be calculated reliably to prepare adequate project specification before more complicated items such as group performance, structural stiffness or pile load distributions can be addressed.

For the settlement prediction and back-calculation of static load test results, Fleming's (1992) 'single pile settlement prediction and analysis' method can be used. This method is based on a simple approach with a few input data, based on the behaviour of a single pile under maintained loading and the use of hyperbolic functions to describe individual pile base and shaft performance. To describe the total pile performance, a hyperbolic function is used that requires the definition of its origin, its asymptote and either its initial slope or a single point of the function. Typically, elastic soil parameters and ultimate loads can be used as input parameters for the hyperbolic function to describe the total pile performance. The author has carried out numerous back-analyses with fully instrumented cast-in-place pile load tests to validate the accuracy of this method.

Chin (1983) suggested deriving a hyperbolic function for the stress–strain relationship for general settlement. He suggested that the stress mobilisation in a soil formation with increased strain is a function of an increasing number of effective soil contacts rather than of a general increase of inter-granular stress on a constant number of grain contacts.

Chin suggests that inter-granular stresses in flocculated clays are virtually constant and independent of the applied effective stresses. This assumption results in the application of a hyperbolic function for the stress–strain relationship.

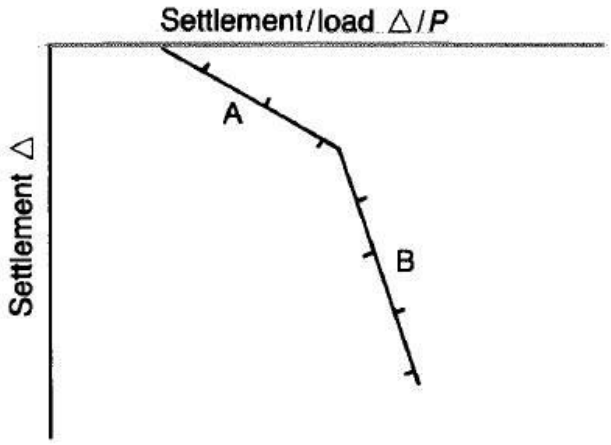

Figure 67 – Relationship of settlement and settlement/load (Chin 1983)

When a soil is loaded under compressive stress, the load is transferred by internal columnar particle structures and ever more columns begin to support the load as the initial column reaches its limits. The yield load for each of the columns is comparable. Chin's suggested relationship of settlement and settlement/load ratio is displayed in Figure 67.

Fleming used Chin's approach and developed a simple hyperbolic function to forecast pile settlements under compressive loads, as single piles typically behave according to a hyperbolic function with respect to shaft friction and end-bearing capacities under constant compression loading.

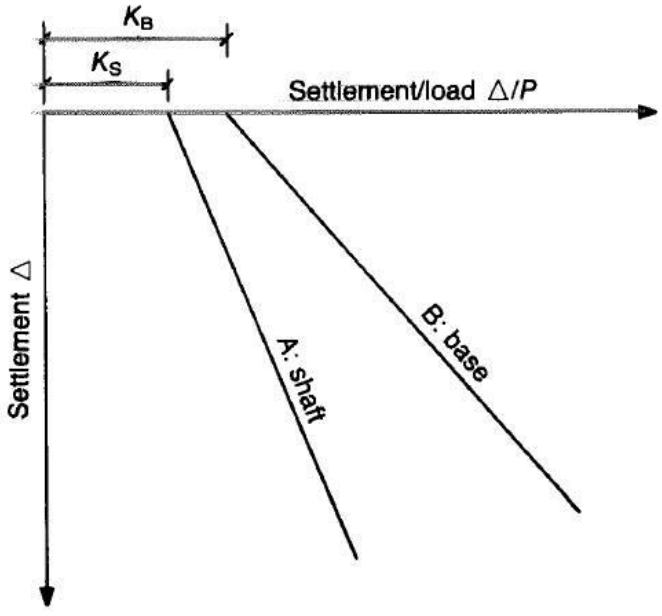

Figure 68 – Individual shaft and base performance (Fleming 1992)

In Figure 68, the slope 'A' represents the ultimate shaft friction of a pile, while the slope 'B' is the ultimate bearing capacity as defined by vertical asymptotes to the load/settlement relationship. K_S and K_B are the corresponding intercepts on the horizontal axis.

Elastic shortening of piles is discussed by Fleming in detail. However, for this research project, the piles are only 4.0 m deep and elastic shortening during ultimate loading conditions is assumed negligible. Therefore, the piles are assumed to behave as rigid and, consequently, the applied load is taken by the shaft and the base, resulting in total pile settlement without any elastic shortening.

According to Fleming's method, the shaft load P_S can be expressed by Equation 24:

$$P_s = \frac{U_s \Delta_s}{M_s D_s + \Delta_s} \tag{24}$$

The base load P_B is written in Equation 25:

$$P_B = \frac{U_B \Delta_B D_B E_B}{0.6 U_B + D_B E_B \Delta_B} \tag{25}$$

Where:

- D_s = Pile shaft diameter (m)
- D_B = Pile base diameter (m)
- Δ_s = Settlement of the pile shaft at a corresponding load P_s
- Δ_B = Settlement of the pile base at a corresponding load P_B
- U_s = Ultimate shaft load, calculated by conventional design methods
- U_B = Ultimate base load, calculated by conventional design methods
- M_s = Shaft flexibility factor, which describes the tangent slope at the origin for the hyperbolic function. This factor is dimensionless and typically varies from 0.004 in soft to stiff and relatively loose soils, to 0.0005 in hard formations or soft rocks, as it decreases with increasing soil stiffness. Fleming stated that in stiff, over-consolidated clays, this factor is found to be in the range of 0.001–0.002. These variations are typically related to construction practice.
- E_B = Soil modulus beneath the pile base after pile installation

Equations 24 and 25 can be expressed more simply by writing the expression for total applied load P_T at a given settlement and inserting the total pile head settlement value Δ_T, as in Equation 26:

$$P_T = \frac{a\Delta_T}{c + \Delta_T} + \frac{b\Delta_T}{d + e\Delta_T} \tag{26}$$

Where: $a = U_s$

$b = D_B E_B U_B$

$c = M_S D_S$

$d = 0.6\ U_B$

$e = D_B E_B$

To solve Δ_T given any specific value for P_T, Equation 26 has to be rearranged in the form:

$$(eP_T - ae - b)\Delta_T^2 + (dP_T + ecP_T - ad - bc)\Delta_T + cdP_T = 0 \quad (27)$$

Fleming suggests introducing the following correlations to simplify Equation 27 further:

$$eP_T - ae - b = f \quad (28)$$

$$dP_T + ecP_T - ad - bc = g \quad (29)$$

$$cdP_T = h \quad (30)$$

This results in Equation 31 written below. Only the positive value of Δ_T is used:

$$\Delta_T = \frac{-g \pm \sqrt{(g^2 - 4fh)}}{2f} \quad (31)$$

It should be noted that conventional pile design methods for the calculation of U_s and U_B are conservative in most cases, as proven by back-analysis of static load test results (Fleming 1992). Installation techniques were found to influence both shaft load and base load significantly. The ultimate shaft capacity can be decreased by faulty construction practice; for example, if CFA piles in sand are not executed correctly, the shaft capacity can be reduced significantly in comparison to the design. Conversely, the installation of displacement piles can potentially enhance both shaft capacity and base capacity considerably. Fleming stated that the soil stiffness at the pile base could be increased by a factor of two or three for driven displacement piles.

The soil modulus beneath the base E_B is one of the most important factors of this method, particularly for the back-analysis of pile load tests. The soil modulus is related to the soil parameters, but is also influenced by the construction technique. The pile base condition is very important for the overall performance of a single pile, and different techniques of pile installation can significantly influence the soil modulus at the pile base. Van Impe's research on Atlas piles in stiff clay (1988) supports this theory, as he discovered clay re-moulding at the flanges of Atlas piles that showed different (higher) strength parameters than the original soil.

Fleming's method was used for the back-analysis of the three static load tests carried out at Lawnton Clay. The load-settlement curves of the three load tests were obtained during the load test procedure. Each curve was used for a back-analysis using Fleming's method, as described above. Critical parameters such as the soil modulus beneath the pile base were determined by iterative processes and these values were compared with the initial soil modulus determined in laboratory tests and *in situ* field tests using DMT and CPT equipment. Further, assumptions about base and shaft capacity distributions were made, also iteratively. The method is well suited to determining changes in soil modulus brought by installation parameters and auger shapes in stiff clay.

7.6 Static load tests

7.6.1 Methodology

Static load tests are used to determine the proof load or ultimate geotechnical strength of a test pile. The test load is increased in pre-defined stages, with the load-settlement curve recorded at each stage of loading and unloading. Pile load tests in general and static pile load tests in particular are suitable methods to verify pile performance estimated from empirical design methods.

It should be noted that static load tests were carried out for three test piles (piles B, C and D). Test pile E was installed a few months after the original three test piles with the initial intention to obtain additional heave monitoring data. Unfortunately, no static load test was carried out on test pile E due to lack of resources and budgetary constraints.

Depending on the load test type adopted (compression, tension or lateral), the applied test load should follow an adequate load step sequence, as laid out in table A1 and A2 of AS2159-2009 or any other applicable standards. With only two types of static load tests available (proof and ultimate), their main objective is to determine the maximum load (P_S, P_G and P_U) that a pile can sustain before reaching a specified failure point or pre-defined settlement. The determination of the applied test loads can be calculated in accordance with relevant codes and pile design methods. As the static load test is a direct measure of the *in situ* performance of a pile, it accurately represents site-specific conditions and can be used to compare and refine pile design calculations for such soil conditions.

Proof load tests are typically used to assess whether the pile foundation is adequate to withstand the design load without failure or yielding. In this test, the load that the test pile must withstand has a factor of safety imposed. This can vary, but is typically in the range of 2. The ultimate geotechnical strength test assesses the ultimate load the test pile can carry before 'failure', which is typically defined as settlements in excess of 10% of the pile diameter (AS2159-2009). There is no factor of safety imposed.

For this research project, all three of the test piles were tested to determine the ultimate geotechnical strength of each pile. The setup of the load tests was carried out in accordance with AS2159-2009, and the test piles were designed to carry the exceeded loads safely without exceeding strength. The test frame was designed to carry 100% more load than the maximum available test load of 1,000 kN. Working load (P_S) was defined at 300 kN and the ultimate geotechnical strength (P_G) was set at 600 kN for all three piles.

Table 6 – Loading program static pile load tests

Stage	***AS2159-2009***		***Test procedure***	
	Load (kN)	Minimum load duration (min)	Load (kN)	Minimum load duration (min)
S1 (proof and ultimate test)	20% P_S	20 min	20% P_S	10 min
Loading to P_S	40% P_S	20 min	40% P_S	10 min
	60% P_S	20 min	60% P_S	10 min
	80% P_S	20 min	80% P_S	10 min
	100% P_S	60 min	100% P_S	10 min
S2 (proof and ultimate test)	30% P_S	10 min	60 % P_S	10 min
Unloading from P_S	0% P_S	20 min	40% P_S	10 min
			20% P_S	10 min
G1 (proof and ultimate test)	30% P_G	20 min		
Loading to P_G	40% P_G	20 min	40% P_G	10 min
	50% P_G	20 min	50% P_G	10 min
	60% P_G	20 min	60% P_G	10 min
	70% P_G	20 min	70% P_G	10 min
	80% P_G	20 min	80% P_G	10 min
	90% P_G	20 min	90% P_G	10 min
	100% P_G	60 min	100% P_G	30 min
	110% P_G	20 min	110% P_G	20 min
	Further increments of 10% P_G	20 min each increment	Further increments of 10% P_G	20 min each increment
G2 (proof and ultimate test)	100 % P_G	10 min	100% P_G	10 min
Unloading from P_G	80 % P_G	10 min	60% P_G	10 min
	60 % P_G	10 min	30% P_G	10 min
	40% P_G	10 min	15% P_G	10 min
	20% P_G	10 min		

The loading program for this project is shown in Table 6; variations to AS2159 are marked in red. Unloading at working load was carried out in more steps than recommended in the code, and unloading after reaching the ultimate geotechnical capacity was carried out with fewer and different loading steps. Further, the minimum loading duration was shortened to 10 minutes for each loading step, as the matter of greatest interest was geotechnical failure. The majority of the settlements for each individual load step were terminated within the first two minutes after application of the new load step and the remaining settlements were generally less than 0.2 mm for the load steps prior to the failure load.

Setup

The general setup of the static load test is shown in Figure 69 and Figure 70. The static load test frame with reaction piles was used for the execution of the tests. Four screw or helical piles (depth 9.00 m and 283 mm in shaft diameter) were used as the reaction piles and two piles were installed to act as guide piles for the stability of the frame during the setup.

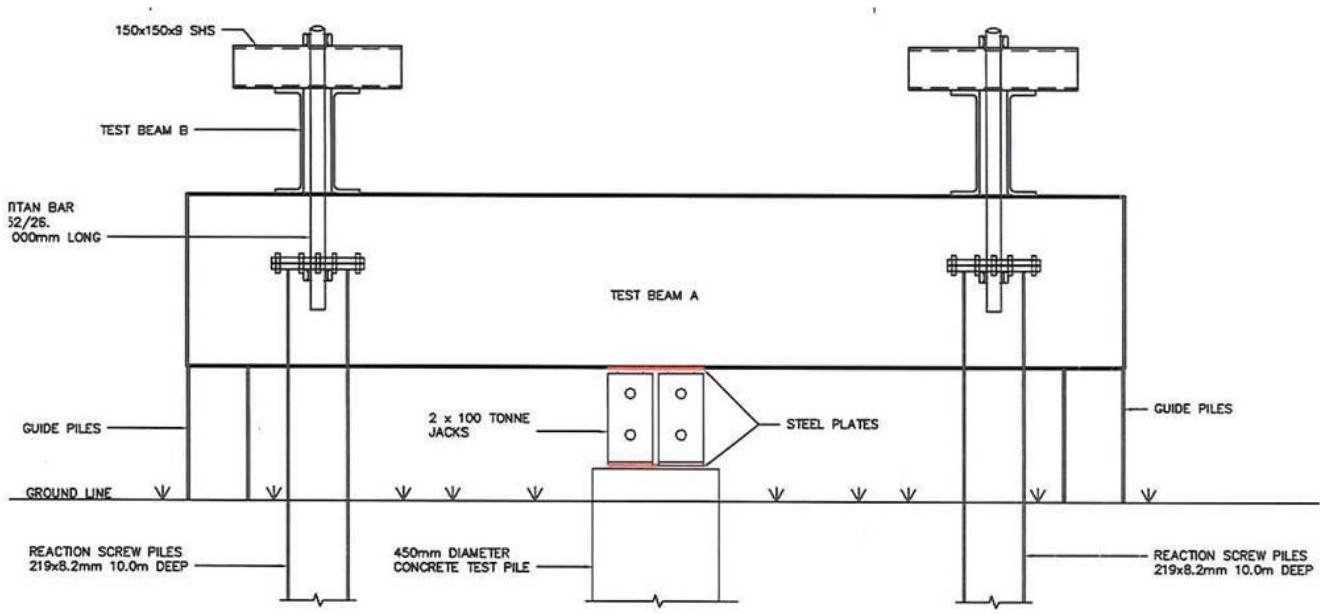

Figure 69 – Typical arrangement of a static pile load test with reaction piles

The static load test frame consisted of several steel beams. It was structurally designed for test loads up to 1,980 kN; however, the maximum test loads were expected to be below 1,000 kN and the hydraulic jack was limited to a 1,200 kN compression load.

Methodology

The pile head was prepared to allow the application of the test load: coaxial with the pile axis for vertical compression or tension tests, and perpendicular to the pile axis for a lateral load test.

Adequate preparation (e.g. through a steel bearing plate) allows the test load to be transferred into the pile with minimal losses and optimal load distribution.

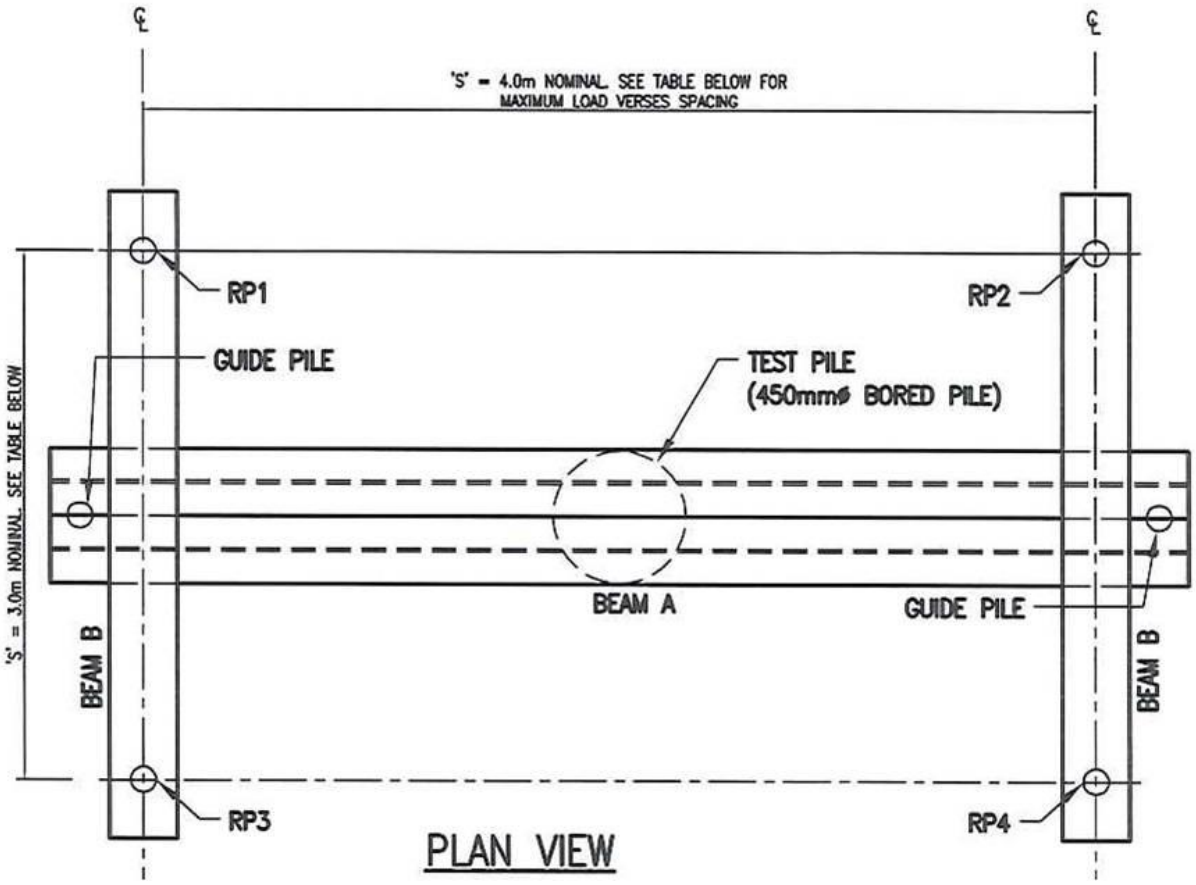

Figure 70 – Plan view of the static pile load test arrangement for this research

For this research project, all test piles were extended to about 700 mm above working platform level by the installation of steel liners with an identical diameter to the individual test piles and 12 mm wall thickness. Structural calculations were done to determine the pile head reinforcement requirement. It was found that no reinforcement was required for test loads up to 1,350 kN.

The test load is usually applied to the pile by jacking against a reaction system using hydraulic jacks, with load cells used to measure the test loads during the execution of the tests. The reaction system may involve ground or rock anchors, reaction piles or, in very rare cases, kentledge.

It is critical that the reaction system is stable and provides safe access for testing personnel. The distances from the centre of the test pile to the centre of the reaction piles or anchors must be more than five times the shaft diameter of the test pile (AS2159-2009) or at least 2.5 m to avoid any interaction. For the tests carried out at Lawnton, the spacing was 2.5 m and complied with AS2159-2009.

For the load application, a calibrated hydraulic jack was used. This was placed on top of the test pile and pushed against the reaction beam to induce a compressive load. The load was applied in pre-defined load step in accordance with Table 6 above, applying incremental load steps of 10 and 20%. The minimum load duration of 10, 20 or 30 minutes was applied, and all three of the test piles received cyclic loading until finally being loaded to the ultimate geotechnical strength.

The following is a detailed description of the methodology that was applied on site for the tests carried out for this research project, with specific reference to the test setup used:

(i) The location of the reaction piles was surveyed and marked. CPT results were used to determine the required depth, to ensure adequate tension capacity and installation torque of the 283 mm diameter steel screw piles. The centre-to-centre spacing of the reaction piles was selected to be 2.5 m.

(ii) Four reaction screw piles and two guide piles were installed to ensure that the setup was perfectly straight to avoid eccentric loading (Figure 71).

(iii) Laser dumpy level survey equipment was used to assess the vertical position of the reaction piles, allowing a margin of error of ±2 mm in accuracy.

(iv) All blank test flanges were attached with fixed titan Ischebeck bars to the screw piles.

(v) The double 610UB113 beam (main beam) and two double 380PFC beams (head stocks) were installed in the correct location, taking care that the beams were appropriately positioned with support of the guide piles. The headstock beams were attached to the Ischebeck bars and locked in place with 52/26 titan nuts (Figure 72).

Figure 71 – Installation of the screw piles as reaction piles on site

(vi) The hydraulic jack was put onto the test pile between two loading plates (25 mm thick steel plates). The circular loading plate was placed underneath and the rectangular loading plate was placed on top of the jack. The circular loading plate was slightly smaller in diameter than the test pile, to allow the test load to be distributed evenly into the concrete shaft, rather than into the steel casing (Figure 72).

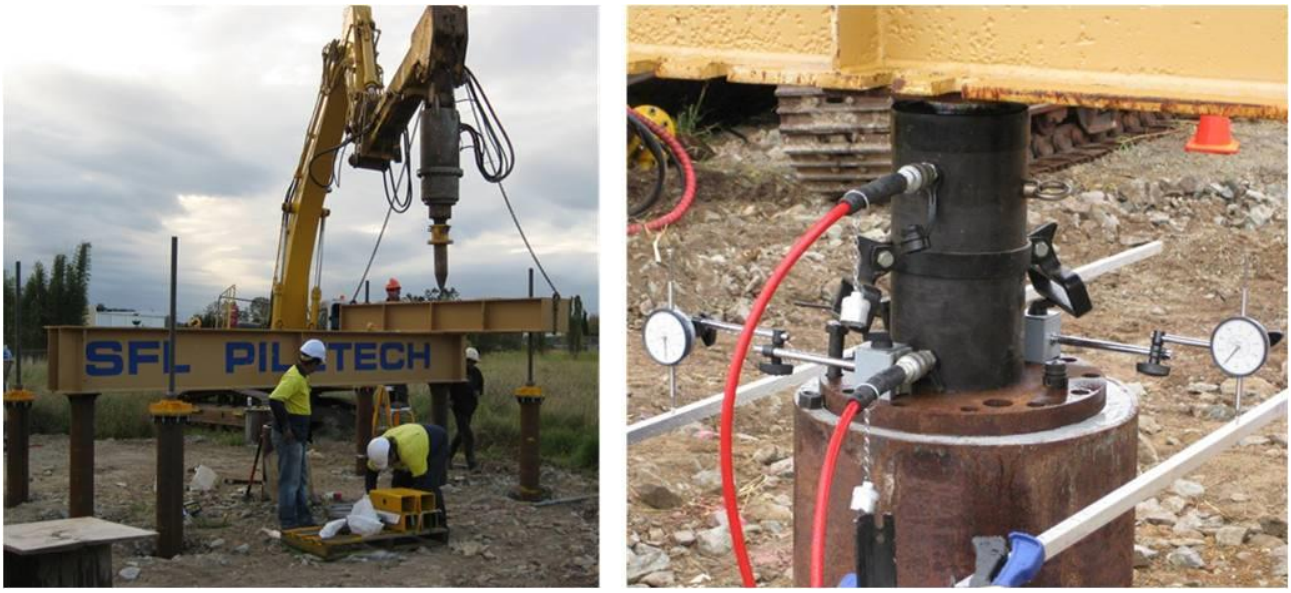

Figure 72 – Installation of the reaction system (left) and preparation of the pile head with the hydraulic jack and dial gauges (right)

(vii) Four rigid star pickets were installed around the test pile, with two corresponding rigid aluminium square bars spanning between them to be used as reference beams to measure the pile head displacement. The position of the star pickets was more than five pile diameters from the test pile (2.25 m). A spirit level was used to ensure that the reference beams were installed horizontally.

(viii) The calibrated spring-loaded dial gauges were attached to the pile head and set as close as possible to the maximum value. The dial gauges were positioned on the perimeter of the loading plate, directly adjacent to each other. Magnetic stands were engaged and the lever arms of the gauges were positioned in a way that they could interact with the reaction frame.

(ix) The inflow and outflow hoses to the 100 ton hydraulic jack were attached and the predetermined loads were applied. The pile head displacements were measured and documented between each load step and recorded every minute.

(x) The positions of the reaction screw piles and reference frame were measured using survey equipment at the start, middle and end of each loading increment to monitor potential movements.

The static load tests for all piles were undertaken in July 2013 by SFL Piletech Pty Ltd, as subcontracted work to UQ.

The following terminology is used for the static load tests, in accordance with AS2159-2009:

P_S = Test load for pile performance assessment at serviceability limit state (E_{ds})

P_u = R_{ug}

P_G = Maximum test load for assessment of geotechnical ultimate limit state $R_{t,ug}$

Where P_u = Load for assessment of ultimate geotechnical strength

R_{ug} = Ultimate geotechnical strength, estimated either by calculation ($R_{d,ug}$) or by test ($R_{t,ug}$)

$R_{d,\,ug}$ = Design ultimate geotechnical strength of pile

$R_{t,\,ug}$ = Ultimate geotechnical strength of a pile as assessed from a load

The following chapter now turns to the presentation of the research observations and results.

CHAPTER 8: RESEARCH OBSERVATIONS AND RESULTS

8.1 Finite element model

8.1.1 Hypo-plasticity

Laboratory oedometer tests and CU triaxial tests were carried out on undisturbed and re-moulded soil samples to determine the five basic hypo-plastic soil parameters for the constitutive soil model used for the numerical model.

Parameters N, λ* and κ*: These parameters were determined from a single loading/unloading oedometer test, as shown in Figure 73. Isotropic loading must exceed the pre-consolidation pressure to find the position of the slope of the normal compression line. Parameter κ* should be calibrated from the slope of the isotropic unloading line of an oedometer test close to the normally compressed state.

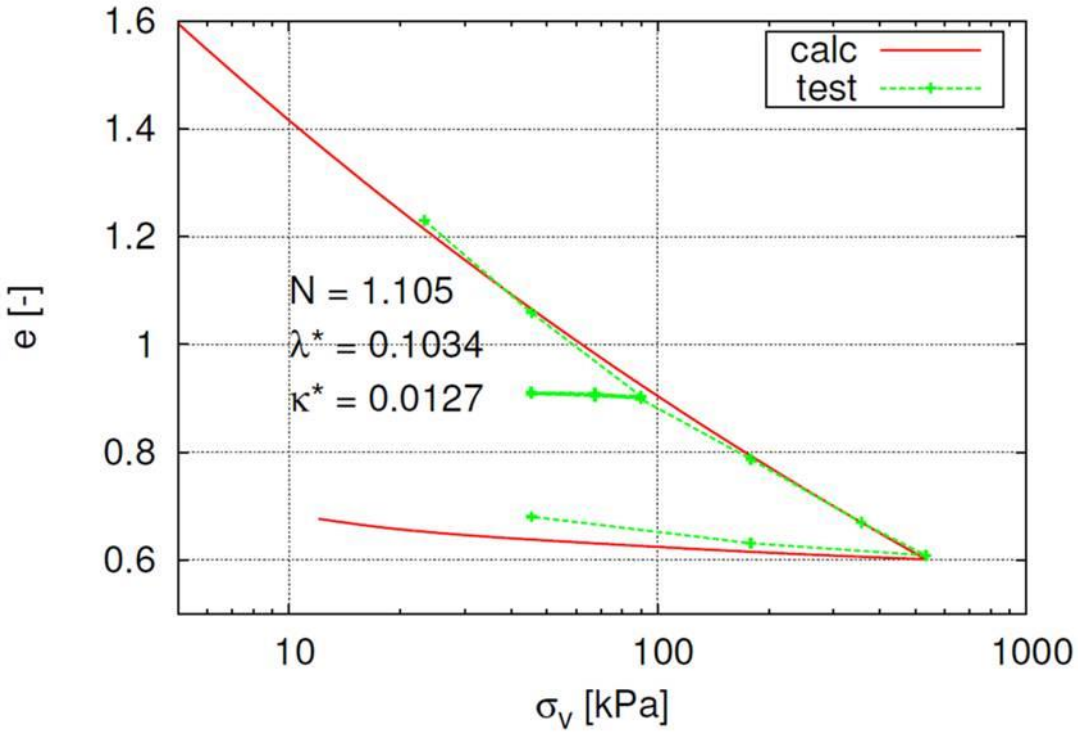

Figure 73 – Oedometer test on grey clay (re-moulded and saturated)

Parameter φ_c: The critical state friction angle was found using a linear regression through the critical state points of all shear tests available, determined from linear regression of the triaxial CU test results on re-moulded and consolidated soil, as shown in Figure 74.

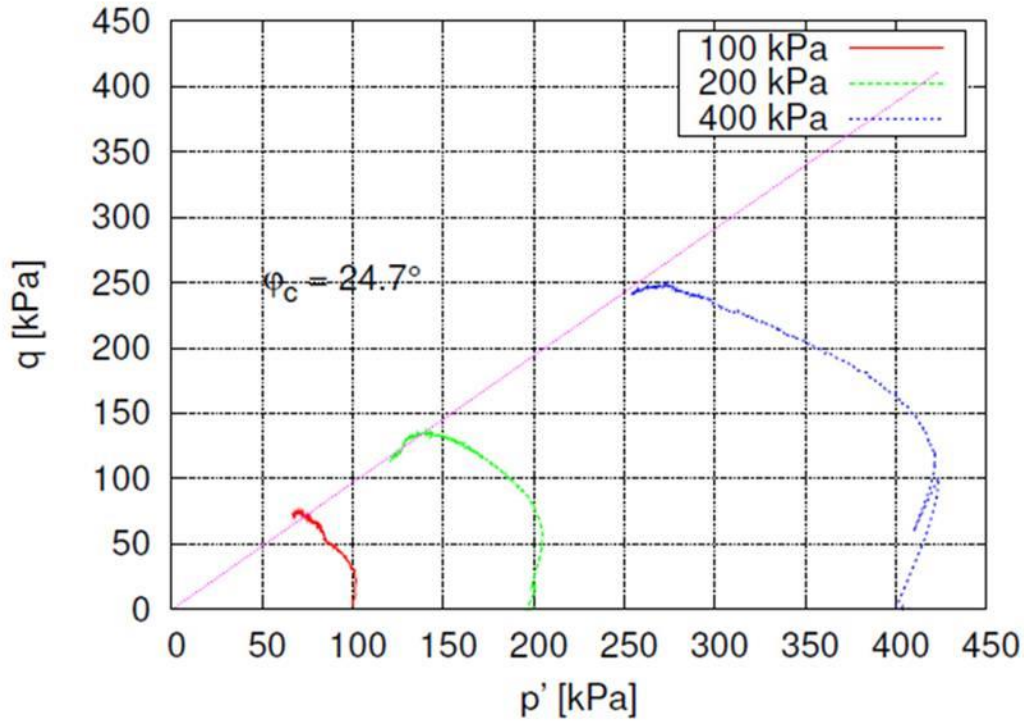

Figure 74 – Triaxial CU test on re-moulded grey clay

Parameter r: Parameter r was evaluated directly, using the definition as the ratio of the bulk to the shear moduli, for tests starting from the isotropic normally compressed stress state, as shown in Figure 75 below.

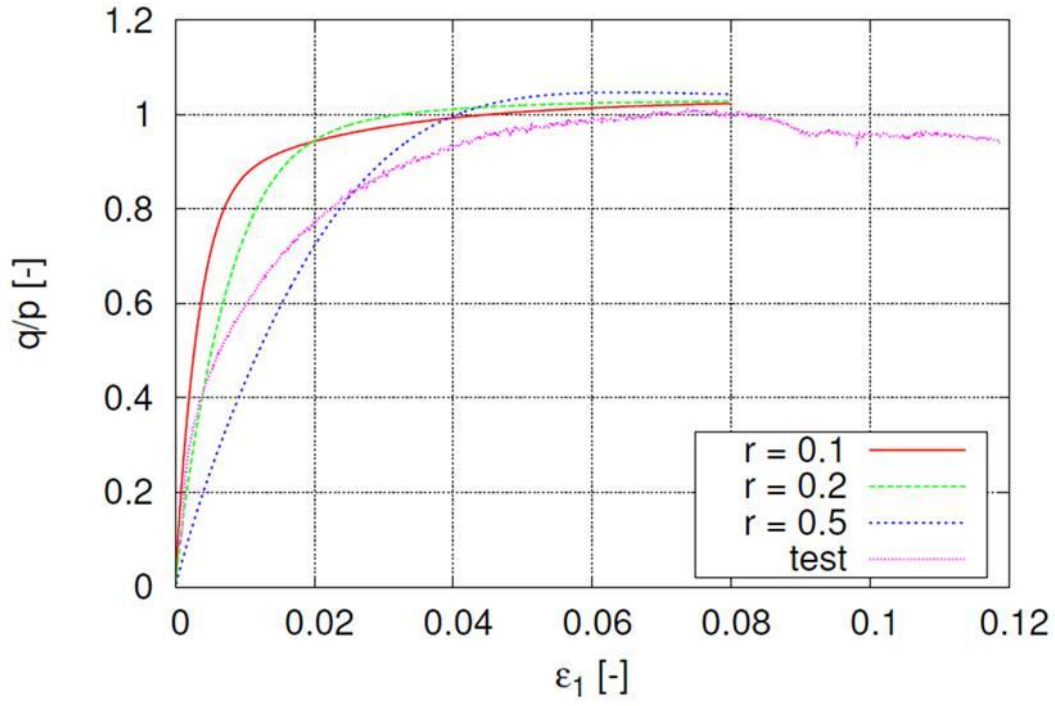

Figure 75 – Recalculation of CU triaxial test (σ_3 = 200 kPa) with different r values

A summary of the calculated hypo-plastic parameters for the hard grey clay are as follows:

φ_c	= 24.7˚	(critical state friction angle)
N	= 1.105	(isotropic compression)
λ^*	= 0.1034	(slope isotropic normal compression line)
κ^*	= 0.0127	(slope isotropic unloading line)
r	= 0.2	(ratio of bulk modulus to shear modulus)

The hypo-plastic parameters were used as parameters for the FE model calculations.

8.1.2 Numerical model

The results of the numerical model are displayed in Figure 76, which shows the effective stresses, pore water pressure and soil displacement during the installation process of a screw auger full-displacement pile, modelled with FE code Abaqus Standard.

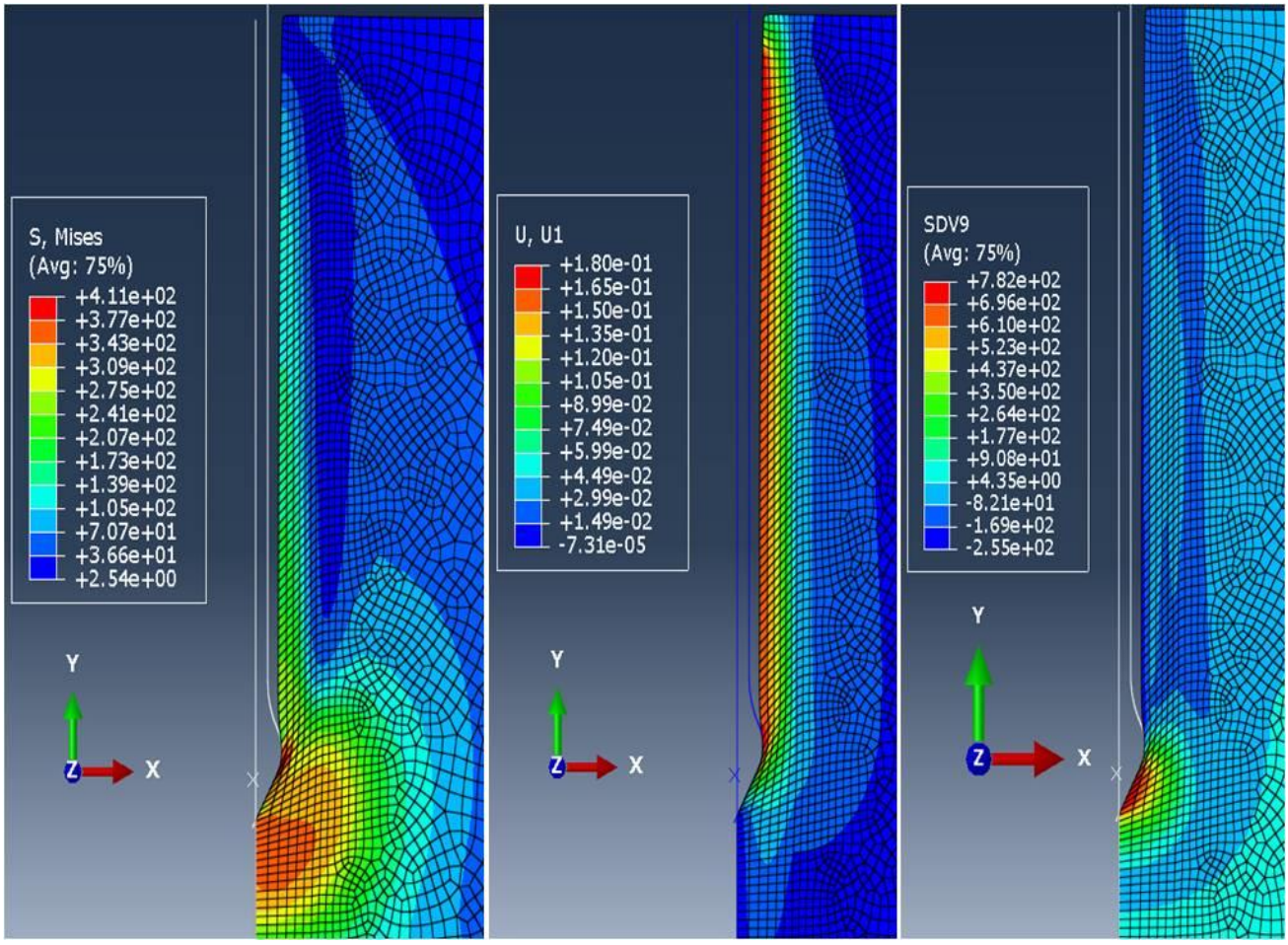

Figure 76 – Expected effective stress field (left), soil displacement (centre) and pore water pressure (right) of ADP to be installed in Lawnton Clay, modelled using Abaqus Standard

For the effective stress modelling, it can be observed that a stress bulb is created in the soil formation traveling downwards as the displacement auger progresses. The maximum stresses are about 400 kPa at a distance of about 225 mm (0.5 pile diameters) from the edge of the pile. Another 225 mm further from the pile, the effective stresses are only around 275 kPa, quickly decreasing to 175 kPa when 1.5 diameters from the pile edge. At 2.0 diameters (or 900 mm from the pile shaft), the stresses are only 139 kPa, further reducing to around 100 kPa at the last layer at 3.0 diameters from the pile centre line.

The remaining effective stresses in the ground after the auger is fully extracted and the concrete is placed using about 5 bar pressure are expected to be around 200 kPa at the pile shaft, which indicates a significant improvement potential. The remaining effective stresses in the soil at 225 mm from the shaft are predicted to be about 80 kPa. At further than 250 mm, no significant lasting effective stress changes are expected. The effective stress bulb below the auger tip is expected to reach about three pile diameters (1,350 mm) below the design depth during auger movement, with the distribution being similar to the horizontal values stated above. The remaining stress changes in the soil are similar to the changes in the horizontal direction. Minor stress changes in the soil continuum are expected as far as three pile diameters from the pile shaft (horizontally and vertically) during installation; however, after the installation process, these are expected to reach only 1.5 pile diameters (675 mm) from the pile shaft.

Soil displacements of about 15 mm are expected to reach up to two pile diameters (900 mm) from the pile centre line during installation; however, most of the displacements are expected to occur within 1.5 pile diameters (675 mm) from the pile centre line. The expected displacements at 0.5 pile diameters from the shaft are predicted to be around 60 mm, further declining to about 35 mm at one pile diameter distance. The displacements are stable after installation and only minor reductions after the installation process occur.

The simulated pore water pressures behave quantitatively in a similar way as the effective stresses. However, the stress bulb reaches only about one pile diameter vertically and horizontally during installation, indicating stresses of around 750 kPa at the auger/soil interface and 200 kPa at 225 mm from the auger tip. The stresses drop quickly to zero at one pile diameter from the pile edge. The pore water stresses remaining after pile installation are predicted to be close to zero. Right at the pile shaft, the program predicts suction of up to 250 kPa.

Based on the numerical model, it was selected to take the CPT, DMT and inclinometer measurements at 225 mm (0.5 diameters) from the pile edge. Further inclinometer measurements were taken at 1.25 and 1.5 diameters from the pile edge.

8.2 Laboratory tests

The field test site is located at Lawnton, Queensland, Australia. In February 2011, two undisturbed, continuous soil samples were taken to bedrock at two locations. The soil samples were taken about 0.5 m from two initial CPTs to allow for a close correlation between CPT values and the soil profile. Three different soil layers were encountered during the site investigations and the relevant index parameters were determined in the laboratory for each of these. The typical soil profile, classification and index parameters are summarised in Table 7 and Figure 77.

Table 7 – Soil profile, index parameters and soil classification of Lawnton clays

Soil Description	*BH1*	*BH2*	*Fines Content <0.15mm*	*Liquid Limit (LL)*	*Plastic Limit (PL)*	*Plasticity Index (PI)*	*Classification USCS*
Stiff, light brown, clay	0.00 m to -1.50 m	0.00 m to -1.50 m	79%	0.43	0.25	0.18	Low plasticity
Hard, grey clay with coloured inclusions	-1.50 m to -6.50 m	-1.50 m to -6.60 m	91%	0.53	0.21	0.32	High plasticity
Hard, grey sandy clay with coloured inclusions	-6.50 m to -8.00 m	-6.60 m to -7.20 m	57%	0.44	0.19	0.25	Low plasticity

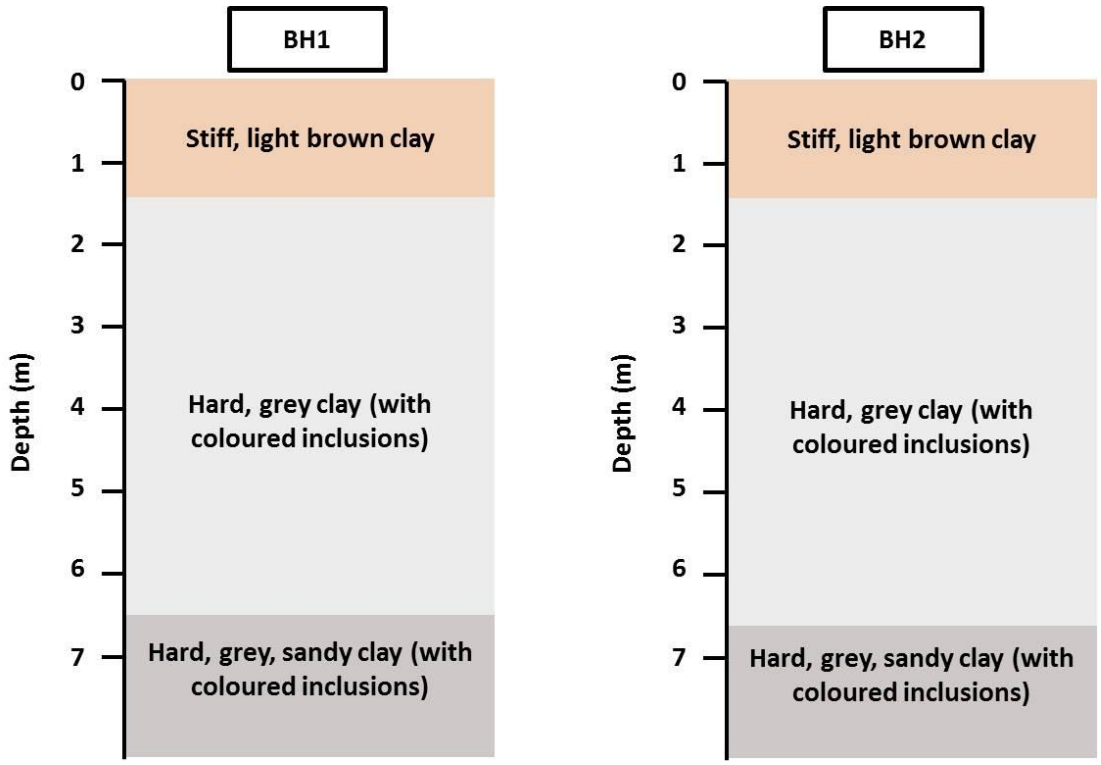

Figure 77 – Typical soil profiles for the field-test site at Lawnton

Undisturbed soil samples of the top layer (taken from 1.40 m depth) are displayed in Figure 78.

Figure 78 – Undisturbed soil samples of light brown clay (0.00 to -1.50 m)

The second clay layer, which was defined as grey clay, was the material in which the screw auger piles were founded. The toe levels of the test piles were located at 4.0 m depth; thus, soil samples were taken from this depth area to determine Young's modulus and the undrained shear strength in the area of the pile toe. As the characteristics of the grey clay are critical for the performance of the test piles, undisturbed samples were also taken at 2.70 m and 5.20 m depth. Typical undisturbed soil samples of the grey clay layer at pile toe level are displayed in Figure 79.

Figure 79 – Undisturbed soil samples of grey clay (-1.50 m to -6.50 m)

In Figure 80, typical undisturbed soil samples of the bottom layer (grey, sandy clay) are presented.

Figure 80 – Undisturbed soil samples of grey, sandy clay (-6.50 to -8.00 m)

The bottom layer has no significance for the pile performance. However, triaxial and oedometer tests were conducted for soil samples of this layer to investigate the characteristics of the full soil profile.

8.2.1 Triaxial tests

Triaxial CU tests were used to determine the Young's modulus E and the undrained shear strength cu of the undisturbed soil samples recovered during the geotechnical investigation of Lawnton site, as shown in Figure 81. The inclination of the linear section of the stress-strain curves (at about 50% of the deviatoric stress level) was used to determine the average Young's modulus of the soil. The confining stress applied in the CU tests was 400 kPa.

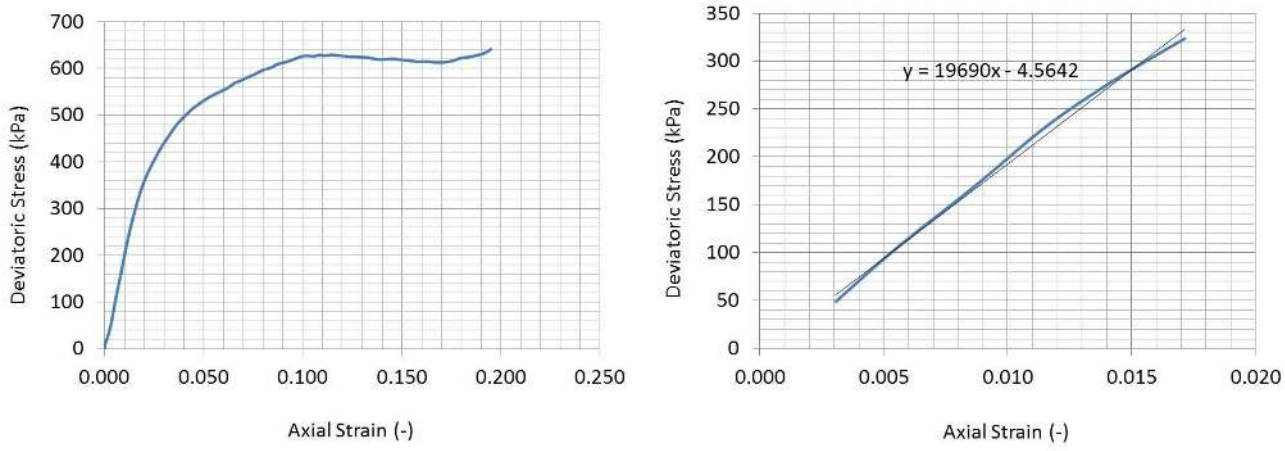

Figure 81 - Young's modulus obtained by triaxial tests (CU) for BH1 at 4m depth

The data obtained for BH2 at 4m depth are displayed in Figure 82. The confining stress applied in the CU tests was 400 kPa.

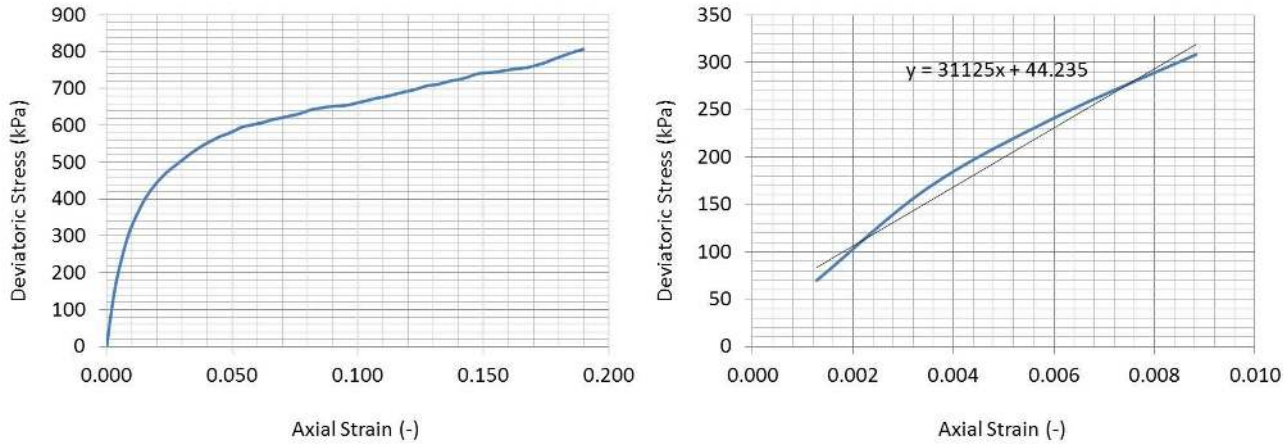

Figure 82 - Young's modulus obtained by triaxial tests (CU) for BH2 at 4m depth

These parameters were used in the pile design calculation. Several soil samples were taken from both borehole locations BH1 and BH2 at different depth levels. The Young's moduli of the soil profile and the different layers at Lawnton are displayed in Figure 83.

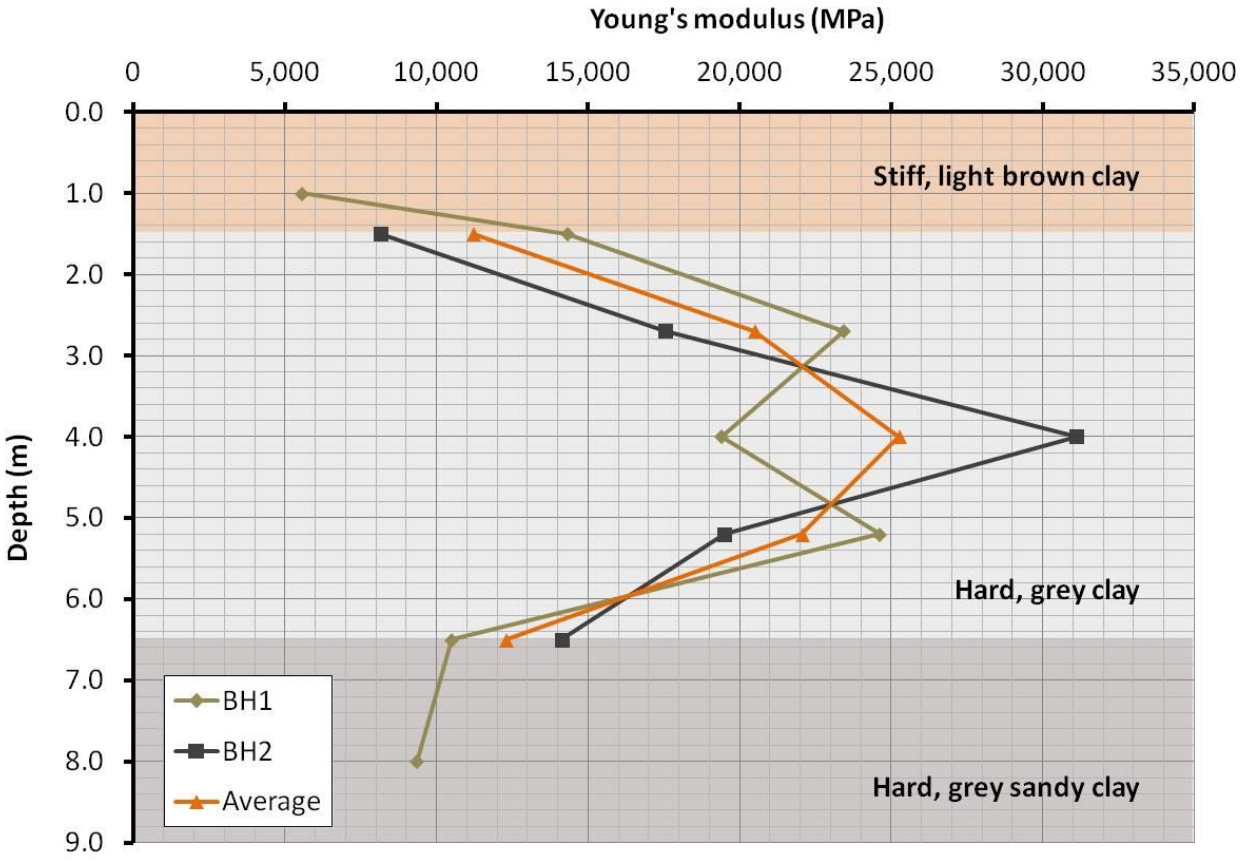

Figure 83 – Young's modulus versus depth for Lawnton field test site

It can be observed that the Young's moduli for BH1 and BH2 are in a comparable range. The only significant difference can be seen at 4.0 m depth, right at pile toe level, where the soil samples taken from BH2 show about 50% higher soil stiffness than those taken from BH1. The author added an average data series (displayed in orange), which was used for the pile design. The average value for Young's modulus utilised for the pile design at 4.0 m depth (the location of the pile toe) was determined with E = 26,000 kPa taking both values at 4.0 m depth into account.

The undrained shear strength c_u of the Lawnton Clay is presented in Figure 84. Up to 4.0 m depth, the c_u values for both locations are quite similar; however, between 4.0 m to 6.5 m, the undrained shear strength varied considerably. Similar to in the determination of Young's modulus, an average data series representing the average values between BH1 and BH2 was added.

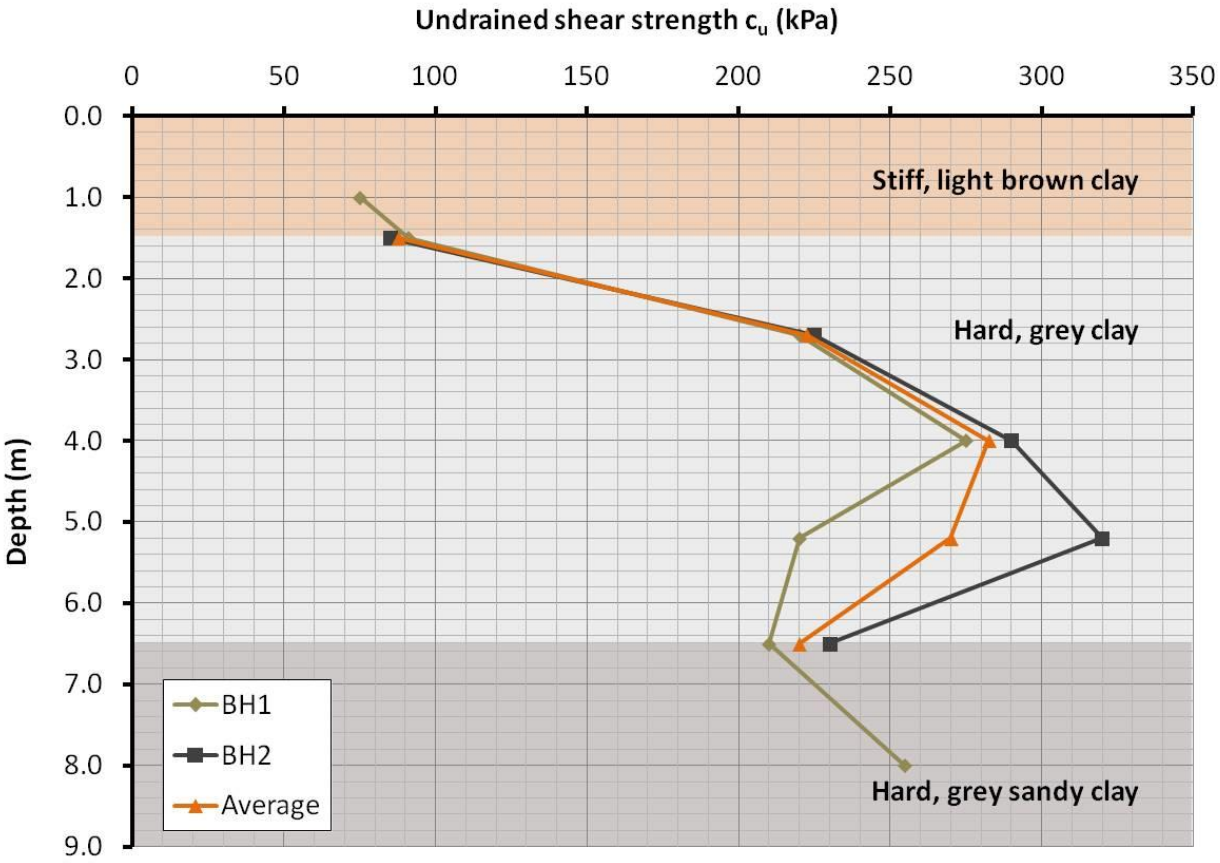

Figure 84 – Undrained shear strength c_u versus depth for Lawnton field test site

The soil strength classification for the Lawnton Clay was defined according to Table 8. The following average values (undrained shear strength c_u) are utilised for the pile design:

- Stiff, light brown clay c_u = 85 kPa
- Hard, grey clay c_u = 250 kPa
- Hard, grey sandy clay c_u = 250 kPa

Triaxial CU test results were also used to determine the parameters for the hypo-plastic soil parameters, as described in Section 8.1.1 above.

Table 8 – Soil strength classification, after Look 2007

Soil Classification	*Undrained Shear Strength c_u*	*Approximate q_c*
Very soft	0–12 kPa	< 0.2 MPa
Soft	12–25 kPa	0.2–0.4 MPa
Firm	25–50 kPa	0.4–0.9 MPa
Stiff	50–100 kPa	0.9–2.0 MPa
Very stiff	100–200 kPa	2.0–4.2 MPa
Hard	> 200 kPa	> 4.2 MPa

8.2.2 Oedometer test

The oedometer test results were used to determine the parameters for the hypo-plastic soil model as described in Section 8.1.1 above. The void ratio versus log of the consolidation pressure was plotted for grey clay on undisturbed and disturbed samples, as shown in Figure 85.

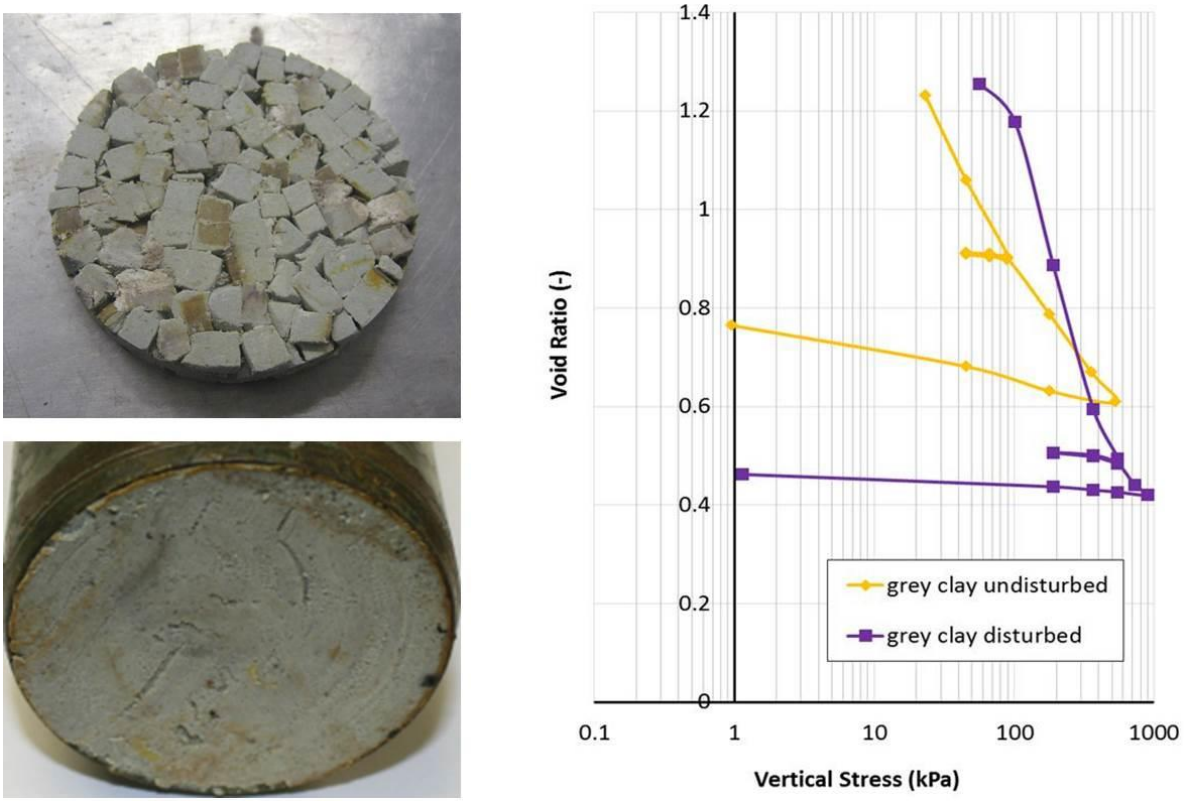

Figure 85 – Plot of void ratio versus consolidation pressure for grey clay

It can be observed in Figure 85 that the disturbed grey clay shows higher compressibility and lower void ratios than the undisturbed sample. It is considered that the grey clay was disturbed during pile installation. However, the mechanism of distortion and disturbance during pile installation was unclear at the time of the laboratory tests and the hypo-plastic parameters used for the finite element analysis were determined from the undisturbed samples.

Figure 85 shows the different response of an undisturbed and disturbed soil sample of grey clay. The stiffer response of the disturbed sample was unexpected and could be more related to sample preparation.

8.3 Pile installation

The three different screw auger types as introduced in Figure 50 in Section 7.3 above are displayed in Figure 86 as they were set up for pile installation on site. The top 250 mm of each pile location was pre-excavated to remove obstructions, stones and rubble, to ensure no auger deviation at the entrance point, which might have resulted in damaging the monitoring equipment. These excavated sections (the top 250 mm of each pile shaft) were not taken into account for the pile design calculations.

Figure 86 – The three different augers on the field test site, CFA (left), progressive displacement (centre) and rapid displacement (right)

Plane pile installation tolerances were within 75 mm, which is in accordance with AS2159-2009. No verticality problems were expected due to the short depths of the piles and the stiff drill stem connection at the piling rigs during installation.

The screw auger full-displacement piles C and D were installed with 450 mm augers, which created a 450 mm pile shaft. The CFA auger measured 500 mm in diameter. This research is mainly concerned with stress changes and displacements in the ground as a result of the pile installation process using different auger shapes and installation parameters. The slightly larger diameter of the CFA pile was not normalised to 450 mm as the total pile capacity was not the main aim of this research. The unit shaft friction and base resistance values in relation to installation effects were more important.

During the penetration phase of the installation of test pile B (CFA pile), a lump of stiff clay became caught inside the auger, as shown in Figure 87. The lump of clay had a diameter of about 650 mm and was located about 1.0 m above pile toe level. At auger extraction, the lump of clay attached to the auger and slowly rotating clockwise created a larger pile diameter than the nominated 500 mm for the upper section of the pile.

Figure 87 – Pile B: Clay became trapped inside the auger during pile installation

For design purposes, it was assumed that the bottom 1.0 m of the shaft had a nominated diameter of 500 mm and that the 2.75 m above the shaft had an enlarged diameter of 650 mm, which is equal to the diameter of the lump of clay. The average pile diameter for test pile B was assumed as 610 mm. The pile was not excavated after the execution of static load tests due to lack of resources and budgetary constraints.

8.3.1 Pile monitoring records

The installation of the test piles was carried out with two different piling rigs. Test piles B (CFA), C (progressive screw auger displacement pile) and D (rapid screw auger displacement pile) were installed in early February 2013 using a Casagrande C30 piling rig, as shown in Figure 88. Test pile E (rapid screw auger displacement pile) was installed a few months later in July 2013 using a Bauer BG28 piling rig (Figure 90).

Figure 88 – Installation of test piles B, C and D with the Casagrande C30 piling rig

Both rigs were equipped with Jean Lutz monitoring software, as described in Section 7.3.1 above. The software-monitored parameters of penetration rate, auger rotation, rotational torque and lifting rate of the auger during concreting were monitored using a 'Taralog' unit in the rig (Figure 89).

Figure 89 – Jean Lutz Taralog pile monitoring unit on site during the test execution

It was intended to use a different rig to install test pile E. The Bauer BG28 is a bigger piling rig, with higher rotational torque and pull-down capacities than the smaller Casagrande C30. The key features of both piling rigs are compared in Table 9.

Table 9 – Comparison of Casagrande C30 and Bauer BG28 piling rigs

Piling rig details	***Casagrande C30***	***Bauer BG28***
Operational weight (ton)	85	110
Year of manufacture	1985	2008
Rotational torque (kNm)	120	280
Vertical pull-down force (kN)	150	300
Automatic drill assistant	NO	YES

The Bauer BG28 rig was used because the originally designated piling rig for this research project, the Casagrande C30, was not rigged up when installing the additional test pile E in July 2013, which was installed to investigate further the heave behaviour of screw auger displacement piles. Instead, test pile E was installed using the much more powerful BG28 rig (Figure 90), which allowed the penetration rate over a depth of 4.0 m to be kept constant. The rig operator used an automatic drill assistant for penetration and extraction, which ensured that the penetration and extraction rates were kept constant as long as the rotational torque and pull-down capacities of the rig were not exhausted. The drill times (shown in seconds) for all test piles are summarised in Table 10 and Figure 91.

From the table, it can be seen that it took 10 seconds to drill pile B to a depth of 500 mm below the surface and that the entire pile was completed after 95 seconds. After 110 seconds, the rig started pumping the concrete, which means that the auger was left at the pile toe for 15 seconds before the concrete placement process started. Reading the table in the same way, pile C was installed to full depth after 179 seconds, pile D was drilled to the same depth after 139 seconds and pile E required only 125 seconds to be drilled to 4.0 m depth.

Figure 90 – Installation of test pile E with the Bauer 'BG28' piling rig

Table 10 – Summary of installation times (in seconds) for all test piles

Depth (mm)	*Pile B*	*Pile C*	*Pile D*	*Pile E*
Penetration				
500	10	15	10	17
1,000	20	25	21	35
1,500	30	38	32	50
2,000	40	50	44	65
2,500	50	65	57	80
3,000	65	97	78	95
3,500	80	134	105	110
4,000	95	179	139	125
Extraction				
4,000	110	192	160	145
3,500	120	204	170	155
3,000	130	215	180	165
2,500	140	225	190	175
2,000	150	235	200	185
1,500	160	245	210	195
1,000	170	255	220	205
500	180	265	230	215
0 (surface)	190	275	240	225

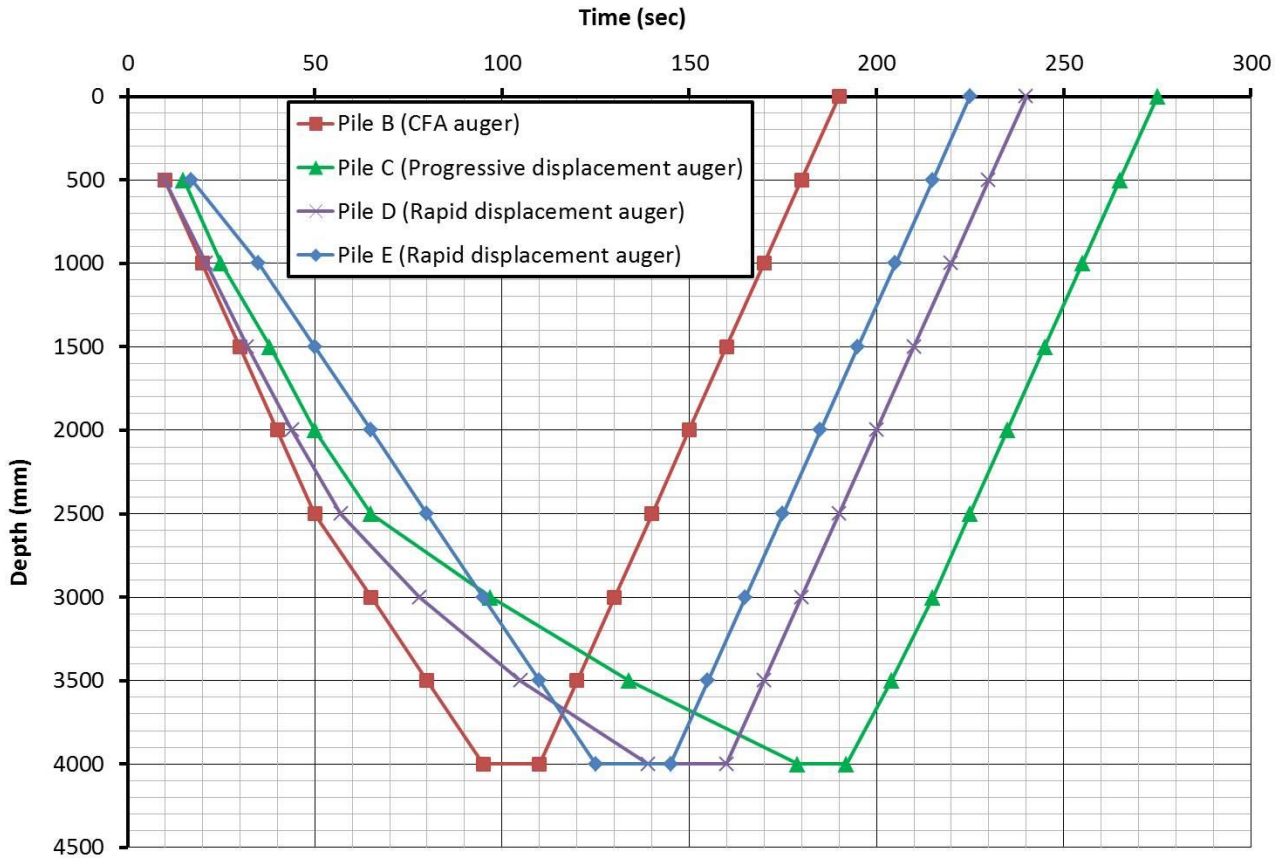

Figure 91 – Summary of installation rates for all test piles

The penetration times and rates for the piles installed with the Casagrande C30 were not constant. Of these piles, test pile B had the closest to linear penetration, whereas the screw auger full-displacement piles C and D showed varying behaviour during penetration, as shown in Figure 91 and Figure 98.

The drill rates for piles C and D decreased as the displacement body started penetrating the soil. The changing slope in the graphs of the installation rates, displayed in Figure 91, indicate a reduction in penetration rate. The progressive displacement auger (pile C) had the most significant decline in penetration with depth.

Pile E, which was installed with a significantly more powerful piling rig, was constructed with a constant penetration rate until 4.0 m below the surface. The rig provided sufficient rotary torque capacity and pull-down force to overcome the friction as the displacement body was pushed into and through the stiff and hard clay formations. Comparing the installation parameters for piles D and E (which were installed using similar rapid displacement augers), it can be observed that pile D was installed with a decreasing penetration rate for the bottom 1.5 m.

Overall, it can be observed that the test piles installed with the C30 piling rig (B, C and D) showed a decreased penetration rate up to 2.0 m below platform level. The reasons for this are now explained.

Test pile B – CFA pile

Test pile B was installed using a CFA auger with a large stem as described in section 2.3. The auger action consisted of the cutting action at the auger tip, the transport of the soil cut through the auger flights and some displacement action of the borehole wall while the soil was being transported to the surface via the auger flights. The penetration rate for test pile B was calculated based on the following assumptions:

Rotations of the auger per minute:	15 (target)
Pitch height of the CFA auger flights:	330 mm
Outer diameter of the auger d:	500 mm
Stem diameter of the auger d_0:	318 mm

For the calculation of the optimal penetration rate, Viggiani's formula as per Equation 8 was used:

$V_{a(min)} \geq nl\ (1 - (d_o^2/d^2))$

$V_{a(min)} \geq 0.33\ m * 15\ rpm * (1 - (0.318^2/0.50^2))$

$\mathbf{V_{a(min)}} \geq 2.95\ m/min = \underline{\mathbf{3\ m/min}}$

For auger B, the optimal penetration rate was calculated to be equal to or faster than 3.0 m/minute.

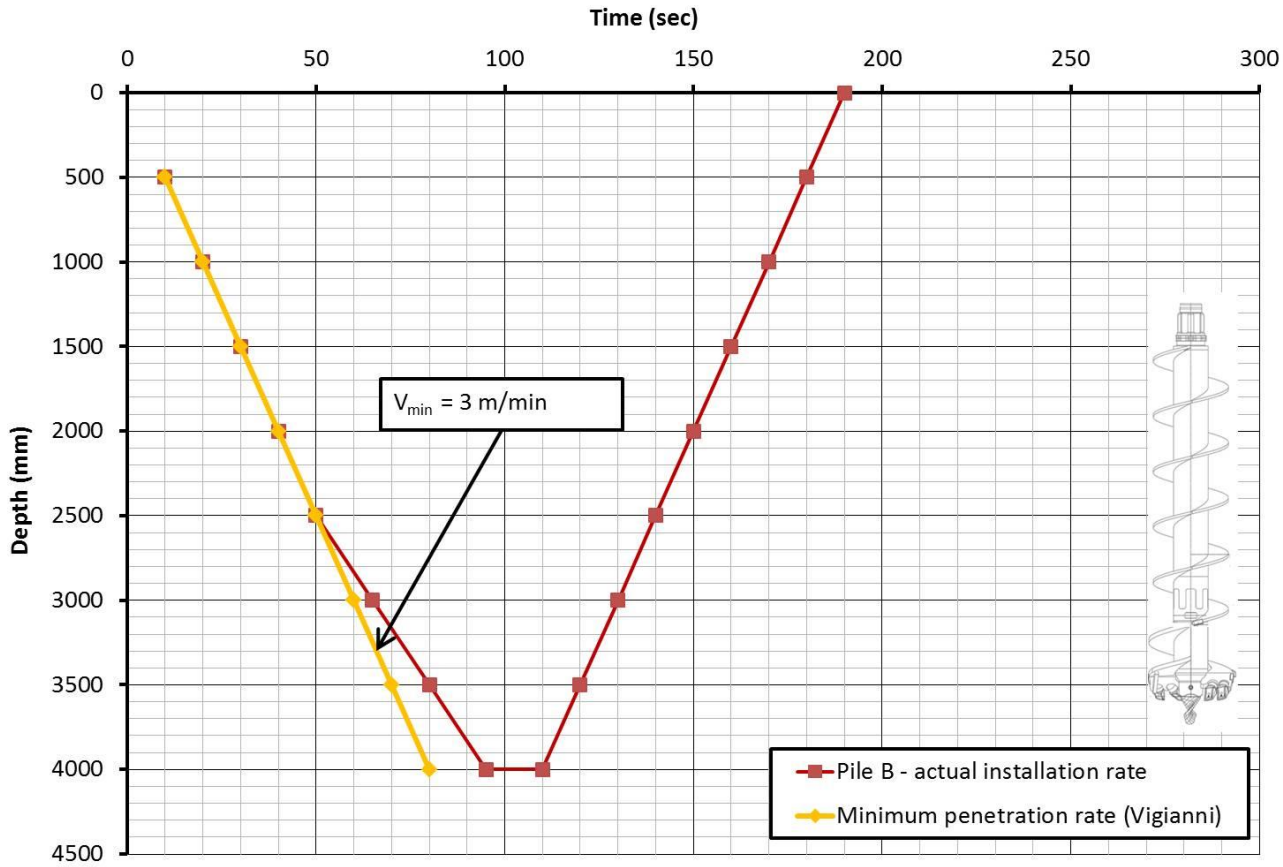

Figure 92 – Summary of installation rates for test pile B (CFA)

Figure 92 shows the drill rate summary for test pile B. The extraction rate of the CFA pile is constant all the way up from the pile toe to the surface. It can also be observed that the penetration rate was constant up to a depth of 2.5 m below ground level. Beneath this depth, the installation rate decreased slightly from 3.0 m/min to about 2.5 m/min until pile toe level.

After review of the pile installation or monitoring record of the rig computer (Figure 93), the auger rotation was observed to be constant over the top 2.0 m, matching the target rotation of 15 rpm.

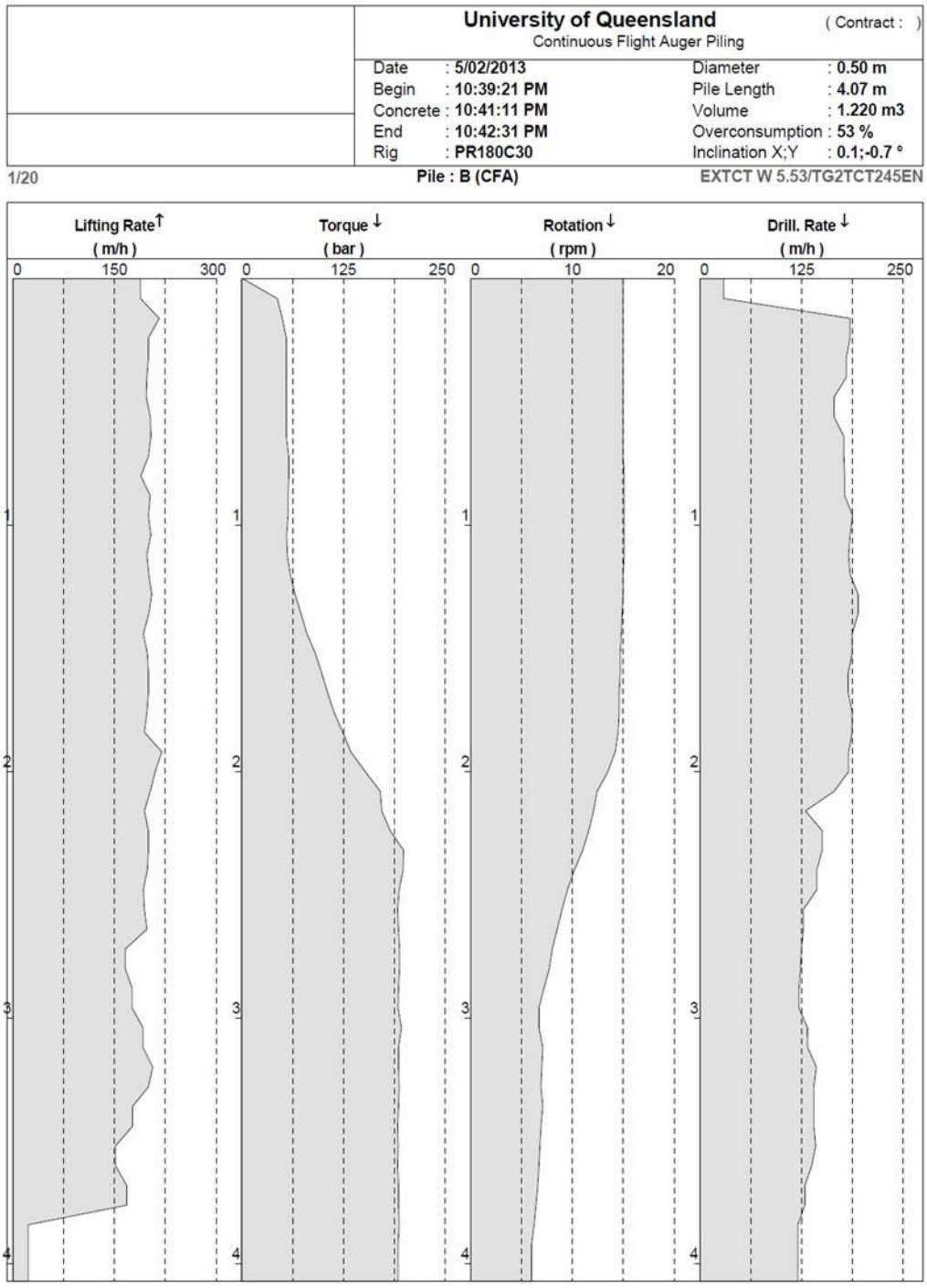

Figure 93 – Pile monitoring record for pile B (CFA pile)

Reduced auger rotations were observed at about 2.0 m below working platform level, as the rotational torque was reaching its maximum such that, within a meter of penetration at 3.0 m below surface level, the number of rotations had halved to reach a value of about 7 rpm. Concurrently, the torque reached its maximum value at 2.5 m below the surface and it remained at this maximum value until the pile reached its final depth of 4.0 m below surface level. As soon as the torque reached its maximum, the penetration slowed. It was then possible to hold this penetration rate constant at the slightly lower rate (2.5 m/min) for the remaining drilling distance.

Considering that the CFA auger had no displacement body or other features that would increase the resistance in the soil, it seems obvious that the rig reached its capacity due to drilling resistance, which caused the penetration to slow. However, this slower penetration rate was then kept linear and constant until the pile toe was reached. The effect of the sheared lump of clay that was trapped inside the auger flights is questionable but it could have influenced the penetration rate.

The slightly reduced penetration rate at about 20% lower than Viggiani's formula seems not to be a major issue in stiff or hard clay with respect to over-flighting and uncontrolled lateral soil transport, as reported for granular soils (Slatter 2000). However, the Casagrande C30 rig was at its limit and would have reached drilling refusal if larger diameters or greater penetration depths had been used.

Test pile C, D and E – screw auger full-displacement piles

The full-displacement test piles were installed using two different auger types:

- Progressive displacement auger (pile C); and
- Rapid displacement auger (piles D and E).

The optimal penetration rates for all full-displacement piles, regardless of the auger geometry or type, were calculated based on the following assumptions:

Rotations of the auger per minute:	12 (target)
Pitch height of the CFA auger flights:	300 mm
Outer diameter of the auger d:	450 mm
Average stem diameter of the auger d_o:	323 mm

The two different auger types were not differentiated further. An identical penetration rate was used as a benchmark for energy input during the pile installation to provide information about increased efforts for one particular type of auger in similar ground conditions. The inner stem diameter was chosen as an average value between the diameters of the displacement body and the lower auger section. The pitch of the flights was taken as an average value of both auger types.

The auger rotations were chosen to be 20% lower as for the CFA pile due to the expected displacement effect and larger auger resistance in the cohesive soil formation.

For the calculation of the optimal penetration rate for the full-displacement augers, Viggiani's formula as per Equation 8 was used, as shown below:

$V_{a(min)} \geq nl\ (1 - (d_o^2/d^2))$

$V_{a(min)} \geq 0.3\ m * 12\ rpm * (1 - (0.323^2/0.45^2))$

$\mathbf{V_{a(min)} \geq 1.75\ m/min =}$ **1.8 m/min**

For the full-displacement screw augers, the optimal penetration rate was calculated to be equal to or faster than 1.8 m/minute.

From Figure 94, it can be observed that only pile E was installed to pile toe level (4.0 m below ground) with a constant penetration rate slightly above the minimum penetration rate of 1.8 m/min.

By contrast, piles C and D show constant penetration rates matching the minimum drill rate over the top 2.0 m, with rates decreased nonlinearly with further depth.

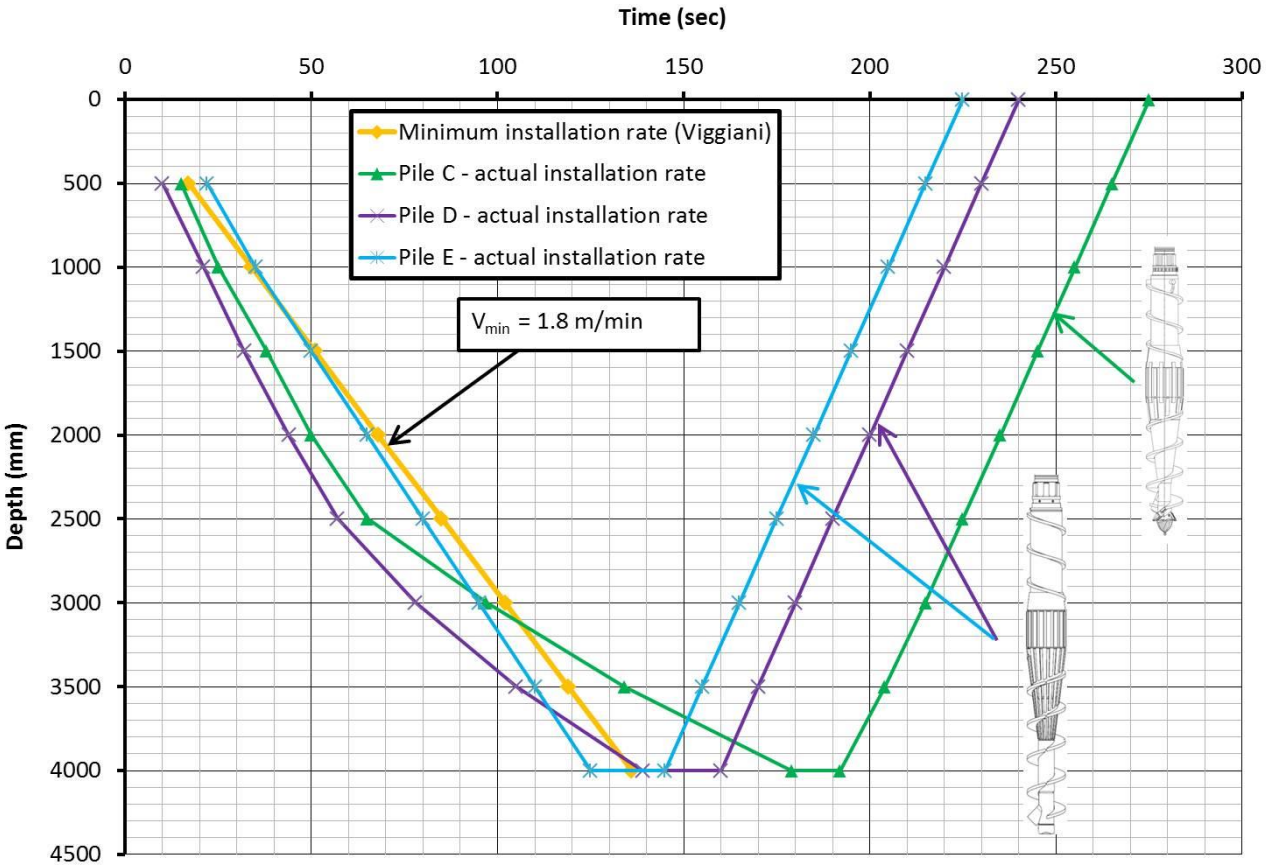

Figure 94 – Summary of installation rates for the test piles C, D and E (screw auger full-displacement piles)

The reductions of penetration rate were more significant for the progressive displacement auger type (pile C). The review of the construction records of the individual piles gives a better understanding of the installation processes for the three test piles installed with full-displacement augers.

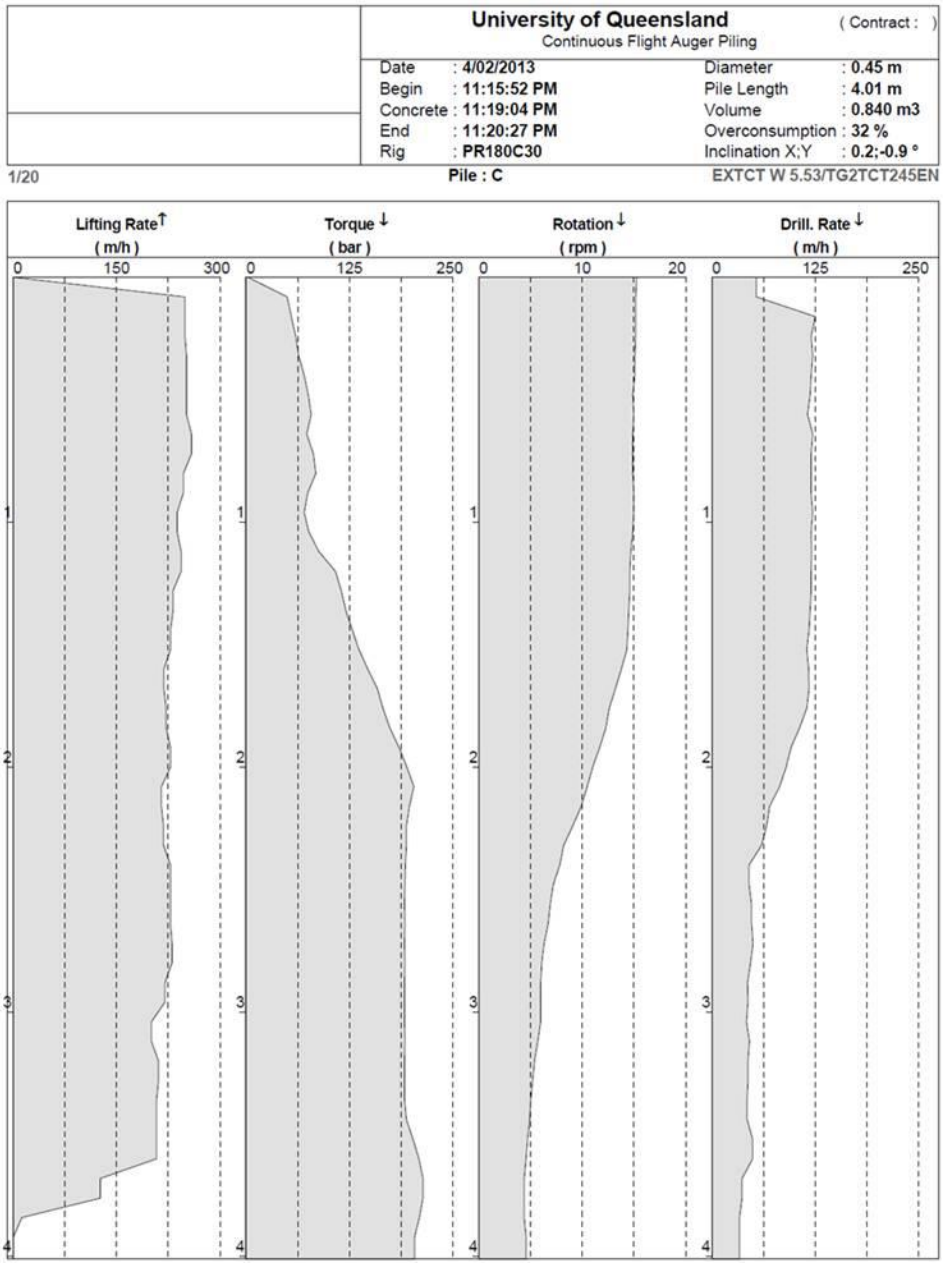

Figure 95 – Pile monitoring record for pile C (progressive displacement auger)

Figure 95 shows the installation record for pile C, installed with a progressive displacement auger. The rotations per minute were constant over the top 1.5 m at 15 rpm, which was higher than the target rotation rate. In the Casagrande C30 piling rig, the auger rotations cannot be operated in a way more sophisticated than by drilling with full or half auger rotations. It is a manual operation process. For this research project, the rig operator applied the maximum number of rotations until the number was reduced by drilling resistance in the soil formation. From 1.5 to 3.0 m depth, the rotations

dropped from 15 rpm to about 5 rpm, which indicates a severe increase in drill resistance, which can be correlated to the entrance of the displacement body into the hard clay layer.

The penetration rate dropped qualitatively in a similar way to the rotations, meaning that it was reduced to a factor of about 35% at 3.0 m depth. The maximum rotational torque was reached at 2.0 m depth, after partial penetration of the displacement body. From this point onwards, the rig operated using its maximum rotational torque capacity and its maximum pull-down force. Even though pile C finally reached the design toe level, the penetration rate was significantly lower at the deeper section of the pile and further penetration into the hard clay formation would have caused auger refusal.

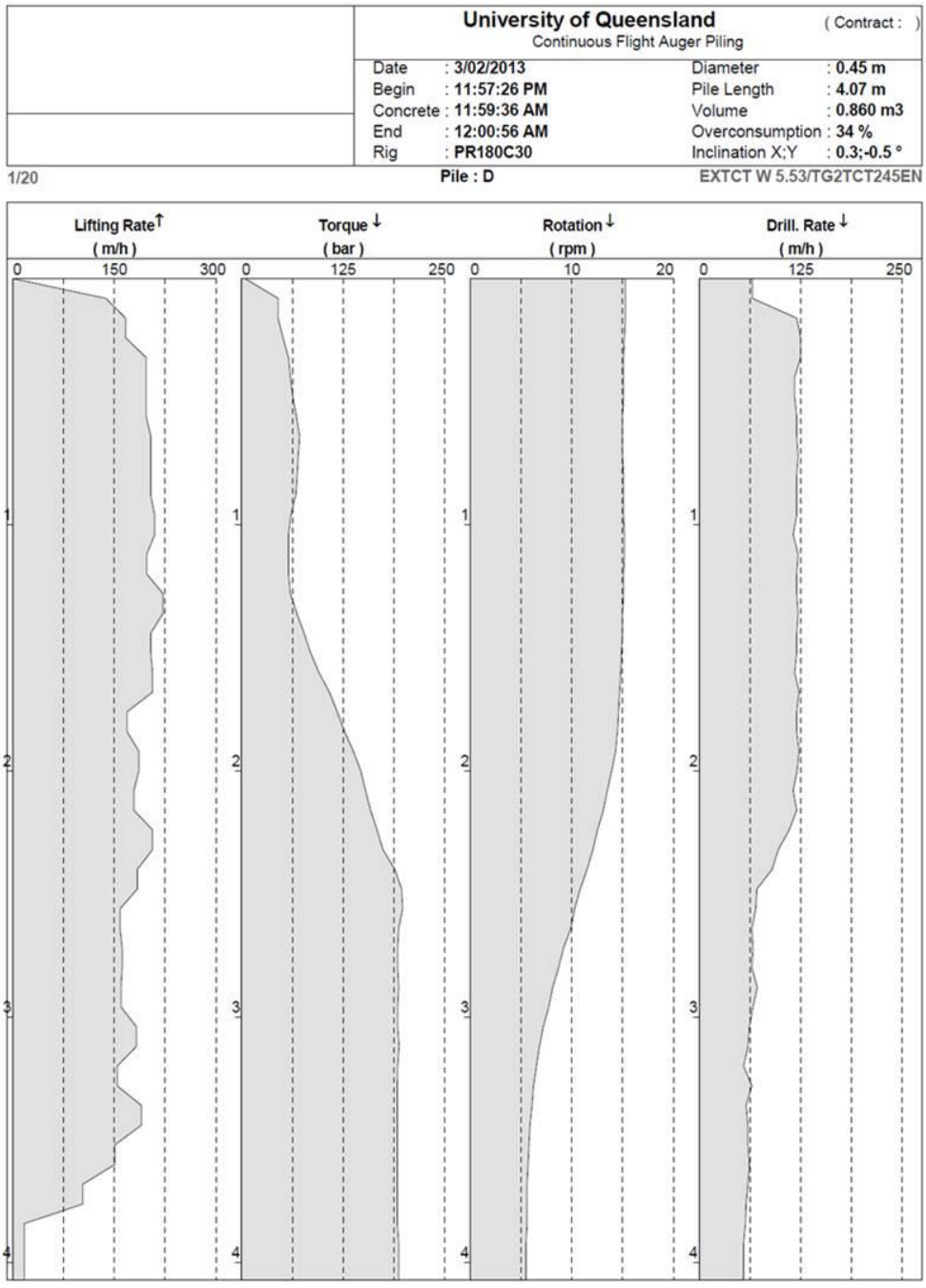

Figure 96 – Pile monitoring record for pile D (rapid displacement auger)

Test pile D was installed with a rapid displacement auger. The penetration rate over the first 2.0 m depth was in excess of the specified rate of 1.8 m/min, as shown in Figure 96. The piling rig operated with maximum auger rotations of 15 rpm for the first 2.0 m of drilling, before the rotations dropped back almost linearly to a value of about 5 rpm at 3.5 m depth below surface. The torque reached a maximum value at about 2.5 m below the surface and stayed at full capacity for the remainder of the drilling process. The penetration rate dropped at a depth of 2.2 m below the surface to about 1.0 m/min, which is about 55% of the calculated drill rate.

For this auger type, the lower auger section is about 500 mm longer than for the progressive auger that was used to install pile C. The maximum rotational torque was reached 500 mm lower than for pile C, at the point of entrance of the displacement body into the stiff clay layer. At this point, there was substantial drilling resistance, causing the auger rotations to decrease considerably and reducing the penetration rate by about 55%, despite working with full rotational torque and vertical pull-down capacities. The reduction was not as severe as for pile C, but with further penetration, the Casagrande C30 rig would have reached refusal.

Test pile E was installed using a considerably more powerful piling rig than the Casagrande C30, the Bauer BG28. This rig has over 140% more rotational torque capacity and 100% additional pull-down force. Further, the auger rotations can be controlled by the operator and the machine offered the assistance of a computerised penetration and extraction process that allowed the desired penetration rate to be defined.

As shown in Figure 94, the penetration rate for pile E is constant and linear for the entire penetration process. The penetration is about 2.0 m/min and is slightly faster than the pre-defined 1.8 m/min after Viggiani's formula. Figure 97 shows the installation or monitoring record of pile E, revealing that the penetration rates and the auger rotations (12 rpm, as per calculation) remained constant throughout the drilling process. The rotational torque increased linearly from about 1.6 m below the surface until the pile design toe level. The full torque capacity was not reached, but it would have been with further penetration, potentially causing a drop in auger rotations or pile penetration in a similar way to in piles C and D.

During pile extraction, the auger was lifted more slowly, directly after concrete placement. This can be observed in the very low extraction rates at the pile base. The Bauer BG28 shows a linear extraction rate, attributable to the fully automated installation procedure.

The extraction rates for all piles installed with the Casgrande C30 were virtually linear; however, due to manual auger extraction, minor variations were observed. Overall, the extraction rate for all test piles was in a similar range, matching 3 m/min.

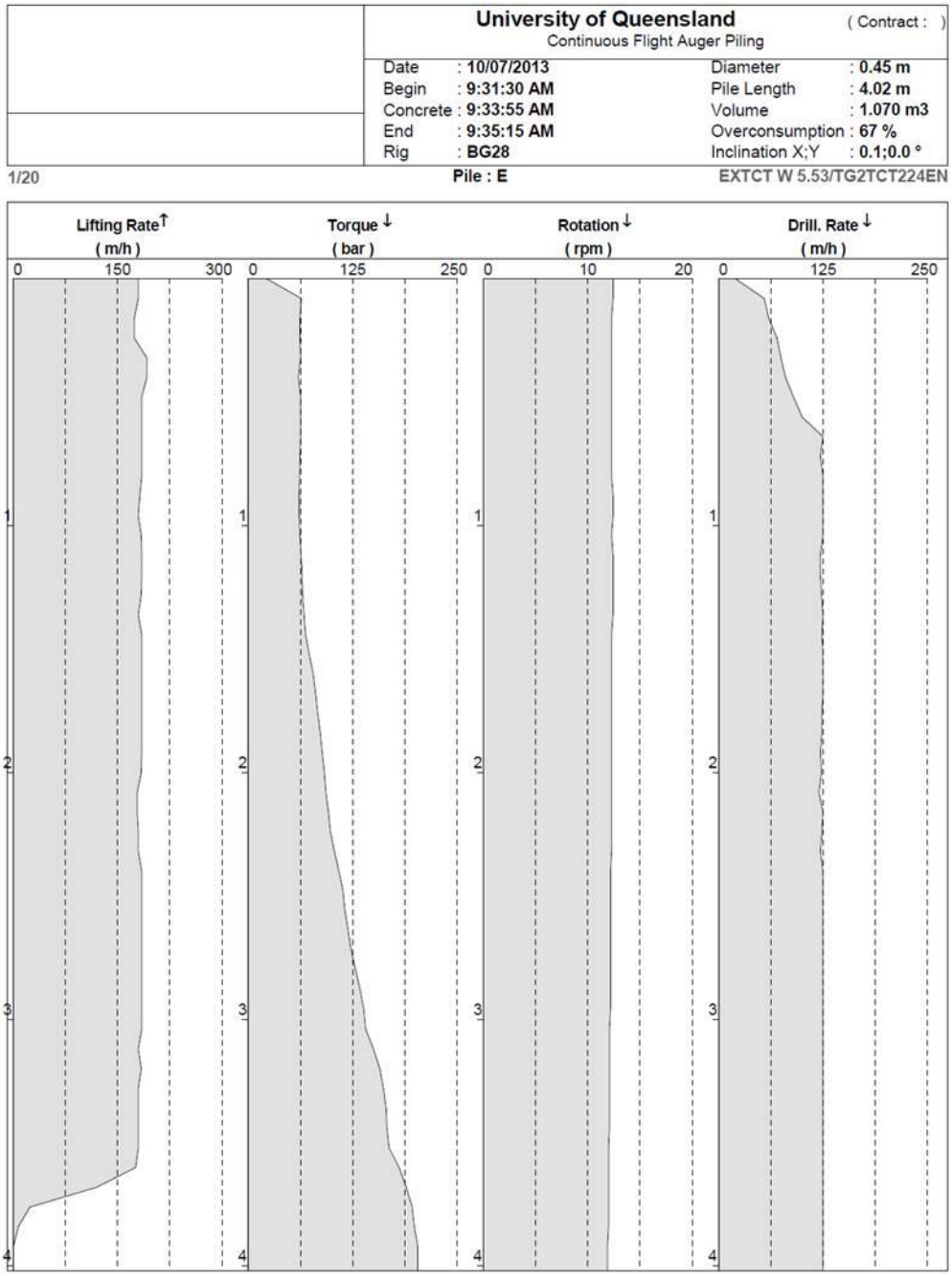

Figure 97 – Pile monitoring record for pile E (rapid displacement auger installed with a more powerful piling rig)

The drill rates for all test piles are summarised in Table 11 and Figure 98. The drill rates are displayed in metres per minute penetration. The extraction rates are constant for all piles (-3.0 m/min).

Only pile E showed penetration rates equal to or above the target value, calculated using Viggiani's formula, throughout the entire drilling process.

Table 11 – Summary of installation rates (in m/min) for all test piles

Depth (mm)	*Pile B*	*Pile C*	*Pile D*	*Pile E*
Penetration TARGET	***3.0/-3.0***	***1.8/-3.0***	***1.8/-3.0***	***1.8/-3.0***
500	3.0	2.0	3.0	1.8
1,000	3.0	3.0	2.7	1.8
1,500	3.0	2.3	2.7	2.0
2,000	3.0	2.5	2.5	2.0
2,500	3.0	2.0	2.3	2.0
3,000	2.8	0.9	1.4	2.0
3,500	2.6	0.8	1.1	2.0
4,000	2.5	0.7	0.9	2.0
Extraction				
4,000	-3.0	-3.0	-3.0	-3.0
3,500	-3.0	-3.0	-3.0	-3.0
3,000	-3.0	-3.0	-3.0	-3.0
2,500	-3.0	-3.0	-3.0	-3.0
2,000	-3.0	-3.0	-3.0	-3.0
1,500	-3.0	-3.0	-3.0	-3.0
1,000	-3.0	-3.0	-3.0	-3.0
500	-3.0	-3.0	-3.0	-3.0
0 (surface)	-3.0	-3.0	-3.0	-3.0

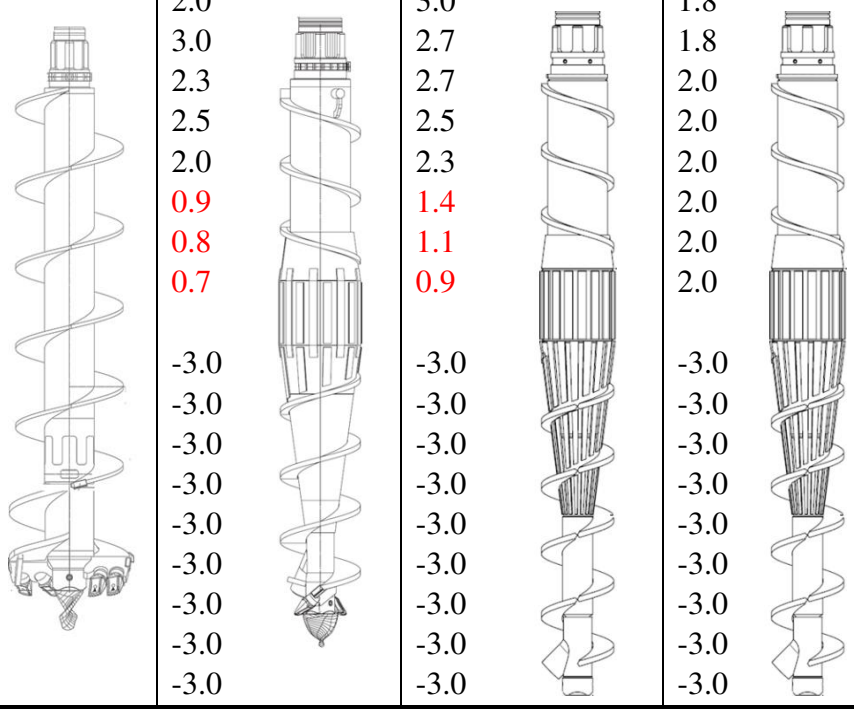

For pile B, the penetration dropped below the target rate of 3.0 m/min over the last 1.0 m of drill depth, from 3.0 m to 4.0 m. However, this was still within 80% of the recommended target penetration rate.

For pile C, which was installed with a progressive displacement auger, the drill rates were sufficient above 2.5 m depth. Below this level, the penetration dropped to 0.9–0.7 m/min, which was between 38% and 50% of the calculated target rate. Close to the surface, the penetration rate was as fast as 167% of the target value for a short distance.

Pile D showed sufficient penetration within the top 2.5 m, before the installation rate dropped to 1.4 m/min and finally to 0.9 m/min for the bottom section of the pile. These values were between 50% and 78% of the calculated target values. Similar to for pile C, the penetration rate close to the surface was between 125% and 167% of the target rate, before slowing drastically at 2.5 m depth.

In summary, the test piles were installed within the following variations, as displayed in Figure 98:

- Pile B: 80–100%
- Pile C: 38–167%
- Pile D: 50–167%
- Pile E: 100–111%

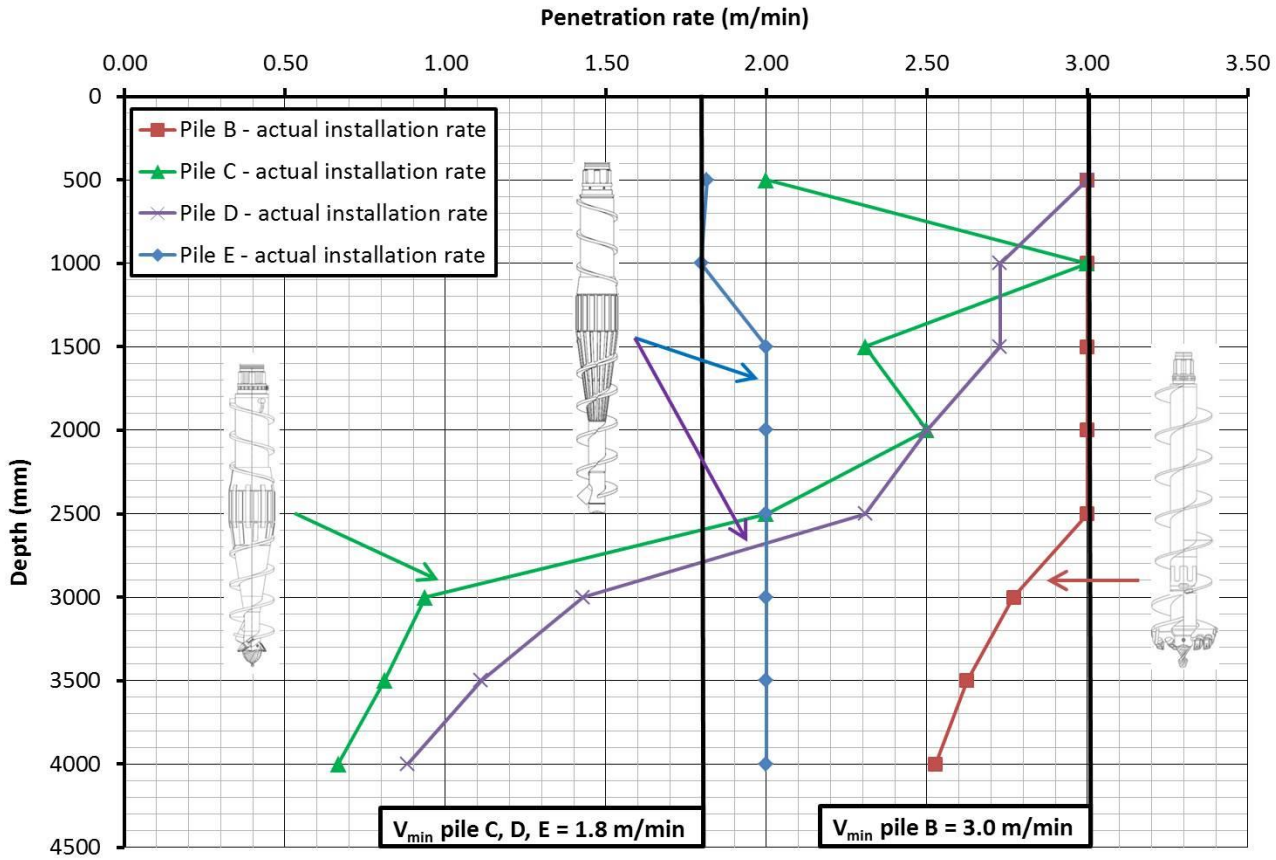

Figure 98 – Summary of the penetration rates for all test piles

8.4 Field test observation methods

8.4.1 Layout details

The three initial test piles were installed within the plane 75 mm tolerances, as specified in AS2159-2009. The target and actual distances of the monitoring equipment installed around each test pile are displayed in Table 12.

The CPT and DMT measurement devices 225 mm from the pile edge were installed within tolerances of ±10 mm.

The inclinometer casings, which were installed by drilling a 100 mm hole in the ground, were installed within ±15 mm tolerance.

Unfortunately, not all inclinometer tubes could be used, as some were damaged during the installation process. Only the tubes spaced 1.25 diameters from the centre line of the pile provided measurements for each pile. The results are displayed in this section.

Table 12 – Distance (target and actual) of the field test monitoring devices from the pile axis of the relevant test pile

TEST	*TARGET DISTANCE*		*PILE B*		*PILE C*		*PILE D*	
	Distance to pile axis	Target (mm)	Actual (mm)	Difference (mm)	Actual (mm)	Difference (mm)	Actual (mm)	Difference (mm)
CPT 1	0.0	0	0	0	0	0	0	0
CPT 2	1.0 d	450	440	-10	455	+5	450	0
DMT 1	0.0	0	0	0	0	0	0	0
DMT 2	1.0 d	450	455	+5	460	+10	440	-10
Inc. 1	1.0 d	450	465	+15	460	+10	445	-5
Inc. 2	1.25 d	563	548	-15	575	+12	560	-3
Inc. 3	1.5 d	675	670	-5	660	-15	670	-5
TDR 1	0.72 d	325	305	-20	315	-10	350	+25
TDR 2	1.0 d	450	420	-30	430	-20	435	-15
TDR 3	1.5 d	675	605	-70	710	+45	695	+20

Note: TDR measurements are not discussed as part of this thesis.

The TDR sensors were installed within tolerances up to +45 mm, -75 mm from the target location. However, again some sensors were damaged during pile installation. This is of no concern here, as the TDR data are not part of this thesis; the associated research results will be published separately.

8.4.2 CPT

Vertical CPTs were carried out for each pile before and after pile installation. For each test pile, the ratio of cone tip resistance q_c before pile installation and after pile installation with depth is displayed. The ratio of shaft friction f_s is not compared because the cone resistance is the governing factor for the pile design methods used for this research work.

It is important to point out that these ratios are of effective stresses: pore water pressures are not included in the figures for vertical CPTs carried out before and after pile installation. The CPTs after pile installation were conducted three to seven days after pile installation, giving sufficient time for pore water pressures to dissipate.

The research focuses on effective stress changes in the soil and potential changes in soil stiffness and shear strength because of the pile installation. For the pile design, it was critical to determine the undrained shear strength c_u at the pile locations. The average value of the undrained shear strength c_u determined from triaxial tests is shown in the following figures as a comparison and reference to the data obtained by CPT and DMT *in situ* measurements. I

n Figure 99, the profiles of undrained shear strength values versus depth are displayed for all pile locations in virgin ground (before pile installation).

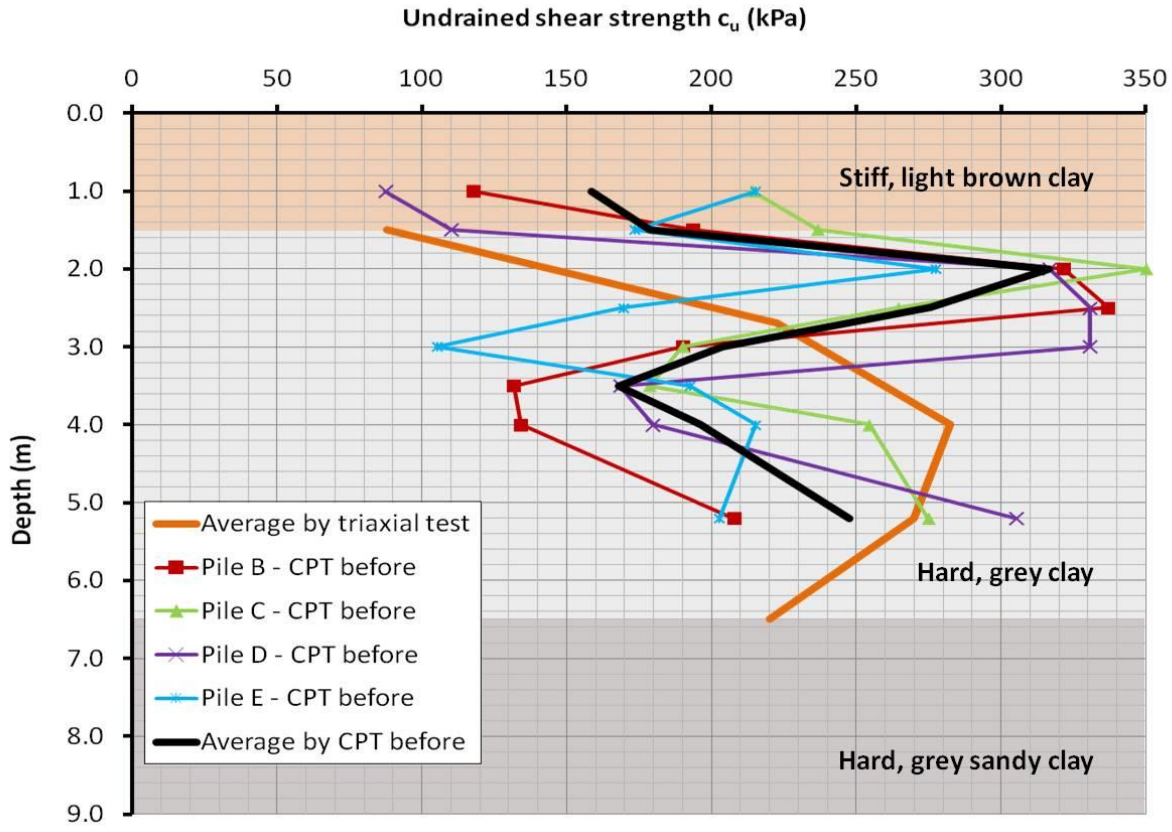

Figure 99 – Shear strength data (by CPT) of Lawnton Clay before pile installation

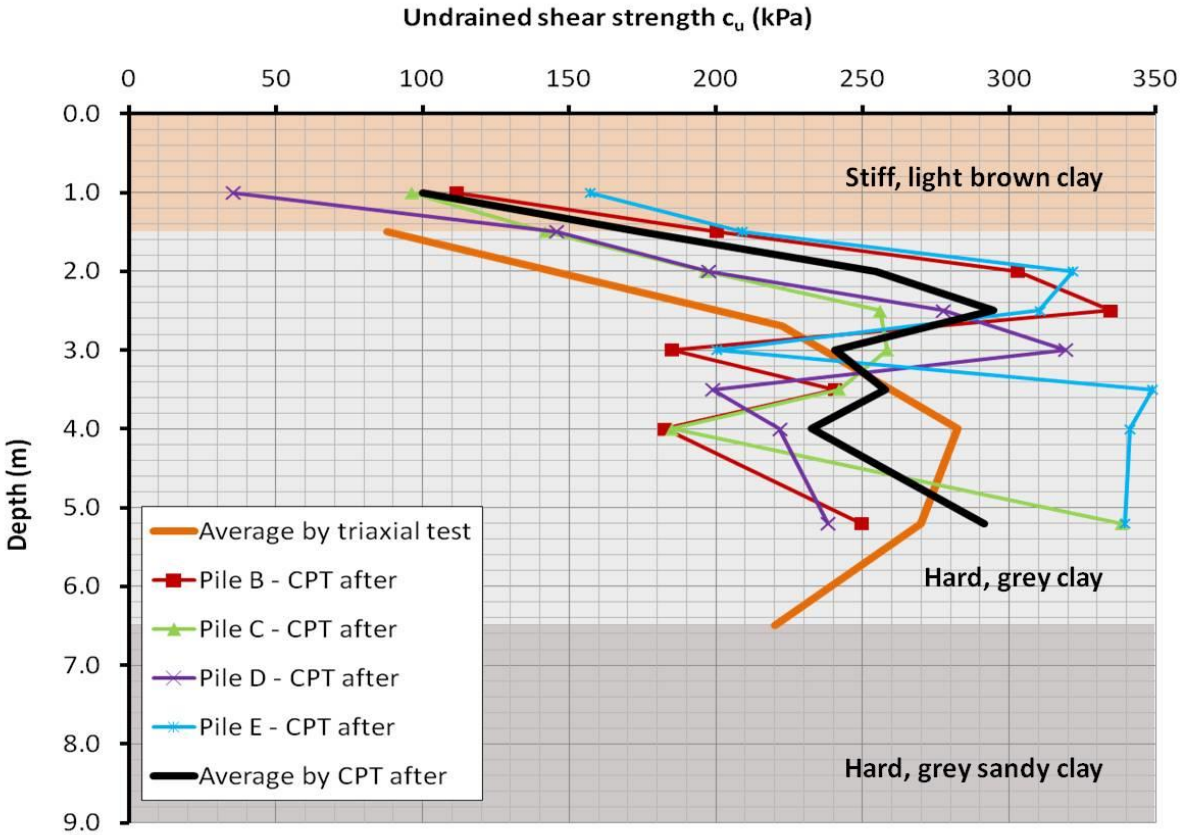

Figure 100 – Shear strength data (by CPT) of Lawnton Clay after pile installation

Figure 100 shows the undrained shear strength data obtained by CPTs and triaxial tests for all pile locations after pile installation. The CPTs were carried out at a distance of one pile diameter from the pile axis of the relevant test pile.

In both figures, the depth profile of the undrained shear strength obtained from laboratory tests (triaxial CU tests) is also displayed for comparison.

In Figure 101, the ratio of the cone resistance qc of test pile B (CFA pile) is displayed, comparing the reading after pile installation with the reading before pile installation. A ratio smaller than 1 is displayed in red and indicates reduced cone resistance q_c as a result of the pile installation process. Conversely, a ratio larger than 1 (displayed in black) indicates increased cone resistance q_c along the pile shaft as a result of the pile installation.

For pile B, along the pile shaft, the ratio was mostly between 0.9 and 1.1. In the top 500 mm close to the surface, the ratio was smaller. Close to the pile toe, at about 3.9 m depth, an increased ratio was observed. This increased ratio of about 1.3–1.4 was located at the pile toe level and reached up to 750 mm (equivalent to 1.5 pile diameters) below the pile base. For the remaining depth, the ratio was close to 1 and the overall improvement of the initial conditions was 3%.

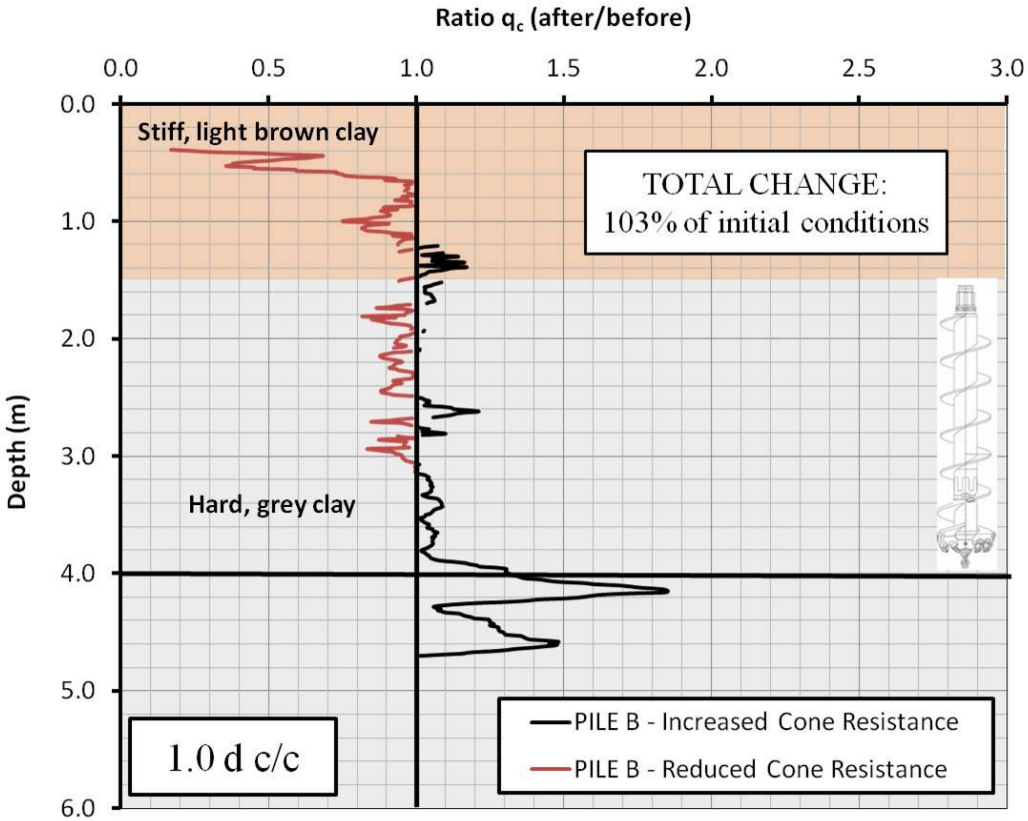

Figure 101 – Pile B: Ratio of cone resistance q_c after and before installation

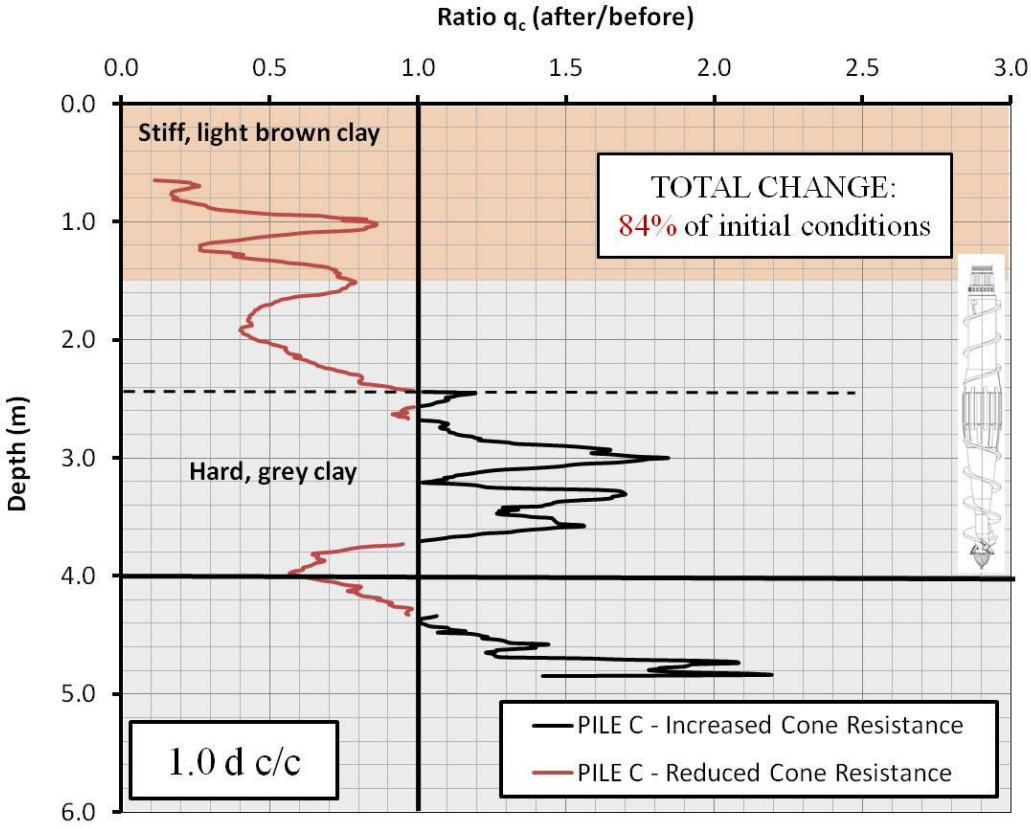

Figure 102 – Pile C: Ratio of cone resistance q_c after and before installation

Pile C showed a different behaviour, as indicated in Figure 102. The pile, which used a progressive displacement auger with decreasing installation rate, showed a significant reduced cone tip resistance of only 60% on average in the top 2.4 m of the pile depth. Below this level, the ratio spiked at about 1.6, with an average improvement rate of about 40% up to 300 mm above the pile toe level. In the area of the pile toe level (300 mm above and below), the ratio was reduced to about 0.8, which means that the cone resistance after pile installation was lower than in virgin soil conditions. Below this level of reduced cone resistance at the pile base, the cone resistance increased significantly up to a level of about 1.0 m below the pile base, where the comparison ended.

For pile D, also installed with a full-displacement screw piling auger, the general pattern is comparable to that for pile C; the installation process of both piles reduced the initial cone tip resistance q_c by 16% for each pile location.

In Figure 103, the ratio for pile D is displayed. The area of reduced cone resistance is shown to reach down to 3.0 m below the surface, with an average ratio of about 0.7 in this region. There is a significant positive spike (reaching 2.8) at the interface of the soil layers at 1.5 m depth.

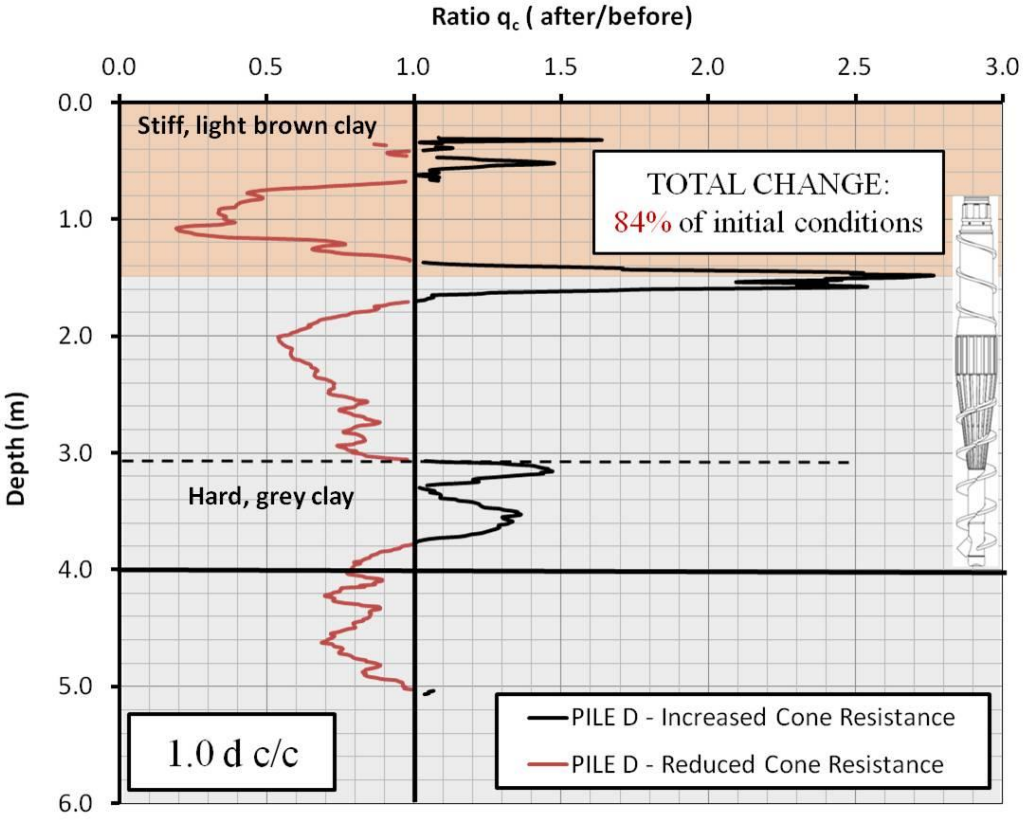

Figure 103 – Pile D: Ratio of cone resistance q_c after and before installation

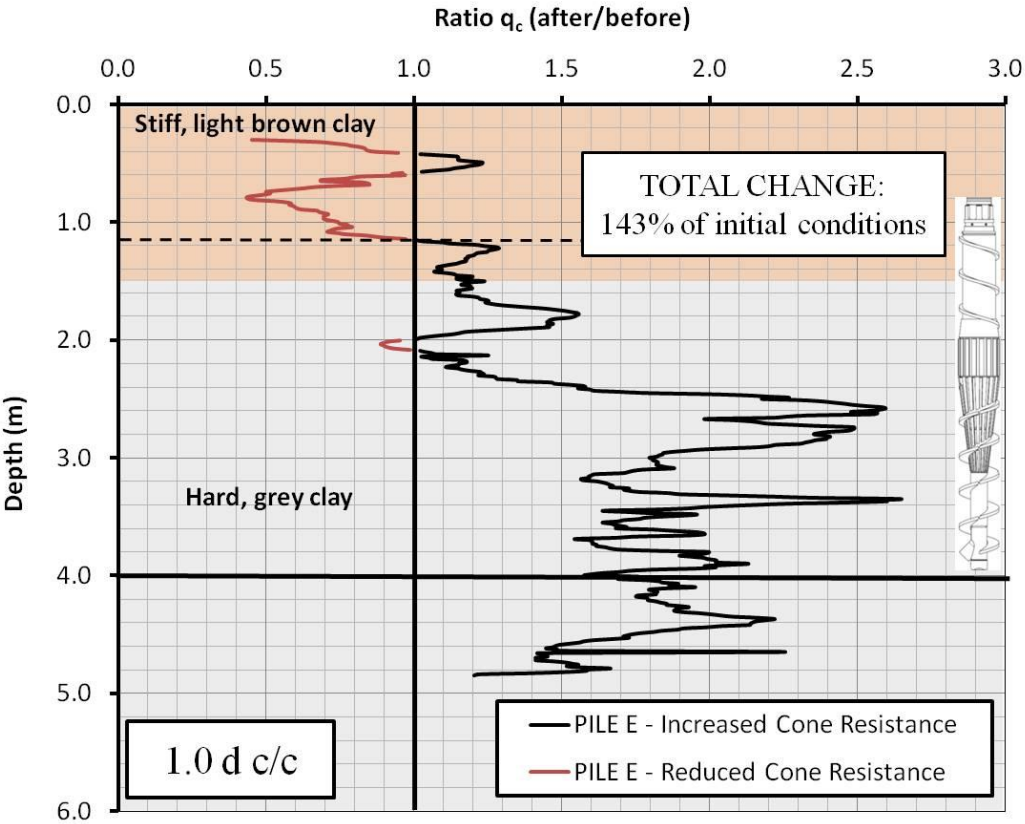

Figure 104 – Pile E: Ratio of cone resistance q_c after and before installation

Another area of improved cone resistance can be seen from 3.0 m to 3.8 m depth, with a slightly positive ratio, reaching an average of about 1.25. At the pile toe level the ratio is only 0.85, reaching down to about 1.0 m below the pile toe, where the ratio becomes 1 again.

Pile E, displayed in Figure 104, presents differently. The only significant reduction in cone resistance occurred in the top 1.2 m, within the stiff, light brown clay layer. Below this depth, the ratio was larger than 1 (with a very minor spike at 2.0 m below the surface, where the ratio was around 0.9 within a 200 mm thin layer). From 2.5 m below the surface to about 1.0 m below pile toe level, the average ratio was close to 2, with spikes up to 2.6. Overall, the installation of test pile E, using a rapid full-displacement auger with a constant, minimum installation rate, in accordance with the recommendations of Viggiani, improved the cone tip resistance q_c by 43%.

The CPT data, collected before and after the pile installation at each pile location, were used for detailed pile design calculations, as presented and discussed in Section 8.5 below. For the stress measurements in the soil formation during pile installation, raked CPT cones were installed, as described in Section 7.4.2 of the previous chapter.

Raked CPTs

The results for test pile B are shown in Figure 105. The change in pressure on the CPT cone and the pore water pressure u_1 were plotted versus time (seconds) to monitor stress changes during the pile installation process. The time intervals for each auger and pile location are shown in Table 14.

For all plots, there were three phases: a penetration phase, during which the auger was drilled down to pile toe level; a pumping phase, during which the auger sat at pile toe level with no movement while concrete was pumped through the supply lines to fill the hollow auger stem; and a penetration phase, during which the auger was extracted whilst concrete being poured to form the pile shaft.

Different points are displayed in each figure, showing the time that the auger tip reached the cone location at 1.5 m depth (A), the moment when the lower point of the displacement body passed the cone location (B) and the time at which the upper point of the displacement body passed the static cone location in the formation. These points are indicated for the penetration and extraction phases. Further, the area of the undrained shear strength c_u for each profile was plotted to show the cone pressure in relation to the undrained shear strength of the individual soil profiles.

Even though the cones were installed a night before the test and left in the ground that the pore water pressure could dissipate, the results shown in the following figures indicate that the pore water pressure did not fully dissipate prior to starting the pile installation. Hence the results should be interpreted more in relative terms.

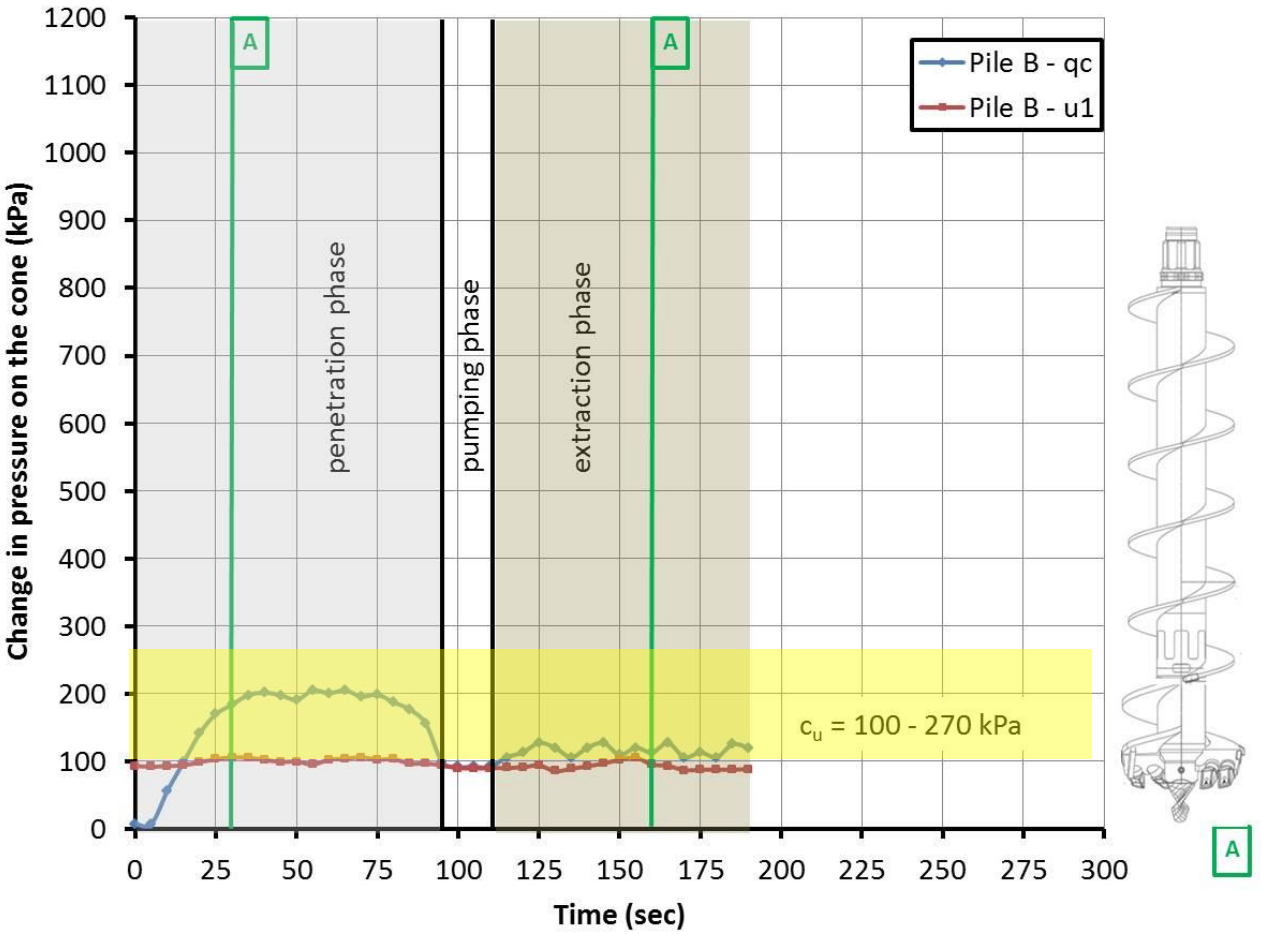

Figure 105 – Change in pressure on the cone v time at 1.5 m depth during installation of pile B

In Figure 105 the changes in pressure on the cone during the installation of pile B are shown. After 30 seconds, the auger tip (point A) passed the cone and the effective stresses reached about 200 kPa. About one minute later, the auger reached the pile toe level and the pumping phase started. At this moment, the lateral stresses dropped to a value of about 100 kPa and then remained constant for the 15 seconds of concrete pumping. During the extraction phase, the lateral stresses varied between 100 and 130 kPa. The passing of the auger tip did not change the effective stress values. At pile completion, the effective lateral stresses were about 120 kPa and the pore water pressure was measured at about 90 kPa. The pore water pressure remained close to constant at this level for the entire pile installation. The changes in pressure on the cone were always below the maximum undrained shear strength of 270 kPa.

In Figure 106 the stresses during the installation of pile C (progressive displacement auger) are shown. The range of undrained shear strength is marked and the changes in pressure on the cone stay within this range for only 30 seconds before they exceed it to reach almost 1,100 kPa as the displacement body of auger C passed the cone location. During the pumping and extraction phases, the pressure on the cone was in the range of 800 kPa, before it quickly dropped to 310 kPa (which is

the upper band of the undrained shear strength for this soil profile) after the auger tip passed the cone during extraction.

The pore water pressure u_1 was at a constant level of about 80 kPa during the installation phase, but as the displacement body (point B) passed the cone, it quickly dropped to about 10 kPa. This value was constant for the remainder of the installation process.

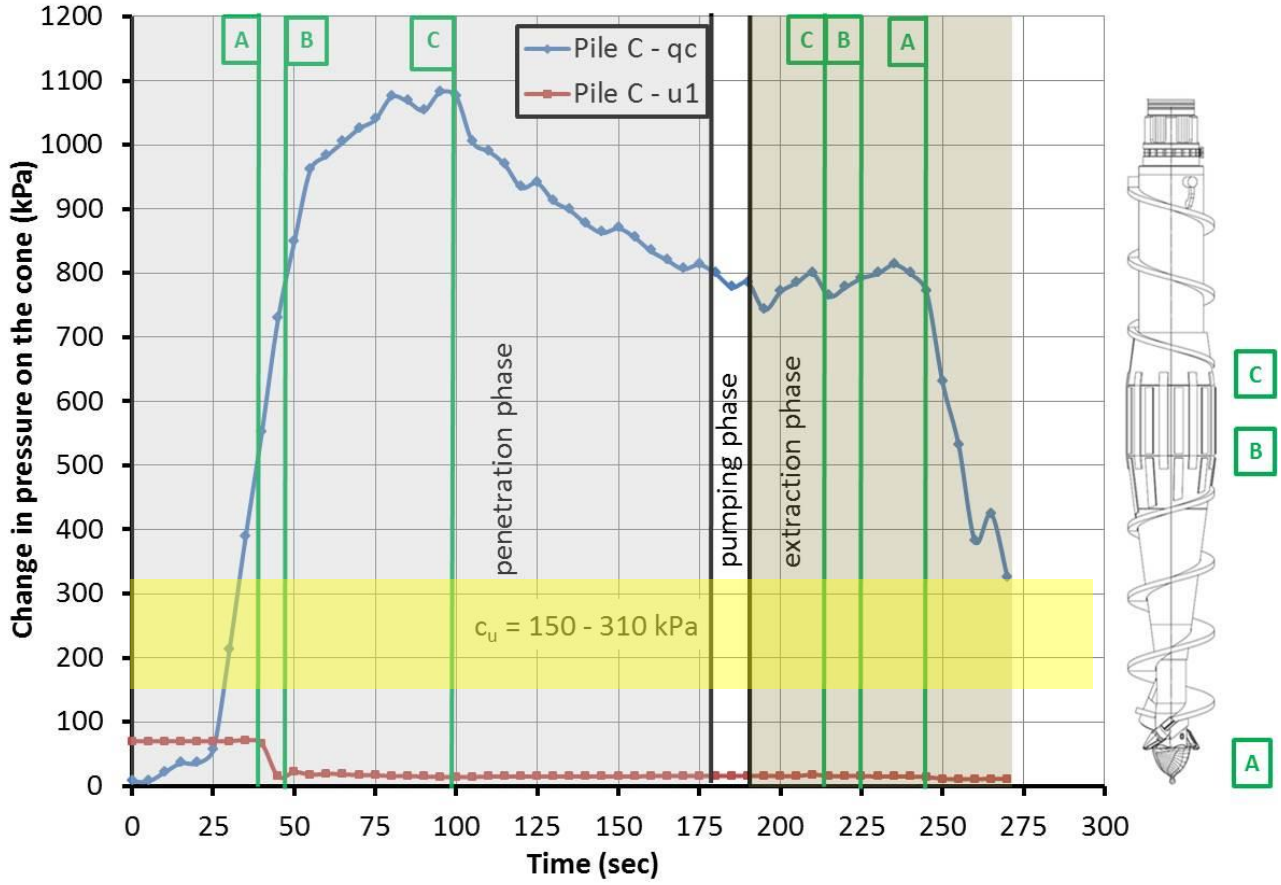

Figure 106 – Change in pressure on the cone v time at 1.5 m depth during installation of pile C

Figure 107 shows the change in pressure on the static cone during the installation of pile D, which was installed using a rapid displacement auger. The quantitative pressure development is comparable with pile C; however, the peak values were only close to 700 kPa (which is about 60% of the peak values of pile C). The maximum pressure changes were measured as the displacement body passed the cone location at 1.5 m depth.

The pressure on the cone dropped from about 450 kPa to 275 kPa after the displacement body passed the cone location. Stress levels between 310 kPa and 220 kPa (in the upper band of the undrained shear strength of this profile) were measured for the remainder of the pumping and extraction phases, with a few variations.

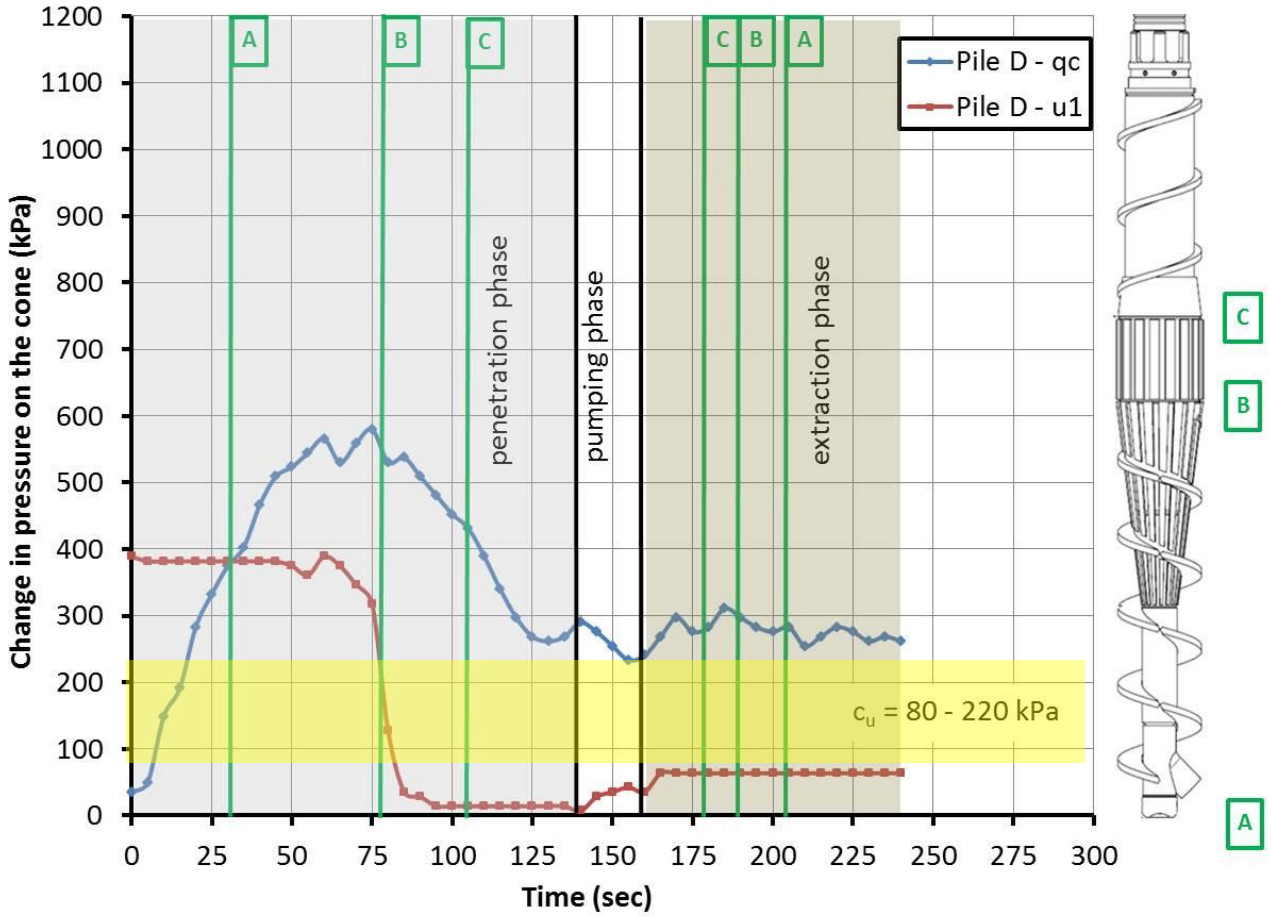

Figure 107 – Change in pressure on the cone v time at 1.5 m depth during installation of pile D

The pore water pressure started as high as 400 kPa and dropped to 30 kPa within 20 seconds just before and after the passing of the lower displacement body (point B). During the pumping phase, the pore water pressure increased to 50 kPa, increasing to 80 kPa about 5 seconds after the commencement of pumping, and remaining constant at this level until the completion of pile D.

8.4.3 DMT

DMTs were conducted for each pile before and after pile installation. For each test pile (except pile E), the ratio of undrained shear strength c_u (determined by DMT) after pile installation and before pile installation with depth is compared. Ratios smaller than 1 are shown in red, indicating strength reductions as a result of the pile installation process. Ratios in excess of 1 are displayed in black, highlighting improved soil strength as a result of the piling process.

For the pile design, it was critical to determine the undrained shear strength at each pile location. As discussed in Section 8.2.1 and shown in Figure 84, the undrained shear strength c_u was also determined using triaxial CU tests and this result is included in the following figures for comparison.

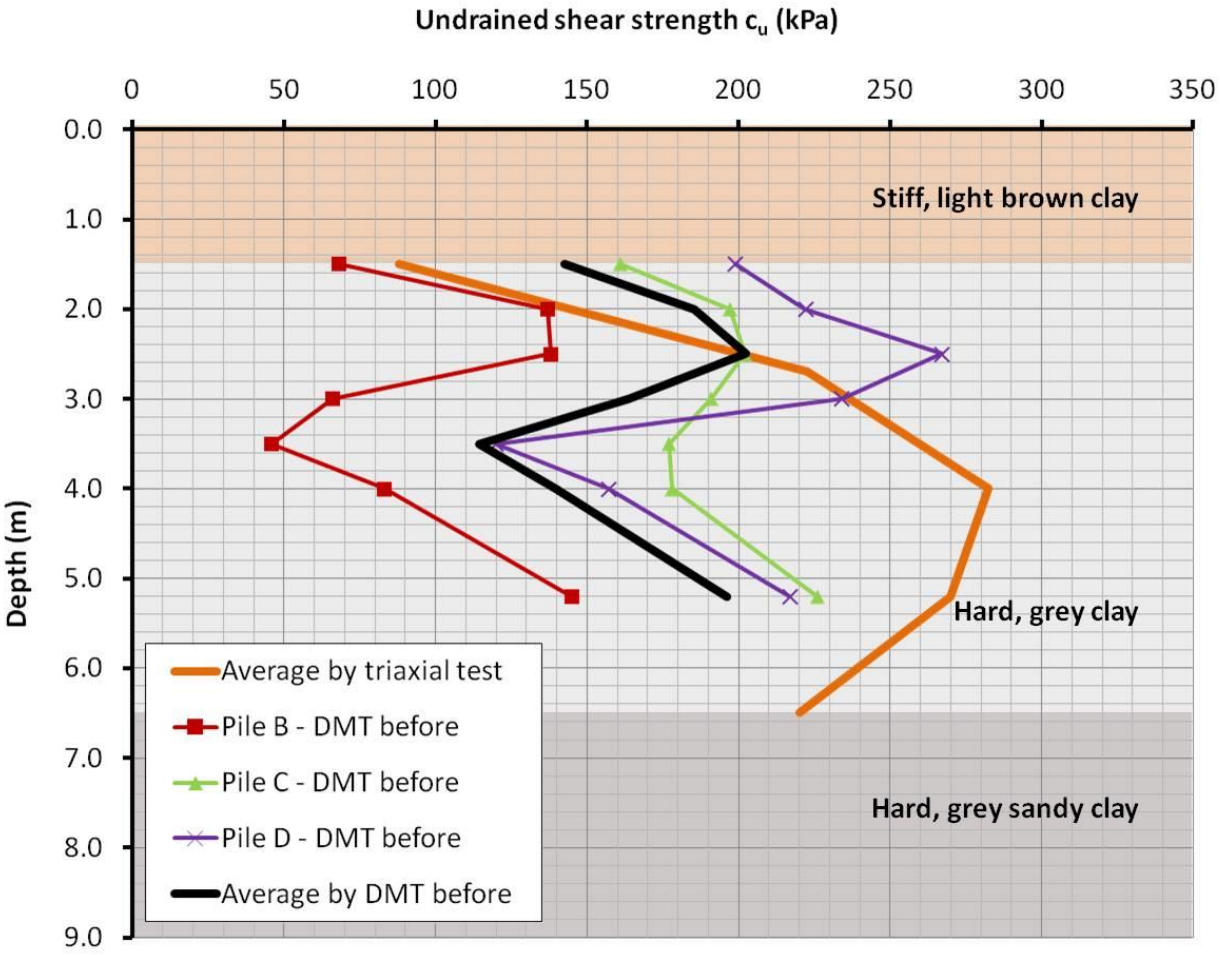

Figure 108 – Shear strength data (by DMT) of Lawnton Clay before pile installation

In Figure 108, the profiles of undrained shear strength values (determined by DMT) versus depth are displayed for all pile locations in virgin ground (before pile installation). Figure 109 shows the undrained shear strength data obtained by DMT for all pile locations after pile installation. The DMTs were carried out at a distance of one pile diameter from the pile axis of the relevant test pile.

Figure 110 shows the ratio of the undrained shear strength c_u before and after pile installation for test pile B (CFA pile). It can be observed that the shear strength after pile installation is about 10% higher on average. The improved shear strength follows the shaft from about 1.0 m below the surface to approximately 1.0 m below the pile base.

The shear strength distribution before and after pile installation for test pile C, installed with a progressive displacement auger, is displayed in Figure 111. A total reduction in shear strength of about 11% can be observed compared to the initial undisturbed condition.

Within the stiff, light brown clay layer from about 0.6 m to 1.0 m depth, a spike of about 1.5 was observed. Below this level, from 1.0 m to 2.7 m, the shear strength was reduced by an average value

of about 0.8. From 2.7 m to 3.8 m depth, well inside the stiff grey clay, the ratio returned to above one, showing a value of about 1.2 on average. At pile toe level and 0.3 m above and below, the shear strength dropped to about 0.8. Below 4.3 m, the shear strength ratio became larger than one again, and no further variations were measured below 4.7 m depth.

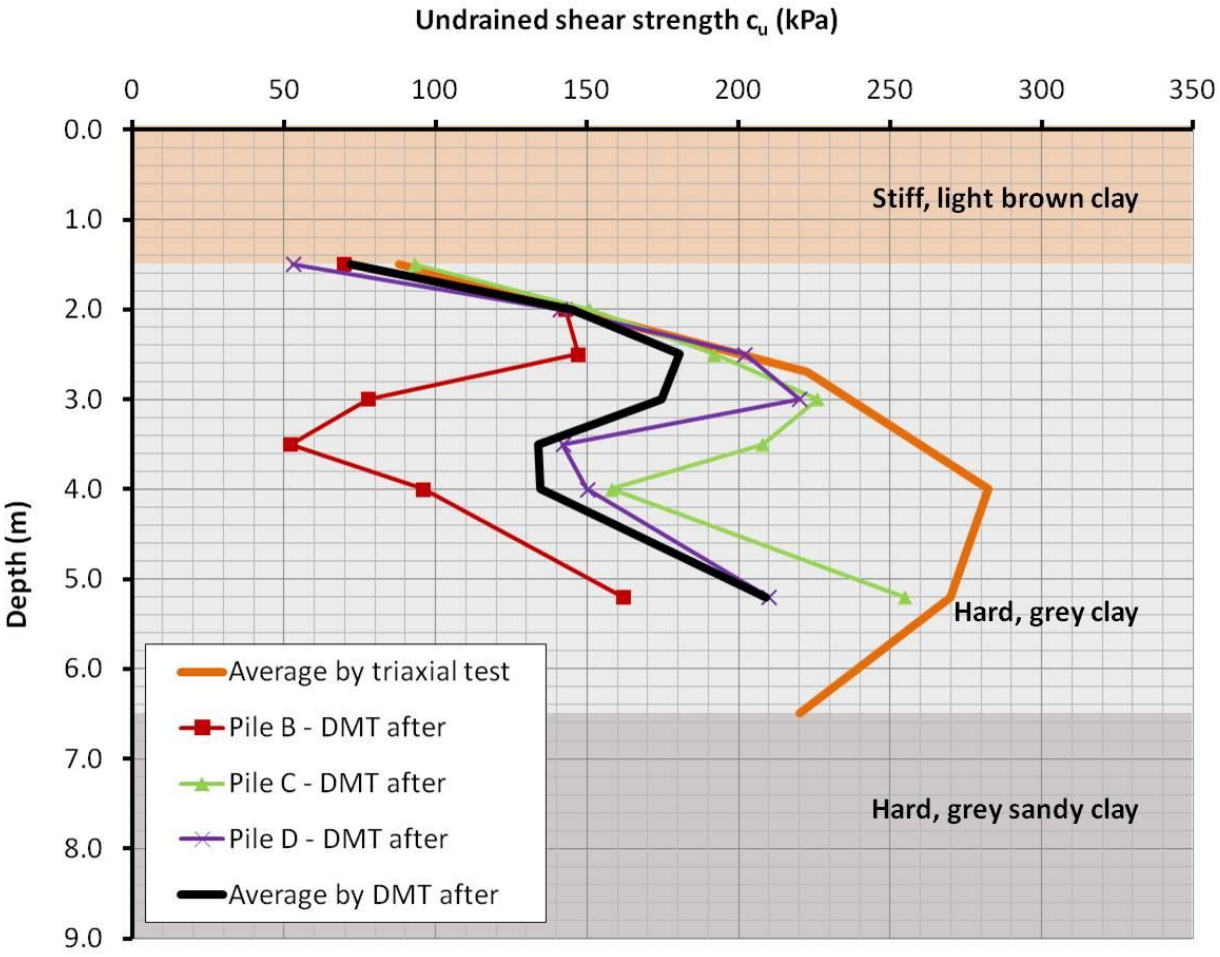

Figure 109 – Shear strength data (by DMT) of Lawnton Clay after pile installation

For test pile D, installed using a screw auger rapid displacement auger, the quantitative graph of the shear strength ratio is comparable with the graph for test pile C. The overall reduction in undrained shear strength for both piles as a result of the pile installation process is 16%.

Figure 112 shows a ratio of 1.1 inside the top soil layer from about 0.7 m to 1.0 m depth. Below this level, the value dropped to an average of 0.65, with single spikes of only 0.35 up to a depth of 3.0 m below ground level. From there, it spiked to 1.3, before the ratio became less than 1.0 again at a depth of 3.9 m. The average value of around 0.9 was maintained for about 800 mm to a depth of about 4.7 m below the surface. Then, the ratio turned above one again, spiking at 1.5 at 5.0 m before measurements were ceased.

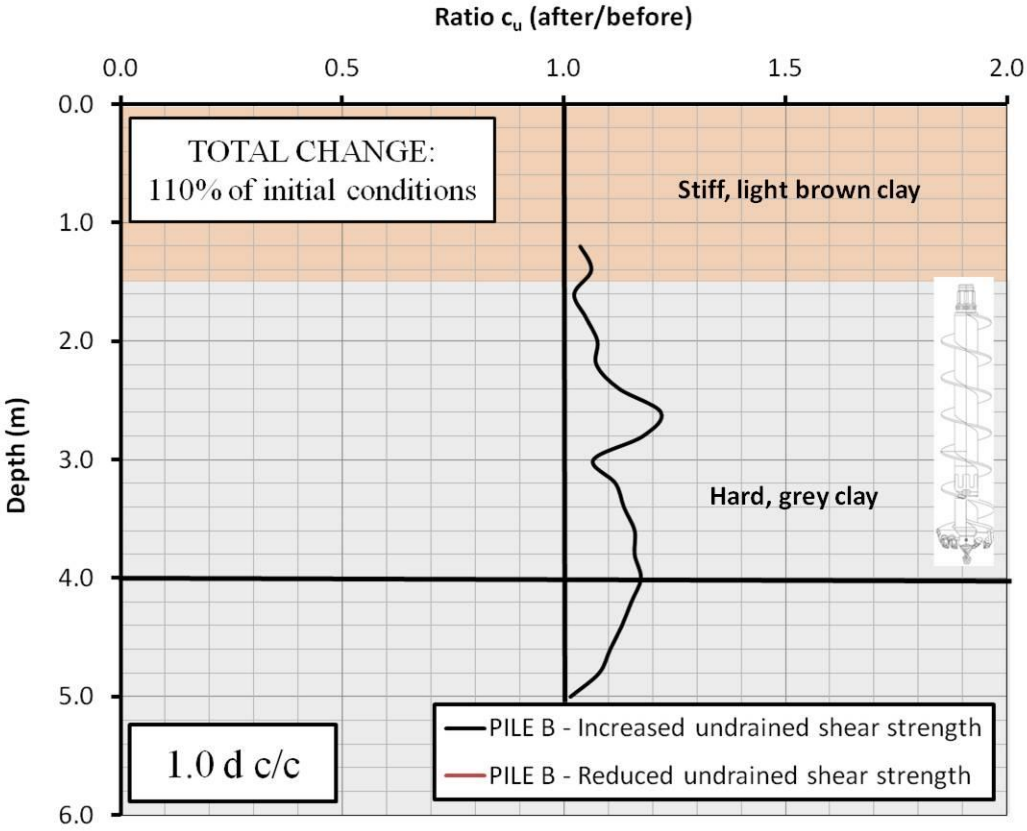

Figure 110 – Pile B: Ratio of undrained shear strength after/before pile installation

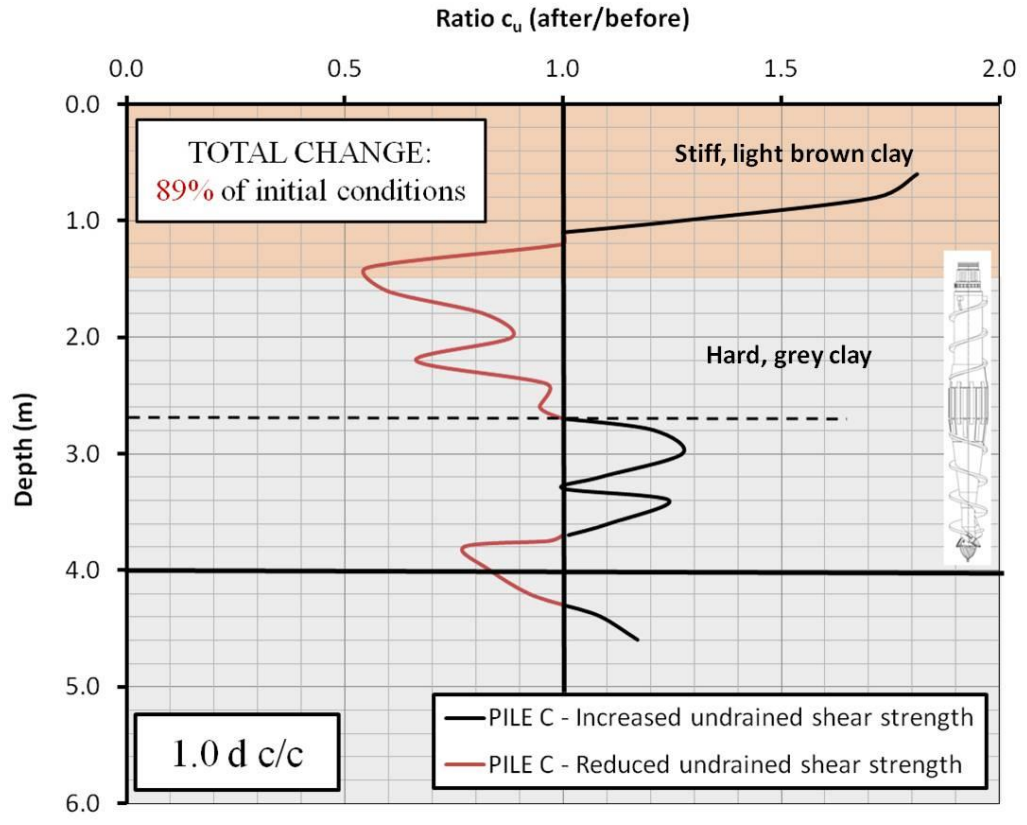

Figure 111 – Pile C: Ratio of undrained shear strength after/before pile installation

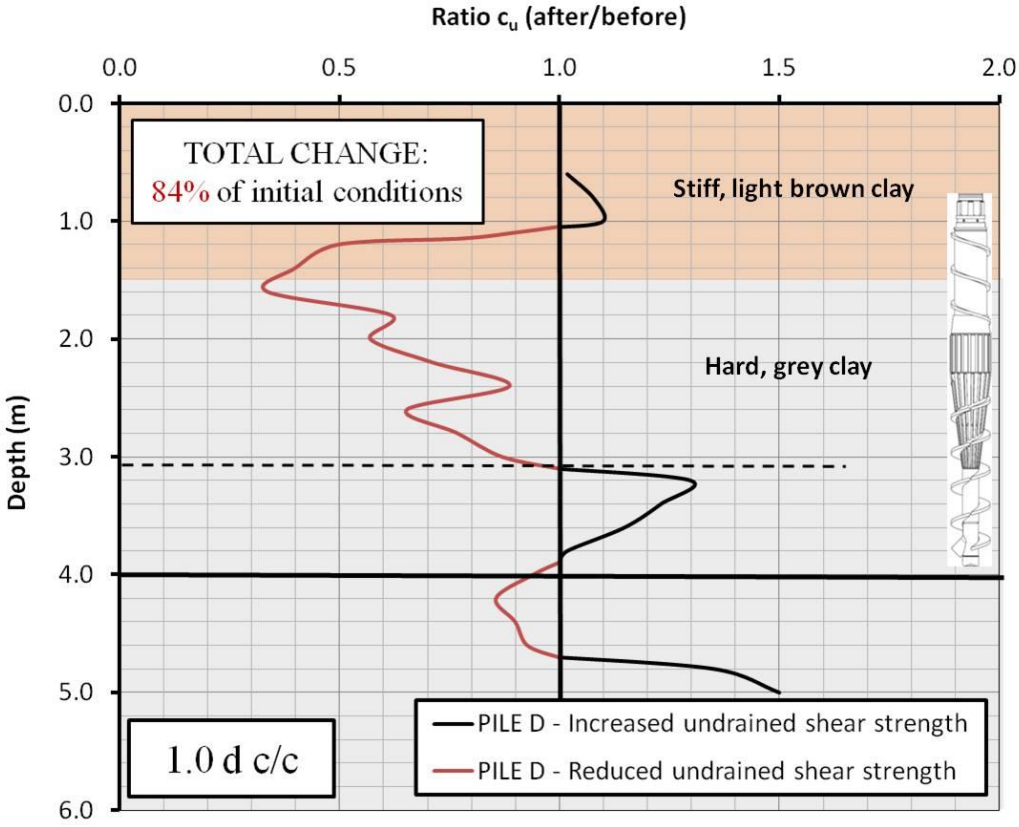

Figure 112 – Pile D: Ratio of undrained shear strength after/before pile installation

8.4.4 Inclinometers

Horizontal displacements in the soil were measured with inclinometer probes placed inside PVC tubes. The tubes were located around each individual test pile, as detailed in Figure 53 and Figure 54 of Section 7.4.1. The tubes were installed at various distances from the test piles; however unfortunately, some of the tubes were damaged during the installation process. Consequently, there is only one common set of data for all three of the test piles: for the inclinometers located 1.25 pile diameters from each test pile centre.

These probes were located about 112.5 mm further away from the pile than the relevant CPT and DMT locations. The horizontal displacements of the inclinometer probe at pile B are displayed in Figure 113. The plot shows displacements up to 5.5 mm from the pile. The maximum deflection was measured at about 0.5 m below the surface, inside the stiff, light brown clay layer. From there, the readings varied between 2.0 and 5.0 mm up to pile toe level. From the pile toe level downwards, the displacements were between 0 and 3.0 mm. Overall, there was not much variation in the displacements measured for pile B. The lateral movements of the PVC tube due to the installation of pile B were almost constant over depth.

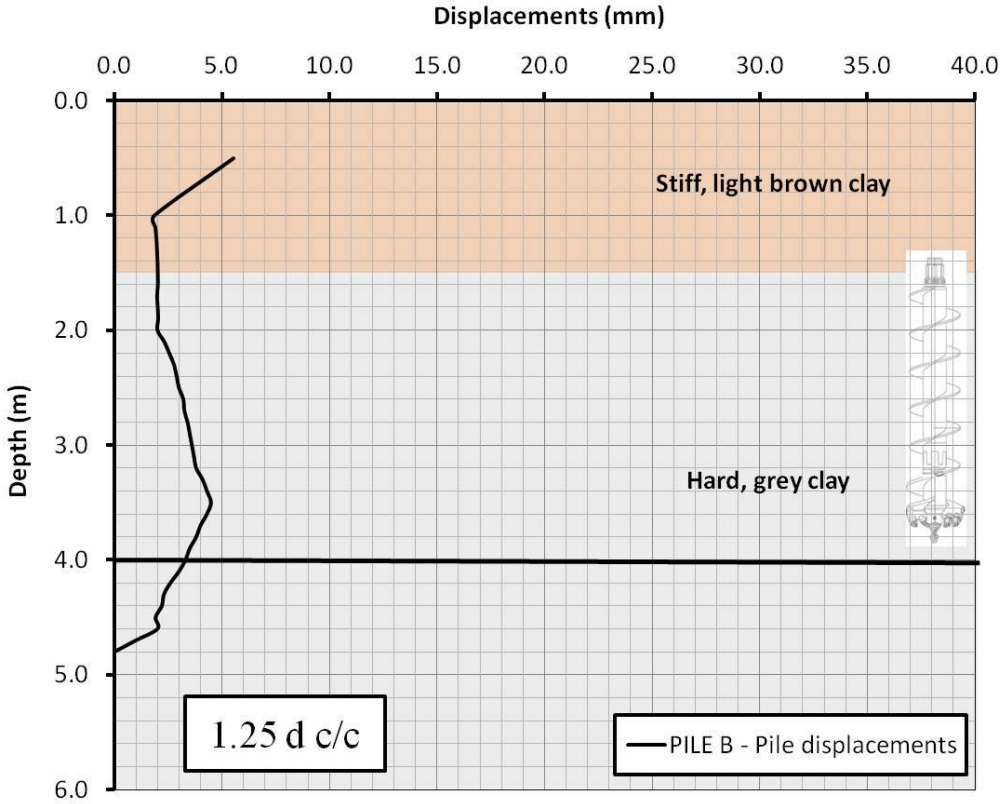

Figure 113 – Pile B: Horizontal soil movements after pile installation

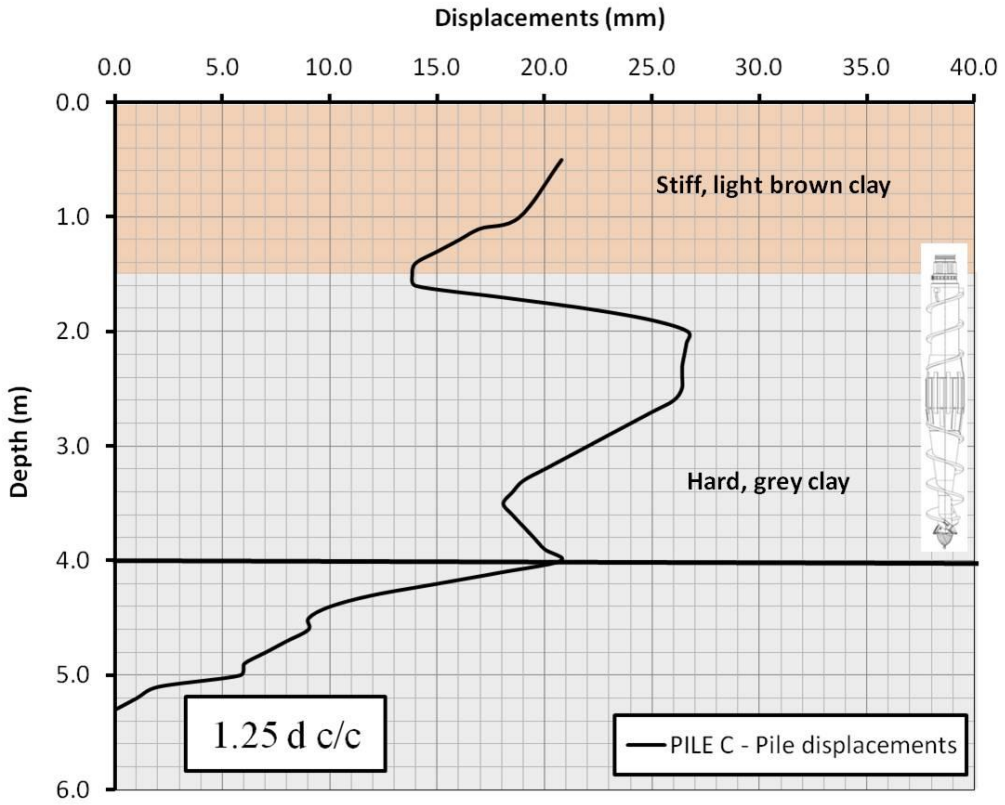

Figure 114 – Pile C: Horizontal soil movements after pile installation

The results for pile C are displayed in Figure 114. The displacements at the pile head and at pile toe level were in the same range of about 20 mm. At the interface of the two soil layers, at 1.5 m depth, the movements were only 14 mm, rising to a maximum value of 27 mm at 2.0 m depth. The displacements remained between 26 and 27 mm for about 0.5 m, before dropping back almost linearly to 20 mm at pile toe level. Below pile toe level, the displacements fell from 20 mm to 0 within 1.3 m with an almost linear regression. For pile C, all displacements were measured as positive, meaning that all displacements occurred away from the pile. The lateral displacements of test pile D, installed with a rapid full-displacement auger, are qualitatively similar to the movements for test pile C.

Figure 115 describes the soil movements for pile D after pile installation with deflection of 31 mm at 2.4 m depth. At pile toe level, the soil movements were about 26 mm.

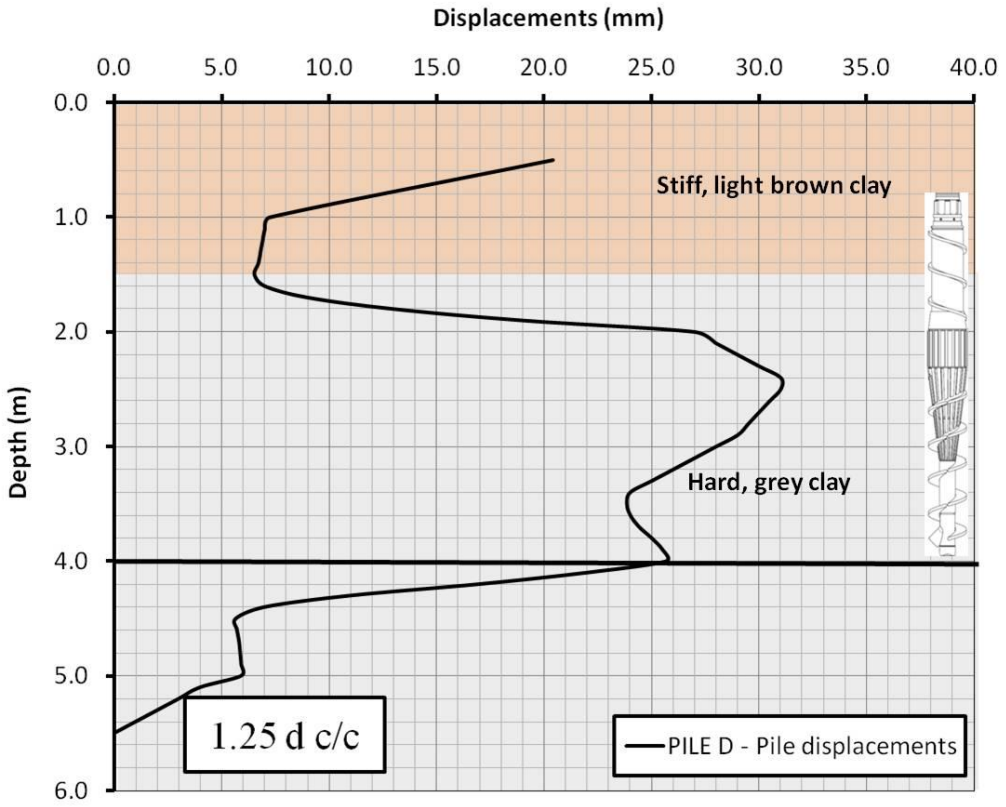

Figure 115 – Pile D: Horizontal soil movements after pile installation

The shapes of the curves for both full-displacement piles are comparable, as shown in Figure 116. In this figure, the soil movements of all three of the test piles are displayed for visual comparison.

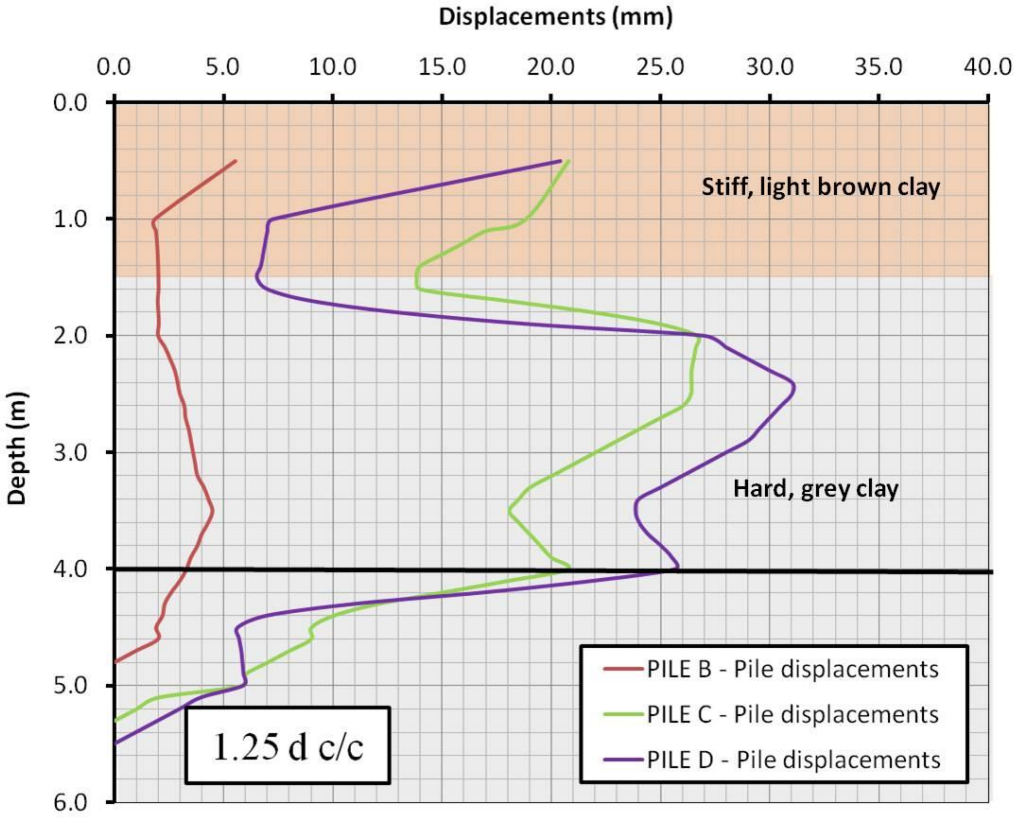

Figure 116 – Summary of horizontal soil movements for all test piles

8.4.5 Heave

Soil heave was measured for the full-displacement piles C, D and E as described in Section 7.4.5 above. Vertical soil movement during the pile installation was measured as shown in Figure 117.

Figure 117 – Pile E: Vertical soil movement (heave) during pile installation

The heave profiles were determined for each of the full-displacement piles and the measurements along the main axis crossing the pile centre are displayed in Figure 118. It can be observed that the radii for piles C and D were about 1.0 m from the edge of the existing pile. The shape of the heave cone was almost linear along the axis. However, for both piles, the heave occurred just in front of the rig and the profiles displayed in Figure 118 are not evenly distributed in all directions. The area of the mast foot of the rig (axis B-B) did not experience as much heave as other areas (axis A-A). For pile E, the heave figure was not perfectly circular, as indicated in Figure 117. The area of the mast foot restricted heave such that more vertical soil displacement was observed in front of the rig and at both sides perpendicular to the mast foot location. The total amounts of soil heave for each individual pile were calculated to be (based on the plots shown in Figure 118):

- Pile C: 0.45 m^3
- Pile D: 0.44 m^3
- Pile E: 0.23 m^3

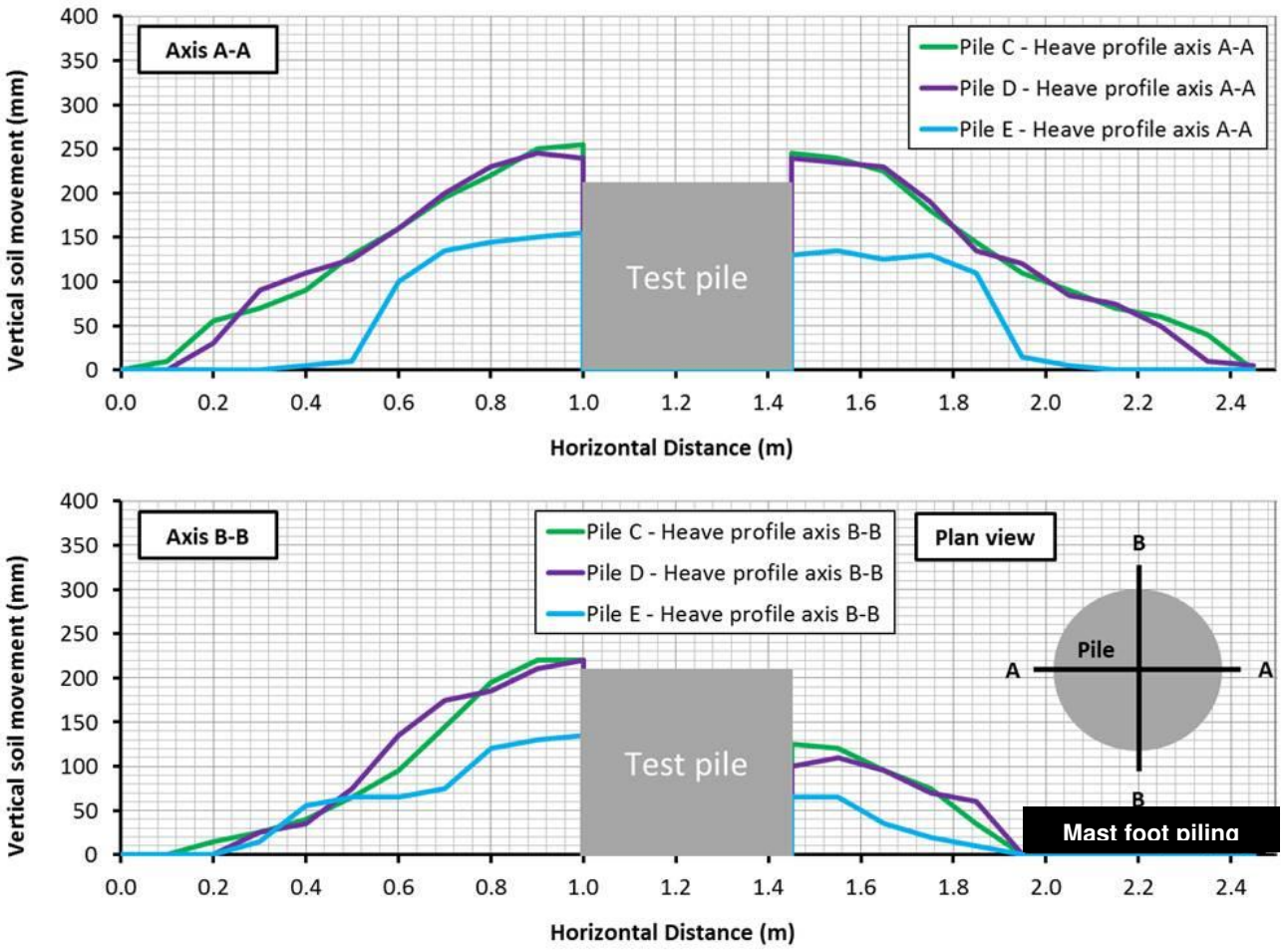

Figure 118 – Heave profiles for test piles C, D and E

8.5 Pile design

Pile design calculations were carried out for tests piles B, C, D and E. The α-c_u method and the method after Bustamante and Gianeselli (1998) were used to determine the pile capacities based on soil investigation results gathered before the execution of the test piles. These results were used for a load-settlement prediction using Fleming's method (1992).

After the execution of the static load tests, the results for each test pile were used to back-calculate the data and to correlate them to soil investigation results carried out after the static load tests, to establish connections between the actual load test data and the individual CPT data after pile installation. Then, the static load test data were correlated to the initial soil investigation data to provide guidance to designers for future projects.

The summary of the average undrained shear strength profiles obtained by CPT, DMT and triaxial tests is displayed in Figure 119. These profiles represent the average of all site measurements calculated from the CPT and DMT profiles for each individual pile location.

Following this, Figure 120 to Figure 123, present the actual CPT and DMT data taken at each pile location in virgin ground before piling and after pile installation.

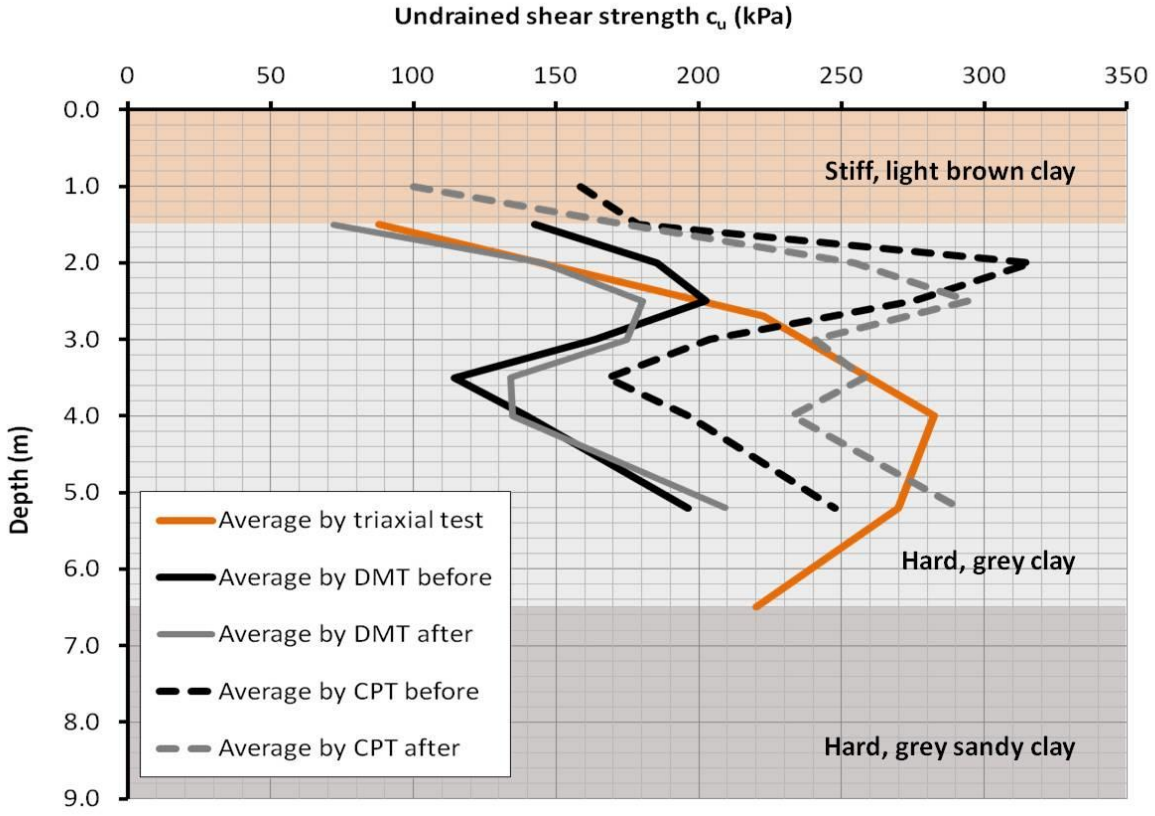

Figure 119 – Summary shear strength data of Lawnton Clay

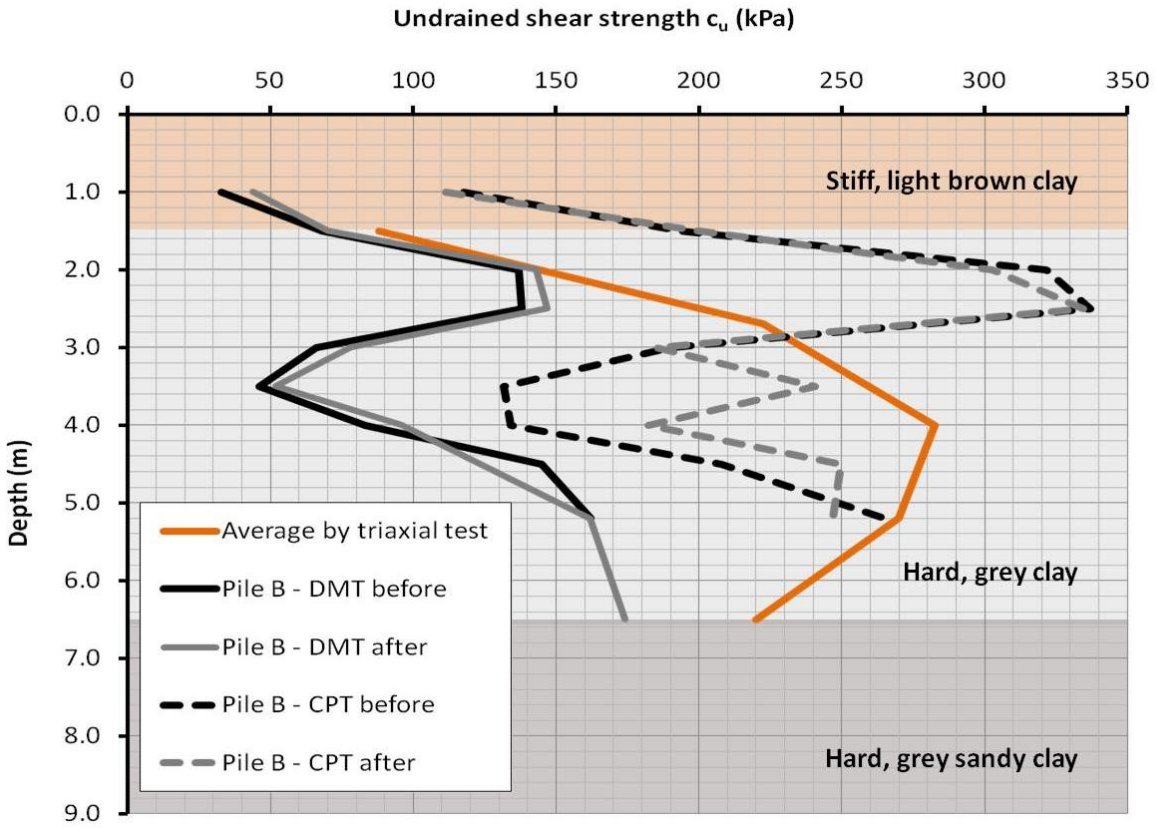

Figure 120 – Summary of undrained shear strength data for test pile B

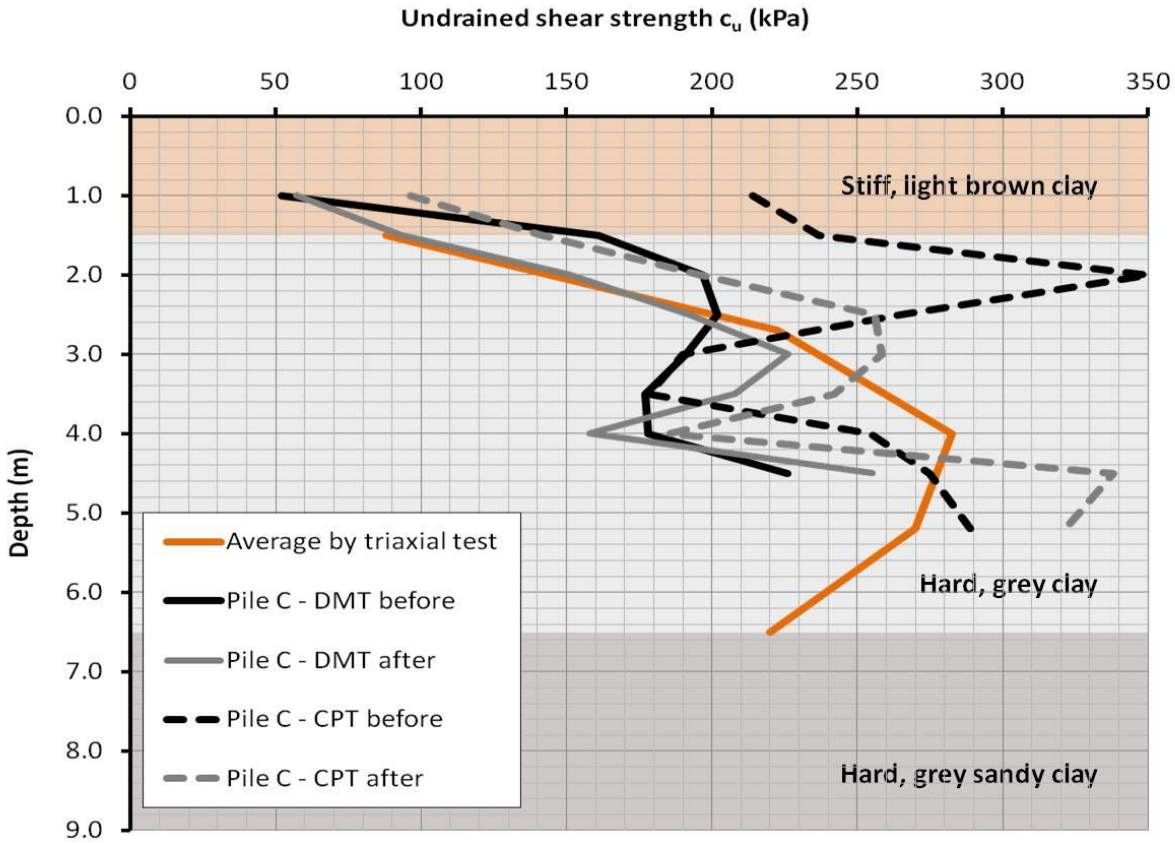

Figure 121 – Summary of undrained shear strength data for test pile C

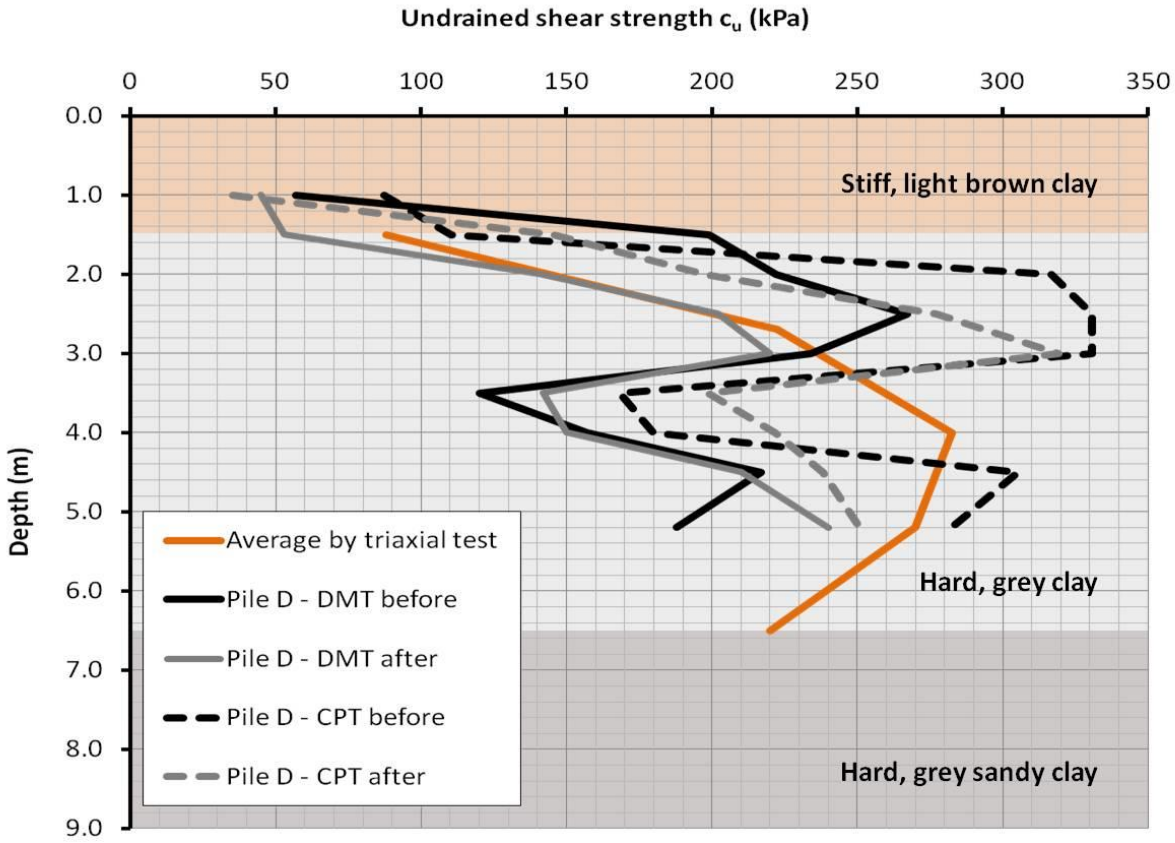

Figure 122 – Summary of undrained shear strength data for test pile D

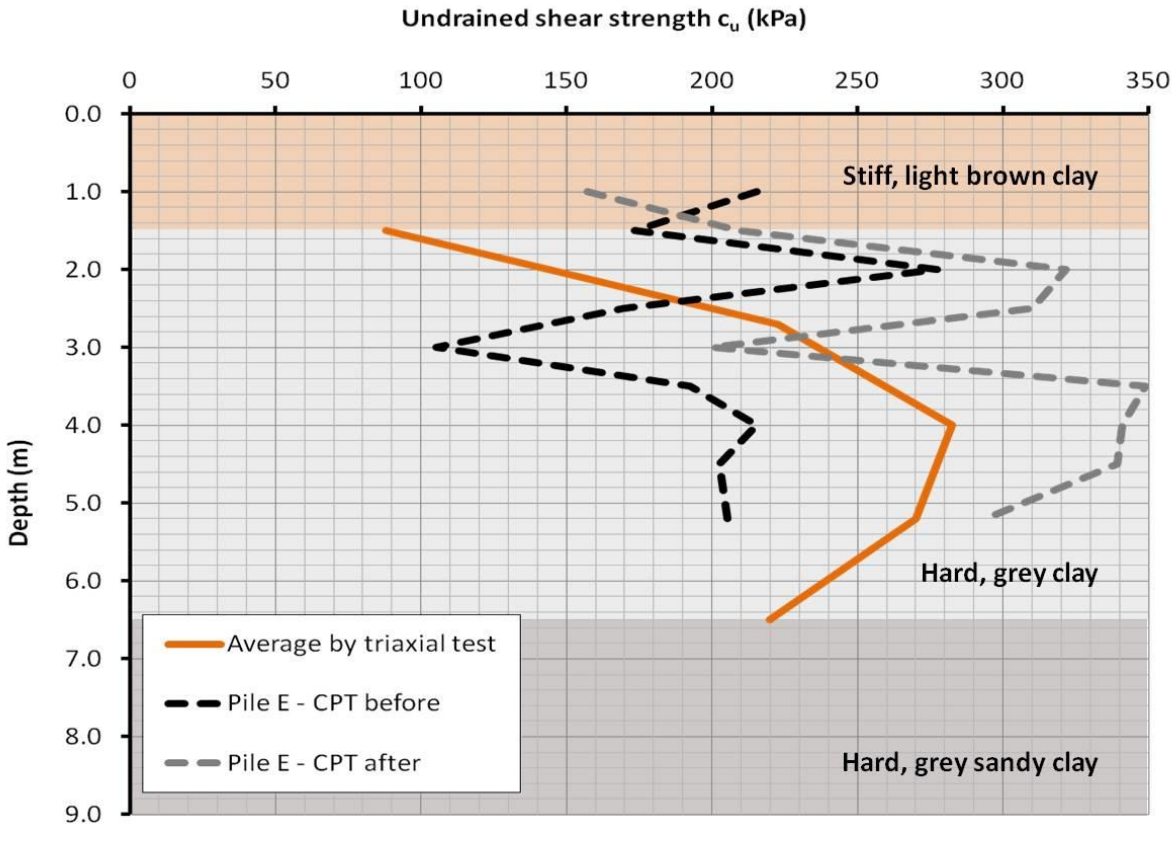

Figure 123 – Summary of undrained shear strength data for test pile E

For the pile design calculations, the actual data obtained at the individual pile location were used as the most representative data for ultimate pile capacity predictions and load-settlement forecasts. However, the average values as well as the triaxial values were also used as input data for detailed pile design calculations to create a range of results for comparison with the actual load test data.

The data obtained after pile installation were used to validate the static load test results with the actual measured stress conditions in the soil formation right next to each pile location. The initial forecasts of pile performance using the virgin soil data and the actual pile load test data with the stress conditions in the soil after pile installation were correlated as part of this research work.

8.5.1 α-c_u method

In this thesis, detailed calculations are only shown for test pile B. The results for the other test piles were calculated following the same principles and these are summarised at the end of this section.

The pile capacities for the test piles were calculated as per Equation 18. The c_u data were taken from the CPTs carried out prior to the pile installation at the location of test pile B. Further calculation using c_u data from other tests and locations are summarised in Table 13.

$$\mathbf{Q_u = \alpha c_u A_s + N c_u A_b}$$

Where:
- α = 0.5 (following the 1984 API proposal)
- c_u = Mean undrained cohesion over the length of the pile shaft: 155 kPa for pile B
- A_s = Pile shaft area: 7.19 m^2 (the top 250 mm of the pile was ignored for the design. The pile shaft was assumed to be 0.61 m in diameter, with 0.65 m over the top 2.75 m and 0.5 m for the bottom 1.0 m. Also refer to Section 8.3 above)
- N_c = Bearing capacity factor = 9.0
- c_u = Undrained cohesion at pile base: 106 kPa for pile B
- A_b = Pile base area: 0.196 m^2

For test pile B, the equation would read as follows:

$Q_{u, \text{pile B}}$ = [0.5 * 155 kPa * (0.61 m * π * 3.75 m)] + [(9 * 106 kPa * ((0.25 m)^2 * π)]

$Q_{u, \text{pile B}}$ = [557 kN] + [187 kN] = **<u>744 kN</u>**

The results for test piles C, D and E are displayed in Table 13. The calculated pile capacities at the pile location determined by CPT results are selected for further comparison. The CPT method is a well-recognised method for the collection of *in situ* c_u data. For a detailed analysis, the particular soil conditions at the pile locations were considered. By contrast, using site average values might be an appropriate method for projects with multiple piles for which only a few CPTs were carried out.

Table 13 – Summary of pile loads for all test piles, calculated with the α-c_u method

Test piles with source of shear strength data	*Shaft capacity*	*Base capacity*	*Total capacity*
Pile B			
- CPT data at pile location	731 kN	237 kN	968 kN
- CPT data site average	789 kN	325 kN	1,114 kN
- DMT data at pile location	351 kN	186 kN	537 kN
- DMT data site average	602 kN	312 kN	914 kN
Pile C			
- CPT data at pile location	642 kN	365 kN	1,006 kN
- CPT data site average	566 kN	263 kN	829 kN
- DMT data at pile location	502 kN	323 kN	825 kN
- DMT data site average	436 kN	253 kN	688 kN
Pile D			
- CPT data at pile location	551 kN	258 kN	808 kN
- DMT data at pile location	533 kN	285 kN	838 kN
Pile E			
- CPT data at pile location	515 kN	308 kN	823 kN
Data from triaxial laboratory test (pile B)	560 kN	499 kN	1,029 kN
Data from triaxial laboratory test (piles C, D, E)	436 kN	404 kN	840 kN

Note: The results shown in grey are not considered in this load-settlement curves presented in this thesis.

The results for the pile capacities using the α-c_u method range from 537 kN to 1,114 kN (about 207% variance), depending on the undrained shear strength values to be used for the calculation. The average prediction is in the range of 850 kN ultimate pile capacity, with a ratio of about 2:1 between shaft friction and base capacity.

For the determination of the undrained shear strength c_u obtained from CPT and DMT data, the following formula was used (Equation 32):

$$C_u = Q_c / N_k \quad (32)$$

Where: Q_c = CPT cone resistance

N_k = Cone factor (assumed as 15 for hard clays)

Note:
The cone factor N_k was assumed to be 15 as an initial value. A smaller cone factor will predict higher pile load capacities. Cone factors between 15 to 20 have been commonly used by the author for pile designs in the past. The cone factor was changed during the back-calculations of the static load test results using Fleming's method (refer to Section 8.6.2 and Table 16). However, Robertson (2014) claimed cone factors could range from 8 to 24 for cohesive ground conditions.

8.5.2 Method after Bustamante and Gianeselli (1998)

The method for the calculation of the ultimate pile capacity Q_u was introduced in Section 7.5.2 and the detailed calculation for test pile B (using CPT data at the pile location before pile installation) is demonstrated here. The summarised pile capacities of the other test piles are shown in Table 13.

$Q_{u,\ pile\ B} = [K * S_{pile\ B} * \alpha] + [q_{s,\ pile\ B} * S_{lat,\ pile\ B}]$

Where:

- K = Base capacity coefficient, selected to be 0.5 (refer to Table 4)
- $S_{pile\ B}$ = Cross-sectional area of the pile base: 0.196 m^2 for pile B
- α = Ultimate point resistance of the cone at the pile tip: 2.014 MPa (this value is the average of all q_c values 750 mm above and below the pile toe level)
- $S_{lat,\ pile\ B}$ = Pile shaft area: 7.19 m^2 (the top 250 mm of the pile was ignored)
- $q_{s,\ pile\ B}$ = Ultimate unit skin friction along the pile shaft: 82.9 kPa (average)

The q_s values are taken in 500 mm depth intervals along the pile shaft. For pile B, the following calculation would be required:

Depth	qc	chart	qs	α (m)	$q_{s,\ i\ (depth\ interval)}$
0.25 m – 0.75 m	1,763	Q3	0.057	0.65	58.2 kN
0.75 m – 1.25 m	1,723	Q3	0.057	0.65	58.2 kN
1.25 m – 1.75 m	2,907	Q3	0.078	0.65	79.7 kN
1.75 m – 2.25 m	4,826	Q4	0.122	0.65	124.6 kN
2.25 m – 2.75 m	5,054	Q4	0.124	0.65	126.7 kN
2.75 m – 3.25 m	2,850	Q3	0.077	0.5	78.7 kN
3.25 m – 3.75 m	1,976	Q3	0.059	0.5	46.4 kN
3.25 m – 3.75 m	2,014	Q3	0.060	0.25	23.6 kN
	TOTAL shaft capacity				596.1 kN

For clay, the curves displayed below are used. The first value of 0.25–0.75 m depth would be determined as follows (marked in red).

The steps shown above are repeated for each layer (each of which is typically around 500 mm thick), to determine the shaft capacity of the entire pile. This design method is particularly suited for displacement piles (partial- or full-displacement), as the actual *in situ* data are used for the design.

For test pile B, the overall pile design would read as follows:

$Q_{u,\ pile\ B} = [0.5 * 0.196\ m^2 * 2{,}014\ kPa] + [82.9\ kPa * 7.19\ m^2]$

$Q_{u,\ pile\ B} = [198\ kN] + [596\ kN] = \mathbf{794\ kN}$

Soils	*Curves qs (MPa)*		p_l	q_c
	Test piles B–E	**Fundex piles**	**(MPa)**	**(MPa)**
Clay	Q1	Q1	< 0.30	< 1.00
Clayey silt	**Q3**	Q2	> 0.50	> 1.50
Sandy silt	Q4	Q2	≥ 1.00	≥ 3.00

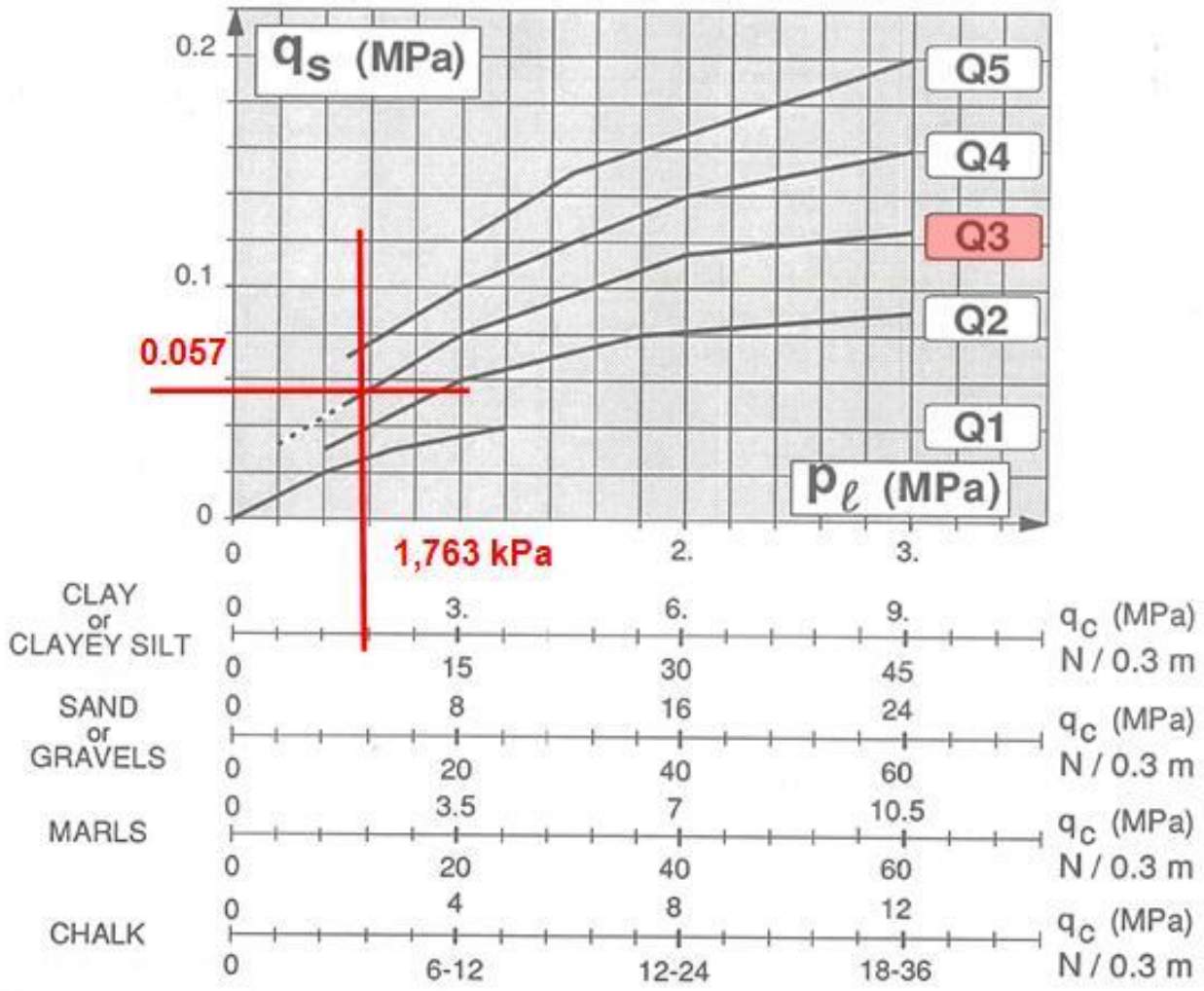

Figure 124 – Example calculation after Bustamante and Gianeselli, for pile B

The calculated ultimate pile capacity results for test piles C, D and E are displayed in Table 14. The calculated pile capacities at the pile location determined with *in situ* CPT results for each individual pile location are selected for further comparison.

The CPT method is one of the distinct applications to be applied for this design approach. However, the table also includes results (q_s values) determined from DMT and triaxial data for comparison and completeness. The q_s values were taken directly from Figure 140 as a function of the q_c value obtained from CPTs on site.

Table 14 – Summary of pile loads for all test piles, calculated with the Bustamante and Gianeselli method

Test piles with source of shear strength data	*Shaft capacity*	*Base capacity*	*Total capacity*
Pile B			
- CPT data at pile location	596 kN	198 kN	794 kN
- CPT data site average	662 kN	271 kN	933 kN
- DMT data at pile location	272 kN	155 kN	427 kN
- DMT data site average	651 kN	260 kN	911 kN
Pile C			
- CPT data at pile location	595 kN	304 kN	899 kN
- CPT data site average	475 kN	219 kN	694 kN
- DMT data at pile location	512 kN	269 kN	781 kN
- DMT data site average	467 kN	211 kN	677 kN
Pile D			
- CPT data at pile location	446 kN	215 kN	660 kN
- DMT data at pile location	383 kN	237 kN	621 kN
Pile E			
- CPT data at pile location	470 kN	237 kN	660 kN
Data from triaxial laboratory test (pile B)	580 kN	506 kN	1,086 kN
Data from triaxial laboratory test (piles C, D, E)	460 kN	426 kN	887 kN

Note: The results shown in grey are not considered in this load-settlement curves presented in this thesis.

The results for the pile capacities produced by the Bustamante and Gianeselli method (1998) range from 427 kN to 1,086 kN (variance of about 250%), depending on the undrained shear strength values to be used for the calculation.

The average prediction is in the range of 670 kN ultimate pile capacity with a ratio of about 2:1 between shaft friction and base capacity.

Overall, the Bustamante and Gianeselli method calculates slightly lower pile capacities than the α-c_u method. The values for the selected piles (CPT at pile location before installation) show a larger difference with less conservative predictions by the α-c_u method. Overall predictions for pile capacities are about 20% lower using the Bustamante and Gianeselli method.

8.5.3 Fleming's method (1992)

The Fleming method was used to predict the load-settlement performance of the test piles. The predicted values calculated by the α-c_u and Bustamante and Gianeselli methods were used to predict the different load-settlement curves for each test pile.

Pile B was again used as an example for the procedure and the remaining piles were calculated following the same principle. All predicted load-settlement curves are displayed in Figure 125 to Figure 128.

As stated in Section 7.5.3 above, Fleming's method for the calculation of the shaft load can be expressed by Equation 24:

$$P_{s,\text{pile B}} = \frac{U_s \, \Delta_s}{M_s D_s + \Delta_s}$$

The base load is written in Equation 25:

$$P_{B,\text{pile B}} = \frac{U_B \, \Delta_B D_B E_B}{0.6 U_B + D_B E_B \Delta_B}$$

Where:

$D_{s,\text{ pile B}}$ =	Pile shaft diameter: 0.61 m
$D_{B,\text{ pile B}}$ =	Pile base diameter: 0.5 m
$\Delta_{s,\text{ pile B}}$ =	Settlement of the pile shaft at a load P_s – to be calculated
$\Delta_{B,\text{ pile B}}$ =	Settlement of the pile base at a load P_B – to be calculated
$U_{s,\text{ pile B}}$ =	Ultimate shaft load, calculated by α-c_u method
$U_{B,\text{ pile B}}$ =	Ultimate base load, calculated by α-c_u method
$M_{s,\text{ pile B}}$ =	Shaft flexibility factor: 0.002 for stiff clay (Fleming 1992)
$E_{B,\text{ pile B}}$ =	Soil modulus at the pile base: 26,000 kPa (average triaxial test result)

The individual settlement values for each load step are calculated using the formulas above. The calculation is complex and the program Microsoft Excel was used to calculate the hyperbolic curves for the load-settlement predictions of the four test piles B, C, D and E. For each test pile, a few individual load-settlement curves are displayed to show the expected pile performance, depending on the data used for the pile design and the pile design method.

The initial CPT data at the pile location (virgin ground) were used to calculate the predicted load-settlement behaviour using the α-c_u method as well as the method after Bustamante and Gianeselli (1998). Additionally, the predicted curve from the laboratory data (c_u values from triaxial tests) using the α-c_u method is displayed for each pile. As the latter curve is seen an average for each pile, it can be compared with the individual CPT data for the individual pile location.

As mentioned above, the Bustamante and Gianeselli method predicts lower pile capacities compared to the α-c_u method (N_k = 15). The data evaluated from triaxial tests provided mid-range predictions for piles B, D and E. For pile C, the laboratory data predicted the most conservative pile performance.

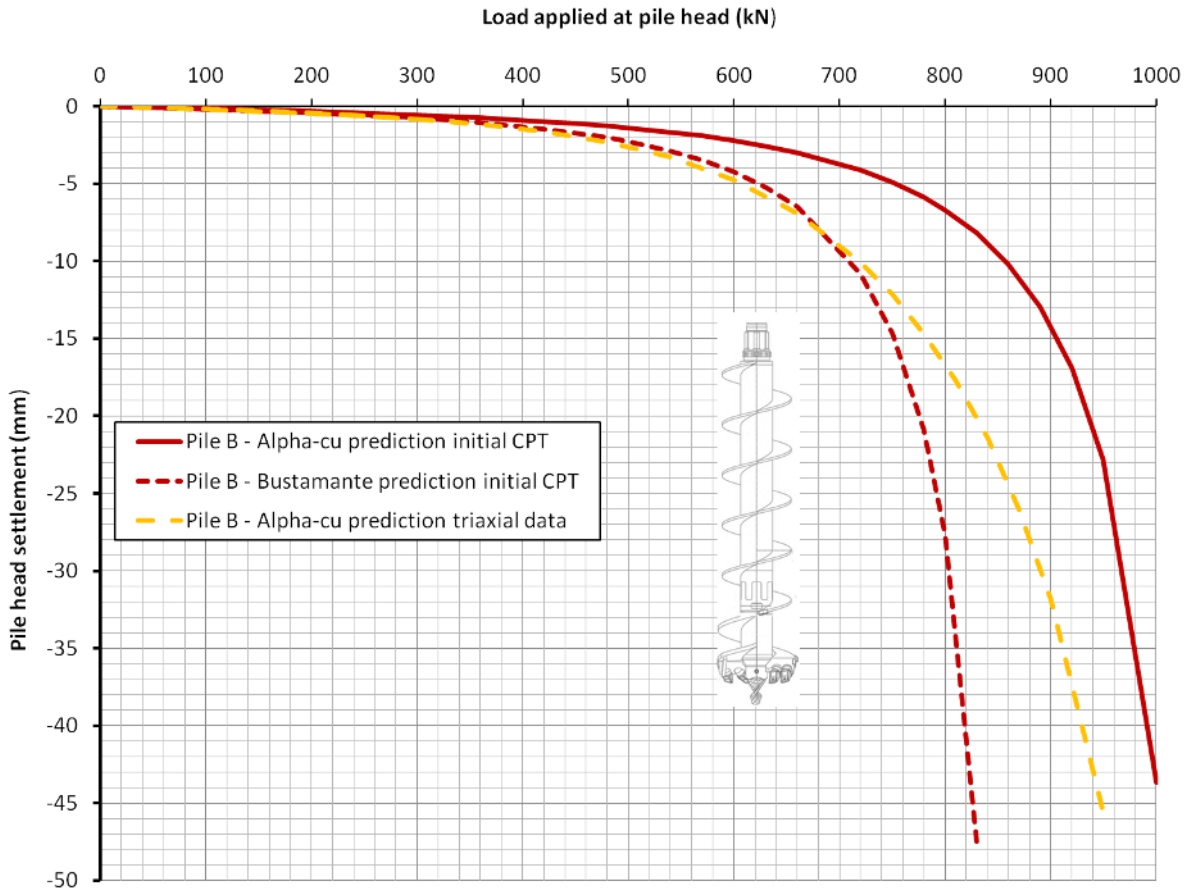

Figure 125 – Pile B: Load-settlement predictions using Fleming's method

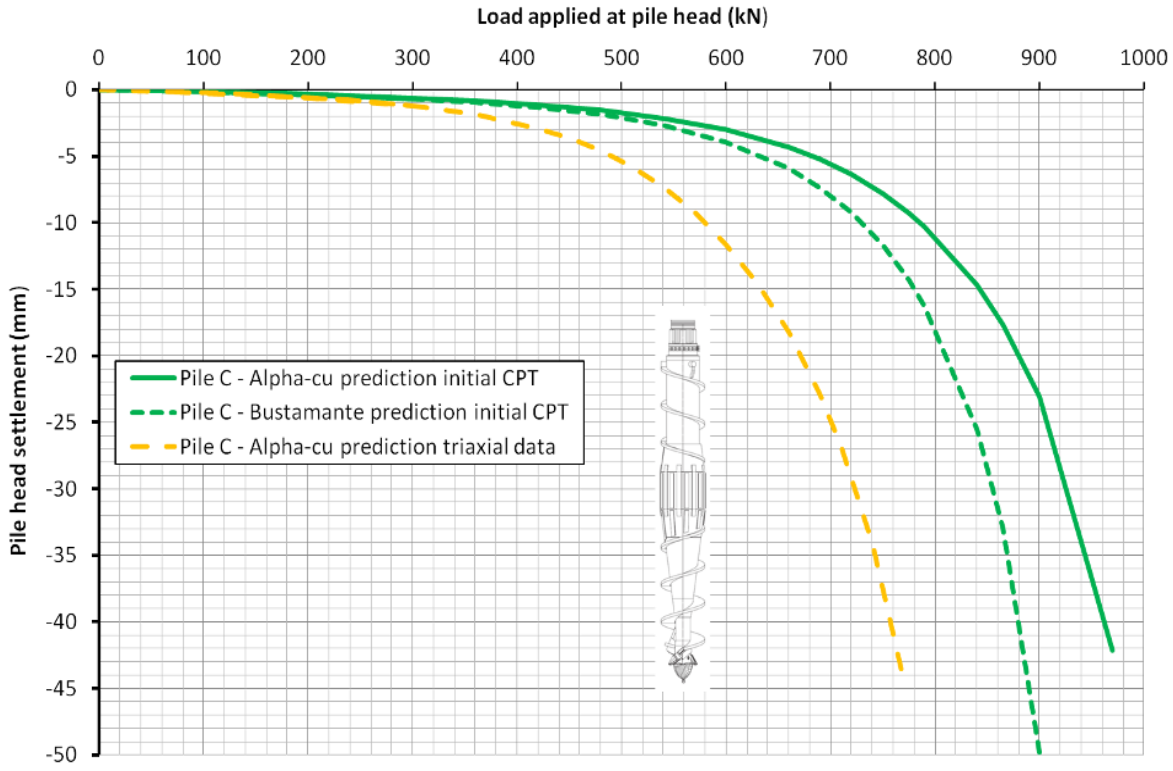

Figure 126 – Pile C: Load-settlement predictions using Fleming's method

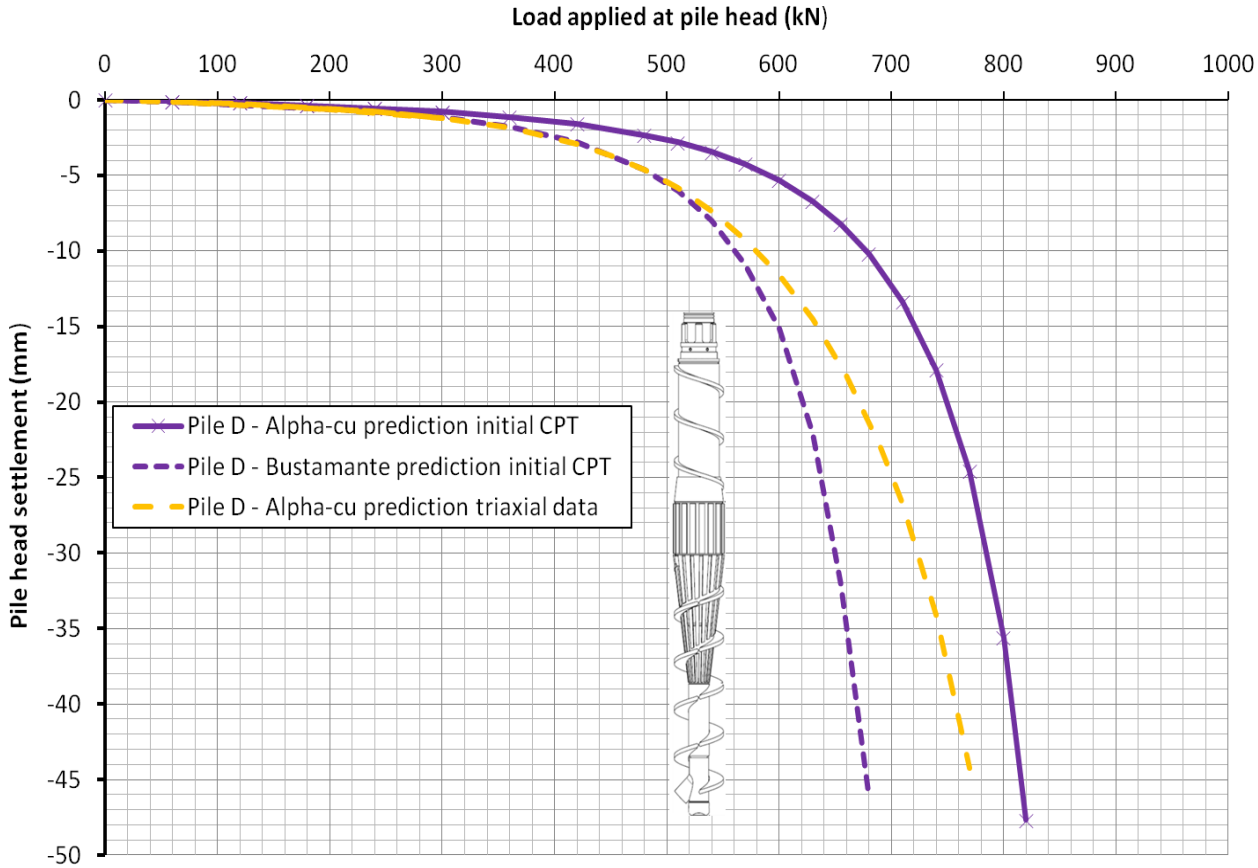

Figure 127 – Pile D: Load-settlement predictions using Fleming's method

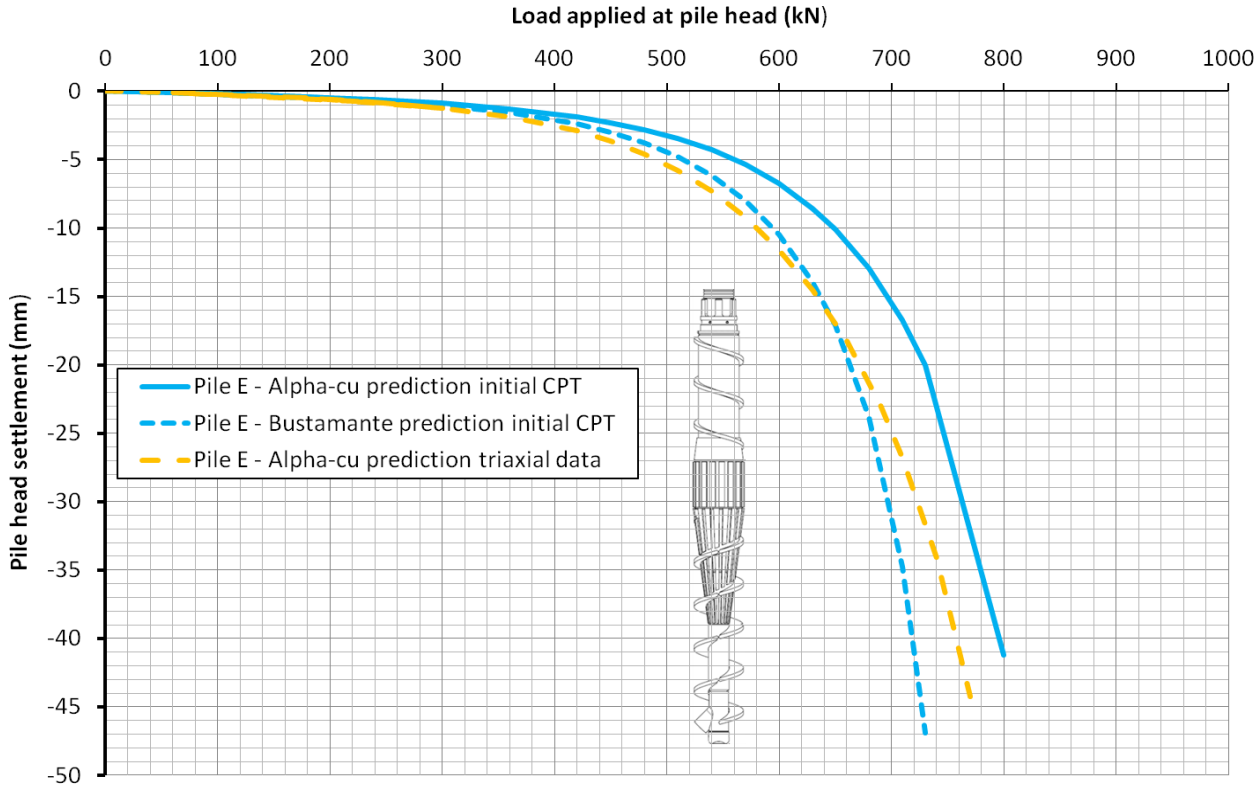

Figure 128 – Pile E: Load-settlement predictions using Fleming's method

8.6 Static load tests

8.6.1 General results

The static load test results are displayed in Figure 129. They show the load-settlement performance of the three test piles installed in Lawnton Clay. The actual settlement data for each test pile are also displayed in Table 15 on the following page.

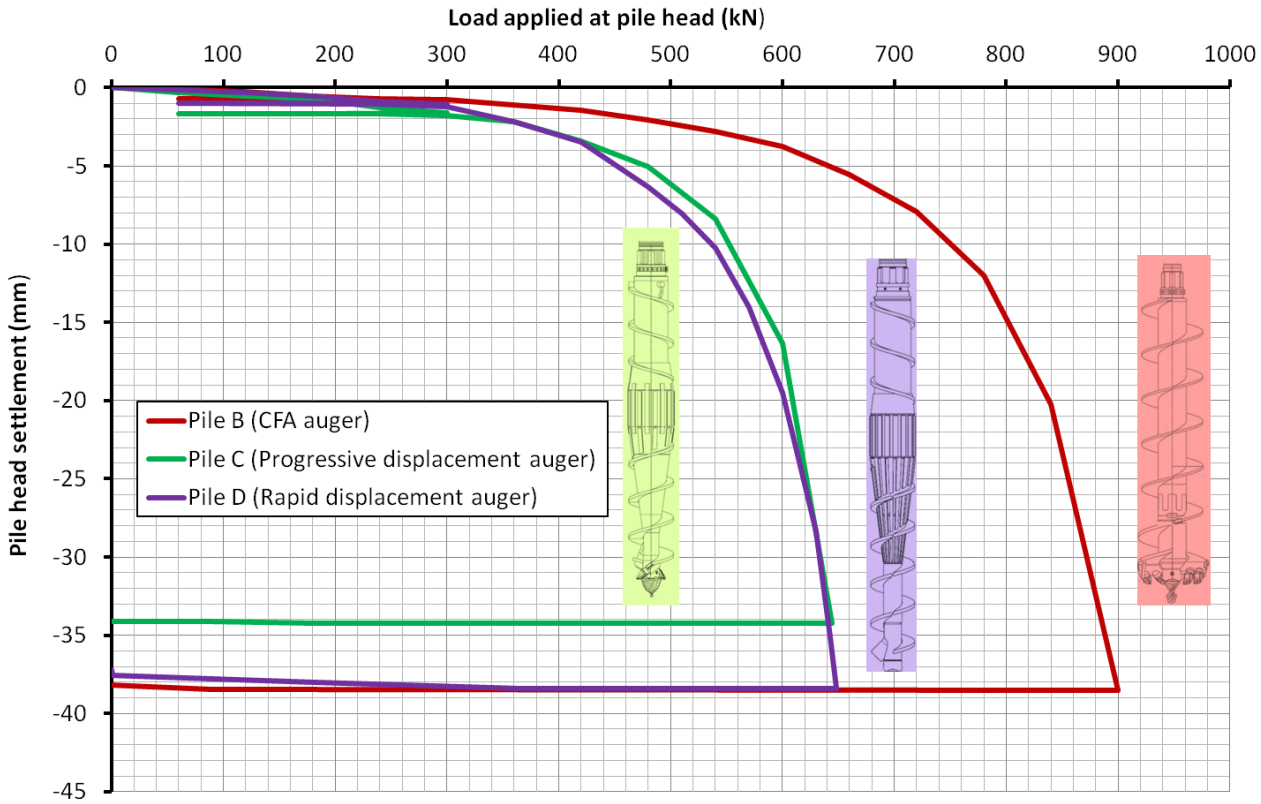

Figure 129 – Static load test results for piles B, C and D

Pile B showed a stiff behaviour up to a test load of 420 kN (which is approximately 50% of it's ultimate geotechnical pile capacity), with pile head settlement below 1.0 mm at 300 kN (working load). With increasing load steps, the settlement increased up to a final settlement of 38.52 mm at 900 kN. The load could not be increased beyond 900 kN and the test was terminated after several attempts.

Pile C behaved stiff up to 300 kN (which is about 45% of the ultimate geotechnical capacity) with pile head settlement of 1.64 mm at this load step. Rapid failure started at 540 kN, and the pile failed at 644 kN with 34.21 mm settlement.

The stiff behaviour for the first 50% of loading was also observed for test pile D, and the settlement at 300 kN test load was 1.07 mm. The ultimate pile capacity was reached at 650 kN with a total settlement of 38.40 mm.

Table 15 – Load-settlement data for the three static pile load tests

Test load (kN)	*Settlement pile B (mm)*	*Settlement pile C (mm)*	*Settlement pile D (mm)*
60	-0.10	-0.32	-0.12
120	-0.24	-0.55	-0.29
180	-0.51	-0.73	-0.53
240	-0.70	-1.25	-0.87
300	-0.76	-1.64	-1.07
180	-0.76	-1.65	-1.01
120	-0.76	-1.65	-1.01
60	-0.69	-1.65	-0.99
240	-0.73	-1.68	-1.05
300	-0.77	-1.80	-1.20
360	-1.09	-2.19	-2.17
420	-1.42	-3.40	-3.50
480	-2.09	-5.08	-6.38
540	-2.78	-8.38	-10.24
600	-3.73	-16.35	-19.49
645	-	-34.21	-35.15
650	-	-	-38.40
660	-5.55	-	-
720	-7.95	-	-
780	-12.02	-	-
840	-20.25	-	-
900	-38.52	-	-
720	-38.52	-	-
540	-38.51	-	-
520	-	-34.21	-38.10
390	-	-34.21	-38.02
360	-38.45		-
260	-	-34.21	-37.79
180	-38.32	-	-
130	-	-34.12	-37.54
0	-38.18	-34.12	-37.24

Overall, the load-settlement curves for the two screw auger full-displacement piles appear very similar, with almost identical ultimate geotechnical load capacities of around 650 kN and corresponding settlements of 34 mm and 38 mm, respectively. Up to 300 kN, test pile D (rapid displacement auger) indicated slightly stiffer behaviour. Between 360 kN and 620 kN, test pile C (progressive displacement auger) responded stiffer, indicating higher shaft capacity compared to test pile D. However, the overall performance of both full-displacement piles was almost equivalent, despite the load distribution between shaft and base capacity being slightly different for both piles (based on the shapes of the load settlement curves based on Fleming's method).

The overall performance of the CFA pile was superior, with about 40% higher ultimate geotechnical load capacity and much stiffer behaviour, particularly in the early and medium load ranges. However, the pile diameter of pile B was 50 mm larger than for test piles C or D. After normalisation and diameter adaptation, the load capacity would still be more than 30% higher compared to the two full-displacement piles.

Overall, it can be observed that the load-settlement behaviour of all three of the test piles up to a load of 300 kN was very similar, and the differences were only marginal in this load range.

8.6.2 Back-calculation after Fleming

The data of the three test piles B, C and D were used to undertake back-analysis after Fleming to obtain the following data for the piles after installation:

E_B = Soil modulus at the pile base
Us = Ultimate shaft load
U_B = Ultimate base load
M_S = Shaft flexibility factor

These four parameters give an indication about the influence of the pile installation method with respect to the shaft flexibility factor. The soil moduli at the pile base provide information of the soil stiffness around the pile toe area. The CPT and DMT values were measured at about 225 mm from the pile shaft and they thus give an incomplete picture of the potential changes of the soil modulus at the pile/soil interface at pile toe level.

The load distribution between shaft and base provides valuable data about the installation method and potential influence of the auger shape or installation parameters on ultimate pile capacity. It should be remembered that the Fleming method matches the actual load-settlement curves of the tested piles, and the data are real test data.

Pile B

The following parameters were obtained after Fleming's method was applied to pile B. The aim was to achieve an optimal match between the hyperbolic curves of the measured values from the load test result and the mathematical back-analysis using the following parameters:

D_S =	Pile shaft diameter (m)	=	613 mm
D_B =	Pile base diameter (m)	=	500 mm
U_S =	Ultimate shaft load for hyperbolic function	=	685 kN
U_B =	Ultimate base load for hyperbolic function	=	295 kN
M_S =	Shaft flexibility factor	=	0.0025
E_B =	Soil modulus beneath the pile base	=	35,000 kPa
P_S =	Estimated load transfer through pile shaft	=	630 kN
P_B =	Estimated load transfer through pile base	=	270 kN
q_S =	Average shaft resistance	=	87.2 kPa
q_B =	Average bearing resistance at the base	=	1.38 MPa

Figure 130 shows a good match for the actual load-settlement curve and the hyperbolic function after Fleming (1992).

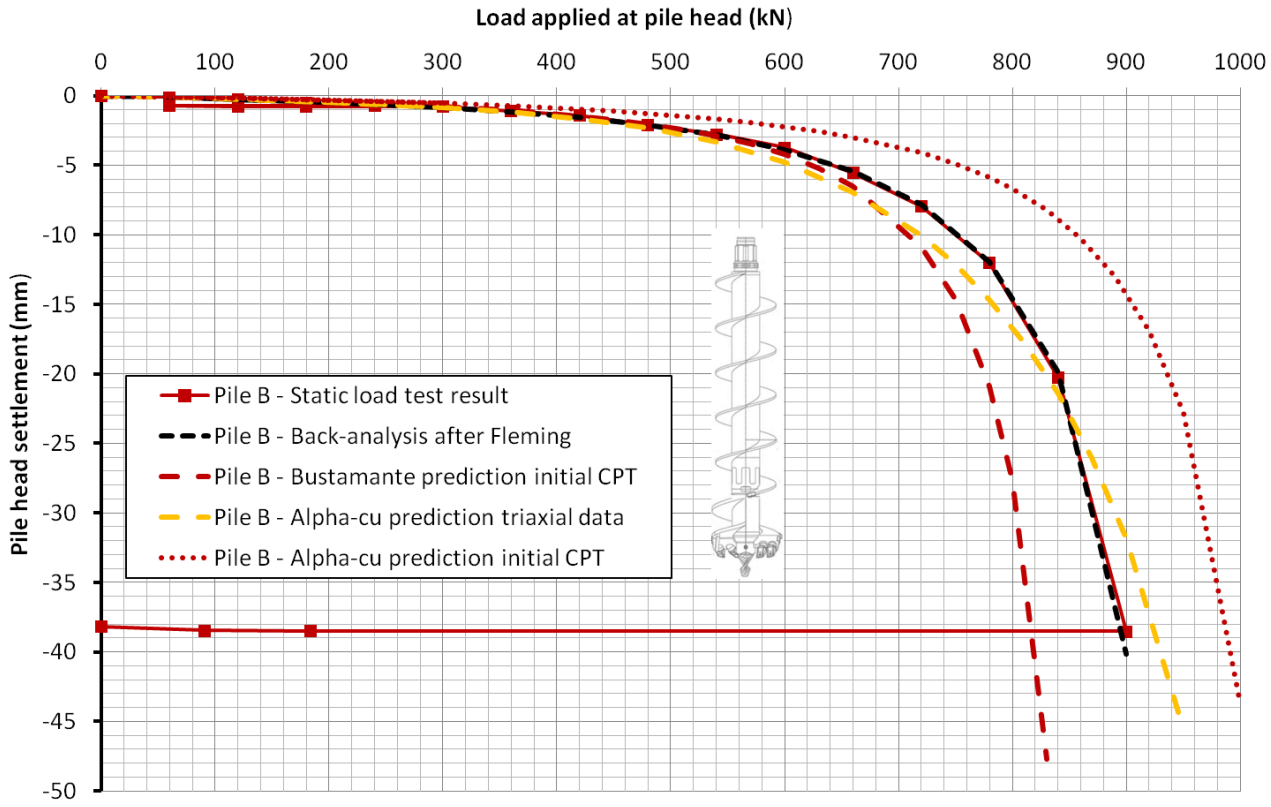

Figure 130 – Load-settlement curve with Fleming back-analysis for pile B

Pile C

The following parameters were obtained after Fleming's method was applied to pile C. The aim was to achieve an optimal match between the hyperbolic curves of the measured values from the load test result and the mathematical back-analysis using the following parameters:

D_S =	Pile shaft diameter (m)	=	450 mm
D_B =	Pile base diameter (m)	=	450 mm
U_S =	Ultimate shaft load for hyperbolic function	=	475 kN
U_B =	Ultimate base load for hyperbolic function	=	225 kN
M_S =	Shaft flexibility factor	=	0.0025
E_B =	Soil modulus beneath the pile base	=	40,000 kPa
P_S =	Estimated load transfer through pile shaft	=	437 kN
P_B =	Estimated load transfer through pile base	=	207 kN
q_S =	Average shaft resistance	=	82.4 kPa
q_B =	Average bearing resistance at the base	=	1.30 MPa

Figure 131 shows a good match for the actual load-settlement curve and the hyperbolic function after Fleming (1992).

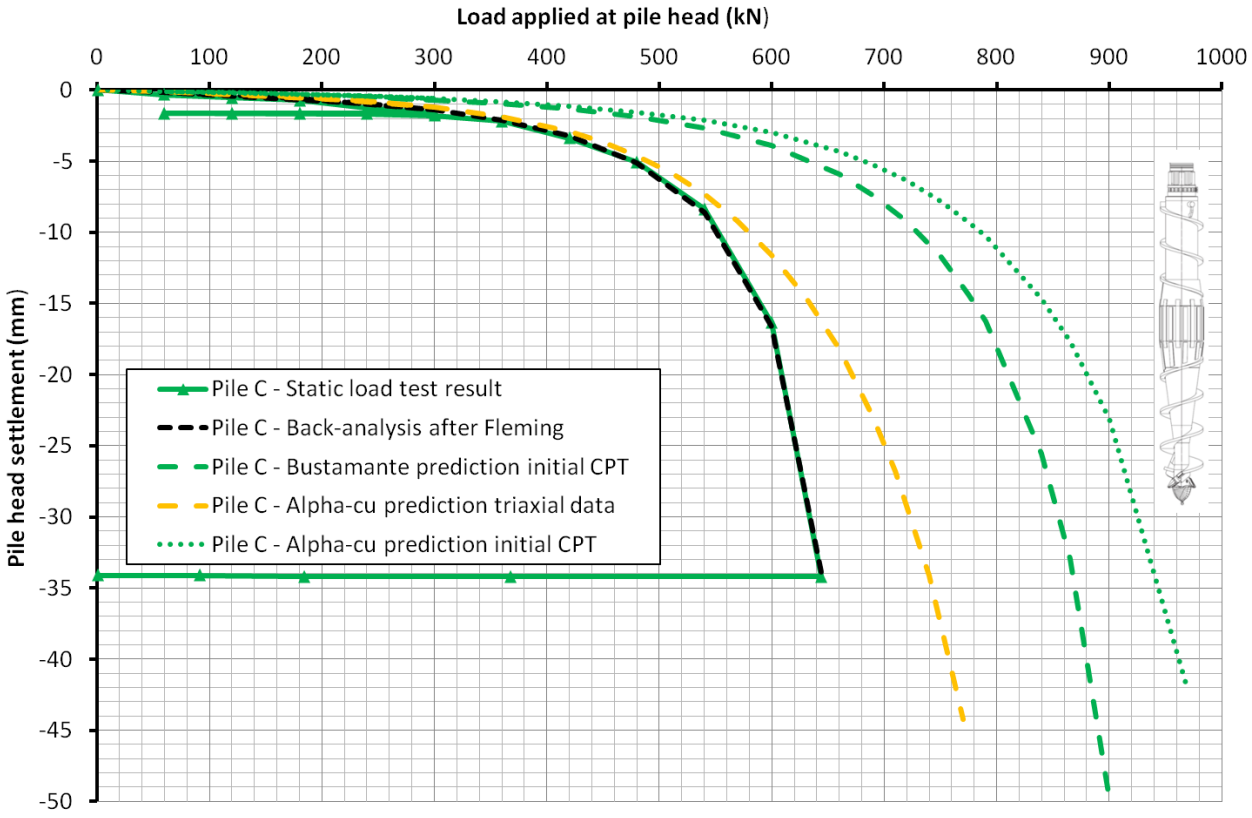

Figure 131 – Load-settlement curve with Fleming back-analysis for pile C

Pile D

The following parameters were obtained after Fleming's method was applied to pile D. The aim was to achieve an optimal match between the hyperbolic curves of the measured values from the load test result and the mathematical back-analysis using the following parameters:

D_S =	Pile shaft diameter (m)	=	450 mm
D_B =	Pile base diameter (m)	=	450 mm
U_S =	Ultimate shaft load for hyperbolic function	=	425 kN
U_B =	Ultimate base loadfor hyperbolic function	=	290 kN
M_S =	Shaft flexibility factor	=	0.002
E_B =	Soil modulus beneath the pile base	=	40,000 kPa
P_S =	Estimated load transfer through pile shaft	=	386 kN
P_B =	Estimated load transfer through pile base	=	264 kN
q_S =	Average shaft resistance	=	72.8 kPa
q_B =	Average bearing resistance at the base	=	1.66 MPa

Figure 132 shows a good match for the actual load-settlement curve and the hyperbolic function after Fleming (1992).

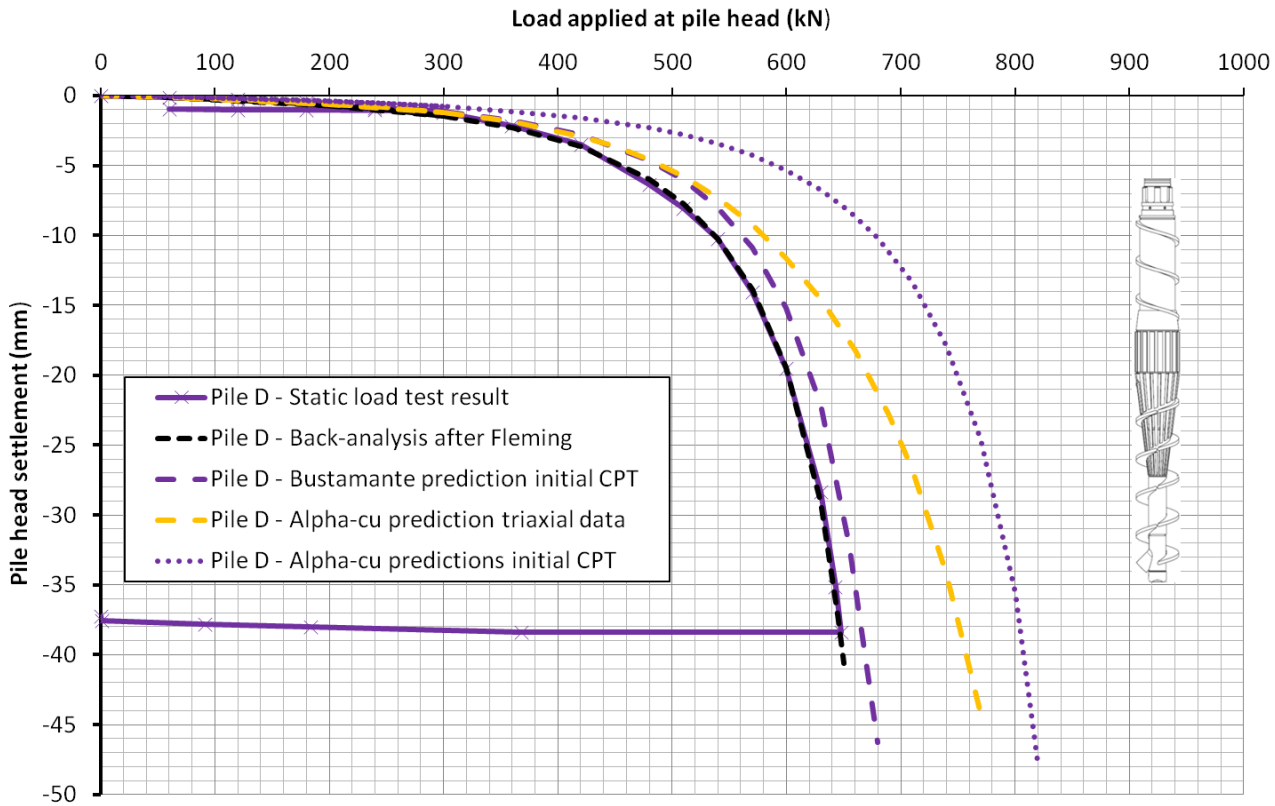

Figure 132 – Load-settlement curve with Fleming back-analysis for pile D

Summarising the back-analysis after Fleming, the soil moduli for the three test piles varied between 35,000 kPa for the CFA pile and 40,000 kPa for both full-displacement piles, indicating that the soil modulus at the pile base was higher than the average soil modulus determined from the triaxial tests (26,000 kPa).

The shaft flexibility factors were in range of Fleming's recommendations for stiff, over-consolidated clay. For pile D, a value of 0.002 was used; while for test piles B and C, a slightly higher value of 0.0025 was required to match the actual load-settlement curves of the relevant piles.

The average base resistance at the pile base was similar for test piles B (1.38 MPa) and test pile C (1.30 MPa). Test pile D showed a higher tip resistance with 1.66 MPa.

For the shaft friction, test pile D had the lowest average value of 72 kPa along the pile shaft. Full-displacement pile C showed an average of 82 kPa, while the CFA pile (test pile B) had the highest shaft capacity with 87 kPa.

The three load-settlement curves for test piles B, C and D indicate that the α-c_u method seems to overestimate pile capacities if the data obtained from the triaxial tests are used for the pile design. For the CFA pile, the over-prediction was about 8%; while for the two full-displacement piles, the laboratory data provided an estimate that was about 30% too high. Further, the load distribution between base and shaft was about 1:1 using the triaxial data. The CPT data obtained at the individual pile locations predicted a ratio of about 2:1 between shaft and base capacity, which is closer to the real results. All data are summarized in Table 16.

Back-calculations with data obtained after pile installation

Further back-calculations were carried out using CPT data obtained after the pile installation at each individual pile location, to correlate those data to the static load test results. The CPT data were measured between 4 and 7 days after pile installation, about one pile diameter from the centre line of the corresponding test pile. Both design methods (the α-c_u and Bustamante and Gianeselli procedures) were applied for each test pile location using the CPT data collected after pile installation. It was found that data obtained by DMT measurements after pile installation showed ranges from 50–120% of the measured test pile loads. CPT data were found to be more accurate, and for the back-analysis, only CPT data were used.

For the α-c_u method, $N_k = 18$ was used (instead of $N_k = 15$, as for the initial pile design) to match the results of the back-calculation as closely as possible with the actual load test data. Further, the c_u data after pile installation were used for the back-analysis and the results are shown in Table 16.

Table 16 – Back-calculated CPT data (after pile installation) and triaxial data correlated to static load test results

Pile and design method	*Shaft capacity (kN)*		*Base capacity (kN)*		*Total capacity (kN)*	
Pile B						
Static load test	**630**	**(100%)**	**270**	**(100%)**	**900**	**(100%)**
α-c_u method (N_k = 18)	639	(101%)	269	(100%)	907	(101%)
Bustamante method	619	(98%)	269	(100%)	888	(99%)
Triaxial data (α-c_u method)	582	(92%)	499	(185%)	1,081	(120%)
Pile C						
Static load test	**437**	**(100%)**	**207**	**(100%)**	**644**	**(100%)**
α-c_u method (N_k = 18)	406	(93%)	221	(107%)	627	(97%)
Bustamante method	424	(97%)	221	(107%)	644	(100%)
Triaxial data (α-c_u method)	436	(100%)	404	(195%)	840	(130%)
Pile D						
Static load test	**386**	**(100%)**	**264**	**(100%)**	**650**	**(100%)**
α-c_u method (N_k = 18)	389	(100%)	265	(100%)	654	(100%)
Bustamante method	379	(98%)	265	(100%)	644	(99%)
Triaxial data (α-c_u method)	436	(113%)	404	(153%)	840	(129%)
Pile E						
Static load test	**-**		**-**		**-**	
α-c_u method (N_k = 18)	563		473		1,036	
Bustamante method	560		473		1,033	
Triaxial data (α-c_u method)	436		404		840	

Both the α-c_u and the Bustamante and Gianeselli design methods provided back-calculated pile capacities within 2% on average of the tested loads for all three of the piles. The accuracy for the load distribution was in the same range. For test pile B, the larger diameter over the top 3.0 m was taken into consideration. For pile E, no static load tests were carried out and the *in situ* CPT data were used to give an indication of potential load capacity. This was assuming that the α-c_u and Bustamante and Gianeselli design methods provided results within at least 5% average accuracy for the back-calculation of the other test piles B, C and D, using soil data (CPT) after pile installation at the location of pile E.

Figure 133 shows the predicted load-settlement curve for pile E using Bustamante and Gianeselli's method and the α-c_u approach, providing data within the 1% range. The overall load capacity can be predicted at around 1,035 kN. This is about 35% higher than the capacity of pile D, which was installed using the same auger type (rapid displacement auger) but a less powerful piling rig, resulting in decreasing and inconsistent penetration rates and auger rotations during pile installation.

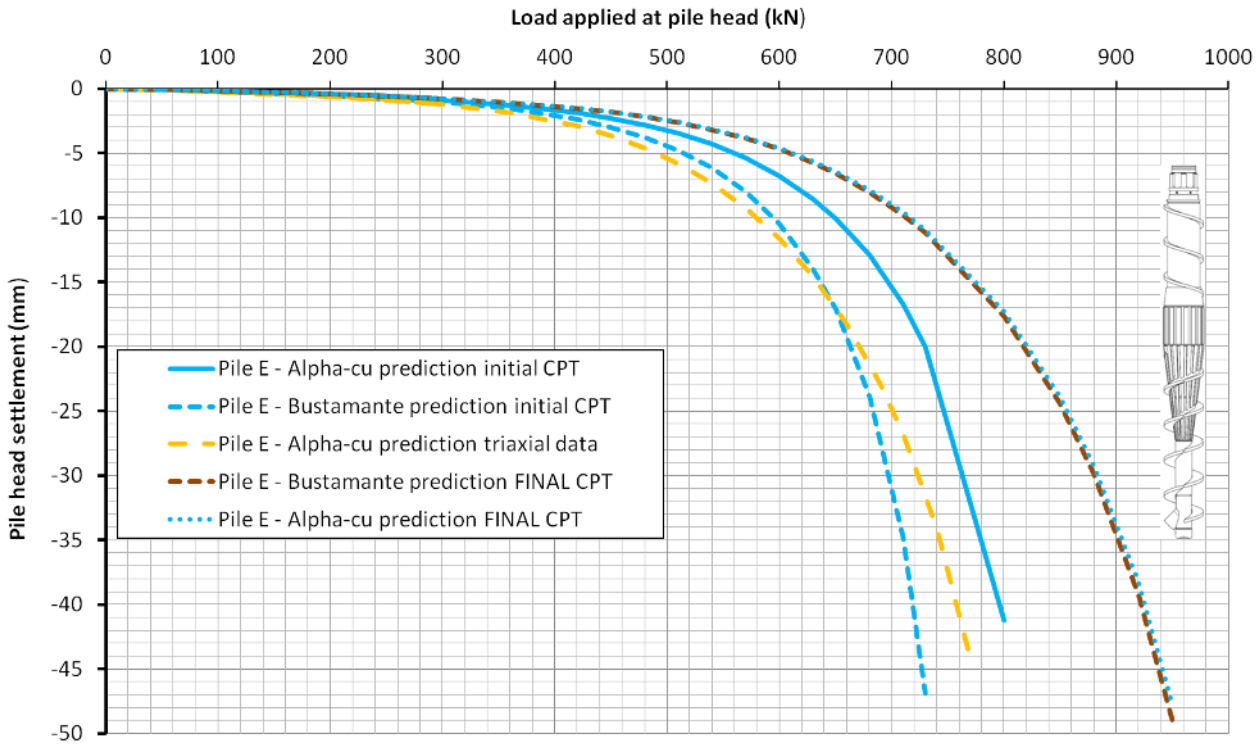

Figure 133 – Pile E: Estimated load-settlement curves using initial CPT data and CPT data collected after pile installation

Further correlation of test results is shown in Table 17, where the design predictions calculated with the initial CPT data are compared with the actual load test results.

For test pile B, installed with almost constant penetration rates according to Viggiani's formula, the pile capacity was slightly under-predicted (12%) when using virgin soil data and Bustamante and Gianeselli's method. The α-c_u method over-predicted the overall pile capacity by 8% using N_k =15.

For test pile C, installed with decreasing penetration rates reaching less than 50% of the recommended rate, the pile capacity was over-predicted by up to 40% using Bustamante and Gianeselli's method. The α-c_u approach (using N_k = 15) using virgin soil data over-predicted the overall pile capacity by 56%.

Test pile D was installed with decreasing penetration rates, reaching more than 50% of Viggiani's recommendations. The Bustamante and Gianeselli approach correctly predicted (within 2%) overall pile capacity, while the α-cu method over-predicted the overall pile capacity by 24% using N_k =15.

The potential load capacity of pile E (Figure 133), installed with the minimum installation speed, was under-estimated by about 20% using the α-c_u method with N_k =15. Bustamante and Gianeselli's approach with virgin soil data also under-predicted the estimated pile capacity by about 28%.

Table 17 – Pile load capacities (initial CPT data) compared to static load test results

	Shaft capacity (kN)	***Base capacity (kN)***	***Total capacity (kN)***
Pile B			
Static load test	**630 (100%)**	**270 (100%)**	**900 (100%)**
α-c_u method (N_k = 15)	731 (116%)	237 (88%)	968 (108%)
Factor to achieve design load	0.86	1.14	0.93
Bustamante method	596 (95%)	198 (73%)	794 (88%)
Factor to achieve design load	1.06	1.36	1.13
Pile C			
Static load test	**437 (100%)**	**207 (100%)**	**644 (100%)**
α-c_u method (N_k = 15)	642 (147%)	365 (176%)	1,006 (156%)
Factor to achieve design load	0.68	0.57	0.64
Bustamante method	595 (136%)	304 (147%)	899 (140%)
Factor to achieve design load	0.73	0.68	0.72
Pile D			
Static load test	**386 (100%)**	**264 (100%)**	**650 (100%)**
α-c_u method (N_k = 15)	551 (143%)	258 (98%)	808 (124%)
Factor to achieve design load	0.70	1.02	0.80
Bustamante method	446 (116%)	215 (81%)	660 (102%)
Factor to achieve design load	0.87	1.23	0.98
Pile E			
Assumed capacity	**562 (100%)**	**473 (100%)**	**1,035 (100%)**
α-c_u method (N_k = 15)	515 (92%)	308 (65%)	823 (80%)
Factor to achieve design load	1.09	1.54	1.25
Bustamante method	470 (86%)	257 (56%)	727 (72%)
Factor to achieve design load	1.16	1.79	1.39

CHAPTER 9: ANALYSIS OF RESULTS AND INTERPRETATION

9.1 Finite element analysis

The FE analysis was used to determine the location of the proposed monitoring equipment prior to the establishment of the field test site. It was not intended to simulate the installation process of screw auger displacement piles into stiff, fine-grained soil exactly, but rather to provide a basic understanding of the soil behaviour during pile penetration and extraction.

The author selected a simplified system consisting of a simple cone matching the basic shape of a standard full-displacement piling head, which was pushed into the ground using constant penetration of 1.8 m/min (in accordance with the computed rate after Viggiani, 1993), and an advance hypo-plastic constitutive soil model to observe the basic soil behaviour.

Overall, the FE model provided a good orientation to the expected stresses and displacements around and along the pile shaft. However, the calculation process of the 4.0 m penetration and extraction of the auger took a high performance computer about 10 hours. Moreover, the program showed some unstable behaviour such that the further improvement and development of the FE model was not considered as a major topic of this research work.

Nonetheless, the simplified FE model provided satisfactory results for the prediction of the permanent stress changes for the CFA pile, with a predicted value of 80 kPa versus 90 kPa as the measured value by raked and vertical CPTs before and after installation. As shown during the raked CPTs, the grey clay was not entirely sheared and re-moulded at 225 mm distance from the edge of the pile. The 200 kPa maximum pressure measured at the cone was only 50% of the FE prediction, but the value was within the range of the undrained shear strength of the grey clay layer.

For the full-displacement piles C and D, the FE model under-predicted the permanent and temporary stresses in the ground at 225 mm distance from the pile shaft. The measured values by the raked CPT cone showed that the stresses created by the installation process were 2 to 3 times higher than the upper boundary of the undrained shear strength, indicating that the soil around the pile shafts of piles C and D was heavily distorted and re-moulded by the auger penetration. These effects were not taken into account by the FE model.

The stress bulb below the pile toe level during installation was not measured, as no sensors were located below pile toe level. The permanent stress changes predicted by the FE model could only be found at pile B, and then at a significantly higher level (a factor of 10) than predicted by the

numerical model. For the two displacement piles C and D, the model predicted stress increments, whereas the measurements in the field indicated stress reductions after the installation process.

The displacements predicted by the FE code were about 48 mm, which is almost 100% higher than the data measured in the field. However, the inclinometers measured the displacements of the PVC tubes rather than of the soil itself. The inclinometer measurements could have been influenced by the sand and grout surrounding the PVC tubes and the fact that the tube material was stiffer than the surrounding ground. In this case, the real soil displacements would be measured conservatively, meaning that the true soil displacements could be higher than the displacements of the grouted PVC tubes. The predictions for pore water pressure were also unsatisfactory, mainly due to problems with the stability of the FE model.

The FE model did not allow for any soil distortion or disturbance from the cutting, transport and displacement actions throughout the entire installation process. The simulation of auger rotation, soil cutting and the transport processes was beyond the capabilities of the continuum methods and thus these parameters have not been considered. The FE model greatly simplified the installation process and no account was taken of soil heave (vertical soil movement).

Constant penetration rates were assumed for the entire installation process, which were not achieved for pile B (CFA pile) or the full-displacement piles C and D. No raked CPT measurements were taken for pile E to measure stress changes in the soil formation during the installation process.

The FE model also assumed pre-excavated soil conditions at the surface, to allow full contact between the auger and the surrounding soil prior to penetration. This assumption was not correct for the field test site conditions and did not model the heave phenomena realistically.

The hypo-plastic soil model after Mašín provided a new approach to simulate the behaviour of stiff clay during the penetration process of a rigid body. The constitutive soil model was able to accommodate larger soil deformations than the conventional elastic, elastic-plastic or Cam Clay approaches. The latter soil models were also used in the simulations; however, as these did not provide any meaningful results, the calculations were ceased after 10 mm of penetration due to excessive mesh distortions. Hypo-plasticity allowed the implementation of a re-meshing rule, allowing for the use of the FE mesh for further calculations, despite excessive deformations.

Overall, the adopted FE model provided data, which indicated that the installation of monitoring equipment will be most efficient if installed within 900 mm around the pile axis to measure the most significant stress and displacement changes during the pile installation. The location of equipment closer than 450 mm was likely to damage monitoring equipment due to large deformations.

9.2 Laboratory tests

Undisturbed soil samples were used for the comparison of laboratory test results for the determination of the E-modulus and the undrained shear strength c_u of the Lawnton Clay using CU triaxial tests. CU tests were used to simulate the behaviour of the cohesive soil during the pile installation, which would initially be consolidated but not drained during the short installation process (typically only a few minutes per pile).

In this research project confining stresses for CU tests of 100 kPa, 200 kPa and 400 kPa were used. In order to simulate the penetration of full displacement tools the measured stresses 225 mm from the auger were measured to be in excess of 1,000 kPa. Larger stresses cause larger displacements and consequently different values for the calculation of Young's Modulus or the undrained shear strength of the soil after the pile installation process. For this research project, no data were available of installation stresses next to the pile shaft during the pile installation process and the standard confined pressures were used for the CU tests. In order to simulate soil behaviour and the associated strength parameters more realistically, the choice of higher confined pressures for future research projects on auger displacement piles should be considered.

Whereas the profiles at the two test locations BH1 and BH2 show good alignment up to a depth of 4.0 m for the undrained shear strength c_u, significant discrepancies between these locations were observed for Young's modulus at pile toe level (Figure 83). This is important to note because the elastic modulus at pile toe level was used to calculate the load-settlement curve of each pile after Fleming's method.

For BH1, the elastic modulus at 4.0 m depth was determined by triaxial test to be about 19 MPa. A few metres from this location (at BH2), the elastic modulus was calculated to be about 32 MPa. For the initial pile design calculations using Fleming's method, the average value of 26 MPa was used.

The average profile of the undrained shear strength c_u for the grey clay layer along the pile shaft had a value of 155 kPa (determined by triaxial tests). This value was used for the initial pile design calculations (α-c_u method, Bustamante and Gianeselli's method and Fleming's method). Assuming the rule of thumb, Young's modulus was calculated according to the formula:

$E = 250 * c_u$

$E = 250 * 155 \text{ kpa} = 38{,}750 \text{ kPa}$

This value is much closer to the 35 MPa and 40 MPa used for the back-calculation of pile B and piles C and D, respectively, according to Fleming's method. It is assumed that the triaxial test at BH1

included some kind of mistake, as the value at pile toe level at BH2 is 32 MPa, which is closer to the 35 MPa and 40 MPa used for the back-analysis.

It was observed that the undrained shear strength values determined by triaxial testing varied significantly from the estimates obtained by indirect methods (CPT and DMT). Triaxial tests are the most direct measure of undrained shear strength, but the tests suffer from the need to prepare the specimen to represent the in situ state of the soil. Both CPT and DMT tests are indirect measures of undrained shear strength, but at least test the material in situ, albeit causing some disturbance during installation. Robertson (2014) stated that the NK value used to estimate the undrained shear strength from the measured cone resistance can vary from 8 to 24. The author assumed an NK values of 15 (initially) and 18 (from back-calculations). It is noted that the average cu distribution over the depth of the pile obtained by CPTs carried out after pile installation (disturbed ground) is closer to the values obtained by triaxial testing. This could be related to some disturbance during the recovery of the samples or some incorrect sample preparation for the laboratory tests.

The undrained shear strength values estimated by DMT vary from pile location to pile location (by about 100%). The resulting plots of DMT-estimated cu all have similar shapes, but these are different to those obtained by triaxial testing.

The plots of CPT and DMT-estimated cu with depth are qualitatively similar, but the quantitative values varied by up to more than 100%.

Oedometer tests were used to calculate the hypo-plastic parameters for the FE calculations and the results are shown in Figure 85.

9.3 Pile installation

The pile installation of piles B, C and D was carried out with a Casagrande C30 piling rig, which could not provide sufficient rotational torque and vertical pull-down forces to maintain a minimum target penetration rate of 3.0 m/min for pile B and 1.8 m/min for piles C and D. The target penetration rates were calculated using Viggiani's formula and were used as a guideline for this research project, as no standard or best practice data were available for screw piling methods in cohesive ground conditions. Screw auger displacement piles are typically installed 'as quickly as possible' to the required depth with the piling equipment that is available on site.

Pile E was installed with a more powerful Bauer BG28 piling rig a few months after the installation of the initial test piles. (The originally used Casagrande C30 rig was not available.) As this pile was installed for the sole purpose of conducting further detailed investigation of the heave behaviour of full-displacement piles, no raked CPT and no static load test were carried out for this pile. Data akin

to that for pile D (installed with the same type of rapid displacement auger) were expected. However, the use of the different rig meant that new data were collected for test pile E (CPT before and after, in addition to the heave data). These detailed CPT ratios and heave data for pile E showed significantly reduced heave values and much higher stresses in the ground after pile installation.

Test pile B was installed using a 500 mm CFA auger with a large stem. The auger can also be defined as a partial-displacement auger, as the ratio between cutting diameter and inner stem is 0.63. This auger was similar to the partial-displacement augers of the same diameter that are commonly used in Europe, as described in Section 2.3. If installed with the appropriate penetration rate, the CFA auger displaces soil into the borehole wall.

Up to 2.5 m depth, the auger advanced with the target penetration of 3.0 m/min into the Lawnton Clay. At about 2.0 m depth, the auger rotations started to slow due to drill resistance as the rotational torque was at about 90% of its maximum capacity. At 2.2 m depth, maximum torque was reached, and the auger rotations slowed further to reach 50% of the initial value at 3.0 m depth. The penetration rate slowed slightly more to a value of 2.6 m/min at pile toe level. Overall, the target penetration rate was maintained within 80% once the torque reached its maximum value and the rotations began to slow.

The capture of the lump of clay during penetration at about 3.0 m depth could be a result of the reduced rotations at depth caused by the insufficient rotational toque capacity of the piling rig. The material cut by the auger tip could not be transported through the auger flights appropriately and, as the auger was pushed down, the lump of clay sheared off, attached to the auger and became ‘trapped’ inside the auger flights.

This incident was only noticed because no auger cleaner was used to remove the spoil during auger extraction. Typically, the application of auger cleaner would have cleaned the auger close to surface level and the potential widening of the pile shaft due to the trapped oversized lump of clay would have gone unrecognised. Due to the pile shaft widening for the top 2.75 m of pile B, the shaft capacity was evaluated with a larger pile diameter.

Ideally, if the penetration rate and auger rotations are kept constant, a pre-defined soil volume is cut and transported by the auger. This soil volume is pushed with a constant rate towards the displacement body and the borehole wall. Due to further auger advancement, the volume of soil pushed into the borehole wall is constant. It is obvious that if the penetration rate slows, the soil volume inside the auger flights will be transported towards the displacement body and from there into the borehole wall. If the auger penetration slows or ceases, the entire soil volume stored inside the

auger flights is pushed against the borewall wall within a very small area, potentially causing over-stressing and resulting in the collapse of the borehole wall.

For the full-displacement piles C and D, the target penetration rates were calculated as 1.8 m/min as per Viggiani's formula (refer to Section 3.4). The auger rotations were set to 12 rotations per minute, as greater drill resistance was expected due to the displacement body of the auger. For the CFA pile, the rotations were set at 15 per minute, as less drill resistance was expected.

The average stem diameter for the full-displacement piles was calculated to be 323 mm, taken as an average between the inner stem diameter, the displacement body diameter and the diameter of the tapered lower auger section.

Full-displacement pile C was installed with a progressive displacement auger. This auger typically showed higher drill resistance, as the soil was transported quickly towards the displacement body and parts of the soil volume inside the auger flights were pushed towards the borehole wall due to the tapered shape of the lower auger section.

Pile C was installed with 15 rotations per minute through the top 1.5 m of the soil formation before the number of rotations declined linearly to five rotations per minute at 3.0 m depth. At about 2.0 m depth, the rotational torque reached its maximum value and the penetration rate started to slow significantly. From being higher than the target limit above 2.5 m depth, the penetration rate dropped to 0.9 m/min at 3.0 m depth and then to 0.7 m/min at pile toe level. This drop is significant considering that the drill rate at pile toe level was less than 50% of the target rate. It is obvious that the piling rig had insufficient energy to maintain a constant target penetration rate, as the resistance of the soil acting at and along the auger was too high for the performance of the rig.

Pile D was installed using a rapid displacement auger, which cuts the soil at the pile tip and transports it towards the displacement body inside the straight lower auger section. The straight bottom part of the lower auger section is tapered below the displacement body and the soil is displaced towards the borehole wall before it is pushed towards the displacement body.

Experience (also Slatter 2000) shows that rapid displacement augers require less input energy than progressive displacement augers due to the lower resistance of the auger in the soil. However, similar to for test piles B and C, the rapid displacement auger could not be installed with a constant penetration rate due to the insufficient rotational torque and pull-down capacities of the piling rig. The installation process started with 15 auger rotations per minute for the top 2.0 m before slowing gradually and constantly to five rotations per minute at the pile's base. The rotational torque reached its maximum value at 2.5 m depth and worked at full capacity until the pile reached the final depth.

The target penetration rate was maintained up to 2.5 m depth, but then the rate dropped to a minimum level of 0.9 m/min, which is equivalent to 50% of the target penetration rate.

Overall, the tests conducted for this research project highlighted the need for rigs to have sufficient rotational torque and pull-down force for the successful installation of screw auger displacement piles. Viggiani's formula seems a good and robust orientation to the required penetration rate; however, the balance between pull-down force and rotational torque is crucial, and this is not included in Viggiani's formula.

9.4 Field observational methods

9.4.1 Layout details

The field observation equipment was installed within tolerances. It should be remembered that small tolerances might influence the result marginally, but that under field conditions tolerances should be incorporated and overall results are only affected insignificantly.

9.4.2 CPT

The vertical CPTs were carried out before and after pile installation for each individual pile location. The results of the tests conducted in virgin ground at the pile location before pile installation were compared with those done at one pile diameter from the pile centre line. As the CPTs after pile installation were carried out between 4 and 7 days after pile installation, it was assumed that pore water dissipation would have occurred by this time.

The test results provided some surprising results, particularly for the full-displacement piles C and D. The overall *in situ* stress reductions in the soil formations measured by CPT were identical and exactly 16% for both piles after the installation process, compared with the initial values at pile location. For both piles, the top 2.7 m to 3.0 m showed reduced cone resistance q_c, indicating soil re-moulding and shearing.

Below this area up to 0.3 m above the pile toe level, cone resistance increased, before a general reduction at the pile toe area. These results indicate a significant soil disturbance because of the pile installation. Due to the reduced penetration rates and limited auger rotations, the borehole walls were over-stressed by punctual soil transport, causing them to collapse. For both full-displacement piles, the maximum rotational torque was reached when the auger tip was located about 2.5 m below the surface, which means that the top end of the displacement body just passed the soil surface and the full drill resistance was activated.

The lower end of the displacement body never reached below 3.0 m depth, and it can be concluded that the displacement body caused the soil to shear and fail. Below the displacement body inside the lower auger section, soil was still pushed upwards and sideways into the borehole wall. This slight lateral soil movement towards the borehole walls seems to have improved the soil formation at the bottom 1.0 m section of the pile moderately (15–25% improvement factor).

The pile base section was weakened with both full-displacement auger types for piles C and D. This reduction in cone resistance could be a result of extended borehole wall collapses, reaching down to 1.0 m below the pile base. Further, the reduced penetration with ongoing auger spinning caused localised zones of stress reductions below the pile toe.

Even though the areas along the pile shafts of piles C and D were sheared and re-moulded, the sheared soil was probably re-compacted by the penetrating lower auger section, indicated by the improved *in situ* stresses between 2.7 m to 3.7 m.

The installation parameters have a significant influence on the effective stress development in the stiff and hard clay formations, which can be demonstrated with the CPT measurements of pile E. This pile was installed using constant auger rotations and penetration rates and the ground around the pile was improved by an average factor of about 1.43. Only the top 1.0 m showed stress reductions, which could be a result of soil heave. From 1.0 m to 2.0 m depth, the improvement factor was only 20%; however, below this level, the rapid displacement auger achieved significant soil improvement of the clay formation. The most significant soil improvement was achieved by the lower, tapered auger section right below the displacement body. The soil below the pile base was improved by the auger penetration as well, which increased the base capacity of pile E significantly.

Pile B was installed using a partial-displacement CFA auger. From the surface to the pile toe level, there were no significant areas of improved or reduced cone resistance of the Lawnton Clay. Overall, the auger slightly improved the soil by about 3% along the pile shaft. However, there is a noteworthy improvement sector (30%) below the pile base, reaching about 1.5 pile diameters below the design level. This is a similar pattern to that observed for pile E, albeit with a smaller magnitude. This could be a result of the almost constant penetration rate of the partial-displacement auger. This effect was predicted by the FE code based on constant tool penetration.

The results show that installation factors are critical for the performance of screw auger piles in stiff clay. The installation of a rapid displacement pile with constant penetration and rotation provided about 60% higher cone resistance along the pile shaft and below the pile base, compared to a pile installed in similar ground conditions, with an identical drill tool but with insufficient installation rates.

These results were confirmed by the partial-displacement auger, which was installed with 80% of the target penetration rate yet still improved the cone resistance at the pile base and achieving a neutral effect along the pile shaft.

Both full-displacement piles installed with insufficient penetration and rotation rates demonstrated significant soil re-moulding and failure along the pile shaft, particularly in the upper part of the pile and the pile base.

9.4.3 DMT

The DMTs were carried out in virgin soil at the pile location and one pile diameter from the test pile after installation, similar to the CPT measurements. The DMT provides the measurements of the undrained shear strength c_u of the soil, with the comparison of the undrained shear strength before and after pile installation providing valuable details about the installation effects of screw auger piles in stiff clay.

The DMT measurements confirm the general findings of the CPT results described in the previous section. The two full-displacement piles C and D showed reduced c_u values at the pile toe area and for the top 2.5 m to 3.0 m of the pile shaft. Slight improvements (15–20%) of the shear strength between 3.0 m to 3.8 m depth were also observed.

Pile B showed a 10% increment in undrained shear strength along the pile shaft and 15% below the pile toe. The overall *in situ* stress reduction for pile C is 11%, which is slightly less than measured by the CPT. However, an obstruction close to the surface increased the stresses after pile installation in the area close to the surface and influenced the overall results accordingly. For pile D, the stress reduction of 16% after pile installation measured by the CPT method was confirmed by DMT. The values for test pile B show an overall improvement of 10%, which is slightly higher than the data obtained by CPT measurements.

There are no DMT results for test pile E, this test was not conducted for this pile, as explained earlier.

9.4.4 Inclinometers

The inclinometer readings for the two full-displacement piles C and D have comparably shaped displacement curves. The magnitude for the rapid displacement auger pile D is about 5.0 mm higher than for the progressive displacement pile C.

However, the measurement of the soil movements using inclinometers for this research project bears some risks for unreliable results. As the inclinometer tubes were grouted into the stiff clay formation, the displaced soil had definitely shifted the PVC tubes during the displacement process. As the

stiffness of the PVC and the grout are different to the stiffness of the surrounding soil, it is questionable whether the displacement of the tube is equal to the expected soil movement.

Overall, the displacements of piles C and D were in a comparable range, whereas the displacements of test pile B were significantly lower and reached a maximum of only 5.0 mm close to the surface. The installation of the CFA auger clearly resulted in significantly lower lateral displacement, mainly due to the higher soil transport work of the auger.

9.4.5 Heave

Pile heave was minimal for test pile B (CFA auger), as most of the spoil was transported to the surface by the auger flights. No heave measurements were carried out and, similar to the horizontal soil movements, the vertical soil movements for the CFA pile were negligible.

For test piles C and D, heave was measured along two main axes, perpendicular to each other. The measured heave volume was similar for both full-displacement piles, with 0.45 m^3 (pile C) and 0.44 m^3 (pile D). The values are approximately 70% of the theoretical excavated pile shaft volume, but it needs to be considered that the measured heave volume contained highly disturbed soil with a high dilation and large voids. Pile heave was lower where the mast foot of the piling rig was positioned, and dilation and voids were reduced in this area.

Compared to test pile E, the heave volume described above seems high, as the latter test pile only showed 0.23 m^3 measured heave volume, which is about half that shown for pile C and D. Whether the soil was similarly disturbed at this pile location is unknown; it is possible that the voids and dilation effects were less significant at this location than for the locations of test piles C and D.

The installation parameters seem to play an important role in the creation of soil heave for screw auger displacement piles. Due to the re-moulding effect, if auger penetration and rotations are insufficient, the re-moulded soil is pushed towards the surface. The CPT and DMT values confirm the existence of re-moulded and sheared soil in the upper 2.5 m along the soil shaft for piles C and D and for pile E, the heave-influenced zone is located up to about 1.0 m below the surface.

Maintaining the required installation parameters reduced the heave volume by about 50% when using a similar piling auger (rapid displacement auger) in identical soil conditions. Constant rotations and penetration keeps the soil transport and displacement rate into the borehole wall at a constant level such that the clay is compacted rather than sheared off and re-compacted or displaced towards the surface.

9.5 Pile design

The pile design was carried out using two well-established and proven methods for screw auger displacement piles. One method (α-c_u method) strongly relies on the undrained shear strength c_u as a critical design parameter. This value can be obtained by laboratory tests or *in situ* tests like the CPT or DMT. Depending on the correlation factor N_k, the results fluctuate considerably. Initial design calculations were carried out using $N_k = 15$, which over-predicted the potential pile capacity. By contrast, an increased value of $N_k = 18$ provided good alignment with the static load test results when using soil data from after pile installation (disturbed soil conditions).

The second method (after Bustamante and Gianeselli) directly relies on the q_c data obtained by *in situ* testing. However, it should be kept in mind that CPTs measure the initial pore water pressure in the soil formation; thus, this method should be used with care in the absence of supporting data from triaxial tests. For this research project, the pore water pressure was insignificant, so the method after Bustamante and Gianeselli worked well.

Installation parameters for different auger types/geometries are not considered by the design methods and the author did not find any design methods for screw auger displacement piles that took into account such parameters. Fleming suggested reducing the pile capacity for bored and CFA piles using a factor of 0.7 when applying the α-c_u method.

Pile design calculations were carried out using the specific CPT and DMT values obtained at the pile location, the site averages using all available CPT and DMT data, and the c_u values obtained by the triaxial tests. These various data were also used to identify the most reliable method after back-analysis of the static load test results.

In general, the DMT data appeared to under-evaluate the undrained shear strength, with the values typically being 10–25% lower than those obtained by CPTs at the same location. Both CPTs and DMTs show a considerable discrepancy between 2.5 m and 5.0 m depth, which is the most critical depth for pile design of this project. The CPT data for the individual pile locations showed relatively homogeneous results; however, at 4.0 m depth (pile toe level), the c_u values varied from 100 kPa for pile B to 200 kPa for pile C. Piles D and E had a comparable value close to 150 kPa. To allow for local changes, the average c_u value over a distance of 0.5 m was selected for the pile designs of each individual pile.

In summary, both methods, α-c_u and the Bustamante and Gianeselli method, provide results in a comparable range. The design calculations use comparable approaches and the choice of the relevant coefficients and necessary input parameters for the different methods are the main dissimilarities.

The author recommends the use of the α-c_u method, as it is easier to apply because no special charts are required for the selection of the design input parameters. Undrained shear strength should be obtained by laboratory tests for initial pile design calculations. Throughout the course of the project, the data can be added to by CPT measurements.

The use of Bustamante and Gianeselli's method bears the risk of some mistakes due to the selection of different q_s data from a chart, as described in Section 7.5.2. This procedure is not required for the α-c_u method, for which the only important input parameters are the undrained shear strength c_u along the shaft and the base and the coefficient α. For screw auger piles, the factor of 0.5, as recommended by API for driven piles, was found to be adequate.

The correct determination of the undrained shear strength c_u is the most important task for an efficient and correct pile design. The c_u value determined by the triaxial CU tests for this research project estimated the pile capacity within an acceptable range, whereas CPT and DMT data tended towards under- and over-prediction. CPT and DMT are quick and economical in situ testing methods from which cu values may be estimated. However, the values obtained should always be calibrated against more direct methods of determining cu, such as triaxial tests (CU). The confining pressures applied in a CU test should be considered carefully as the installation method of auger displacement piles causes large deformations and installation stresses, which should be allowed for.

The pile design data for the different test piles were used to calculate predictions about the load-settlement behaviour of each test pile. For all piles but pile D, the parameters derived from the triaxial tests provided the pile capacity that was closest to the static load test results.

9.6 Static load tests

The static load tests were the core element of the research project. These tests provided load-settlement data for piles B, C and D and allowed the author to back-calculate the pile capacities for the individual test piles. Further, pile design calculations were carried out using the CPT and DMT data taken after the pile installation process, and the results of the pile load tests were correlated to the installation parameters for each pile before and after installation.

It was interesting to note that the CPT data measured after the pile installation of piles B, C and D provided an accuracy of 98% using either the Bustamante and Gianeselli or the α-c_u method (with a modified N_k value) when compared with the static load test results. Slight variations between shaft and base capacity for some piles using different methods were observed, but the calculated values were always within 10% of the tested values. This indicated that both design methods are reliable and robust tools for the design of screw auger displacement piles in stiff clay using CPT data. The results

of the different installation methods and rates are reflected by the *in situ* soil conditions after the pile installation, measured by CPT as close to the pile shaft as practicable (0.5 pile diameters from the shaft).

Test pile B was tested with an ultimate geotechnical capacity of 900 kN. Back-calculations after Fleming showed that about 630 kN were contributed by the pile shaft and the remaining 270 kN came from base resistance. The initial design predictions using triaxial data from the original soil investigations over-predict the pile capacity by about 20% for test pile B. The Bustamante and Gianeselli approach under-estimated the pile capacity by 12% using the virgin soil data and the α-c_u method predicted 8% more capacity with the original CPT data at the pile location. Indeed, the pile installation process using the CFA auger with a large stem and penetration rates between 80% and 100% of the target penetration rate of 3.0 m/min achieved a pile capacity that fell between the predictions of the two methods. In particular, the base capacity was improved by the constant installation method. This was to be expected after analysing the DMT and CPT data after pile installation, which showed significant improvement of the soil strength below the pile base for pile B.

The larger diameter of the CFA pile (500mm) compared to the screw auger displacement pile diameters (450mm) was of minor importance for this particular project, as the main goal of the research was to correlate the pile design predictions and actual load-settlement data and the stress and displacement changes within the soil formation caused by the pile installation. The direct comparison of load capacities between the CFA pile and the full-displacement piles in stiff clay was not a research target. The normalisation of the pile diameter of the CFA pile from 500 mm to 450 mm could have distorted or influenced the direct comparison.

Test pile C, installed with the progressive displacement auger, was tested with a geotechnical capacity of 644 kN (437 kN shaft capacity and 207 kN base resistance). Estimates using virgin soil data over-predicted the pile capacity by up to 40%. The back-calculation using the CPT data collected after pile installation predicted the pile capacity within a range of 2% accuracy. It is obvious that the reduced installation parameters had a negative effect on the overall pile capacity. The initial CPT data over-predicted the pile capacity for the shaft by an average of 40% and for the base by 60%. From the reduced CPT and DMT data (average reduction by 16%) taken after pile installation, lower pile capacities could be expected. The lack of rotational torque of the Casagrande C30, combined with the high drill resistance of the progressive displacement auger, resulted in installation rates of less than 50% of the target values, reducing the estimated pile capacity by a factor of 0.64.

Test pile D was installed with a rapid displacement auger and penetration rates between 50-100% of the target penetration value. The tested geotechnical pile capacity of 650 kN (386 kN shaft capacity and 264 kN base resistance) was predicted within 2% accuracy using the virgin soil data and Bustamante and Gianeselli's method. The initial triaxial data and the α-c_u method over-predicted the pile capacity by about 20–25% compared with the test data. The cone resistance q_c taken after the pile installation using the CPT method was 16% below the original conditions, resulting in reduced pile capacities compared with the initial predictions. For pile D, no improvement or reduction factors for the base need to be applied. However, a reduction of the shaft capacity by about 30% was necessary, and an installation factor of 0.7 is recommended.

The result of the analysis of the static load tests for piles B, C and D, together with the reliability of the pile design methods used for the back-analysis of piles B, C and D, proved that the α-c_u method and the Bustamante and Gianeselli approach with CPT data collected after pile installation can be used to estimate the pile capacity of pile E, which was installed using constant penetration rates and auger rotations. Using an average value of both design methods, pile E has an estimated capacity of 1,035 kN, split into 562 kN shaft capacity and 473 kN base resistance. The original design calculations carried out with virgin soil conditions would require an improvement factor of 1.1 for the shaft capacity and 1.5 for the original base capacity estimates.

This is an important discovery, as it means that constant auger penetration in stiff clay can increase pile capacity by about 50%, assuming 4.0 m penetration into stiff clay layers. Conversely, a pile installed with insufficient penetration rates, of less than 50% of the recommended target values, only achieves 80% of the design load capacity, which is equivalent to a 2.5 m penetration with a sufficient piling rig. Significant savings in pile quantities and production rates on site can be expected if penetration rates are kept at or above the recommended target values.

The author recommends the general use of the α-c_u method, as it is more user friendly than the Bustamante and Gianeselli approach. The undrained shear strength can be obtained directly from laboratory tests. Bustamante and Gianeselli's method might be slightly more accurate (based on data collected during this research project); however, the robustness of the α-c_u method and its familiarity among practitioners are perceived by the author as advantages for the method's practical application. The alpha value can be chosen as per the API recommendation for the installation of driven piles considering the displacement effect during pile installation:

$\alpha = 1.0$ for clays with $c_u < 25$ kPa

$\alpha = 0.5$ for clays with $c_u > 75$ kPa

Values of 25–75 kPa need to be interpolated and the skin friction is solely dependent on the cohesion of the soil. Effective stress changes with depth are disregarded with this method.

As an addition, and because of this research work, the author wants to introduce an installation factor λ to account for the installation effects of screw auger piles in hard clay. The minimum required penetration rate as per Vigianni's formula in hard clay is the governing criteria and c_u data collected from *in situ* tests on site can be used:

- Screw auger full-displacement pile $v_{actual} < 50\%$ (at any time)
  - λ_{shaft}: 0.65
  - λ_{base}: 0.6

- Screw auger full-displacement pile $100\% > v_{actual} \geq 50\%$ (at any time)
  - λ_{shaft}: 0.7
  - λ_{base}: 1.0

- Screw auger full-displacement pile $v_{actual} \geq 100\%$ (at any time)
  - λ_{shaft}: 1.1
  - λ_{base}: 1.5

- Screw auger partial-displacement pile $v_{actual} \geq 80\%$ (at any time)
  - λ_{shaft}: 0.8
  - λ_{base}: 1.1

For screw auger partial-displacement piles the rules for full-displacement piles should be adopted.

The installation factors λ are based on the use of the α-c_u method. In Figure 134 both, partial- and full-displacement tools are combined as the research has proven that in hard Lawnton Clay, the installation rate is more important than the auger shape to achieve high pile/column capacities.

However, the author suggests care in using the installation factors λ for either method until more data is collected and further correlations between installation parameters and design methods in fine-grained soil conditions become available.

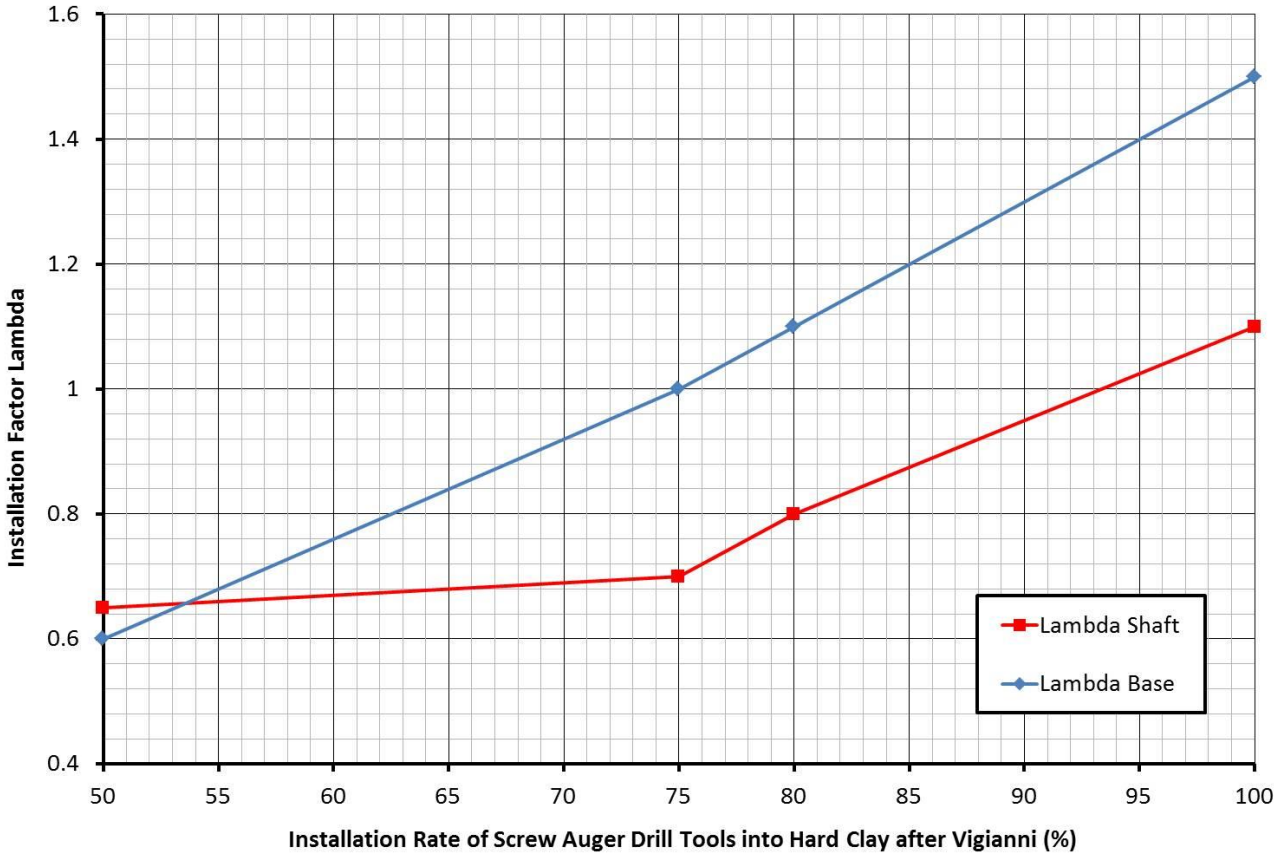

Figure 134 – Installation factors lambda for screw auger piles in hard clay

CHAPTER 10: BENEFITS AND TECHNOLOGY TRANSFER ACTIVITIES

The findings of this research work will be available to practitioners and academics who are involved in the design or execution of screw auger displacement piles and columns in Australia and around the world.

Piling Contractors Pty Ltd, one of the research project's industry partners, is part of the globally operating Keller Group, which has over 40 offices and subsidiaries around the globe. The results of this research will be available to the Keller Group and its employees. Additionally, the findings of this research will be communicated during national and international workshops and conferences within the next few years. The author is confident that within the Keller Group further research projects will be initiated that will further explore the behaviour of screw piling augers in fine-grained and granular soil formations.

The results of this research are also available to Golder Associates, a globally operating consultancy firm with a strong geotechnical branch in Australia. The author is optimistic that the research findings will be communicated throughout the organisation and the findings could be applied in the design and specification of rigid inclusion projects in Australia.

Over the last five years, contacts with other researchers and universities inside and outside Australia were established by the author. In 2011 and 2012, the Go8 and DAAD generously funded an exchange program with the Technical University of Dresden (Germany). The German research team had significant expertise in numerical modelling using hypo-plastic soil models. With the support of the German researchers, a numerical model was developed to simulate the penetration of the rigid body into the cohesive soil continuum, as presented earlier. The comparison of the actual test data with the predictions provided by the FE model highlighted that the model needs to be further improved and future collaborations in this area are probable and desirable.

Contacts with the University of Wollongong, The University of Newcastle, The University of Western Australia, The University of Luxemburg and the Universiti Tunku Adbul Rahman (Malaysia) were also established during the course of this research project, and these will be used to explore further options to continue investigating screw auger displacement pile behaviour in fine-grained soil conditions.

CHAPTER 11: CONCLUSION AND RECOMMENDATIONS

11.1 Conclusions

The aim of this research project was to investigate the behaviour of fine-grained soil during the installation of screw auger displacement piling augers. Here, soil behaviour was measured in changes in stresses and displacements in the soil formation before, during and after pile installation.

With respect to the gaps that were identified after the literature review (refer to Chapter 5 and displayed here in *italics*), the following conclusions are drawn from this research work:

(i) *Screw auger pile behaviour in stiff, cohesive soils has not been investigated in detail. Stiff clays are often used as a bearing layer for piles and rigid inclusions and it is important to understand the interaction of screw piling augers and the surrounding soil, particularly as concerns the influence of auger shape and installation parameters in relation to possible load capacities and soil behaviour around the pile shaft.*

The auger shape of a long screw auger full-displacement auger seems not to have a major influence on the load-bearing capacity of piles in stiff or hard clay formations. More important is the maintenance of a constant penetration rate and auger rotations during the tool installation. With minimum penetration rates as calculated using Viggiani's formula, embedment lengths into stiff clay could be reduced by about 25%, maintaining similar load capacities due to the soil displacement effect around the toe and along the shaft. Overall production rates on site could be increased significantly, as socket penetration usually requires most of the drill time.

This research has investigated the influence of installation parameters (Figure 134) and auger shapes (for long displacement augers) on pile performance in stiff to hard clay formations. The results and recommendations of this research provide valuable data for future research investigate this field further in detail.

(ii) *There are no qualifications in design standards and specifications in regards to the performance of different drill tools and auger geometries, despite the fact that the auger mechanics are different for each individual tool.*

Minimum auger penetration rates should be included in specifications for auger displacement piles and rigid inclusions, whereas different auger shapes seem not to play an important role in hard clay.

The author recommends at least 1.8 m/min penetration rates for 450 mm full-displacement augers (after Viggiani's 1993) as a starting point unless the auger geometry makes a new calculation necessary. The extraction rate should be kept constant at about 3.0 m/min.

(iii) *Over the last two decades, different screw auger displacement tools have been manufactured by numerous different suppliers around the world; yet no classification of the different auger types has been carried out.*

The author categorised the different screw augers into short and long sections. The latter category can be separated into progressive and rapid displacement augers.

(iv) *Several researchers have carried out pile load tests to compare the load capacities of different screw auger types in similar ground conditions. However, no efforts have been made to compare and consider the particular installation parameters (e.g. penetration rates, pull-down forces, rotational torque readings) to investigate whether those parameters have any influence on the pile capacity and stress development in the soil formation.*

Installation parameters seem to have a significant influence on the pile capacity of screw auger displacement piles. With constant minimum penetration rates of at least 1.8 m/min, total pile capacities in stiff to hard Lawnton Clay could be increased by about 25% on average due to 'controlled' clay re-moulding along the pile shaft (10% increment) and particularly below the pile toe level (up to 50% increased load capacity).

Reduced penetration rates, at between 50–100% of Viggiani's recommendation, seem to shear-off and re-mould the clay in an unpredictable way. Potentially 'soft' pile toes with reduced bearing capacity can be created and shaft friction can be reduced by up to 30%.

Penetration rates below 50% in any part of the installation process can reduce the calculated design capacity, with the most severe reductions below the pile toe (up to 40%).

These significant findings indicate that potential settlement problems of completed structures can be directly linked to the pile installation parameters. The author has developed a chart for installation parameters for screw auger displacement piles installed in hard (Lawnton) clay (Figure 134). The chart is valid for both, partial- and full-displacement piles in hard clay but needs further verification in other ground conditions than Lawnton Clay.

(v) *There is no evidence as to whether the current theoretical auger models described in this thesis sufficiently describe screw auger behaviour in cohesive soil conditions. All current auger models are based on the Archimedean screw principle, which might not reflect the real behaviour of screw piling augers with absolute certainty, but which might be sufficient for the current state of knowledge.*

The simple auger model after Viggiani worked well for this research project to investigate the fundamental behaviour of screw auger piles in stiff clay. The auger model greatly simplifies certain mechanical processes and does not allow for vertical thrust (pull-down force) or any correlations between vertical thrust and rotational torque dependent on the strength of the formation of interest.

However, the penetration rates provided a robust starting point and indicated that reduced penetration significantly diminishes the pile capacity of screw auger displacement piles in stiff clay.

(vi) *The effects of lateral soil displacement and heave on screw auger displacement piles are well known from practical experiences on numerous piling projects; however, these are not well understood in detail. Heave has not previously been related to installation parameters and has not been applied to designs or specifications for screw auger displacement piles or rigid inclusions.*

Heave was not investigated in detail in this research project. However, soil heave was about 35% of the theoretical pile volume for piles installed using the minimal penetration rate. If piles were installed with penetration rates less than 100% of the recommended 1.8 m/min, soil heave doubled. This indicates significant and uncontrolled soil re-moulding and shearing due to reduced auger penetration.

It needs to be considered that the measured heave volume contains voids and sheared material. The dilatation factor of the vertically displaced soil volume is unknown.

(vii) *Load tests indicated the improvement of skin friction of screw auger piles due to soil displacement or re-moulding processes in stiff clay formations; however, no detailed research has been carried out in regards to potential weakening of the surrounding pile by insufficient installation parameters.*

The test piles C and D of this research project showed significant reductions in estimated shaft capacities if the minimum penetration rates were not met.

Test pile E provided evidence that the clay can be re-moulded in a controlled way if the penetration rate is kept constant at a pre-defined limit, as mentioned by van Impe (1988) with respect to clay re-moulding during the installation of Atlas piles (the installation of Atlas piles follows constant installation rates).

(viii) *The influence of installation parameters (e.g. penetration rate, torque, pull-down force, rotations) for different screw piling auger types has not been studied in detail and no theoretical models are available to predict pile capacities in relation to different installation parameters.*

The influence of the installation parameters was investigated for two screw auger full-displacement piles (piles D and E) installed with a similar long rapid displacement auger in similar ground conditions using different piling rigs. As rotational torque capacities were limited for one rig, the penetration rate could not be kept constant, which resulted in strength reductions in the cohesive soil formation.

Test pile E, which was installed with the minimum and constant penetration rates and rotations, achieved about 50% more theoretical load capacity than pile D.

For this research project, Bustamante and Gianeselli's (1998) design approach and the well-known α-c_u method both worked well for the prediction of pile capacities for partial and full-displacement piles in stiff to hard clay. The author recommends the α-c_u method due to its more straightforward use.

The recommended α value of 0.5 worked well for this research project, as did the use of CPT data at the pile location together with pile installation factors λ.

In addition to the conclusions arrived at above, the author summarises the following important additional findings resulting from this research project that do not directly relate to the gaps identified in the literature review:

(ix) Piling rigs must provide sufficient torque and pull-down capacities to ensure constant penetration rates in stiff to hard clay formations. As a rule of thumb, the author recommends using piling rigs of at least 250 kNm rotational torque capacity and 250 kN pull-down force for 4.0 m penetration into stiff clay. For each meter less, penetration torque requirements and thrust rates can be reduced by 50 kN(m). However, the minimum requirement should not be less than 150 kNm torque and 150 pull-down force for 2.0 m penetration into stiff clays. If the required constant penetration rate and auger rotations cannot be maintained during the penetration of the bearing layer, a bigger rig must be used

or the pile installation factors λ should be applied accordingly to reduce pile load as recommended in this thesis.

(x) Stresses in the soil during auger penetration were measured *in situ* by using stationary CPTs installed under a 45-degree rake. It was observed that the stresses in the ground reached a peak of up to 500% of the initial stresses when the displacement body of the auger passed the measurement device. After the whole displacement body had passed, the pressure dropped back significantly, which indicates that (full-)displacement augers can increase stresses in cohesive soil formations. Despite the fact that the stresses created by the penetrating drill tool in the Lawnton Clay were higher for progressive displacement augers than for rapid displacement augers, the stress changes in the soil after the installation process were similar for both auger types (just above the undrained shear strength of the soil). This finding is supported by CPT measurements and the static load test results, as both displacement piles achieved almost identical ultimate geotechnical pile capacities of about 650 kN. The stress plot for the CFA column followed a slight zigzag pattern, which indicates that stress increments and reductions changed with auger penetration and rotation. Increments of initial stresses of up to 10% were observed, indicating that the small diameter CFA auger displaced and 'improved' the Lawnton Clay partially, albeit not as significantly as did the full-displacement augers.

(xi) The stress pattern predicted in the FE model, showing a stress bulb moving downwards with auger penetration, was proven quantitatively with field measurements using raked CPTs. The values provided by the FE model did not match the measured values exactly, but the prediction for the CFA pile was close. Further, the stress bulb below the pile toe, indicating strength increments, was proven for piles B and E, for which the penetration rates were kept constant (as per the FE model assumption).

(xii) *In situ* stress measurements by CPT and DMT should be considered carefully without the support of laboratory results for the determination of the undrained shear strength c_u. The cones or blades are installed quickly under undrained conditions and in many cases, the pore water pressure (or fluid pressure) is measured rather than the effective stresses in the soil.

(xiii) The correlation factor $N_k = 15$ worked well for the back-analysis using the α-c_u method. Consideration should be given to varying this value depending on application and soil conditions.

Static load test results and the back-analysis on the test piles provided evidence that the piles installed with the minimum and constant penetration rate of 1.8 m/min and constant auger had improved load capacities by about 25% more than predicted. Reduced penetration rates due to lack of piling rig power decreased pile capacities below predicted levels. It can be concluded from this that the impact of installation parameters on rigid inclusion and displacement pile design is significant. The choice of installation rate is the most critical consideration, as only a constant installation rate ensures full pile or column capacities. Declining penetration rates due to insufficient drill rig torque will reduce the base capacities of rigid inclusions, causing the neutral line of settlements to move further downwards, increasing the overall settlement of the soil block.

The reason for the reduced load capacity and the additional soil heave can be attributed to the different mechanics of the screw full-displacement augers. During penetration, the auger flights fill with spoil, cut by the auger tip. The spoil is transported towards the displacement body of the auger, where it is pushed into the borehole wall, resulting in improved strength and higher *in situ* stresses of the soil formation at the pile/soil interface. As long as the penetration rates are constant, a continuous amount of soil is fed from the auger flights into the borehole wall. With declining penetration rates and constant auger rotation, more soil from the auger flights will be pushed into the borehole wall, causing overstressing of the borehole wall and resulting in a failure of the wall inside the excavation. The soil might fail towards the pile toe, where the lower auger section temporarily supports the borehole wall, causing the wall to collapse. The sheared and collapsed soil will be fed back towards the displacement body and into the borehole wall as the auger slowly progresses. The soil is then re-compacted, but the initial strength cannot be re-achieved. The *in situ* stresses measured by CPT and DMT show stress reductions below the pile toe, indicating that failure mechanism potentially reached up to this zone. If penetration rates decrease close to the surface, the amount of soil heave can also increase, as the failure pattern could reach out towards the surface as the zone of least resistance.

The possible impact on stress level dependence in the case of longer piles has not been investigated and discussed in this research study. Stress level dependence of longer screw auger displacement piles is strongly dependent on the specific site conditions and need to be analysed based on soil conditions (granular, cohesive or layered formations), drill tools (progressive, rapid or CFA augers) and the installation forces of the pile rig. It is unlikely that socket lengths for longer piles into stiff/hard clay or dense sand formations will extend four meters as even the most powerful piling rigs might struggle to achieve deeper embedment length maintaining minimum penetration rates.

This research demonstrated that declining penetration rates reduce pile load capacity significantly. The disadvantage is three-fold: the contractor will create a pile/column with a reduced load capacity, heave and soil movement will increase potentially damaging adjacent structures and completed piles/columns and production rates will be lowered by the effort required to penetrate stiff layers.

Finally, the author would like to remark that the conclusions of the thesis were formulated on the basis of testing only four piles at Lawnton Clay. The piles were relatively short and installed within one experimental area. Consequently, the experimental findings, and especially the quantitative relationships recorded, cannot be considered as universally valid. They rather have to be treated as signalling the potential problem and will be subject to verification by subsequent research studies.

11.2 Recommendations for further works

Further research is strongly recommended, particularly to investigate the heave mechanism and soil re-moulding processes during the installation of screw auger displacement tools. Considering that displacement piles installed in cohesive soil conditions cause heave due to soil displacement or re-moulding effects, a potential reduction of shaft friction inside the heave disturbed zone is important for design considerations.

Also of interest is the further investigation of soil displacement into the borehole wall during pile penetration and the potential over-stressing of the borehole wall resulting in failure patterns within the formation due to ‘uncontrolled’ soil re-moulding.

The positive and ‘controlled’ re-moulding effect describes by van Impe (1988), observed during the installation of screw auger piles with controlled and constant penetration rates (refer to pile E of this research project), should be investigated in more detail and supported by field and laboratory tests.

It is also important to investigate whether cavity failure occurs in granular material. The author considers that the reduction of the tool penetration in granular soil formations will cause an overstressing pattern at the bottom section of the displacement body, similar to in cohesive ground conditions. A comparable failure pattern might also occur.

The shape and geometry of screw auger displacement augers should be reviewed and optimised for applications in fine-grained cohesive soil conditions to minimise the energy required for auger penetration while maintaining pile/column load capacities. It was concluded that the shape of the drill tool is not significantly important for the load capacity of piles/columns and thus new auger shapes and geometries should be trialled with the aim to reduce drill resistance.

The refinement of Viggiani's auger model, or the development of a new auger model valid for stiff/hard cohesive soil conditions, would be an important achievement to understand better the relationship between installation parameters, auger geometry and pile capacities. In particular, the influence of vertical pull-down force combined with rotations and torque needs to be investigated in detail.

Further, the development of a more detailed numerical model would aid in improving understanding of the auger mechanics and installation parameters of screw auger piles during penetration and extraction in general. With new generations of computer hardware processors and advances in software applications, further research in this area is anticipated in the next few years. Auger rotations, pull-down forces, different auger shapes and soil heave could be implemented in future analyses.

The different behaviour of CFA piles and partial-displacement piles with small diameters (<600 mm) should be investigated further, particularly as regards potential increments in load capacities due to displacement effects for partial-displacement tools.

This research measured effective stress levels around a drilled displacement pile in excess of 1,000 kPa. In order to determine the soil parameters of the disturbed soil around the pile shaft, higher confining pressures should have therefore been applied in the triaxial tests to provide more realistic undrained shear strengths for the stiff to hard clays subjected to displacement piling operations. More research needs to be carried out in this area to more reliably predict undrained shear strengths.

Finally, the distinction between rigid inclusions (which is a soil improvement technique) and auger displacement piles (piles are structural elements) should be clearly defined and published. Different test methods should be proposed to differentiate these two applications (e.g. pile load tests versus plate load tests for proof of capacity).

REFERENCES

Anderson, WF 1988, 'Effective stresses on the shaft of bored and cast-*in situ* piles in clays', in WF Van Impe (ed.), *Proceedings of the 1st International Geotechnical Seminar on Deep Foundations on Bored and Augered Piles, Ghent, 7–10 June 1988*, A. A. Balkema, Rotterdam, pp. 387–394

ASIRI 2011, Amélioration des sols par inclusions rigides [Soil improvement with rigid inclusions] (French), viewed at <www.irex-asiri.fr>

Ayfan, EF, Van Impe, WF and Imbo, R 2003, 'Influence of pile installation and of pile test procedure on the test load results of Atlas pile—A case study', in WF Van Impe (ed.), *Proceedings of the 4th International Geotechnical Seminar on Deep Foundations on Bored and Auger Piles, Ghent, Belgium, 2–4 June 2003*, Millpress, Rotterdam, pp. 287–293

Bauer, *FDP: Full-displacement pile system, Process and equipment*, Company brochure, Bauer Maschinen GmbH, Schrobenhausen

Bjerrum, L 1972, 'Embankments on soft ground', *Proceedings of ASCE Special Conference on Performance of Earth and Earth-Supported Structures*, Purdue University, Indiana, 1–54

Brueckner, *CFA piling and installation of cased bored piles*, Company brochure

Bottiau, M, Meyus, IA, Van Impe, PO and Russo, G 1998, Load testing at Feluy test site: Introducing the Omega B* pile, *Proceedings of the 3rd International Geotechnical Seminar on Deep Foundations on Bored and Auger Piles, Ghent, Belgium, 19–21 October 1998*, Millpress, Rotterdam, pp. 187–199

Budhu, M 2011, *Soil mechanics and foundations*, 3rd edn, John Wiley & Sons, Inc., pp. 235–241

Busch, P, Grabe, J and Geressen, F-W 2012, 'Influence of the installation process of full-displacement bored piles on the subsoil', *Proceeding of the Baltic Piling Days 2012 Conference*, Tallin, Estonia

Bustamante, M and Gianeselli, L 1988, 'L'experience des LPC en matiere de pieux vises moules et tarieres creuses', *Proceedings of the 1st International Geotechnical Seminar on Deep Foundations on Augered and Bored Piles, Ghent, 7–10 June 1988*, A. A. Balkema, Rotterdam, pp. 35–46

Bustamante, M and Gianeselli, L 1993, 'Design of auger displacement piles from *in situ* tests', *Proceedings of the 2nd International Geotechnical Seminar on Deep Foundations on Bored and Auger Piles, Ghent, Belgium, 1–4 June 1993*, A. A. Balkema, Rotterdam, pp. 21–34

Bustamante, M and Gianeselli, L 1998, 'Installation parameters and capacity of screwed piles', *Proceedings of the 3rd International Geotechnical Seminar on Deep Foundations on Bored and Auger Piles, Ghent, Belgium, 19–21 October 1998*, Millpress, Rotterdam, pp. 95–108

Bustamante, M 2003, 'Auger and bored pile construction monitoring and testing', *Proceedings of the 4th International Geotechnical Seminar on Deep Foundations on Bored and Auger Piles, Ghent, Belgium, 2–4 June 2003*, Millpress, Rotterdam, pp. 27–41

Butterfield, AA 1979, 'Natural compression law for soils', *Geotechnique*, vol. 29, no. 4, pp. 469–80

Campanella RG and Robertson PK 1991, 'Use and interpretation of a research dilatometer : Can Geotech', *International Journal of Rock Mechanics and Mining Sciences & Geomechanics Abstracts*, Volume 28, Issue 6, Elsevier Ltd., November 1991

Chen, BS-Y and Mayne, PW 1996, 'Statistical relationships between Piezocone measurements and stress history of clays', *Canadian Geotechnical Journal*, vol. 33, pp. 488–498

Chin, FK 1983, 'Bilateral plate bearing tests', *Proceedings of the International Symposium on in situ Testing*, Paris, pp. 29–33

Cudmani, RO 2001, 'Statische, alternierende und dynamische Penetration nicht bindiger Boeden, Publications of the Institute of Soil Mechanics and Rock Mechanics, University of Karlsruhe (Germany), Issue 152

De Cock, F, Van Impe, WF and Peiffer, H 1993, 'Atlas screw piles and tube screw piles in stiff tertiary clays—Assessment of pile performance and pile capacity on basis of instrumented loading tests', *Proceedings of the 2nd International Geotechnical Seminar on Deep Foundations on Bored and Auger Piles, Ghent, Belgium, 1–4 June 1993*, A. A. Balkema, Rotterdam, pp. 359–367

Combarieu, O 1974, 'Effet d'accrochage et method d'evaluation du frottement negative', *Bulletin de liaison des laboratoires des ponts et chaussées*, no. 71, Mai – Juin, pp. 93–107 (French)

Combarieu, O 1985, 'Frottement negatif sur les pieux', *Rapport de recherche des Laboratoires des ponts et chaussées*, no. 136, Octobre, p. 151 (French)

Combarieu, O 1988, 'Amélioration des sols par inclusions rigides verticals, Application à l'edification des remblais sur sols mediocre', *Revue française de géotechnique*, no. 44, pp. 57–79 (French)

Craig, RF 2004, 'Consolidation theory', in *Craig's Soil Mechanics*, 7th edn, Spon Press, Padstow, Cornwall, pp. 227–233

Derbyshire, PH, Turner, MJ and Wain DE 1989, 'Recent developments in continuous flight auger piling', *Proceedings of International Conference on Piling and Deep Foundations*, London

Dettman, M 2010, *Shear Strength of Soil*, Power Point slides, Western Kentucky University

Durham Geo-Enterprises 2011, *Durham Geo-Enterprises Inclinometer User Manual,*

EN 12699:2000, European Committee for Standardization, *Execution of special geotechnical work—Displacement piles*, Brussels

England, M and Harding, J 1993, 'Instrumentation of pile installation as a management tool', *Proceedings of the 2nd International Geotechnical Seminar on Deep Foundations on Bored and Auger Piles, Ghent, Belgium, 1–4 June 1993*, A. A. Balkema, Rotterdam, pp. 199–206

Fleming, WGK 1992, 'A new method for single pile settlement prediction and analysis', *Geotechnique*, No. 3, pp. 411–425

Fleming, WGK 1995, 'The understanding of continuous flight auger piling, its monitoring and control', *Proceedings of the Institution of Civil Engineers Geotechnical Engineering*, pp. 157–165

Geomil 2012, *Electrical CPT*, Moordecht, Netherlands, viewed 11/12/2013, at: <http://www.geomil.com/products/cones-probes/eletrical-CPT/>

Smoltczyk, U 2006, *Geotechnical engineering handbook, volume 3: Elements and structures*, Ernst & Sohn

Gudehus G 1996, 'A comprehensive constitutive equation for granular materials', *Soils and Foundations*, vol. 36, no. 1, pp. 1–12

Gupte, AA 1989, 'Integrity control of bored piles using SID', *Proceedings of International Conference on Piling and Deep Foundations*, London

Hanna, TH 1968, 'The bending of long H-section piles', *Canadian Geotechnical Journal*, vol. 5, no. 3, pp. 150–172

Henke, S 2010, 'Influence of pile installation on adjacent structures', *International Journal for Numerical and Analytical Methods in Geomechanics*, vol. 34, no. 11, pp. 1191–1210

Herle, I and Kolymbas, D 2004, 'Hypo-plasticity for soils with low friction angles', *Computers and Geotechnics*, vol. 31, no. 5, pp. 365–373

Holden, JC 1988, 'Integrity control of bored piles using SID', *Proceedings of the 1st International Geotechnical Seminar on Deep Foundations on Augered and Bored Piles, Ghent, 7–10 June 1988*, A. A. Balkema, Rotterdam, pp. 587–597

Holtz, R. and Jamiolkowski, M 1985, 'Discussion of 'Time Dependence of Lateral Earth Pressure' by Edward Kavazanjian, Jr., and James K. Mitchell', April 1985, *Journal of Geotechnical Engineering*, 111(10), pp. 1239–1242.

Holeyman, A E 2001, *Screw Piles – Installation and design in stiff clay*. A.A. Balkema, Netherlands

Huegel, HM, Henke, S and Kinzler, S 2008, 'High-performance Abaqus simulations in soil mechanics', *2008 Abaqus Users' Conference*.

Huybrechts, N 2001, 'Test campaign at Sint-Katelijne-Waver and installation techniques of screw piles', *Proceedings of the Symposium on Screw Piles—Installation and Design in Stiff Clay, Brussels*, A. A. Balkema, pp. 151–203

Huybrechts, N and Maertens, J 2008, 'Some new insights with regard to load distribution in piles, based on a detailed interpretation of a large number of instrumented pile load tests', *Proceedings of the 5th International Geotechnical Seminar on Deep Foundations on Bored and Auger Piles, Ghent, 8–12 September 2008*, CRC Press, London, pp. 249–256

Imre, E and Rozsa, P 1998, 'Consolidation around piles', *Proceedings of the 3rd International Geotechnical Seminar on Deep Foundations on Bored and Auger Piles, Ghent, Belgium, 19–21 October 1998*, Milpress, Rotterdam, pp. 385–390

ISSMFE standards TC-16 (1989)

Kolymbas, D 1991, 'An outline of hypo-plasticity', *Archive of Applied Mechanics*, vol. 61, pp. 143–151

Kolymbas, D 2001, *Introduction to hypo-plasticity*, Taylor & Francis, London, New York

Kolymbas, D and Herle, I 2003, 'Shear and objective stress rates in hypo-plasticity', *International Journal for Numerical and Analytical Methods in Geomechanics*, vol. 27, pp. 733–744

Larisch, MD, Arnold, M, Uhlig, M, Schwiteilo, E, Williams, DJ and Scheuermann, A 2013, 'Stress and displacement monitoring of auger displacement piles', *Proceedings of Pile 2013—State of the Art of Pile Foundations and Case Histories, Bandung Indonesia*, B3, pp. 1–13

Larisch, MD, Williams, DJ and Slatter, JW 2012, 'Load capacity of auger displacement piles', *Proceedings of the International Conference on Ground Improvement and Ground Control (ICGI 2012), Wollongong, Australia*, pp. 739–745

Legrand, C 2001, 'Deep foundations and the need for research on screw piles in Belgium', *Proceedings of the Symposium on Screw Piles—Installation and Design in Stiff Clay*, A. A. Balkema, Brussels, pp. 3–9

Look, B 2007, *Handbook of geotechnical investigation and design tables*, Taylor & Francis, London

Machan, G and Bennett, VG 2008, *Use of inclinometers for geotechnical instrumentation on transportation projects*, E-C129, Transportation Research Board, Washington, DC

Maertens, J and Huybrechts, N 2003. *Belgian Screw Pile Technology – Design and Recent Developments*. 1st edition A.A. Balkema, Netherlands

Marchetti, S 1980, '*In situ* tests by flat dilatometer', *Journal of the Geotechnical Engineering Division, GT3*, pp. 299–321

Marchetti, S and Crapps, D.K 1981, *Flat Dilatometer Manual*, GPE Inc., USA

Mašín, D 2005, 'A hypo-plastic constitutive model for clays', *International Journal for Numerical and Analytical Methods in Geomechanics*, vol. 29, no. 4, pp. 311–336

Mašín, D and Khalili, N 2008, 'A hypo-plastic model for mechanical response of unsaturated clay', *International Journal for Numerical and Analytical Methods in Geomechanics*, vol. 32, pp. 1903–1926

Massarsch, KR, Brieke, W and Tancre, E 1988, 'Displacement auger piles with compacted base', *Proceedings of the 1st International Geotechnical Seminar on Deep Foundations on Augered and Bored Piles Ghent, 7–10 June 1988*, A. A. Balkema, Rotterdam, pp. 333–342

Metcalf, JR 1965, 'The mechanics of the screw feeder', *Proceedings of the Institute of Mechanical Engineers, Manipulative and Mechanical Handling Machinery Group*, vol. 180, pt. 1, no. 6

NeSmith, WM 2003, 'Installation effort as an indicator of displacement screw pile capacity', *Proceedings of the 4th International Geotechnical Seminar on Deep Foundations on Bored and Auger Piles, Ghent, Belgium, 2–4 June 2003*, Millpress, Rotterdam, pp. 177–181

NeSmith, WM, Jr and NeSmith, WM 2008, 'Installation effort, current calculation methods and uses in design and construction in the US', *Proceedings of the 5th International Geotechnical Seminar on Deep Foundations on Bored and Auger Piles, Ghent*, *8–12 September 2008*, CRC Press, London, pp. 317–321

NCHRP 2007, *Cone penetration testing state-of-practice*, Project 20-05, Georgia Institute of Technology, Atlanta, GA

Niemunis, A 2002, 'Extended hypo-plastic models for soils', Habilitation Thesis, Ruhr-University, Bochum

Niemunis, A and Herle, I 1997, 'Hypo-plastic model for cohesionless soils with elastic strain range', *Mechanics of Cohesive Friction Materials*, vol. 2, pp. 279–299

Pagliacci, F, Bertero, A, Siepi, M and Zuffi, P 2003, 'Recent developments on Continuous Flight Auger (CFA) pile: Technology, equipment and application', *Proceedings of the 4th International Geotechnical Seminar on Deep Foundations on Bored and Auger Piles Ghent, Belgium, 2–4 June 2003*, Millpress, Rotterdam, pp. 251–257

Peiffer, H, Van Impe, WF, Cortvrindt, G and Bottiau, M 1993, 'Evaluation of the influence of pile execution parameters on the soil condition around the pile shaft of a PCS pile', *Proceedings of the 2nd International Geotechnical Seminar on Deep Foundations on Bored and Auger Piles, Ghent, Belgium, 1–4 June 1993*, A. A. Balkema, Rotterdam, pp. 217–220

Peiffer, H, Van Impe, WF, Van Impe, PO and Haegeman, W 1998, 'Soil parameters relevant to screw pile research testing at Feluy test site', *Proceedings of the 3rd International Geotechnical Seminar on Deep Foundations on Bored and Auger Piles, Ghent, Belgium, 1–4 June 1993*, A. A. Balkema, Rotterdam, pp. 411–415

Peiffer, H 2008, 'The DMT as tool for the monitoring of the effect of pile installation on the stress state in the soil', *Proceedings of the 5th International Geotechnical Seminar on Deep Foundations on Bored and Auger Piles, Ghent, 8–12 September 2008*, CRC Press, London, pp. 135–142

Plomteux, C and Lacazedieu, M 2007, 'Embankment construction on extremely soft soils using controlled modulus columns for highway 2000 project in Jamaica', *Proceedings of the 16th Southeast Asian Geotechnical Conference*, Kuala Lumpur

Prezzi, M and Basu, P 2005, 'Overview of construction and design of auger cast-in-place and drilled displacement piles', *Proceedings of the 30th Annual Conference on Deep Foundations*, Chicago, pp. 497–512

Robertson, PK 1990, 'Soil classification using the cone penetration test', *Canadian Geotechnical Journal*, vol. 27, no. 1, pp. 151–158

Robertson, PK 2014, pers. comm.

Roscoe, KH and Burland, JB 1968, 'On the generalised stress-strain behaviour of wet clay', in J Heyman and FA Leckie (eds.), *Engineering plasticity*, Cambridge University Press, Cambridge, pp. 535–609

Scheuermann, A and Huebner, C 2009, 'On the Feasibility of Pressure Profile Measurements With Time-Domain Reflectometry', *IEEE Transactions on instrumentation and measurement*, Vol. 58, No. 2, February 2009

Schmitt, A and Katzenbach, R 2003, 'Particle based modeling of CFA and soil displacement piles', *Proceedings of the 4th International Geotechnical Seminar on Deep Foundations on Bored and Auger Piles, Ghent, Belgium, 2–4 June 2003*, Millpress, Rotterdam, pp. 217–224

Scott, JN, Suckling, TP and Wren, C 2006, 'Business benefits of an integrated CFA rig instrumentation system', *Proceedings of the 31st Annual Conference on Deep Foundations*, Washington, DC, pp. 535–540

Simon, B and Schlosser, F 2006, 'Soil reinforcement by vertical stiff inclusions in France', *Proceedings of the Symposium on Rigid Inclusions in Difficult Subsoil Conditions*, Mexico

Slatter, JW and Seidel, JP 2000, 'A proposed model for soil/auger interaction during installation of screw piling augers', *25th Annual Members Conference and 8th International Conference and Exhibition*, New York

Slatter, JW 2000, 'The fundamental behaviour of displacement screw piling augers', PhD thesis, Monash University, Melbourne

Standards Australia 2009, *Piling—Design and installation*, AS2159-2009, Standards Australia, Sydney

Tchepak, S 1998, 'The performance of CFA piles in residual clays', *Proceedings of the 3rd International Geotechnical Seminar on Deep Foundations on Bored and Auger Piles, Ghent, Belgium, 1–4 June 1993*, A. A. Balkema, Rotterdam, pp. 349–354

Terzaghi, K, Peck, RP and Mesri, G 1996, *Soil mechanics in engineering practice*, 3rd edn, John Wiley and Sons, Inc.

Thorburn, S, Greenwood, DA and Fleming, WGK 1993, 'The response of sand to the construction of continuous flight auger piles', *Proceedings of the 2nd International Geotechnical Seminar on Deep Foundations on Bored and Auger Piles, Ghent, Belgium, 1–4 June 1993*, A. A. Balkema, Rotterdam, pp. 429–443

Van Impe, WF 1988, 'Consideration on the auger pile design', *Proceedings of the 1st International Geotechnical Seminar on Deep Foundations on Augered and Bored Piles, Ghent, 7–10 June 1988*, A. A. Balkema, Rotterdam, pp. 193–218

Van Impe, WF, Viggiani, C, Van Impe, PO, Russo, G and Bottiau, M 1998, 'Load-settlement behaviour versus distinctive Omega-pile execution parameters', *Proceedings of the 3rd International Geotechnical Seminar on Deep Foundations on Bored and Auger Piles, Ghent, Belgium, 1–4 June 1993*, A. A. Balkema, Rotterdam, pp. 355–366

Van Impe, WF 2001, 'Considerations on the influence of screw pile installation parameters on the overall pile behaviour', *Proceedings of the Symposium on Screw Piles—Installation and Design in Stiff Clay*, A. A. Balkema, pp. 127–149

Van Impe, WF 2003, 'Screw piling: Still a challenging discussion topic?' *Proceedings of the 4th International Geotechnical Seminar on Deep Foundations on Bored and Auger Piles, Ghent, Belgium, 2–4 June 2003*, Millpress, Rotterdam, pp. 4–23

Van Weele, AF 1988, 'Cast-*in situ* piles—Installation methods, soil disturbance and resulting pile', *Proceedings of the 1st International Geotechnical Seminar on Deep Foundations on Augered and Bored Piles, Ghent, 7–10 June 1988*, A. A. Balkema, Rotterdam, pp. 219–226

Van Weele, AF 1957, 'A method of separating the bearing capacity of a test pile into skin friction and point resistance', *Proceedings of the 4th International Conference on Soil Mechanics and Foundation Engineering*, vol. 2, London, pp. 76–80

Vermeer, P 2008, 'Screw piles: Construction methods, bearing capacity and numerical modeling', Bautechnik 85, Heft 2

Viggiani, C 1993, 'Further experiences with auger piles in Naples area', *Proceedings of the 2nd International Geotechnical Seminar on Deep Foundations on Bored and Auger Piles, Ghent, Belgium, 1–4 June 1993*, A. A. Balkema, Rotterdam, pp. 445–455

Von Wolffersdorff, PA 1996, 'A hypo-plastic relation for granular materials with a predefined limit state surface', *Mechanics of Cohesive-Frictional Materials*, pp. 251–271

Wong, P and Muttuvel, T 2011, 'Support of road embankments on soft ground using controlled modulus columns', *Proceedings of the International Conference on Advances in Geotechnical Engineering*, Perth, pp. 621–626

Wood, DM 1990, *Soil behaviour and critical state soil mechanics*, Cambridge University Press, New York

Zhang, Z and Tumay, MT 1999, 'Statistical to fuzzy approach toward CPT soil classification', *Journal of Geotechnical and Geoenvironmental Engineering*, vol. 125, no. 3, pp. 179–186